# AN IMPROVED BACKCALCULATION METHOD TO PREDICT FLEXIBLE PAVEMENT LAYERS MODULI AND BONDING CONDITION BETWEEN WEARING COURSE AND BASE COURSE

by

BACHAR AL HAKIM
BSc, MSc, MASCE, MIHT

A thesis submitted to Liverpool John Moores University
for the degree of Doctor of Philosophy

Liverpool John Moores University
School of the Built Environment
Liverpool
United Kingdom.

April 1997.

This thesis is dedicated to the souls of my mum and my twin brother,
whom I lost during this research period.

# ACKNOWLEDGEMENTS

The author wishes to express his sincere appreciation to Dr H. Al-Nageim, Professor L. Lesley and Mr D. Morley under whose supervision this research project was conducted.

Sincere thanks are due to Dr D. Pountney for his advice concerning the mathematical, statistical and computer works.

A special thank is also extended to Professor D. Jagger, the School Deputy Director for Research and Developments for his help and support.

The author acknowledges the co-operation of Cheshire County Council for permission of access to the A34 road pavements, University of Ulster for the Nottingham Asphalt Tester provision and SWK Pavement Engineering Limited for providing the A41 pavement results for analysis.

Researchers, staff and technicians of the School of the Built Environment are thanked for their friendship and help.

Finally the author wishes to dedicate this thesis to his parents, his wife and his son for their understanding, love and moral support.

# ABSTRACT

The aim of this research project is to develop an improved backcalculation procedure, for the determination of flexible pavement properties from the Falling Weight Deflectometer (FWD) test results.

The conventional backcalculation methods estimate the pavement layer moduli assuming full adhesion exists between layers in the analysis process. The method developed in this research can predict the interface condition between the wearing and the base courses in addition to the layer moduli, which can be considered an improvement to the existing procedures. A two stage database procedure has been used to predict the above parameters and to facilitate the determination of the deflection insensitive parameters.

The need for this improvement arises from the large number of debonding failures which have been reported in the literature between the wearing and base courses, and the theoretical studies which identified the significance of including the interface bonding condition in the analysis process.

The validation of the improved method has been carried out firstly by comparing the backcalculated results for ninety theoretical pavements with their hypothetical values, and secondly by comparing the improved procedure results with other well known programs such as WESDEF and MODULUS.

Full scale pavement testing using the FWD has been performed and the backcalculated results compared with measured values for the pavement materials. Indirect tensile tests for resilient modulus of bituminous materials were carried out on cores extracted for the pavements, whereas Dynamic Cone Penetrometer (DCP) tests were conducted for the unbound materials. The Backcalculated and the physically measured results correlated well, validating the improved procedure.

# CONTENTS

# LIST OF TABLES

# LIST OF FIGURES

# Chapter 1

# INTRODUCTION

## 1.1 BACKGROUND TO THE PROBLEM

The majority of highway networks have been constructed during the 1960's and 70's in many countries (1), therefore monitoring, evaluating and improving these highways to meet the increasing traffic loading and frequency has become major concern for highway engineers.

Pavements deteriorate after construction under traffic and environmental effects. The assessment of existing pavement conditions with sufficient accuracy is an important part of a pavement management system. Therefore, different maintenance and rehabilitation schemes can be considered together with the financial constraints to achieve the optimum rate of return.

Pavement condition can be classified as functional and structural (2):

i) The functional properties include the pavement ride quality related to surface roughness and the pavement safety related to skid resistance.

ii) The structural properties include the strength of the pavement and its bearing capacity.

The structural condition will depend on the material properties and thicknesses of the different layers in the pavement structure including the subgrade. Predicting the material properties of the pavement layers to assess its structural performance is the main concern of this research.

Pavement structural condition deteriorates gradually during its life to reach the state of failure. Two main criteria are considered for flexible pavement failure, permanent deformation or rutting, and fatigue cracking (3).

In the UK a rut depth of 10 mm in the wheel tracks has been proposed to describe the pavement critical life. If the deterioration progresses the failure will be reached eventually at 20 mm rut depth or extensive surface cracking in the wheel path (4).

An evaluation method based on the maximum measured deflection under standard wheel load to assess the pavement strength is also implemented. Empirical relationships between the deflection and the residual pavement life developed from experience on full scale experimental roads are used (5). However, this method describes the whole pavement as one number which does not indicate the individual layers' properties within the pavement.

With increasing use of the mechanistic pavement design and evaluation methods, which are based on fundamental engineering principles, the knowledge of each pavement layer property becomes important(2). The layers moduli can be use to calculate the stresses and strains within the pavement structure and hence predict its life.

To determine the mechanical properties of the pavement materials two different approaches can be employed; either laboratory testing on samples taken from the pavement structure or by mean of non-destructive testing (NDT) on existing pavements. The former suffer from many drawbacks such as the tests being tedious, time consuming, destructive to the structure and can cause traffic delays. Furthermore, it is difficult, if not impossible, to simulate an exact state of field stress in the laboratory testing of pavement materials (6). NDT methods have gained popularity in the past decade because of their ease of use and their ability to collect large amounts of data in a short time period (7).

Among the pavement responses to surface load such as stresses, strains and deflections, the only practical measurements are deflections. Many NDT devices have been developed to measure the pavement surface deflections. The Falling Weight Deflectometer (FWD) is one of them, where an impact load is applied to the pavement surface and the deflections are measured at seven locations. The FWD provides a pulse shape load that tends to simulate moving-wheel load better than any other device (8). The deflection basin is analysed in a

procedure known as backcalculation, to predict the insitu elastic modulus for each pavement layer. Knowledge of the pavement geometry (layer thickness) and the interface condition between the layers is essential for the process. The pavement properties are then input into a mechanistic pavement model to calculate stresses and strains resulting from the applied loads. These stresses and strains are used with fatigue and deformation distress relationships to evaluate the pavement structural condition and predict the pavement failure.

The surface deflections under the falling weight reflect the real insitu pavement conditions in term of layer moduli, thicknesses, Poisson's ratios and the interface condition between the individual layers.

Conventional backcalculation programs for flexible pavements have assumed that full adhesion exists between the pavement layers in the analysis process. However, debonding failure between the wearing course and base course has been reported in flexible pavements (9,10,11).

## 1.2 OBJECTIVE OF THE PROJECT

The scope of the present research project is to develop and validate an improved backcalculation procedure for flexible pavements. The process is based on mechanistic analysis of the pavement response under the FWD.

The new two-stage backcalculation method should predict the pavement layer moduli and the interface shear reaction modulus between the wearing and base courses from the FWD test results. This can be considered as an improvement in the existing backcalculation methods since the common assumption of full adhesion between the wearing and base course has been relaxed.

## 1.3 OUTLINE OF THE THESIS

A review of literature relating to flexible pavement evaluation using the FWD and backcalculation techniques, including pavement and materials modelling, deflection analysis, assumptions and sources of errors in backcalculation methods are discussed in Chapter Two.

The reported practical evidence of slippage failures and their causes, together with the mathematical model and the existing methods for predicting the interface condition, are presented in Chapter Three.

The effect of the interface bonding condition between the wearing and base courses on backcalculated moduli and pavement life is discussed in Chapter Four.

Surface deflection sensitivity to pavement parameters is investigated in Chapter Five.

The development of the improved two-stage backcalculation procedure is detailed in Chapter Six.

The theoretical and empirical validation of the improved method including the discussion of the full scale pavements testing results are provided in Chapters Seven, Eight and Nine.

Finally, the conclusions of this thesis with the recommendations for further investigation are given in Chapter Ten.

# Chapter 2

# FLEXIBLE PAVEMENT EVALUATION USING THE FWD AND BACKCALCULATION TECHNIQUES

## 2.1 INTRODUCTION

Pavement structural evaluation using the Falling Weight Deflectometer (FWD) and backcalculation of its properties has been widely used (12). This is due to its economic and environmental advantages, and its ability to represent the insitu pavement condition under traffic load.

Pavement analytical design methods involve specifying the layers' material property and thickness and calculating the stresses, strains and deformations produced within the pavement structure under design load employing an appropriate theoretical model. Hence the proportions of the pavement and the constituent materials are adjusted until a design results in which the stresses and strains are within their permissible limits (4).

Pavement structural evaluation, on the other hand, requires the measurement of its response in terms of surface deflections under the FWD and optimising the best set of layers properties to fit the deflection basin. These properties describe the existing pavement condition. The predicted properties are used to forecast the pavement's remaining life employing empirical performance models. Therefore the rehabilitation requirements, such as overlay, can be decided. However, overlay design is not the objective of this research and only the pavement's structural evaluation is considered.

Therefore to understand the pavement assessment procedure the following elements need to be detailed:

i) The pavement structure representation by an appropriate model.

ii) The pavement materials behaviour modelling.

iii) FWD testing.

iv) The analysis of deflection basin.

## 2.2 PAVEMENT MODELLING

The earliest model for calculating the stresses in a body subjected to a load on the boundary surface is that developed by Boussinesq (13). Boussinesq solved the equilibrium equations for a semi-infinite half-space, providing solutions that are accurate for a single-layer system. The Boussinesq general equation for deflection due to point load (P), as reported by Zhou et al (14), is:

$$d_{z,r} = \frac{(1+\nu)P\,[2(1-\nu)+\mathrm{Cos}^2\theta]}{2\pi R E} \qquad [2.1]$$

where,

$d_{z,r}$ , deflection at a depth z and radius r (see figure 2.1),

R , distance from point load to the location deformation occurs,

E , modulus of elasticity,

$\nu$ , Poisson's ratio,

$\theta$ , angle between centreline of the load and location of analysis.

Provided that the top layer is stiff, Boussinesq equations for point load will usually give satisfactory results to evaluate the stresses, strains and displacements for a uniformly distributed surface load (15).

To extend the use of these equations to a multilayered pavement structure, the method of equivalent thickness can be applied. This method assumes that any two layers with similar structural stiffness will distribute loading in the same way (14,15). According to this

assumption, all layers in a multilayered system can be transformed to a one layer system with equivalent stiffness. The structural stiffness of a layer is given by:

$$\frac{E\,I}{(1-\nu^2)} \qquad [2.2]$$

where,

I , second moment of area of the layer = $bh^3 / 12$

h, layer thickness

b, unit width.

For a two layer structure, the equivalent thickness of a layer with a modulus $E_2$ and Poisson's ratio $\nu_2$ to a layer of thickness $h_1$, modulus $E_1$ and Poisson's ratio $\nu_1$ may be expressed by equating the structural stiffness of both layers, that is:

$$\frac{E_1 h_1^3}{12(1-\nu_1^2)} = \frac{E_2 h_2^3}{12(1-\nu_2^2)} \qquad [2.3]$$

Rearranging the equation,

$$h_2 = h_1 \left[\frac{E_1(1-\nu_2^2)}{E_2(1-\nu_1^2)}\right]^{\frac{1}{3}} \qquad [2.4]$$

By expanding this concept for a multilayered system, a general form of the equation may be written as:

$$h_{ei} = \sum_{i=1}^{n-1} h_i \left[\frac{E_i(1-\nu_n^2)}{E_n(1-\nu_i^2)}\right]^{\frac{1}{3}} \qquad [2.5]$$

where,

$h_{ei}$ , equivalent thickness for the ith layer

$h_i$ , thickness of the ith layer

$E_i$ , modulus of the ith layer

$E_n$ , modulus of the nth layer

$\nu_i$ , Poisson's ratio for the ith layer

$\nu_n$ , Poisson's ratio for the nth layer.

The thickness of n-1 layers of a multilayered structure above the nth layer is replaced by an equivalent additional thickness ($h_e$) of the semi-infinite half-space, as shown in figure 2.2.

Peattie and Ullidtz (15) suggested that a correction factor should be applied to the equivalent thicknesses, varying between 0.8 and 1. A value of 0.9 is commonly adopted except for a two-layer system where the factor should be 1.

Therefore by transforming the multilayered structure into its equivalent semi-infinite space, Boussinesq's equations can be used to evaluate stresses, strains and deflections. However, Ullidtz (2) stated two limitations for using this method; namely: pavement layer moduli should decrease with depth probably by a factor of at least two between consecutive layers and that the equivalent thickness of a layer should preferably be larger than the radius of the loaded area.

Burmister (16), presented the first solution for a multilayered elastic system by developing a solution for deformation of specific two and three-layer systems. Full contact was assumed at the interface between the layers. Acum and Fox (17) extended this analysis to include deformations and stresses for three-layer systems and subsequently Peattie (18) presented graphically coefficients which enable a range of three-layer structures to be evaluated.

In a layered linear elastic model of a pavement, each layer can be characterised by its modulus of elasticity (E) and Poisson's ratio ($\nu$) as shown in figure 2.3. Knowing these elastic properties and the thickness of each layer together with the continuity condition at the interface, a unique pavement response to circular surface loading can be calculated numerically. A number of documented computer programs are now available to calculate the pavement response such as BISTRO, BISAR, CHEVRON, ELSYM5 and WESLEA (19). Full adhesion is normally assumed at the interface between the layers, although some programs (such as BISAR) are capable of varying the interface condition between the layers.

Several assumptions have to be made for using the multilayered elastic system theory (16). These are:

i) Uniform static load is applied on a circular area of the surface.
ii) The material in each layer is linear elastic, homogeneous, isotropic for which Hooke's law is valid.
iii) The first (n-1) layers overlaying the elastic half-space are weightless and finite in thickness, but are infinite in the horizontal direction.
iv) The nth layer is infinite in the two directions.
v) The solution of the problem must satisfy certain boundary conditions, namely that the top of the surface layer must be free of normal and shearing stresses outside the loaded area and for the elastic half-space, stresses and displacement are assumed to approach zero at a infinite depth.
vi) The solution of the problem must satisfy certain continuity conditions of stress and displacement.

Some of the above assumptions are violated in real pavements, where both traffic and FWD loads are dynamic. Furthermore bituminous mixes are visco-elastic with their mechanical properties dependent on the temperature and the time of loading, while soil and granular materials exhibit non-linear stress dependent behaviour. Therefore in the above theory the modulus of each layer represents an equivalent or effective modulus.

Mamlouk et al (20) found that within the stress range of the FWD tests, the effect of material non-linearity is negligible compared with the effect of spatial variability in material properties.

Due to their simplicity, static multilayered linear elastic analysis methods are the most widely used for pavement design and analysis (21-28). In principle it is possible to use algorithms that account for dynamic effects and non-linear materials behaviour, but they involve significantly greater computation times, which make them unacceptable for practical use (28-30).

Currently, calculation of stresses, strains and displacements, may be applied through the use of the following (29):

i) Traditional layered elastic programs based on numerical integration procedures such as, BISAR, CHEVRON, ELSYM5 and WESLEA.

ii) The method of equivalent thickness instead of numerical integration.

iii) Finite-element programs such as ILLIPAVE or MICHPAVE.

iv) Plate theory such as the Westergaard solution for concrete pavements.

v) Neural networks trained to reproduce the results.

## 2.3 PAVEMENT MATERIALS BEHAVIOUR MODELLING

The relationship between stress due to applied load and the corresponding strain is the most important mechanical property of the material. Therefore to analyse the pavement structure under the FWD it is necessary to determine the stress-strain model for each pavement material.

Typical materials found in flexible pavements are bituminous materials, granular materials and fine-grained subgrade soil. The complex characteristics and variability of the pavement materials and their sensitivity to temperature and moisture, have lead researchers to consider simplifying the models to describe, with reasonable accuracy, the materials behaviour under FWD load.

The deformation of a pavement structure under loading is composed of two parts, the resilient or recoverable component and the permanent or non-recoverable component (19). In the case of transient loads the pavement strains are governed by the resilient characteristics of the materials.

The resilient modulus is defined as the applied deviatoric dynamic stress divided by the recoverable resilient strain, measured between successive stress application in the triaxial test (22,31), namely;

$$M_r = \sigma_d / \varepsilon_r \qquad [2.6]$$

where,

$\sigma_d$ , repeated deviatoric stress $\sigma_1 - \sigma_3$

$\varepsilon_r$ , recoverable axial strain in the direction of principal stress $\sigma_1$

$\sigma_1$ , $\sigma_2$ , $\sigma_3$ , principal stresses.

### 2.3.1 Bituminous Materials

Bituminous mixes are visco-elastic materials, where the stress-strain relationship is a function of temperature and loading time. At low temperature and short loading time, they behave like fully elastic whereas at high temperature and long loading time they become visco-elastic (32).

The modulus of bituminous material is usually represented by the complex modulus, dynamic modulus or resilient modulus (33). Because of the short loading time associated with pavement load, the response of the bituminous layer may be assumed to be linear elastic (19). Mamlouk et al (34), indicated that the resilient modulus may be more appropriate in analysing the FWD deflection basin using a multilayer elastic system than other moduli. And the moduli predicted from NDT of pavements are more representative of the insitu resilient moduli of the materials. Furthermore, other researchers (35,36) have claimed that the Indirect Tensile Test (ITT) is the most suitable testing method for estimation of the bituminous material modulus of elasticity in the laboratory.

The ITT for measuring the stiffness modulus of bituminous materials has been used for many years (36). The principle of the test is that a cylindrical core extracted from the pavement, or moulded in the laboratory, is subjected to a repeated load pulse along the vertical diameter, and the resultant deformation along the horizontal diameter is recorded (see figure 2.4). The stiffness modulus is a function of applied load, horizontal deformation, Poisson's ratio and the specimen thickness.

### 2.3.2 Unbound Materials

Modelling unbound materials is complex since their resilient modulus is a function of many parameters such as, moisture content and stress level (37).

A simplified approach widely used in pavement design, is to relate the unbound material resilient modulus to the insitu California Bearing Ratio (CBR) value using the following empirical equation (38):

$$E\ (MPa) = 10\ CBR \qquad [2.7]$$

The Transport Research Laboratory (TRL) proposed other relationship (4):

$$E\ (MPa) = 17.6\ CBR^{0.64} \qquad [2.8]$$

Furthermore, many insitu test results can be correlated to the CBR value such as, the Standard Penetration Test (SPT) (39) and the Dynamic Cone Penetrometer (DCP) (40).

The main advantage of using the CBR value as an indicator to the modulus of elasticity for unbound material is its simplicity. However the CBR value should only be regarded as a qualitative measure of the unbound material stiffness.

Uzan (12) describe the general model for non-linear behaviour of the unbound material found in repeated load triaxial tests:

$$M_R = K_1\ P_a\ (\theta / P_a)^{K2} (\tau_{oct} / P_a)^{K3} \qquad [2.9]$$

where,

$M_R$ , resilient modulus of unbound material

$\theta$ , bulk stress or first stress invariant ($\sigma_1 + \sigma_2 + \sigma_3$)

$\tau_{oct}$ , Octahedral shear stress or second deviatoric stress invariant
$= (\sqrt{2} / 3)(\sigma_1 - \sigma_2)$ in the triaxial test

$P_a$ , atmospheric pressure used in the equation to make the coefficient independent of the unit used

$K_1$, $K_2$, $K_3$, material parameters.

Two types of unbound materials are found in pavement structures namely granular materials and fine grained subgrade soil. The stiffness of the fine soil is predominantly a function of

the deviatoric stress. This stress decreases with depth resulting in an increase in effective stiffness. Sandy or granular materials are affected by both the confining pressure and the deviatoric stress. The weight of the materials causes the confining pressure, and thus the bulk stress, to increase with depth. This and the decreasing load-related stress result in a rapid increase in effective stiffness (26)

However, in the backcalculation techniques, including the non-linear behaviour of the unbound materials will result in a large number of parameters to be predicted. This is not likely to produce an effective and reliable solution (12,26).

It has been suggested that linear elastic system computation can analyse granular layers with sufficient accuracy when an appropriate modulus value is assigned to them (41). Similar is the difficulty of establishing a feasible model for the subgrade which can accurately deal with all situations that may occur. It seems that a linear elastic layered model is a necessary approximation provided that an appropriate modulus is assigned to the subgrade (20).

Rohde et al (26), suggested accounting for changes in subgrade stiffness with depth, using a layered elastic approach, by including a rigid layer underlying the subgrade. Many backcalculation programs assume an apparent stiff layer at certain depth into the subgrade to simulate its non-linear behaviour.

## 2.4 THE FALLING WEIGHT DEFLECTOMETER (FWD)

The FWD has been established as the most effective testing device for the structural evaluation of a pavement (42). A trailer-mounted NDT device applies an impact load to the pavement surface by mean of a falling weight on 300 mm diameter circular plate. The load magnitude can be adjusted by varying either the mass of the weight or the drop height. The impact load has a total duration typically between 25 to 30 ms and a peak force up to 125 kN. The applied force is measured with a load cell. Peak deflections at the centre of the load plate and at six other locations, away from the plate, are obtained by velocity transducers (geophones) in contact with the pavement surface (see figures 2.5 and 2.6).

The geophones settings are usually selected to be 300 mm apart, therefore the seven deflection values can represent the deflection basin under the FWD load, assuming symmetry around the load.

The FWD has the following advantages over laboratory testing (6,14,43):

i) Low operating cost. A laboratory test programme for measuring layer moduli will be 60-80 times more costly than a corresponding field test program using the FWD (43). This includes factors such as traffic control cost and the monetary value of project delay.
ii) Short test duration and rapid data collection.
iii) Simple testing procedures.
iv) No physical damage to the pavement structure.
v) No disturbance effect to the sample.
vi) It can simulate the effect of moving traffic loads.
vii) Full scale model test where the test measures the insitu pavement behaviour under traffic load.

## 2.5 ANALYSIS OF DEFLECTION BASIN

Typical deflection analysis involves estimating the modulus of each layer to describe the structural condition of the pavement. However, since there is no direct solution that predicts the layer moduli from surface deflections, the procedures generally utilise iterative inverse solution techniques, which have been termed as backcalculation. The backcalculation procedure has the following steps (see figure 2.7):

i) Assume the initial seed layer moduli.
ii) Calculate the pavement surface deflection using any structural analysis model, such as BISAR (44).
iii) Compare the calculated deflections with the measured deflections under the FWD.
iv) Adjust the layer moduli until the two deflection basins match within an acceptable tolerance.

### 2.5.1 Backcalculation Methods

Some backcalculation programs use the properties of the deflection basin to adjust the layer moduli, where these moduli influence different parts of the deflection basin as shown in figure 2.8. These methods form the basis of many backcalculation programs such as, PADAL (42), the New Mexico State Department of Transport (45) and MODCOMP2 (46).

Brown et al (42), studied the moduli influence indices for certain pavement structures. The variations in the deflections relative to the variation in the considered modulus are calculated at each deflection location, and named as the stiffness influence. The influence index (II) of the deflection basin is defined as the ratio of the stiffness influence calculated at a specific radial position to the maximum stiffness influence computed at any radial position. The index number, ranging from 0 to 1, measures the sensitivity of the change of deflection to the change in layer modulus. When the influence index equals one, the radial position which is most sensitive to the change of modulus is located.

By allocating to each layer modulus a deflection location from the influence index, the initial seed assumed modulus can be adjusted using the following equation (42):

$$(E_{new})_j = (E_{old})_j \left( d_c / d_m \right)_i^k \qquad [2.10]$$

where,

$E_{new}$ and $E_{old}$ , new and old computed modulus respectively for layer j,

$d_c$ and $d_m$ , calculated and measured deflections respectively at radial location i,

k , an index number which increases as iteration progresses.

Thus the iteration process continues modifying the moduli of all the layers until a satisfactory match is achieved between the calculated and measured deflection basins.

De Almeida et al (47) at Nottingham University considered that the above method which they used earlier in PADAL backcalculation program (42), has some limitations, i.e.

i) It requires a decision on which geophone location should be assigned to each parameter.

ii) The remaining deflections are ignored in the deflection matching and, consequently, more poorly matched.

Therefore they concluded that all measured deflections should be taken into account in the backcalculation procedure, using the concept of a least squares method.

The method of least squares was first conceived by Hou (48) and has been used in many iterative backcalculation programs. Newton's method for adjusting the pavement parameters, in order to minimise the error between the measured and the calculated deflections, is used.

Starting with an initial estimate of the solution (P), a linear Taylor expansion of the response function $f( P + \Delta P )$ is taken around (P), i.e.

$$f( P + \Delta P ) = f( P ) + \nabla f . \Delta P \qquad [2.11]$$

where $f( P + \Delta P )$, is the measured response corresponding to the value of the function at the solution $( P + \Delta P )$, and $f( P )$ is the value of the function at the solution (P).

Equation [2.11] is written in matrix form as follow

$$f_i ( P + \Delta P ) - f_i ( P ) = \frac{\partial f_i}{\partial P_j} \Delta P_j \qquad [2.12]$$

where,

i = 1,2, ..., m (number of equations)

j = 1,2, ..., n (number of independent parameters).

Equation [2.12] can be non-dimensionalized by dividing both sides by $f_i ( P )$,

$$r = F . \alpha$$

or $$F^T . r = F^T . F . \alpha \qquad [2.13]$$

The vector $r = [ r_i ]^T$, and $$r_i = \frac{f_i ( P + \Delta P ) - f_i ( P )}{f_i ( P )}$$

where, $f_i ( P + \Delta P )$, represent the measured surface deflection at sensor location i of the FWD and $f_i ( P )$ represent the most recently calculated surface deflection at the location i. Therefore the vector r is completely determined.

The matrix $F = [ F_{ij} ]$, and $$F_{ij} = \frac{\partial f_i}{\partial P_j} \frac{P_j}{f_i ( P )}$$

The matrix F is usually called the sensitivity matrix, because its elements ($F_{ij}$) reflect the sensitivity of the deflections to pavement parameters. Since the analytical solution is not available the derivatives ( $\partial f_i / \partial P_j$ ), where $f_i$ (i = 1,2,..m) represent the pavement deflections and $P_j$ (j = 1,2,...n) represent the pavement parameters, are computed numerically using the forward derived differences. The initial parameters are increased by 5% and the resulting deflections are calculated using the BISAR program. For these small variations the derivatives ( $\partial f_i / \partial P_j$ ) can be assumed equal to ( $\Delta f_i / \Delta P_j$ ). Thus the sensitivity matrix (F) can be generated by n + 1 runs of BISAR program.

The vector $\alpha = [\alpha_j]^T$, and $$\alpha_i = \frac{\Delta P_j}{P_j} .$$

The unknown vector $\alpha$ reflects the relative changes of the parameters. The set of equations can be solved using any equation solver, such as a Gauss elimination method. As soon as $\alpha$ is obtained, a new set of parameters is determined as, $P_{new} = P_{old} ( 1 + \alpha )$.

The iteration process is continued until the observed convergence is reached, i.e. the changes in the pavement parameters are sufficiently small and the computed and measured deflections match closely.

Wang and Lytton (49), at Texas Transportation Institute developed the System Identification method (SID) for backcalculating the pavement layer properties. The parameter adjustment algorithm used in their program (SID) was identical to equation [2.13] in the method of least squares.

Other computer programs have been developed by the US Army Corps of Engineers at the Waterways Experimental Station (50). They are named BISDEF, CHEVDEF, ELSDEF and WESDEF, using different forward calculation programs, i.e. BISAR, CHEVRON, ELSYM5 or WESLEA. These programs employ a gradient search technique for iteration toward the correct set of layer moduli, where a successive linear least squares approach is used. All the above programs use the multilayered elastic system for the forward calculation method.

The method of equivalent thickness can be used as a forward model to convert the multilayer system to a single layer. Therefore backcalculation will be faster and simpler. Both ELMOD (2) and BOUSDEF (14) programs use this method, however as stated earlier in this chapter this method has some limitations.

A completely different approach is used by MODULUS program (51) which has been developed at Texas A&M University. A database is computed for deflection basins using the BISAR program with layer moduli that cover the range of moduli anticipated in the field. The database is stored before the actual backcalculation process starts. The measured deflection basin is compared with the database and a pattern search algorithm is used to predict the layer moduli that minimises the error between the measured and calculated basins. When a large number of deflection measurements are made on pavements with the same configuration, the MODULUS program will be distinctly faster than the iterative methods. This is because of the reduction in computing time, since the database will be the same for all cases. The MODULUS program excludes the user dependency in selecting the initial seed moduli.

A table listing of the most common backcalculation procedures was presented by the Strategic Highway Research Program (SHRP), and shown in table 2.1. These programs were used by SHRP for backcalculation software selection and do not represent a comprehensive list of all available programs.

### 2.5.2 Problems Encountered in Backcalculation

Non-unique solution is one of the main problems of backcalculation techniques. It is possible for two or more combinations of pavement parameters to result in the same deflections (52, 53, 54). Engineering judgement is the prime measure used to decide if the process has converged to the correct parameters or not. However, reducing the number of backcalculated parameters by combining pavement layers with the same properties will decrease this problem (27,61).

May and Van Quintus (27), in describing the proposed ASTM standard for backcalculation suggested assigning the thin wearing course modulus a known value in the backcalculation process. This is because the thin layer modulus has little influence on deflection and its contribution to the structural pavement strength is small, therefore its prediction will be difficult and may cause a non-unique solution.

An other problem encountered in backcalculation is the irregularity in pavement deflection measurement, due to the difference between measured pavement response and the theoretical models used to predict that response (29). These irregularities may result from a number of reasons, including pavement distress, variation in layer thickness, non-linear material response, presence of bedrock or other stiff layers and moisture and temperature effects.

Uzan et al (55), summarised the possible sources of error in backcalculated moduli as follows:

i) Measuring devices, which include deflection sensors and load cell.
ii) Pressure distribution on the loaded area.
iii) Pavement structure geometry and condition.
iv) Material modelling.
v) Analysis technique.

#### 2.5.2.1 Errors due to measuring devices and pressure distribution

These errors can be minimised by repeating the FWD test several times at the same location.

### 2.5.2.2 Errors due to pavement geometry and condition

The errors associated with the geometry and the condition of the pavement structure are:

i) The layer thickness variation with location.

ii) The existence of voids and cracks.

iii) The existence of water table or bedrock.

vi) The adhesion properties between the layers.

Theoretically, surface deflection at specified location ( i ), under the FWD load is a function of pavement parameters, i.e.

$$d_i = f(E_j, \upsilon_j, h_j, K_{sj}) \qquad [2.14]$$

where,

$E_j$ , $\upsilon_j$ , $h_j$ , modulus, Poisson ratio and thickness of layer j

$K_{sj}$ , interface shear reaction modulus between layers j and j +1

Most backcalculation techniques seek to define layer moduli $E_j$ on the basis that all other pavement parameters are assumed or known. The surface deflections under the falling weight reflect the real insitu pavement conditions in terms of layer moduli, thicknesses, Poisson ratios and the interface condition between the individual layers. Therefore any errors in assuming one parameter will affect the backcalculated moduli, and this error depends on the sensitivity of surface deflections to this parameter.

Layer thicknesses can be measured from cores extracted from the pavement or from ground penetrating-radar test (56). However some computer programs can backcalculate the thicknesses in addition to the moduli (49,57). Poisson ratios appear to have insignificant effect in predicting the pavement moduli (24,58,59).

Full adhesion is commonly assumed to exist between the layers in flexible pavement evaluation. However, variations in the bonding condition may cause some errors in

predicting the layer moduli (60). Lee (30) stated that the actual interface behaviour is not fully understood and therefore it was not considered in the backcalculation procedures.

However, the interface condition can be assigned as full smooth in some backcalculation programs, if the forward calculation model can handle this condition.

### 2.5.2.3 Errors due to material modelling

The lack of an accurate material description may introduce an error in the pavement evaluation. Assuming the materials as elastic, isotropic and homogeneous does not represent their real behaviour. Using the multilayer pavement model, the subgrade thickness is assumed to be infinitely thick and has a uniform linear stiffness. The actual condition varies considerably from this model where the thickness of subgrade is not infinity and often a rigid layer or bedrock occurs at certain depth. Furthermore, subgrade stiffness changes with depth due to the stress dependent characteristics of most soils.

Rohde et al (26) suggested, in analysing the deflection basin, placing an apparent rigid stiff layer of high modulus below the multilayer elastic system to account for an actual bedrock, a non-linear elastic subgrade or both.

Many backcalculation procedures include this layer at some depth, normally six metres, into the subgrade (27).

Rada et al (61), proposed using the radial modulus to indicate the degree of non-linearity of subgrade. Calculating the radial modulus of the pavement at each radial distance can be carried out using the measured deflection data as input into Boussinsq's one-layer half-space deflection equation:

$$E_r = \frac{p \cdot a^2 ( 1 - \nu^2 ) \cdot C}{d \cdot r} \qquad [2.15]$$

where,

$E_r$ , Radial composite modulus,

p , applied pressure by the FWD,

a , load plate radius,

$\nu$ , Poisson ratio of the subgrade,

d , measured deflection at a given radial distance (r) from the load centre,

C , deflection constant = $1.1 \text{ Log}_{10} ( r/a ) + 1.15$.

Plotting the radial modulus against radial distance as shown in figure 2.9, will give a clear indication of the degree of subgrade stress dependent properties.

In FWD testing it is known that the outermost deflections are completely controlled by the subgrade (2,42) and therefore the computed radial moduli corresponding to these sensor deflections reflect the subgrade contribution. According to Ullidtz (2), if the radial moduli ($E_{r6}$ and $E_{r7}$) calculated at the sixth and seventh radial locations are identical, the subgrade response is linear, and if $E_{r6}$ and $E_{r7}$ are not identical, the response is non-linear. The nonlinearity might occur because of subgrade behaviour, the presence of a rigid layer at a shallow depth, or both.

Some backcalculation programs such as MODULUS and ELMOD can detect the presence of a rigid layer using regression equations (26). Hossain et al (62), presented a method for detecting the rigid layer depth from deflections under the FWD. They backcalculated the subgrade thickness as any other modulus.

### 2.5.2.4 Errors due to the analysis technique

Most of the current backcalculation procedures use static analysis to model the pavement response under the dynamic FWD test. Only the peak deflections and the peak load are considered in the analysis. A comparison between static and dynamic analysis for surface deflections was carried out by Mamlouk and Davis (63). They found small differences for stiff pavements but the differences were large for weak and thinly surfaced pavements.

Zaghloul et al (64), used dynamic analysis of the FWD test results employing the finite element model. Dynamic analysis suffers from many disadvantages such as the computational capacity and time required to run the program and the additional parameters needed to characterise the materials. In a dynamic analysis, the viscous and visco-elastic properties of the materials should be considered, Poisson's ratio becomes more critical when using wave propagation and the density of the different materials must also be known (29).

## 2.6 SUMMARY

The Falling Weight Deflectometer has been in use for many years for pavement evaluation due to its ability to simulate the insitu conditions of the pavement under traffic load.

Static analysis for a layered linear elastic system is the most widely used method for pavement design and assessment, and it can be considered appropriate for many practical applications.

The analysis of pavement deflections to predict the effective layer moduli can be performed using the backcalculation technique. Some backcalculation programs aim to determine a set of layer moduli, in an iterative manner, that minimise the error between the calculated and measured deflections employing a suitable convergence criterion. Other programs build a database for different pavement structures, from which the layer moduli can be determined using an appropriate search technique.

In predicting the layer moduli, some errors might arise due to the following:

i) Material modelling as linear elastic homogeneous.
ii) Static analysis of the dynamic FWD test results.
iii) Variation in layer thicknesses and the presence of stiff layer.
iv) Variation in the interface condition between layers.
v) Non-unique backcalculation solution.

However to obtain a reliable solution, engineering judgement has to be employed and some simplifications have to be made in order to minimise the number of predicted parameters.

Table 2.1, List of the common pavement layer moduli backcalculation programs (29).

| Program name | Developed by | Forward calculation method | Forward calculation subroutine | Back-calculation method | Rigid layer analysis | Seed moduli |
|---|---|---|---|---|---|---|
| BISDEF | USACE WES | Multilayer elastic theory | BISAR (proprietary) | Iterative | Yes | Required |
| BOUSDEF | Zhou et al | Equivalent thickness | Equivalent thickness | Iterative | Yes | Required |
| CHEVDEF | USACE WES | Multilayer elastic theory | CHEVRON | Iterative | Yes | Required |
| ELMOD | Ullidtz | Equivalent thickness | Equivalent thickness | Iterative | Yes (variable) | None |
| ELSDEF | USACE WES | Multilayer elastic theory | ELSYM5 | Iterative | Yes | Required |
| EMOD | PCS/LAW | Multilayer elastic theory | CHEVRON | Iterative | No | Required |
| EVERCALC | Mahoney et al | Multilayer elastic theory | CHEVRON | Iterative | Yes | Required |
| FPEDD1 | W. Uddin | Multilayer elastic theory | BASINPT | Iterative | Yes (variable) | Program generated |
| ISSEM4 | R. Stubstad | Multilayer elastic theory | ELSYM5 | Iterative | No | Required |
| MODCOMP | L. Irwin | Multilayer elastic theory | CHEVRON | Iterative | Yes | Required |
| MODULUS | Texas Trans. Inst. | Multilayer elastic theory | WESLEA | Database | Yes (variable) | Program generated |
| PADAL | S.F. Brown et al | Multilayer elastic theory | UNKNOWN | Iterative | Unknown | Required |
| WESDEF | USACE WES | Multilayer elastic theory | WESLEA | Iterative | Yes | Required |
| MICHBACK | Michigan State | Multilayer elastic theory | CHEVRON | Iterative | Yes | Required |

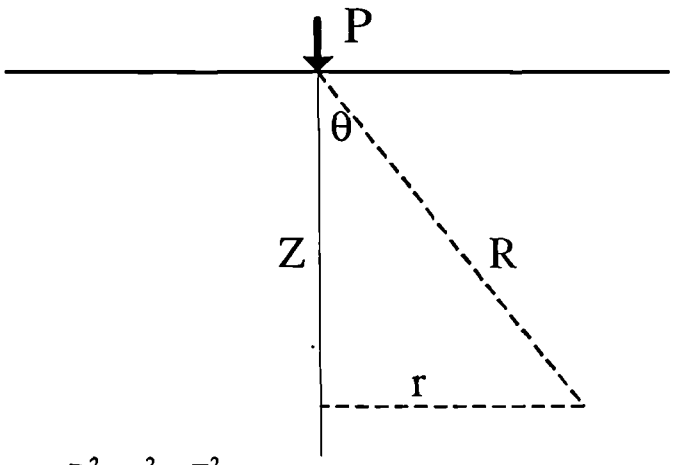


Figure 2.1, Boussinesq 's half-space loading system (14).

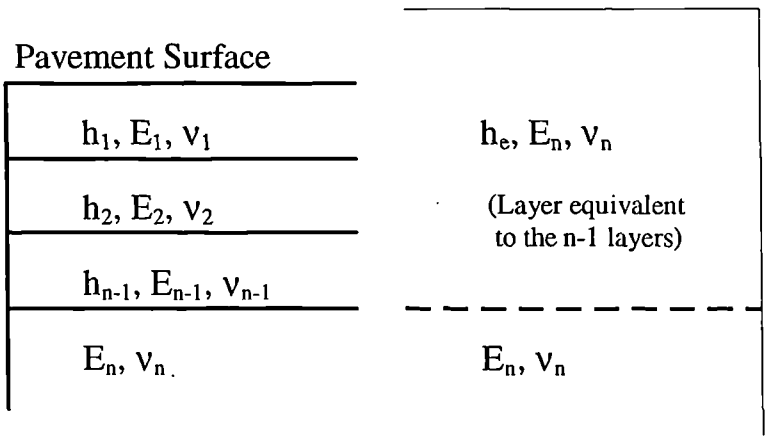


Figure 2.2, Conceptual representation of method of equivalent thicknesses (14).

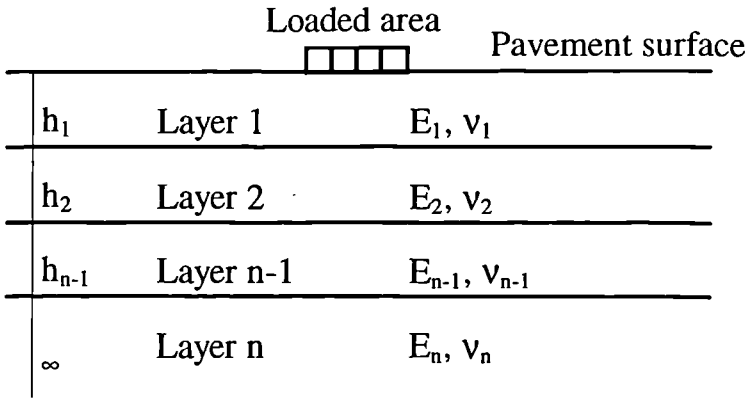


Figure 2.3, Multilayer linear elastic model of pavement.

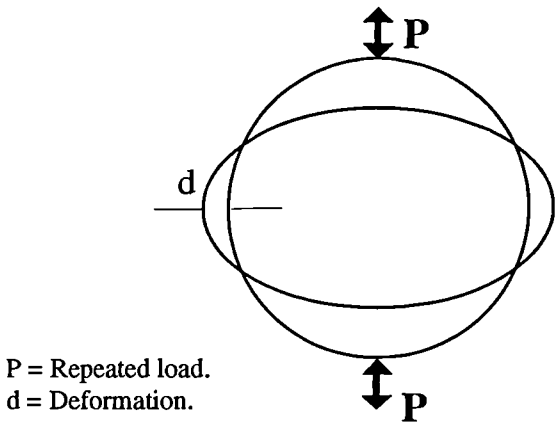


Figure 2.4, Repeated load indirect tensile test for stiffness prediction (35).

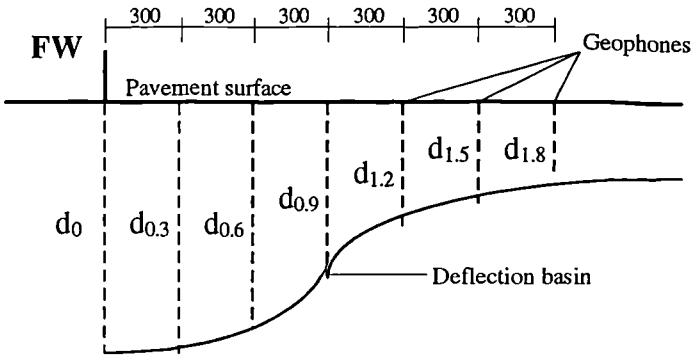


Figure 2.5, Configuration of the FWD.


Figure 2.6, The Falling Weight Deflectometer.

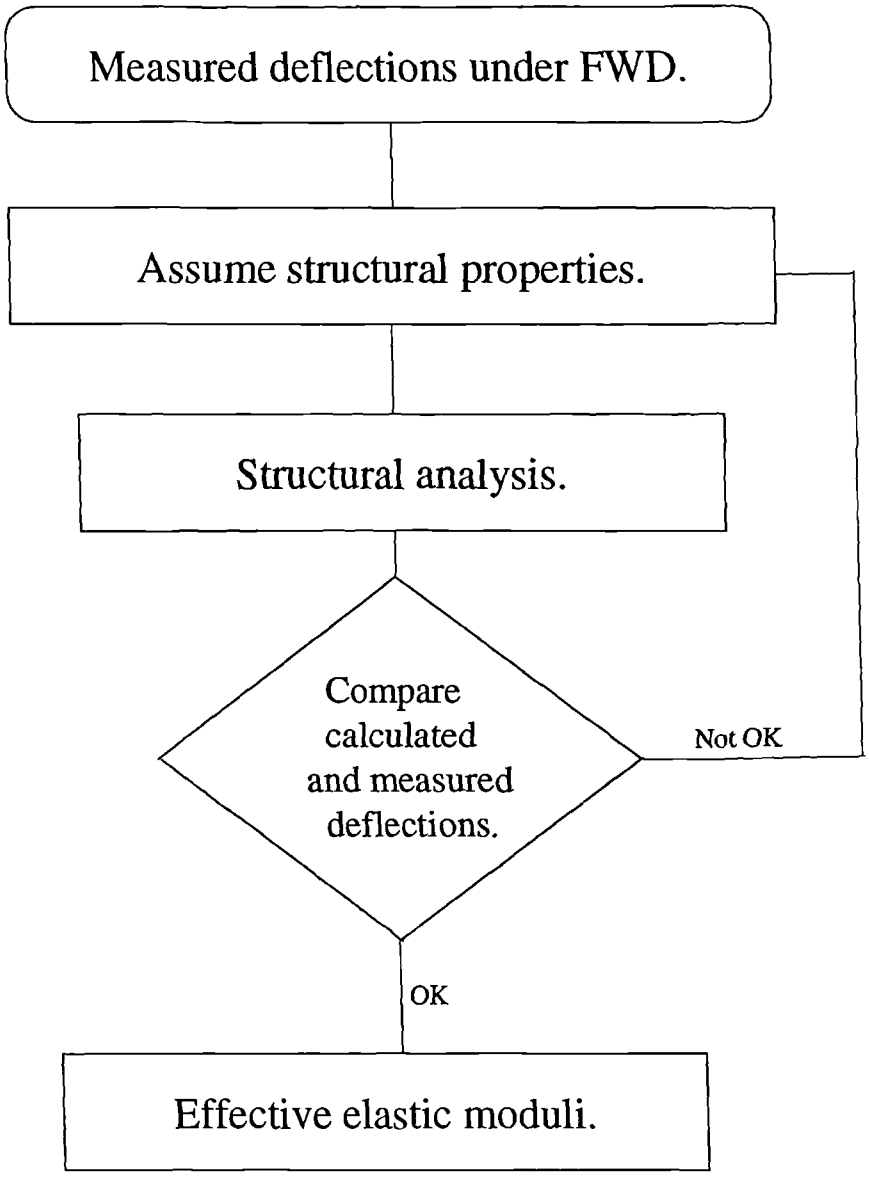


Figure 2.7, Flow diagram for a typical backcalculation procedure (37).

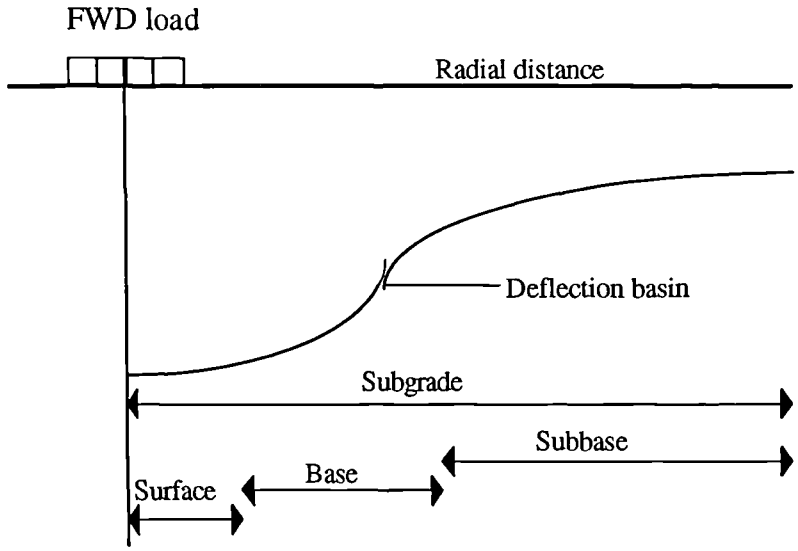


Figure 2.8, General influence of layer on deflection basin (42).

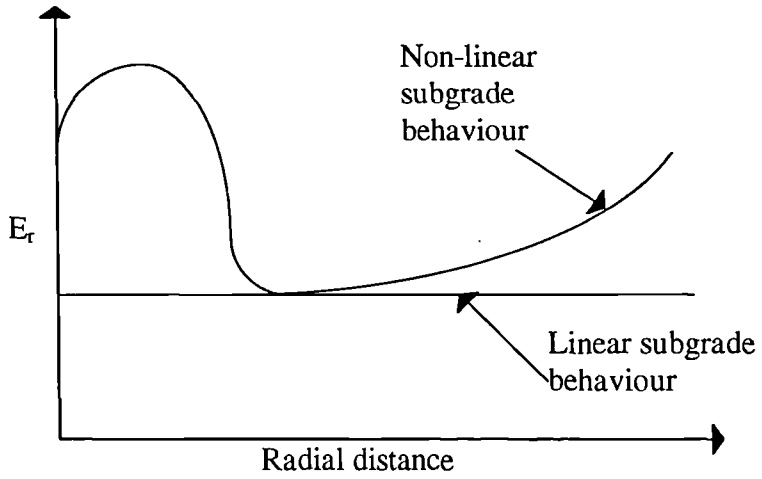


Figure 2.9, Radial modulus ($E_r$) Vs radial distance (61).

# Chapter 3

# BONDING CONDITION BETWEEN PAVEMENT LAYERS

## 3.1 INTRODUCTION

Slippage failure between bituminous layers is hardly a new phenomenon in flexible pavements (65). If the bonding between the wearing course and base course is poor, slippage arises. This is a failure condition which is local and does not imply complete structural failure of the road, though it obviously becomes unserviceable (66).

The state of adhesion at the interface between various layers affects the pavement performance through its influence on the stressing level of the materials (67). This fact is of significant importance, since the upper layers are sometimes constructed in stages, causing poor adhesion between the existing surface and the new layer.

In the UK a large number of debonding failures between wearing and base courses have been reported in road pavements (9,10,66,68). As a result the Transport Research Laboratory (TRL) investigated the factors which might contribute to slippage failure by testing existing pavements (9). Pavement structural condition was assessed with the Deflectograph. The Ring and Ball softening point of the binder recovered from the wearing courses were also measured. Figure 3.1 shows the relationship between deflection, hardness of the wearing course binder and the slippage. The results illustrate that slippage can occur on a stiff pavement if their binder has been hardened unduly and also on a weak pavement whose wearing courses have been hardened to a normal extent.

TRL also carried out full-scale experiments on pavements under controlled conditions (9). The results show that the slip plane is most likely to develop with wearing course rolled at

elevated temperatures on chilled base courses founded on pavements of inadequate stiffness. Therefore the following recommendations have been suggested to reduce the risk of slippage:

i) Improving the quality of unbound materials used in roadbases and subbases by paying attention to compaction.
ii) Avoiding high rolling temperatures when laying the wearing course.

Pell (69) stated that neither the above TRL laboratory experiments nor site studies throw much light on the development of slippage at the slip plane.

During late 1980, the Department of the Environment for Northern Ireland observed a number of premature debonding failures on several pavement sections of recent overlaid roads (65). Whereas in France, a 1986 survey showed that the slippage problem affected 5% of the French highway network at that time (11).

The studies of Van Cauwelaert et al (50) indicated that partial friction is the best representation of the insitu interface condition between pavement layers but no experimental data to quantify this parameter has been reported.

The report of the discussion group on practical limitations of pavement non-destructive testing using the FWD and backcalculation techniques (70), stated that "the methodology is not sensitive to the degree of bonding between pavement layers".

Brown and Brunton (66), stated that relatively little is known about the actual shear strengths at the interface, and that more research is needed.

Therefore the common assumption of full adhesion between pavement layers in the design and evaluation of flexible pavement does not represent the real conditions.

## 3.2 CAUSES OF PAVEMENT LAYERS DEBONDING

Good bonding between bituminous pavement layers is clearly desirable since it improves the strength of the overall structure. However slippage occurs when the shear stress at the interface is greater than the adhesion or bonding between the layers (68).

Shuab (71) summarised the connection between the types of failures in flexible pavements and the reasons for the damage. Table 3.1 shows an extract from his table which includes the effect of poor bonding between pavement layers and slippage failure.

Pavement corrugation is a deformation parallel to the direction of vehicles progress, where the waves are short in length but relatively large in amplitude. This deformation type can be caused by instability of the asphalt pavement, lack of base layer or poor bonding between layers (71). Moreover slipping, peeling and plucking of the wearing course can develop due to insufficient adhesion between the wearing course and the layer under it (71).

Previous works (11,65,67,68,71) suggested that a slip plane may develop between pavement layers due to many reasons such as:

i) Lack of binder coat or defficient binder coat.
ii) Pollution of the base before spreading of the binder.
iii) Surfacing or overlaying in cold weather.
iv) Construction in stages.
v) Insufficient compaction of the base.
vi) Absorption of the binder coat by the base materials.
vii) Under designing of the wearing course resulting in excessively large shear stresses at the interface.

As a result the interface will fail to ensure the continuity of displacements between the layers, hence the slippage will start to progress under the effect of traffic and environmental conditions.

## 3.3 MATHEMATICAL MODEL

A numerical solution of a multilayered system requires the knowledge of the boundary conditions between layers in order to predict the structural responses to surface loading. These conditions can be either full bonding, with the same shear stresses on both sides of the interface, or complete debonding where no shear stress will transfer between layers. A more general fundamental model to describe the interface condition is needed.

Considering the interface as a thin layer of thickness (t), the shear stress ($\tau$) at the interface produces shear strains ($\gamma$) according to the following equation;

$$\tau = G \gamma \qquad [3.1]$$

where, G is the shear modulus of the interface material.

For small horizontal displacements of the thin interface layer, the shear strain may be defined as;

$$\gamma = \Delta u / t \qquad [3.2]$$

where, $\Delta u$ is the relative horizontal displacement of the two faces at the interface.

Therefore;

$$\tau = G (\Delta u / t) \qquad [3.3]$$

$$\tau = K_s (\Delta u) \qquad [3.4]$$

where, ($K_s = G / t$ ) is the horizontal shear reaction modulus at the interface.

This equation represents Goodman's constitutive law to describe the interface behaviour (72).

This model has been used in many pavement analysis programs, such as BISAR, to predict the stresses and strains in multilayered system due to surface load.

## 3.4 THEORETICAL EFFECT OF THE SHEAR REACTION MODULUS ON PAVEMENT PERFORMANCE

Many researchers have demonstrated theoretically the effect of the bonding condition between layers on overall pavement performance (67,73,74,75).

Romain (73), carried out a systematic theoretical investigation into the influence of the interface condition in several four-layer pavements. He presented the variation of stresses, strains and deflections due to bonding conditions. Table 3.2 illustrates the summary of some of his finding as cited by Uzan et al (67).

The actual magnitude of stresses, strains and deflections for three cases of different interface conditions relative to the stresses, strains and deflections computed for the case of full adhesion at all the interfaces were presented in table 3.2. It can be seen that in most cases, stresses, strains and deflections increase when any one of the interfaces changes from prefect adhesion to full debonding. Table 3.2 also shows an increase in tensile strain at the bottom of the layer which is located adjacent to the interface whose properties have been changed.

Uzan et al (67), demonstrated the distribution of the radial strains within the pavement layers by changing the interface condition between the first two layers, using the BISAR program. They stated that by changing that interface from full rough to complete smooth, the tensile radial strain at the bottom of the first layer becomes higher and the tensile radial strain at the top of the second layer reverses to compression (see figure 3.2). Similar results were presented by Shahin et al (75) in figure 3.3.

Brown and Brunton (66) investigated the effect of poor bonding between layers on the lives of pavements (see table 3.3). As a reference case, the structures were initially analysed with rough interfaces, which implies complete bonding. Subsequently the structures were re-analysed with the top interface, then the lower interface, being taken as partly rough and smooth, but with all other interfaces rough. Table 3.3 shows the poorly bonded pavements' lives as percentage of the good bond case. However for good bonding at both the interfaces all the results would be 100 per cent. Brown and Brunton concluded that a very poor bond

would lead to premature local failure and a mediocre bond at either interface could reduce pavement lives by up to 30 per cent.

The above authors expressed the importance of including the actual interface condition between layers in the design and assessment of pavements.

## 3.5 THEORETICAL EFFECT OF THE SHEAR REACTION MODULUS ON PAVEMENT FAILURE MECHANISM

A pavement does not fail suddenly, its deterioration is considered as a fatigue phenomenon in that it is the result of the stresses and strains in the pavement caused by the magnitude and number of load applications.

The two main failure mechanisms in flexible pavement are rutting and fatigue cracking. Rutting arises from the accumulation of permanent strain throughout the pavement structure. If the vertical strain at the top of subgrade is kept below a certain level, excessive rutting will not occur unless, of course, poor bituminous mix design and inadequate compaction are involved. Cracking of the bituminous materials on the other hand is considered to arise from repeated tensile strain, the maximum of which occurs at the bottom of the bituminous layer. The crack, once initiated, propagates upwards and causes a gradual weakening of the pavement (76).

The distress mode due to fatigue cracking may be influenced by the presence of layer debonding in two possible scenarios:

i) The crack will initiate at the bottom of the bituminous layer and propagate towards the surface. If the crack reaches a debonded or partially bonded interface it may propagate in the horizontal direction causing more slippage between the layers, rather than vertically as shown in figure 3.4.

ii) If complete slippage occurs between pavement layers, additional tensile strain will result at the bottom of the bituminous layer above the interface as the two layers will act independently (see figures 3.2 and 3.3). Therefore two cracks may initiate at

both bituminous layers as shown in figure 3.5. This will lead to a faster deterioration in the bituminous layers and quicker pavement failure.

The effect of interface debonding on theoretical and practical failure mechanisms in a flexible pavement is not the objective of this research. However it is stated here to show the importance of predicting the condition of bonding at the interface in order to analyse the causes of pavement failure.

## 3.6 EXISTING METHODS FOR PREDICTING THE INTERFACE CONDITION

Vergne et al (74) used the shear box test for measuring the interface shear reaction modulus ($K_s$) between any two concrete materials prepared in the laboratory, employing Goodman's law, i.e.

$$\tau = K_s (\Delta u) \quad .$$

The slope of the shear stress-relative displacement curve can describe the shear reaction modulus at the interface as shown in figure 3.6.

Uzan et al (67) carried out an extensive testing programme to investigate the interface properties between laboratory prepared bituminous materials using the shear box test. They studied the effect of tack coat rate, testing temperature and normal pressure during testing. An example of their results is shown in figure 3.7.

The reported tests were conducted at only one rate of shear (2.5 mm/min). Uzan et al stated that this rate is appropriate for bearing capacity computations, but not for stress analysis in flexible pavements where the loading rate is dictated by the vehicle velocity. Hence, the measured interface shear reaction modulus should be corrected.

They reported a value for $K_s$ between bituminous layers at 25 °C of $10^4$ MN/m$^3$. However the practical prediction of the interface condition from existing pavement using the shear box test has some limitations such as;

i) The difficulty in cutting intact square samples from an existing pavement for laboratory shearing.

ii) It is destructive testing.

iii) Many testing parameters will affect the measured $K_s$ , such as sample size, rate of shearing and the magnitude of the applied normal load during shearing. Therefore it is difficult to select the appropriate testing configuration to represent the real insitu pavement conditions.

iv) The non-linear properties of the interface condition between bituminous layers, where the relationship between the shear stress and relative displacement is not linear (see figure 3.7).

Woodside et al (77,78), used the shear box test on circular cores to investigate the properties of Stress Absorbing Membrane Interlayer (SAMI). Similar tests can be carried out at the layer interface on cores extracted from an existing pavement. However, coring may damage the interface properties through the torque applied by the cutter.

Researchers at the "Laboratoire Central des Ponts et Chausees" in France have developed a wave propagation technique (COLEBRI) to diagnose the state of adhesion between the pavement layers (11). The COLEBRI is designed to measure the impedance of pavement materials in the frequency range 300 to 3000 Hz. The ongoing French development, which is at the early prototype stage, is considered to offer a promising approach to the detection of pavement layer debonding in bituminous pavements. Test results suggest that pavement impedance measured at the wave propagation frequency of 1500 Hz, is most sensitive to the presence of layer debonding. Future work is aimed at developing a robust version of the COLEBRI and at obtaining a better understanding of the factors that affect the reliable detection of layer debonding. However the test results are indicative only and can not be incorporated in the structural analysis model for pavement evaluation.

Tschegg et al (79) have recently developed a wedge splitting test for evaluating the bonding condition on cores extracted from the pavement. They used the energy required to fracture the core at the interface by splitting to describe the interface behaviour (see figure 3.8). The load-displacement curve is obtained by plotting the force ($F_H$) versus the displacement ($\delta$) as illustrated in figure 3.9. The energy required to fracture the specimen (G) is derived from

the area below this curve. The specific fracture energy ($G_F$) is obtained by dividing the fracture energy through the fractured area;

$$G_F = G / A \qquad [3.5]$$

While this method describes fundamentally the interface condition the results can not be incorporated into the structural analysis model for multilayered elastic system, such as the BISAR program, to calculate the pavement strains and its remaining life. Furthermore, some other limitations can be highlighted such as the sample stressing conditions not being the same as in the pavement and the likelihood of interface damage during coring.

## 3.7 SUMMARY

Considering the literature stated above and the practical evidence of debonding failure in flexible pavements, it is certain that the common assumption of full adhesion between the pavement layers does not represent the real insitu condition of the pavement. Therefore a method for predicting the insitu interface condition in addition to the pavement structural properties is required for a more reliable pavement model. These parameters need to be included in the structural analysis model to predict the pavement performance and its remaining life.

Goodman's constitutive law has been suggested to describe the interface condition.

Several testing methods are under development for predicting the interface condition, however their results can not be incorporated into the pavement analysis model, based on non-destructive testing techniques.

Table 3.1, Relationship between the causes and types of failure in flexible pavements (71).

| Failure Type / Cause of distress | Rutting | Corrugation | Hair cracking | Net Cracking | Transversal cracking | Irregular cracking | Layer joint defect | Slipping | Scaling | Peeling |
|---|---|---|---|---|---|---|---|---|---|---|
| Heavy traffic load | C | C | P | P | L | P | - | L | - | P |
| Increased horizontal load | - | C | - | - | - | - | - | C | - | - |
| Slow traffic | C | C | - | - | - | - | - | - | - | - |
| Canalised traffic | C | P | - | - | - | - | - | P | - | - |
| Extraordinary weather | L | P | - | - | L | - | - | - | P | - |
| Unfavourable local condition | P | C | - | P | - | P | - | L | P | P |
| Drainage deficiency | - | - | - | L | - | - | - | - | - | - |
| Frost and thaw damage | - | - | - | L | - | - | - | - | - | - |
| Large normal use | P | - | P | - | - | - | - | - | - | - |
| Insufficient bearing capacity | L | - | P | C | L | - | - | - | - | P |
| Subsequent compaction of base | L | - | - | - | - | - | - | - | - | - |
| Failure of back fill | - | - | - | - | - | - | - | - | - | - |
| Poorly constructed widening | - | - | - | - | - | | - | - | - | - |
| Inappropriate bitumen hardness | L | L | L | - | P | P | P | L | P | P |
| Inappropriate bitumen quantity | L | L | L | - | L | P | P | L | L | L |
| Burnt bitumen | - | - | L | - | - | P | - | - | L | P |
| Improper composition | C | C | L | - | P | - | P | P | P | P |
| Inappropriate aggregate | - | - | P | - | P | P | - | - | P | P |
| High void content | P | P | - | - | - | P | - | - | P | P |
| Low void content | - | - | - | - | - | - | - | - | L | P |
| Poor binding of layer | - | C | - | - | P | P | L | C | - | C |
| Insufficient spraying | - | P | - | - | - | - | P | P | - | L |
| Improper construction | P | P | P | - | P | P | L | P | L | L |
| Poor maintenance works | - | - | P | P | - | - | P | - | - | L |

( P = Possible, L = Likely, C = Certain )

Table 3.2, Relative results of four layer pavement with different interface conditions (73).

| Interface condition | First interface = Second interface = Third interface = | Smooth Rough Rough | Rough Smooth Rough | Smooth Smooth Rough |
|---|---|---|---|---|
| First layer | Max. compressive stress | 0.79 | 1.07 | 0.89 |
| | Max. tensile stress | 2.19 | 1.92 | 2.69 |
| | Max. compressive strain | 2.83 | 1.07 | 3.07 |
| | Max. Tensile strain | 1.93 | 1.10 | 2.07 |
| | Deflection | 1.20 | 1.19 | 1.43 |
| Second layer | Max. compressive stress | 1.74 | 0.98 | 1.81 |
| | Max. tensile stress | 1.08 | 2.26 | 2.73 |
| | Max. compressive strain | 1.27 | 1.72 | 2.25 |
| | Max. tensile strain | 1.30 | 1.44 | 1.89 |
| Third layer | Max. compressive stress | 1.55 | 1.48 | 2.29 |
| | Max. tensile stress | 1.38 | 1.23 | 1.77 |
| | Max. compressive strain | 1.28 | 0.92 | 1.18 |
| | Max. tensile strain | 1.22 | 0.92 | 1.29 |
| Fourth layer | Max. compressive stress | 1.40 | 1.74 | 2.40 |
| | Max. compressive strain | 1.37 | 1.37 | 1.97 |
| | Deflection | 1.19 | 1.39 | 1.58 |

Table 3.3, The lives of pavements with poorly bonded layer expressed as percentages of the good bonding case (66).

| Structural details | 1st interface: Partly rough | 1st interface: Smooth | 2nd interface: Partly rough | 2nd interface: Smooth |
|---|---|---|---|---|
| 40mm HRA<br>60mm DBM<br>60mm DBM<br>330mm S-base | 79% | 48% | 100% | 37% |
| 40mm HRA<br>60mm DBM<br>230mm DBM<br>450mm S-base | 86% | 61% | 69% | 32% |
| 40mm HRA<br>60mm DBM<br>190mm W-mix<br>330mm S-base | 81% | 65% | - | - |
| 40mm HRA<br>60mm HRA<br>50mm HRA<br>330mm S-base | 87% | 43% | 82% | 25% |
| 40mm HRA<br>60mm HRA<br>125mm HRA<br>450mm S-base | 93% | 61% | 82% | 23% |
| Average | 85% | 56% | 83% | 29% |

HRA, Hot Rolled Asphalt,
DBM, Dense Bitumen Macadam,
S-base, Subbase,
W-mix, Wet mix.

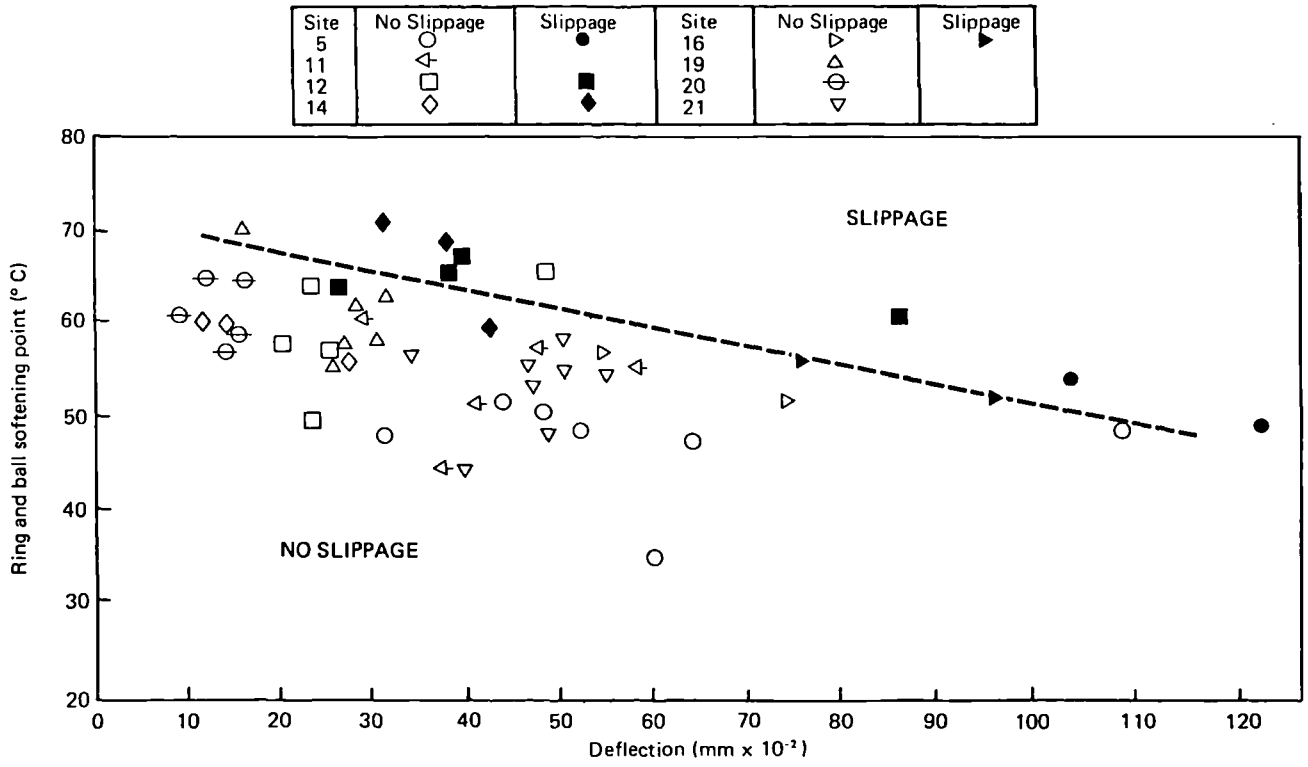


Figure 3.1, Relation between deflection, hardness of the binder in the wearing course and the incidence of slippage (9).

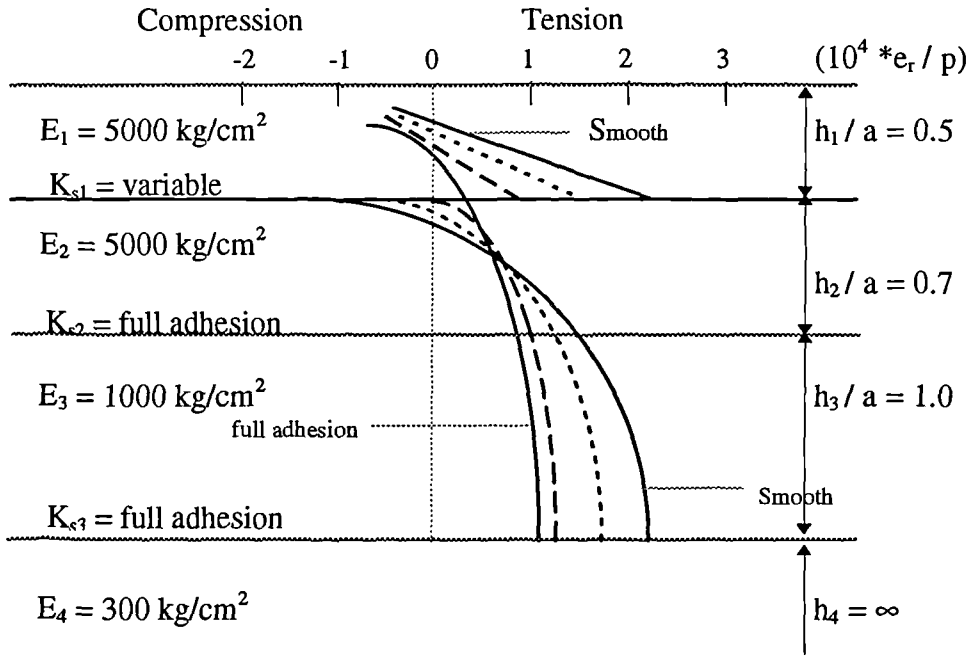


p, surface pressure (kg/cm$^2$) (1kg/cm$^2$ = 9.81*10$^{-4}$ N/m$^2$)
a, radius of the loaded area.

Figure 3.2, Distribution of radial strain ($e_r$) with depth using different interface condition between the top two layers (67).

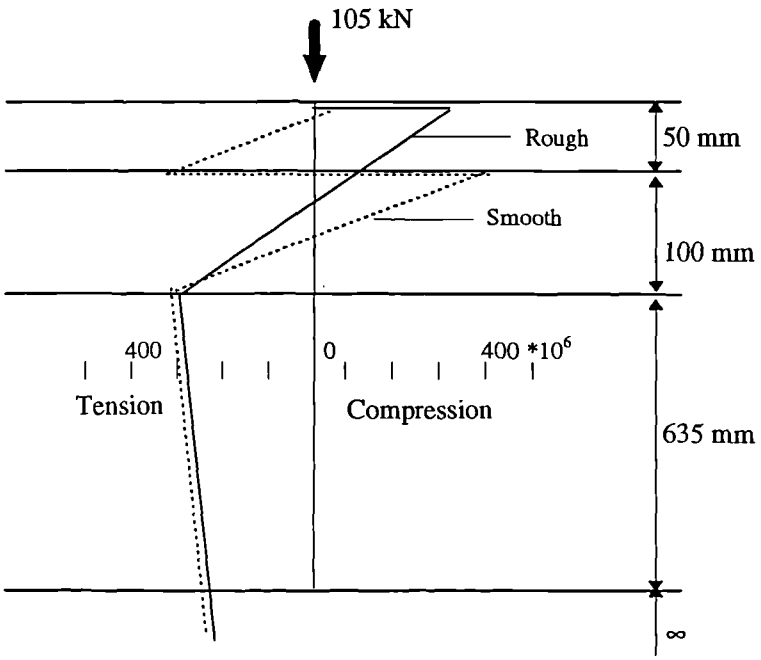


Figure 3.3, Horizontal strain under centreline of a single DC-9 wheel (75).

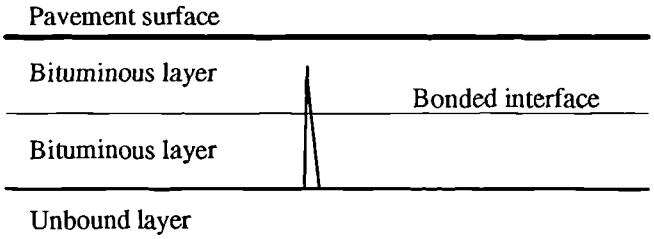


a) Possible crack shape when there is no debonding failure.

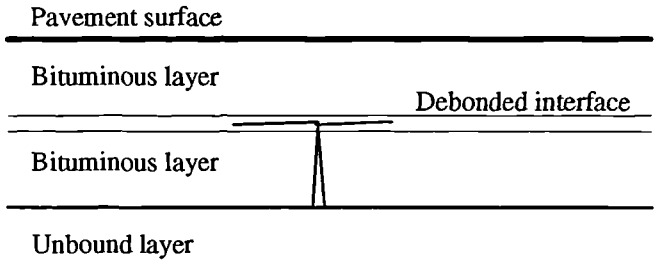


b) Possible crack shape when there is an interface debonding.

Figure 3.4, Effect of debonding between layers on crack's propagation in flexible pavement.

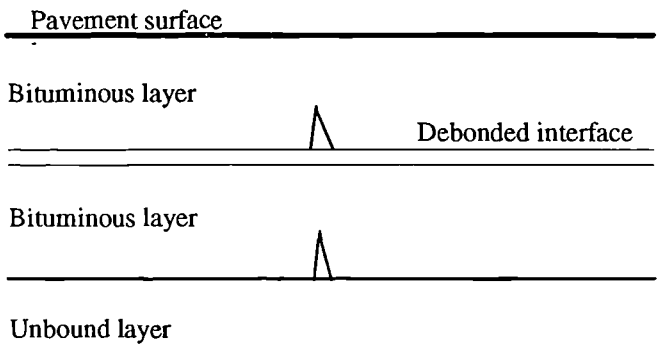


Figure 3.5, Effect of debonding failure on possible crack initiation in flexible pavement.

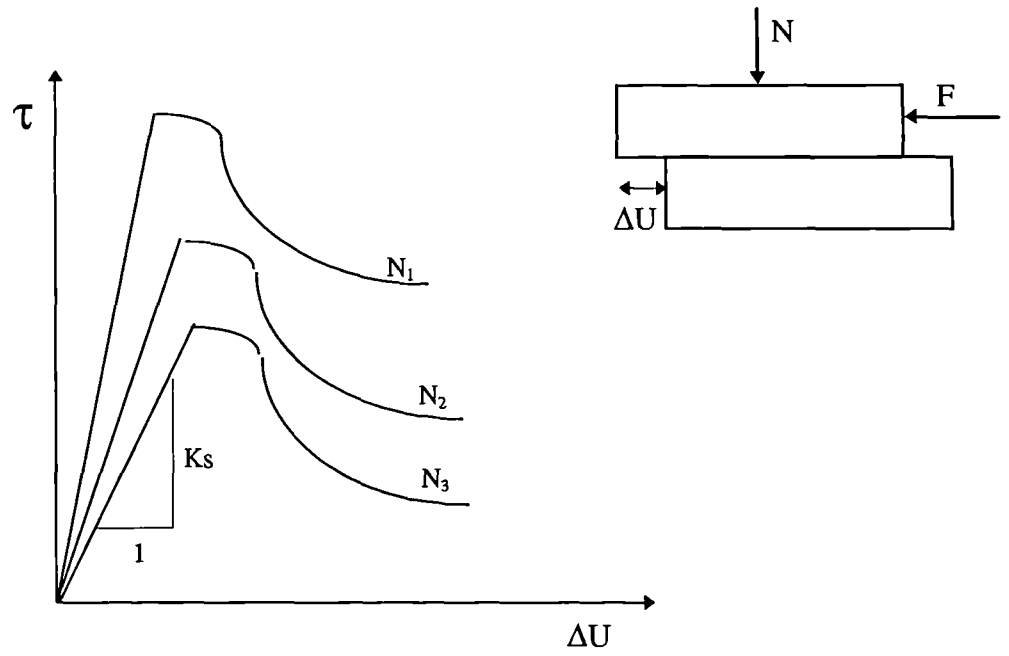


Figure 3.6, Shear stress-relative displacement curve at the interface as a function of normal load (74).

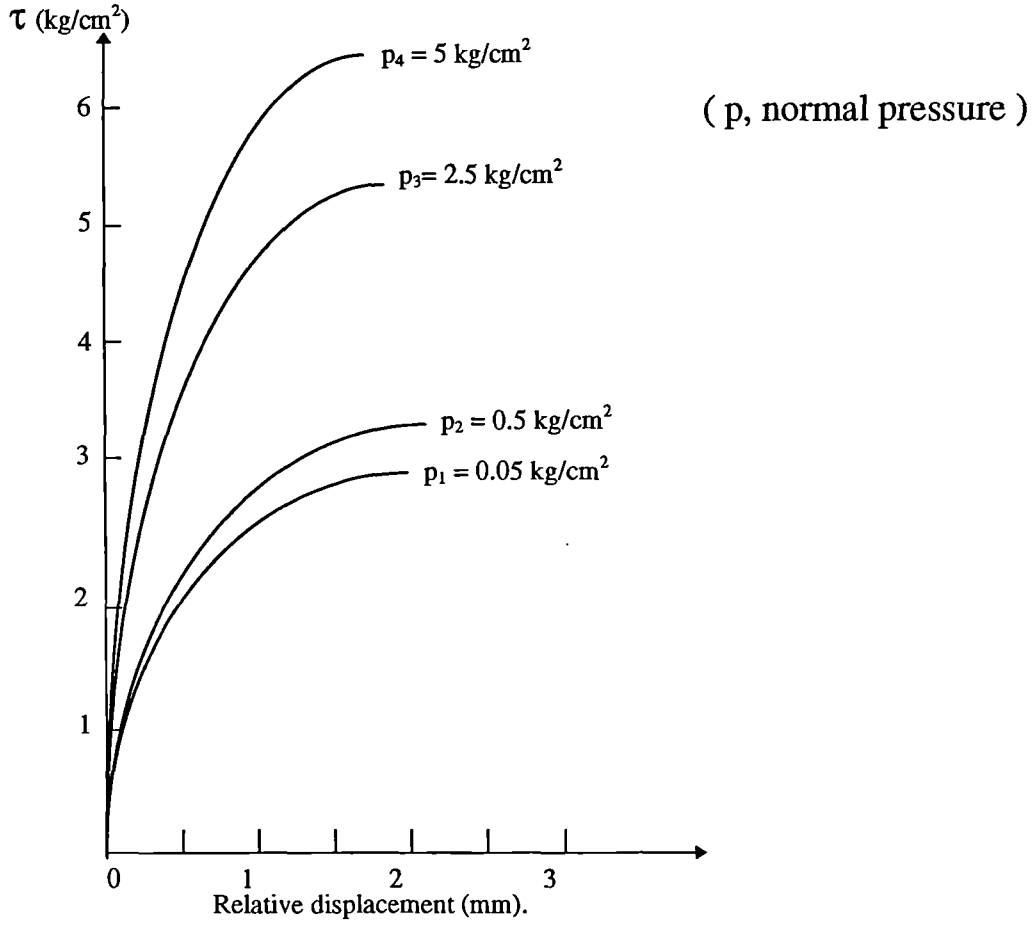


Figure 3.7, Shear test results for bituminous materials at 25 °C (67).

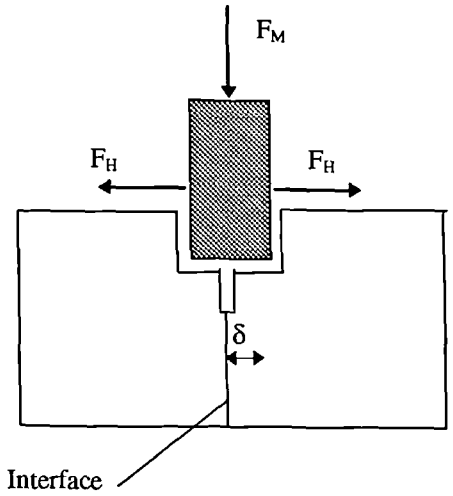


Figure 3.8, Wedge splitting test to measure the interface properties (79).

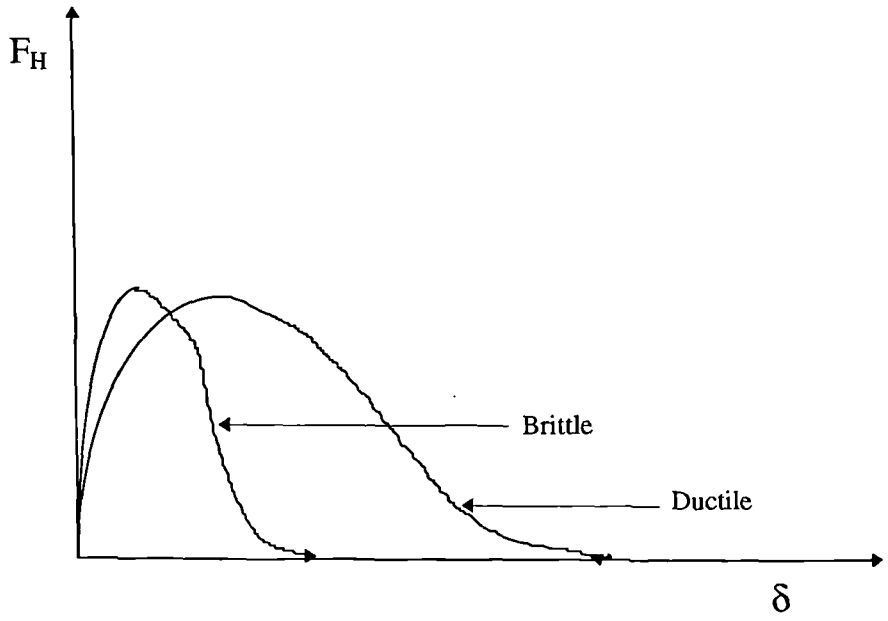


Figure 3.9, Load displacement curve under wedge splitting test (79).

# Chapter 4

# SIGNIFICANCE OF THE BONDING CONDITION BETWEEN WEARING AND BASE COURSES ON PAVEMENT LIFE AND BACKCALCULATED MODULI

## 4.1 INTRODUCTION

Most flexible pavement design and evaluation methods have assumed that full bonding exists between the pavement layers in the analysis process. This is probably due to modelling limitations and the assumption that good quality control will take place during construction. However, debonding failure has been reported between wearing and base courses in flexible pavements (9,10,11).

The literature review in the previous chapter showed that the adhesion properties between the pavement layers affect the performance of flexible pavement through their influence on the stressing level of the materials (67).

Therefore, in this chapter the investigation of the theoretical influence of bonding condition between wearing and base courses has been carried out. Firstly the reduction in the pavement life calculation during the design stage has been studied and secondly the reflection of the interface condition modelling error on backcalculated moduli has been analysed.

The study of the impact of the bonding condition between wearing and base courses for this research is due to the following reasons:

i) Practical evidence of slippage failure that has been reported between the wearing and base courses.

ii) Lepert et al (11) indicated that the road base subbase interlayer is rarely damaged in bituminous and semi rigid pavements. In contrast the interlayer between the wearing course and the layer just below it is most often defective.

However in principle the bonding condition between any two layers of the pavement can be investigated.

## 4.2 PAVEMENT LIFE PREDICTION

Most of the analytical design procedures for flexible pavements adopt the concept of limiting the horizontal tensile strain at the bottom of bituminous layer to control fatigue cracking and the vertical compressive strain at the top of subgrade to control permanent deformation. In this study the semi-empirical relationship developed by Transport Research Laboratory (TRL) (4), between the above strains and the pavement life in terms of the number of standard axle load of 80 kN was used, namely

$$\text{Log } N_t = -9.38 - 4.16 \text{ Log } e_t \qquad [4.1]$$

$$\text{Log } N_z = -7.21 - 3.95 \text{ Log } e_z \qquad [4.2]$$

where,

$N_t$ , is the number of standard axle load to cause fatigue cracking,

$N_z$ , is the number of standard axle load to cause permanent deformation,

$e_t$ , is the horizontal tensile strain at the bottom of bituminous layer,

$e_z$ , is the vertical compressive strain at the top of subgrade.

The final pavement remaining life (N) is the smallest of the fatigue and deformation lives. The selection of the above relationships is due to their wide use in the UK.

## 4.3 PAVEMENT STRUCTURE MODELLING

Here the pavement is modelled as a layered linear elastic system. The stresses, strains and displacements within the structure due to external load are calculated numerically, using the BISAR program (44).

Four theoretical structures were investigated in this study to represent a wide range of flexible pavements in terms of strength. Weak, medium, strong and very strong pavement terms were used for comparison purpose. The thicknesses and Poisson ratios were fixed in all pavements whereas the moduli of wearing course, base, subbase and subgrade were varied as shown in figure 4.1. The pavements consist of four layer systems with an additional rigid layer at 6m depth, to represent either bedrock or the depth where the vertical deflection is negligible.

For each pavement structure the interface shear reaction modulus between the wearing and base courses was changed gradually from complete debonding to full adhesion, with $K_{s1}$ varying as, $10^1$, $10^2$, $10^3$, $10^4$, $10^5$ MN/m$^3$. All other interface conditions were kept constant and assumed as full adhesion.

Numerical analysis using the BISAR program to identify the range of shear reaction modulus between wearing and base courses for flexible pavements has been carried out.

The BISAR program was used to calculate i) the surface deflections at the load centre, at 300 and 600 mm radial distance, and ii) the two critical strains for pavement life under 40 kN load for the four pavements. The 40 kN load is selected to represent the impact of traffic loading (80). The shear reaction modulus between wearing and base courses was changed gradually from 1 to $10^7$ MN/m$^3$ for each case.

Figures 4.2 and 4.3 show the deflections and strains respectively as a function of ($K_{s1}$) for the four structures. Two limits can be established from the above figures, beyond them there are no significant changes in pavements response such as deflections and strains.

Therefore ($K_{s1}$) can be taken to vary from 10 MN/m$^3$ (complete debonding) to $10^5$ MN/m$^3$ (full adhesion) in flexible pavements.

The effect of $K_{s1}$ on surface deflections decreases as the radial distance increases with its maximum influence on the deflection at the load centre ($d_0$) (see figure 4.2). Hence deflections beyond the 600 mm radial distance were not considered in the analysis.

## 4.4 INFLUENCE OF THE SHEAR REACTION MODULUS BETWEEN WEARING AND BASE COURSES ON DESIGN LIFE OF PAVEMENTS

Flexible pavements are designed, in term of material selection and layer thickness, to carry traffic load during a specified life. However if a slip plane develops between the wearing and base courses, due to lack of binder coat or surfacing in cold weather, the stress distribution within the structure will change, reducing the pavement performance and life (75).

The four pavement structures shown in figure 4.1 have been studied in this section. The two calculated critical strains were used to predict the fatigue and deformation lives employing the TRL equations mentioned above, for each bonding condition. The pavements' lives were presented for each case in table 4.1.

Figure 4.4 shows the percentage reduction in pavement lives due to variation in the first shear reaction modulus from full adhesion. An average decrease in pavement life of 20% was recorded in figure 4.4 when the value of $K_{s1}$ reached $10^4$ MN/m$^3$. Further reductions of up to 50% were observed when complete debonding occurs between wearing and base courses.

These findings agree with the results of Brown and Brunton (66) shown in table 3.2.

## 4.5 INFLUENCE OF THE SHEAR REACTION MODULUS BETWEEN WEARING AND BASE COURSES ON PAVEMENT BACKCALCULATED MODULI

Most of the procedures followed in this section are based on the methodology proposed by Briggs and Nazarian (81), in studying the effects of unknown rigid layer on backcalculated moduli.

Five surface deflection basins under 40 kN load were calculated for each pavement structure shown in figure 4.1 using the BISAR program. Each basin represents an interface condition between wearing and base courses, with $K_{s1}$ varying as, $10^1$, $10^2$, $10^3$, $10^4$, $10^5$ $MN/m^3$. The twenty deflection basins were assumed as the measured basins under Falling Weight Deflectometer (FWD) tests.

The twenty basins were used to backcalculate the layer moduli. The pavement parameters assumed in the backcalculation process were identical to those in the theoretical structures shown in figure 4.1, except the first interface condition was fixed as full adhesion as is commonly found in most backcalculation programs.

The moduli of the second, third and fourth layers were backcalculated, and the modulus of the 40 mm wearing course was fixed as recommended by May and Van Quintus (27), in describing the proposed ASTM standard for backcalculation. These backcalculated moduli should carry some errors to compensate for modelling the interface conditions as full adhesion rather than the actual values.

Figure 4.5, illustrates the ratio of backcalculated to actual modulus of the layer 2 versus the ratio of actual to assumed interface condition between bituminous layers, (note that log $K_{s1}$ was used in the graphs). The above moduli ratio of layer 2 has decreased on average by 35% for a full adhesion assumption instead of complete debonding in the backcalculation procedure.

Figure 4.6, shows the ratio of backcalculated to actual modulus of the layer 3 versus the ratio of actual to assumed interface condition between bituminous layers. The ratio of backcalculated to actual subbase modulus varied between 70% and 120%. These results may be interpreted not only as error in modelling $K_{s1}$, but also as error in predicting the subbase moduli. The prediction of a weak subbase modulus for a pavement with a strong bituminous base will be difficult, since its contribution to the structural pavement response is small (47).

Figure 4.7, demonstrates the ratio of backcalculated to actual modulus of the layer 4 versus the ratio of actual to assumed interface condition between bituminous layers. It is apparent that by modelling the interface condition as full adhesion instead of the real cases, there is no significant effect on backcalculated $E_4$.

## 4.6 SUMMARY

Lower pavement life than the specified design value may result if a slip plane develops between the bituminous layer during construction. Up to 50% reduction in pavement life was recorded when complete debonding exists between the wearing and base courses and therefore weaker pavement will be produced.

Flexible pavement evaluation using the FWD and backcalculation of moduli, assuming full adhesion between wearing and base courses may cause some errors in moduli prediction. For the analysed structures, a maximum errors of 35% was recorded for bituminous base.

Due to the above results and all the practical evidence of debonding failures, an improvement in the existing backcalculation methods is required to give better modelling possibilities. The new method should predict the interface shear reaction modulus between the wearing and base courses in addition to the layer moduli from FWD test results.

**a) Pavement structure**

| | | |
|---|---|---|
| $h_1$ = 40 mm | Bituminous Wearing Course Layer 1 | $\nu_1$ = 0.4 |
| | | $K_{s1}$ = variable |
| $h_2$ = 200 mm | Bituminous Base Layer 2 | $\nu_2$ = 0.4 |
| | | $K_{s2}$ = full adhesion |
| $h_3$ = 300 mm | Granular Subbase Layer 3 | $\nu_3$ = 0.3 |
| | | $K_{s3}$ = full adhesion |
| $h_4$ = 5460 mm | Subgrade Layer 4 | $\nu_4$ = 0.4 |

Rigid Layer

**b) E values of different pavements**

| Pavement | $E_1$ (MPa) | $E_2$ (MPa) | $E_3$ (MPa) | $E_4$ (MPa) |
|---|---|---|---|---|
| **Weak (W)** | 1000 | 2500 | 80 | 40 |
| **Medium (M)** | 2500 | 4000 | 100 | 80 |
| **Strong (S)** | 5000 | 7000 | 200 | 80 |
| **Very Strong (VS)** | 7500 | 10000 | 500 | 200 |

Figure 4.1, Summary of pavements properties.

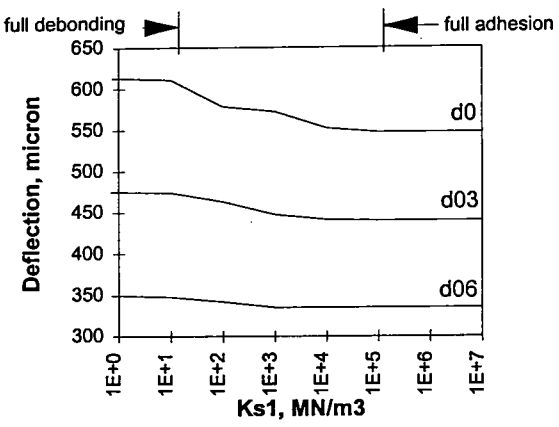


Weak Pavement

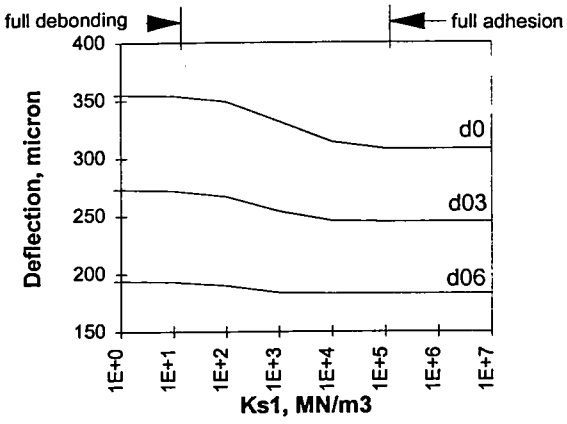


Medium Pavement

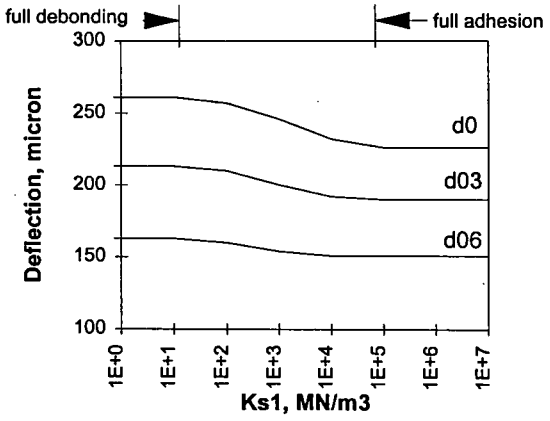


Strong Pavement

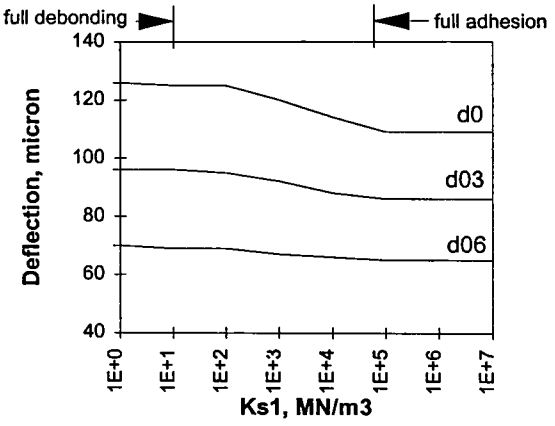


Very Strong Pavement

Figure 4.2, Surface deflection as a function of first shear reaction modulus ($K_{s1}$) for the Weak (W), Medium (M), Strong (S) and Very Strong (VS) pavements.

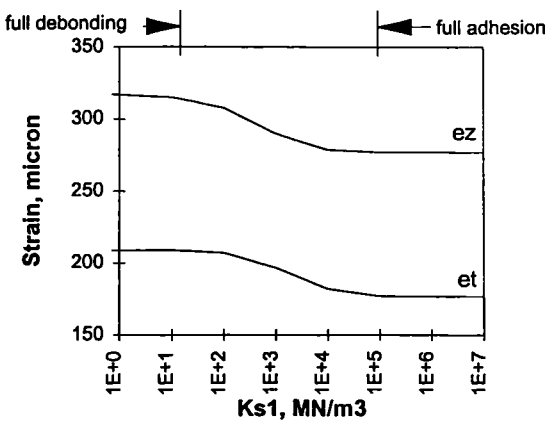


Weak Pavement

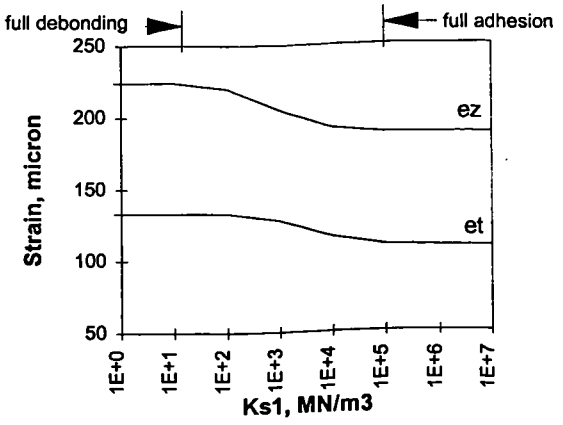


Medium Pavement

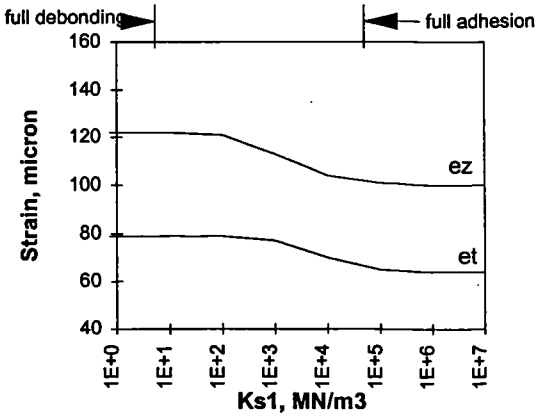


Strong Pavement

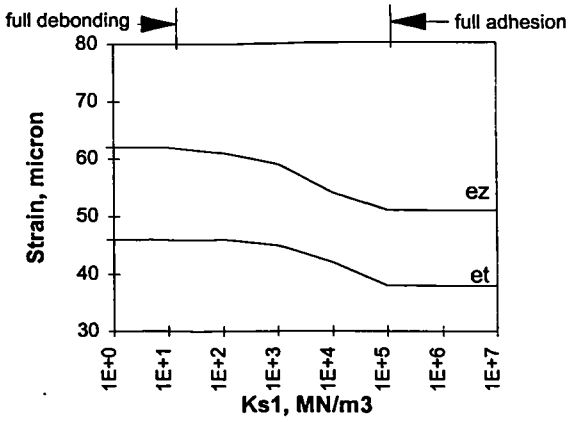


Very Strong Pavement

Figure 4.3, Horizontal strain at the bottom of bituminous layer ($e_t$) and vertical strain at the top of subgrade ($e_z$) as a function of first shear reaction modulus ($K_{s1}$) for the Weak (W), Medium (M), Strong (S) and Very Strong (VS) pavements.

Table 4.1, Effect of variation of first shear reaction modulus on pavements life in million of standard axle (msa).

| | $K_{s1}$ ($MN/m^3$) | | | | |
|---|---|---|---|---|---|
| **Pavement** | **10** (full debonding) | $10^2$ | $10^3$ | $10^4$ | $10^5$ (Full adhesion) |
| **Weak** | 0.8 | 0.9 | 1.1 | 1.5 | 1.7 |
| **Medium** | 5.6 | 5.6 | 6.5 | 9.8 | 12.2 |
| **Strong** | 48.5 | 48.5 | 54.0 | 80.2 | 109.2 |
| **V.Strong** | 460.2 | 460.2 | 504.2 | 671.9 | 1018.8 |

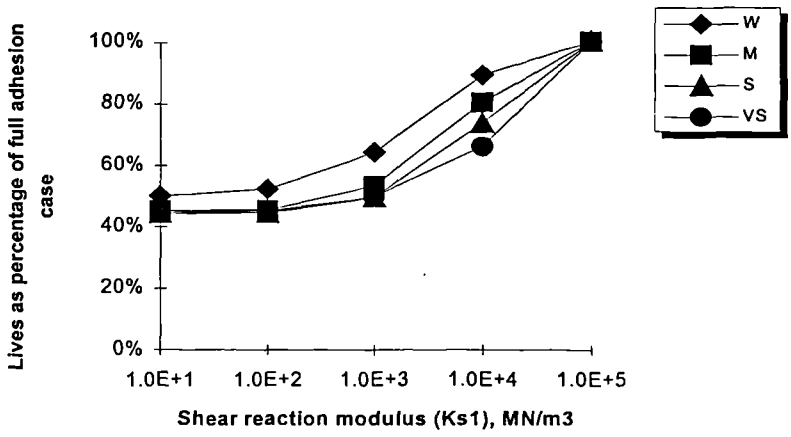


Figure 4.4, Reductions in pavements life due to variations in the first shear reaction modulus, as percentage of full adhesion case.

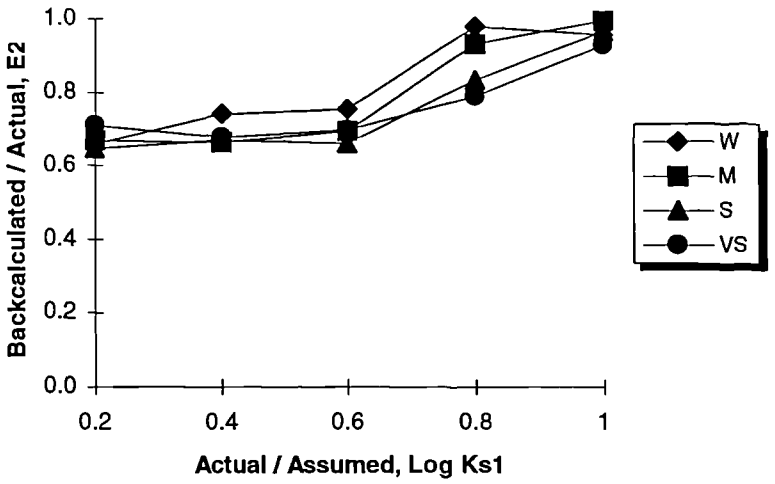


Figure 4.5, Influence of the first shear reaction modulus modelling error on backcalculated modulus of bituminous base.

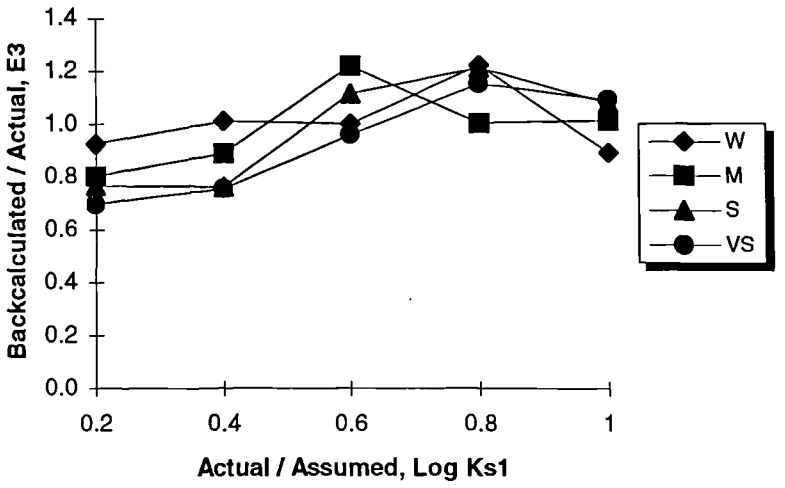


Figure 4.6, Influence of the first shear reaction modulus modelling error on backcalculated modulus of unbound subbase.

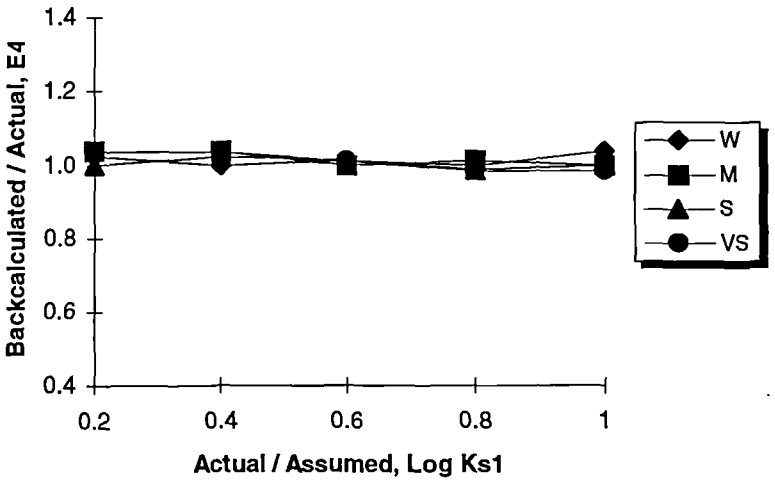


Figure 4.7, Influence of the first shear reaction modulus modelling error on backcalculated modulus of subgrade.

# Chapter 5

# THE INFLUENCE OF PAVEMENT PARAMETERS ON SURFACE DEFLECTIONS

## 5.1 INTRODUCTION

The pavement surface deflections under the falling weight deflectometer reflect the real insitu pavement conditions in terms of layer moduli, thicknesses, Poisson ratios and the interface condition between the individual layers. Theoretically all the above parameters can be predicted from the surface deflections, however the number of parameters should be reduced to eliminate the likelihood of a non-unique solution from the backcalculation process (27).

In this chapter, the influence of each pavement parameter on pavement deflection variation is determined. The result of the analysis together with the practical applications and mathematical limitations will be used for the selection of the parameters to be backcalculated, and hence the development of the proposed improved backcalculation procedure.

## 5.2 SURFACE DEFLECTION SENSITIVITY TO PAVEMENT PARAMETERS

### 5.2.1 Methodology

The methodology used to investigate the deflection sensitivity analysis is summarised in the following steps:

i) Assume a standard pavement structure with known properties.

ii) Vary one parameter at the time keeping the remaining as in the standard structure, and calculating the resulted deflection basin using the BISAR program.
iii) Analyse the variation in both the shape and magnitude of the deflection basin due to the parameter variation.

The larger the influence of the parameter on surface deflections the higher its contribution to the pavement strength and the easier its backcalculation (1,2,12,42). Therefore a strong thick layer will be backcalculated more reliably from surface deflections than a weak thin layer.

Conventional backcalculation programs predict the layer moduli assuming all the other pavement parameters are known. Hence any error in assuming one parameter will affect the backcalculated moduli, and this error depends on the sensitivity of surface deflections to this parameter (60).

Figure 5.1 illustrates a four layer pavement with additional bedrock at 6m depth from the surface. This standard structure represents a typical flexible pavement with two bituminous layers, i.e. wearing and base courses, and granular subbase over subgrade.

The properties of the standard pavement in term of moduli, layer thickness, Poisson's ratio and the interface condition between layers are shown in figure 5.1. The deflection basins for this structure were computed using the BISAR program (44) under 40 kN surface load.

### 5.2.2 Deflection Sensitivity to the Layers Moduli

Each layer modulus was changed by ±50% from the original value, keeping all the other parameters as in the standard structure, and the deflection basins were calculated under 40 kN load for each case. Figures 5.2 to 5.6 demonstrate the influence of varying the modulus of each layer on surface deflections. It is observed that changes in the modulus of bituminous layers only influence the deflections close to the load centre, up to a distance of 900 mm. However the modulus of the wearing course has very little effect on the deflection compared with the base modulus.

The moduli of subbase and subgrade influence the whole deflection basin with $E_4$ having the largest effect on surface deflections. However the quantification of these effects will be carried out later in this chapter. The modulus of the rigid bedrock ($E_5$) has no influence on the deflection basin, and therefore its assumed value will not affect the backcalculated parameter results.

### 5.2.3 Deflection Sensitivity to the Layers Thickness

Figures 5.7 to 5.10 show the effect of layer thickness variations on surface deflections. The base layer thickness has the largest influence on deflection near the loaded area, whereas the depth of the bedrock has influenced the whole deflection basin. Both the thicknesses of wearing course and subbase have little effect on surface deflection.

Therefore, accurate measurements of bituminous layer thickness and the depth of the rigid layer, especially if it exists at shallow depth, is essential for a good estimate of the backcalculated parameters. These results support the finding of many researchers (27,57,61,81).

### 5.2.4 Deflection Sensitivity to the Poisson's Ratio

Figures 5.11 to 5.15 present the effect of Poisson's ratio variations on surface deflections. Poisson's ratios of all the pavement layers including the rigid bedrock have insignificant influence on surface deflections and therefore on predicting the pavement parameters (24,58,59).

### 5.2.5 Deflection Sensitivity to the Interface Shear Reaction Moduli

The influences of the interface shear reaction modulus ($K_s$) between the pavement layers on deflection basins were illustrated in figures 5.16 to 5.18. The ($K_s$) value has changed from a standard structure of full adhesion with $K_s = 10^5$ to an intermediate case of $10^3$ and finally to 10 MN/m$^3$ which represents complete debonding.

The upper layers' interface properties have most influenced the deflections near the loaded area, whereas most of the deflection basin has been affected by the bonding condition

between the lower layers. Generally ($K_s$) has little influence on surface deflections compared to that exerted by the thick layers' moduli.

### 5.2.6 The Selection of the Pavement Parameters to be Backcalculated

The following findings can be drawn from the above studies:

The upper pavement properties mostly affect the deflections near the load centre, whereas the deflections far from the loaded area are influenced only by the lower properties. These findings are supported by other researchers (1,21,42,82).

The modulus of the thin wearing course has very little influence on deflection. Therefore assigning its modulus as a known value in the backcalculation process, as recommended by May and Van Quintus in describing the proposed ASTM standard for backcalculation (27) and SHRP's layer moduli backcalculation procedures (61), will be acceptable. The modulus value may be measured in the laboratory, using the Nottingham Asphalt Tester (NAT) for indirect tensile test for resilient modulus of bituminous mixtures (35), or mathematically estimated using the Asphalt Institute regression equations (83) or Shell International monographs (84).

The modulus of the rigid layer has no effect on surface deflections, therefore a typical value of 7000 MPa is to be assumed for this layer in the calculation process as found in the literature (50,85).

The layers' thicknesses have variable influences on the deflection basin, however their value can be measured physically and they can be excluded from the backcalculation process.

Poisson's ratios for all the layers have not influenced the surface deflections, hence they can be assumed as known values in the backcalculation procedure. A typical value for each material can be assumed in the backcalculation process as found in the literature (37).

The shear reaction moduli between layers ($K_s$) have varying influence on deflections. However, as explained in previous chapters and from the practical evidence of debonding failure, the interface condition between the wearing and base courses prediction is the

objective of this work, and the other interface conditions are to be assumed as full adhesion in the analysis process.

Therefore, the moduli of bituminous base, subbase and subgrade in addition to the shear reaction modulus between wearing and base courses ($K_{s1}$) are the only parameters to be backcalculated from surface deflections, using the proposed improved backcalculation procedure. However, if the radial modulus investigations indicate the presence of a rigid layer at shallow depth, the subgrade thickness should be included in the backcalculation process.

These parameters are commonly predicted using the conventional backcalculation programs apart from the shear reaction modulus between the wearing and base courses, which is the proposed improvement to the current methods.

## 5.3 THE DETAILED ANALYSIS OF THE INFLUENCE OF THE SELECTED PARAMETERS ON SURFACE DEFLECTIONS

The percentage variations in surface deflections due to the effect of each layer modulus and the shear reaction modulus between wearing and base courses ($K_{s1}$), are investigated for the Weak (W), Medium (M), Strong (S) and Very Strong (VS) pavements shown in figure 4.1 (see chapter 4).

The absolute relative errors in deflections at the load centre due to each of the above parameter variations are presented in figures 5.19 to 5.23. Maximum deflection errors of 5%, 22%, 12% and 46% were recorded when varying the moduli of wearing course, base, subbase and subgrade respectively by 50%. The interface condition variation from full adhesion to complete debonding between wearing and base courses has changed the central deflection by up to 15% as shown in figure 5.23.

Similar studies have been carried out to investigate the influence of the above parameters on the whole deflection basin. The absolute sum of the relative errors in deflection locations due to each parameter variation is illustrated in figures 5.24 to 5.28.

Maximum deflection errors of 18%, 50%, 69% and 535% were found due to 50% alternation in $E_1$, $E_2$, $E_3$ and $E_4$ respectively, whereas a maximum value of 44% was recorded in figure 5.28 for ($K_{s1}$).

The subgrade modulus has the largest influence on surface deflection followed by both the base and subbase. The shear reaction modulus ($K_{s1}$) has a lower effect on surface deflections, hence its prediction may be more difficult. Finally the modulus of the thin wearing course has the lowest influence on deflections, therefore the literature recommendation of fixing the wearing course modulus in the backcalculation process is acceptable. However, it is not likely to estimate the wearing course modulus from laboratory testing with 50% error and a small variation in its value will not affect the calculation results (27).

However, if the wearing course thickness is more than 75 mm its modulus should be included in the backcalculation process (27,61).

## 5.4 CONCLUSIONS

The results of the deflections sensitivity to pavement parameters and the mathematical limitation of the backcalculation process in reducing the number of parameters to be predicted, lead to the following recommendations for the proposed improved method:

i) Radial modulus analysis should be performed to detect any rigid layer at shallow depth.

ii) If the wearing course is a thin layer, as commonly used in the UK (86), its modulus should be assigned a fixed value as recommended in the literature. However a small variation in this modulus will not influence the calculation process since it has little effect on surface deflections.

iii) The shear reaction modulus between the wearing and base courses in addition to the normal layer moduli of base, subbase and subgrade are to be backcalculated from surface deflections using the proposed improved backcalculation procedure.

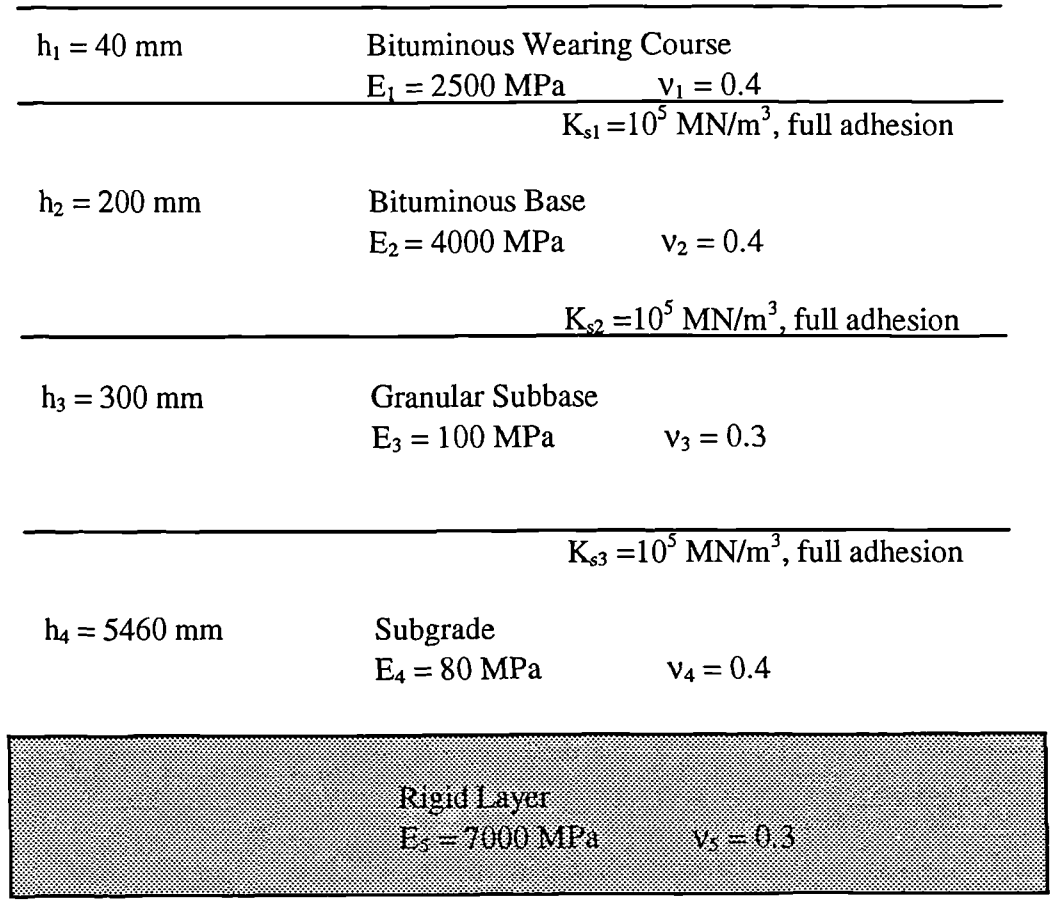


Figure 5.1, Standard pavement structure for the sensitivity analysis.

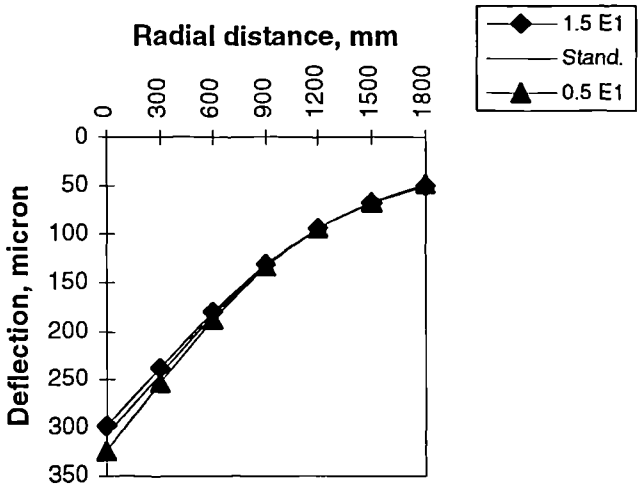


Figure 5.2, Effect of variation of the wearing course modulus ($E_1$) on surface deflections.

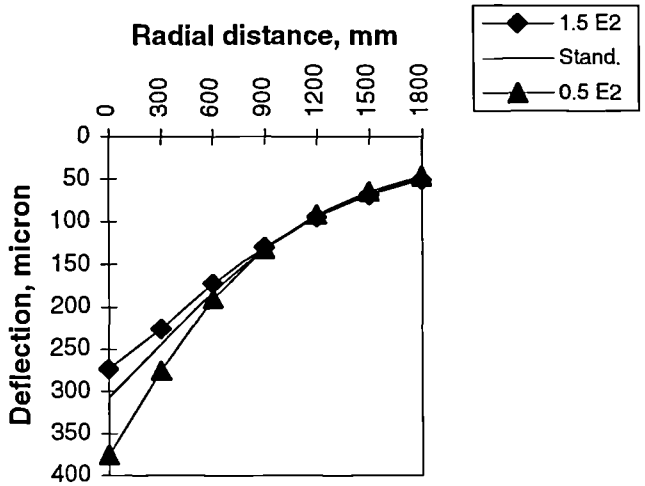


Figure 5.3, Effect of variation of the base modulus ($E_2$) on surface deflections.

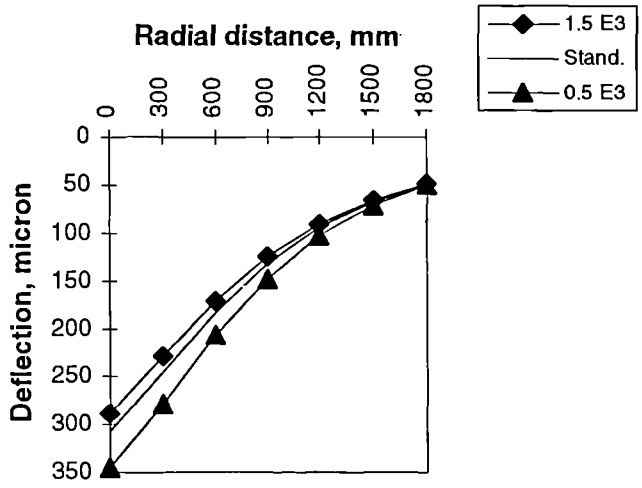


Figure 5.4, Effect of variation of the unbound layer modulus ($E_3$) on surface deflections.

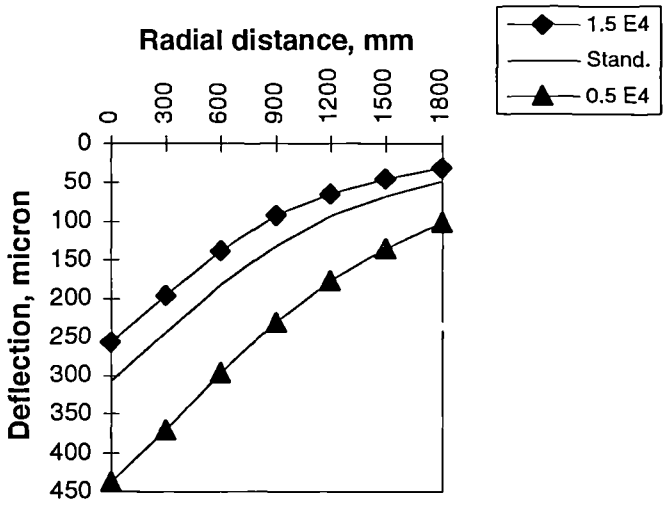


Figure 5.5, Effect of variation of the subgrade layer modulus ($E_4$) on surface deflections.

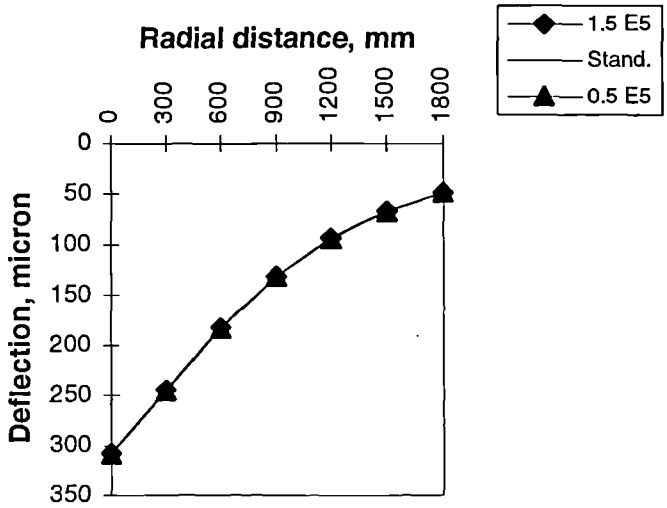


Figure 5.6, Effect of variation of the rigid layer modulus ($E_5$) on surface deflections.

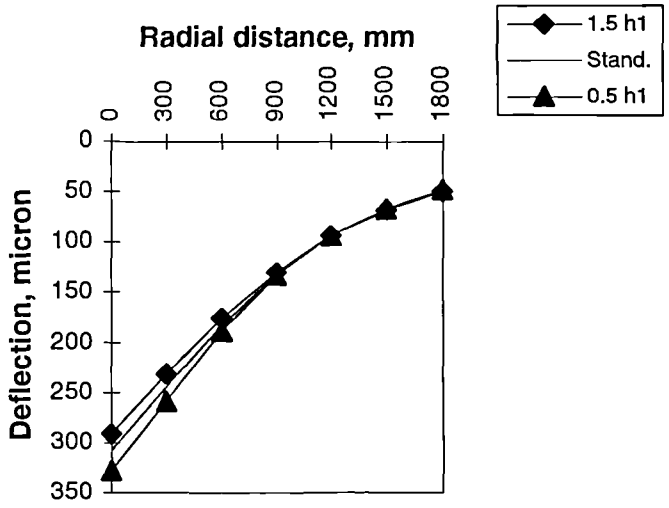


Figure 5.7, Effect of variation of the wearing course thickness ($h_1$) on surface deflections.

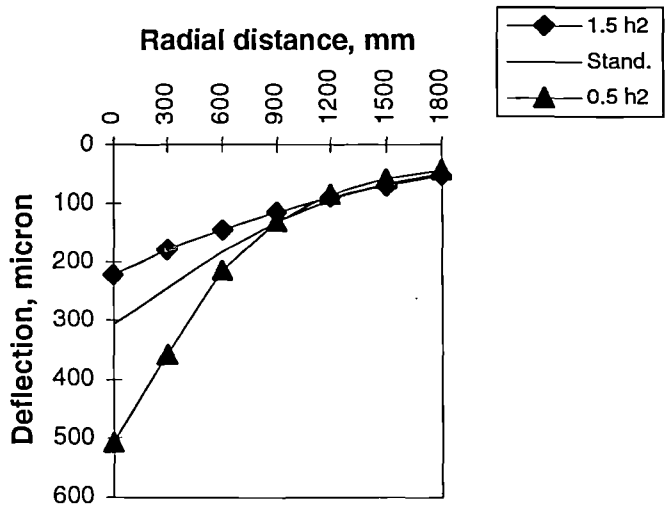


Figure 5.8, Effect of variation of the base layer thickness ($h_2$) on surface deflections.

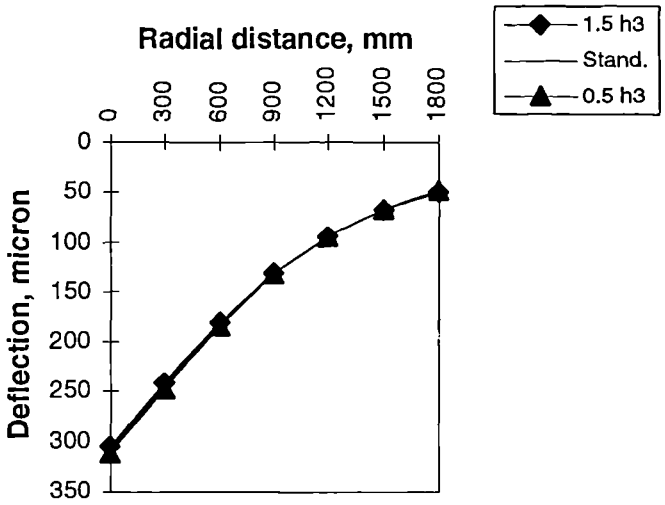


Figure 5.9, Effect of variation of the unbound layer thickness ($h_3$) on surface deflections.

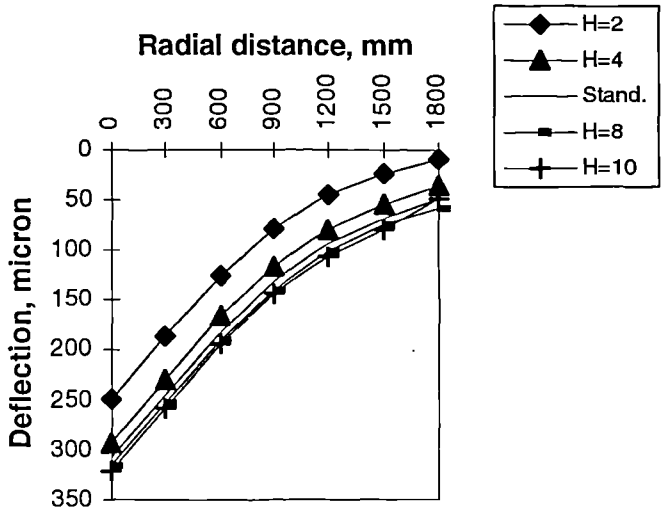


Figure 5.10, Effect of variation of the rigid layer depth on surface deflections.

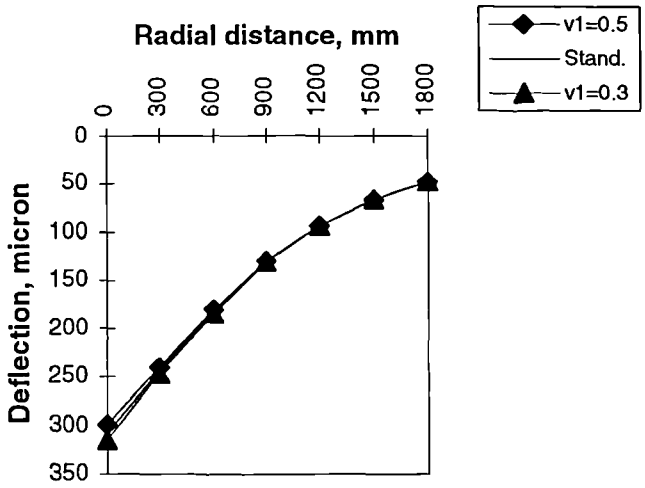


Figure 5.11, Effect of Poisson's ratio of the wearing course ($\nu_1$) on surface deflections.

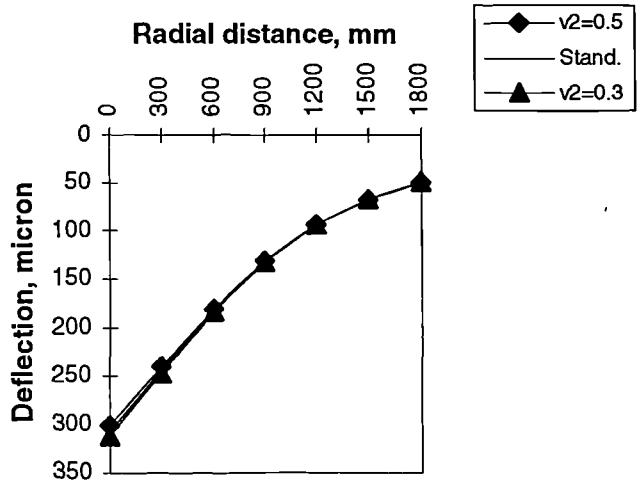


Figure 5.12, Effect of Poisson's ratio of the base layer ($\nu_2$) on surface deflections.

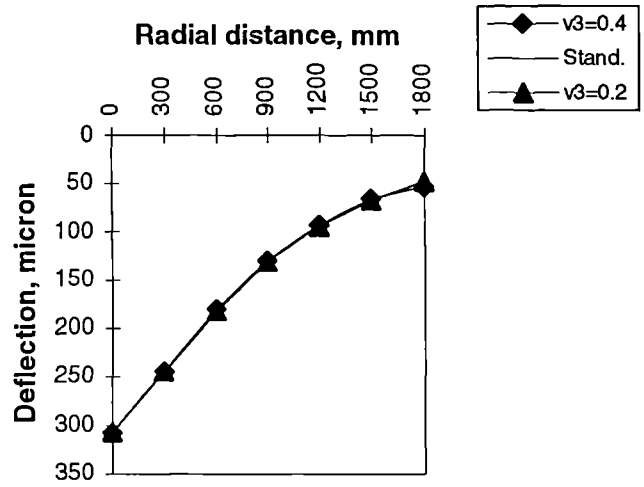


Figure 5.13, Effect of Poisson's ratio of the unbound layer ($\nu_3$) on surface deflections.

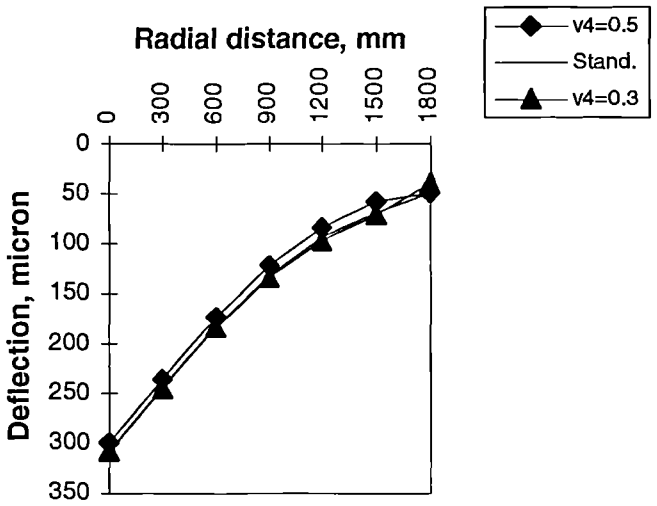


Figure 5.14, Effect of Poisson's ratio of the subgrade ($v_4$) on surface deflections.

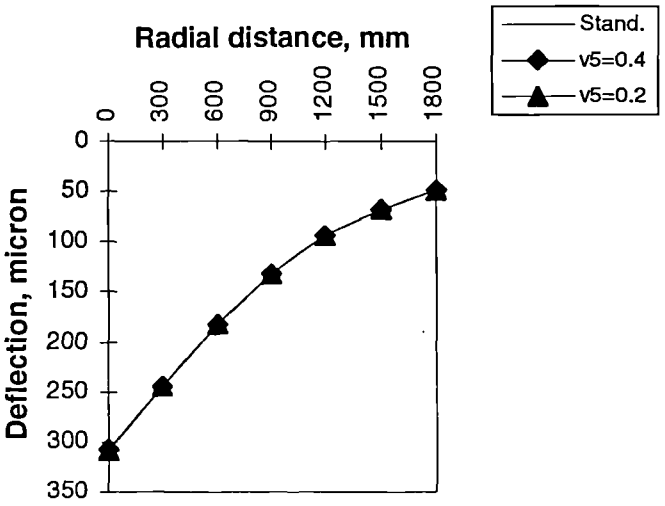


Figure 5.15, Effect of Poisson's ratio of the rigid layer ($v_5$) on surface deflections.

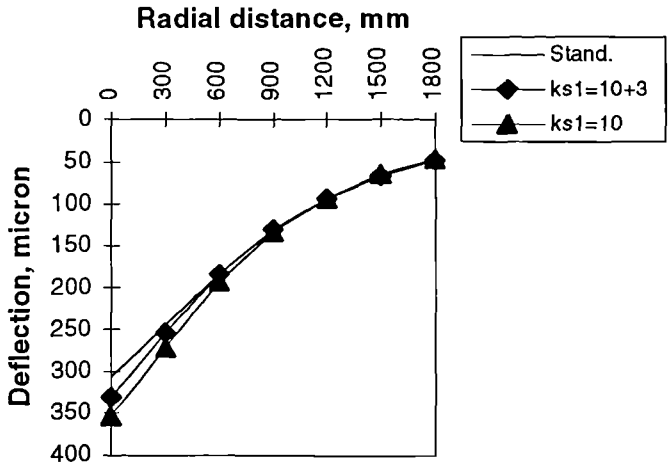


Figure 5.16, Effect of the first shear reaction modulus ($K_{s1}$) on surface deflections.

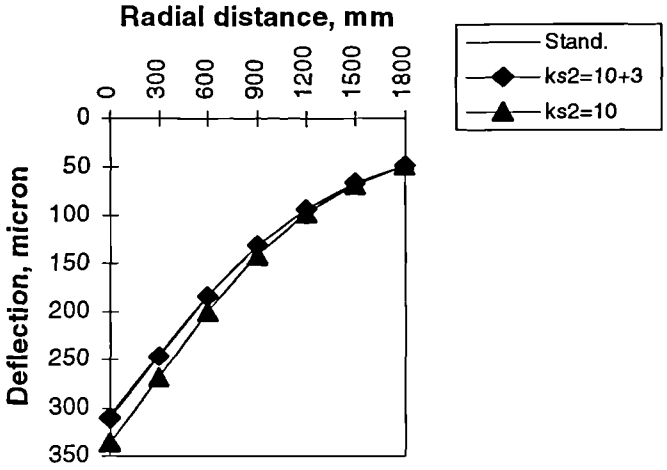


Figure 5.17, Effect of the second shear reaction modulus ($K_{s2}$) on surface deflections.

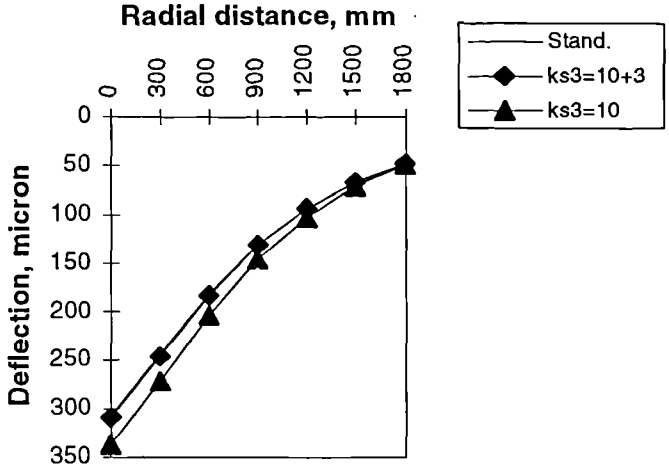


Figure 5.18, Effect of the third shear reaction modulus ($K_{s3}$) on surface deflections.

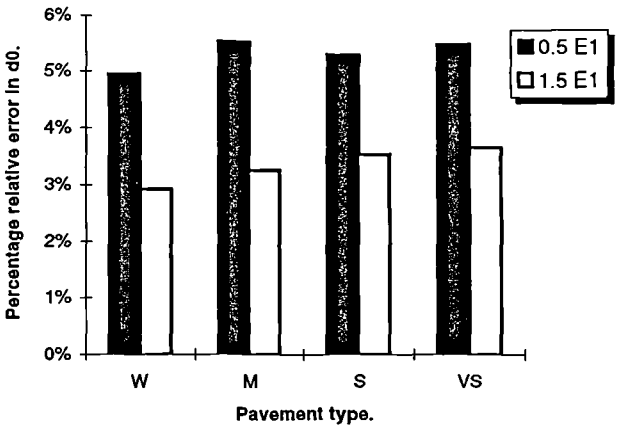


Figure 5.19, Absolute relative error in deflections at the load centre due to the wearing course modulus variations.

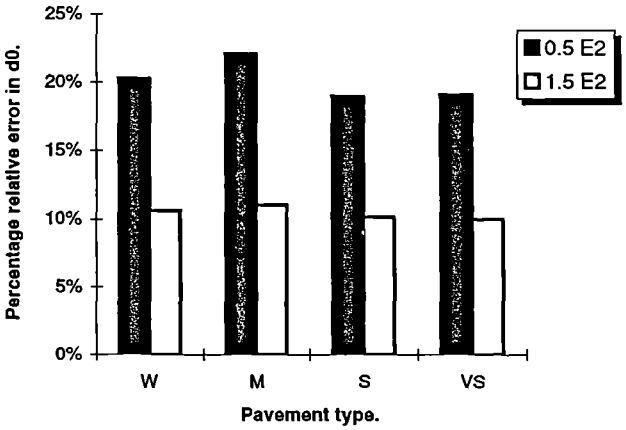


Figure 5.20, Absolute relative error in deflections at the load centre due to the bituminous base modulus variations.

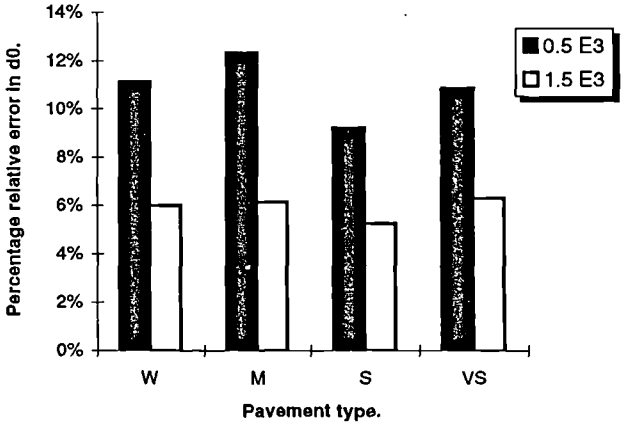


Figure 5.21, Absolute relative error in deflections at the load centre due to the subbase modulus variations.

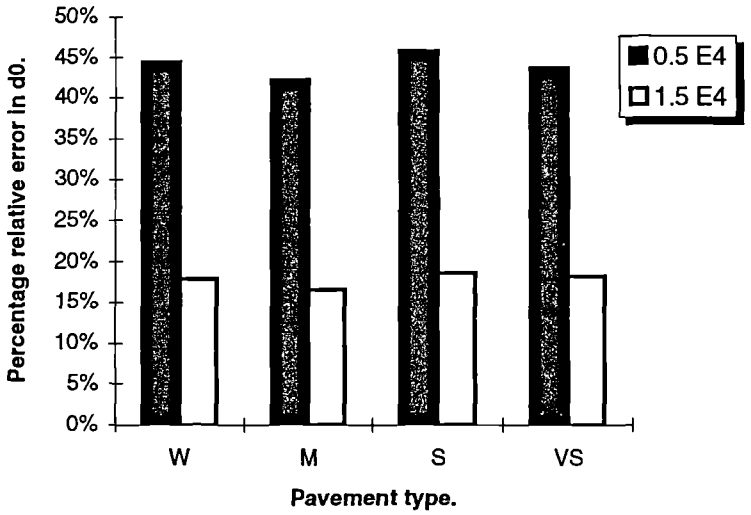


Figure 5.22, Absolute relative error in deflections at the load centre due to the subgrade modulus variations.

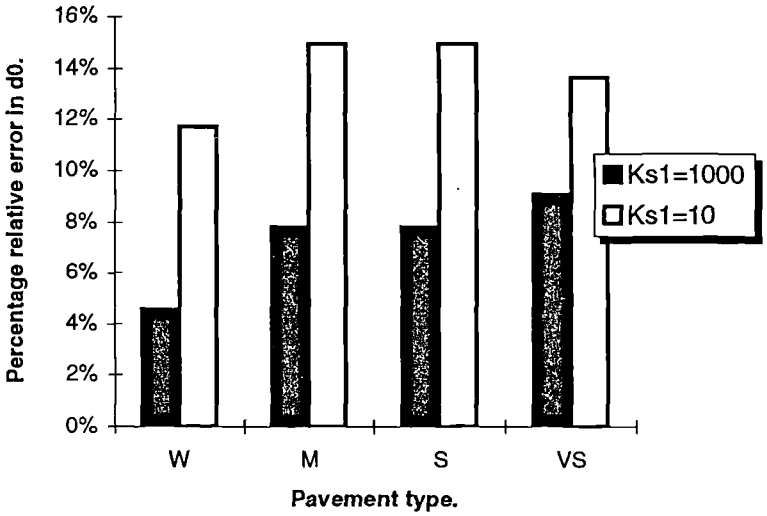


Figure 5.23, Absolute relative error in deflections at the load centre due to the interface shear reaction modulus between wearing and base courses variations.

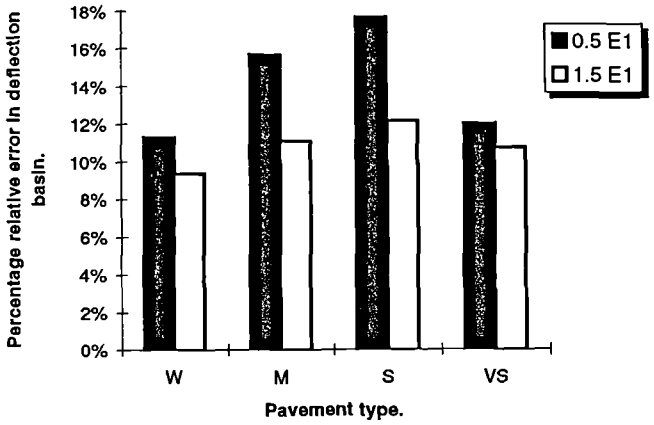


Figure 5.24, Absolute relative error in deflections basin due to the wearing course modulus variations.

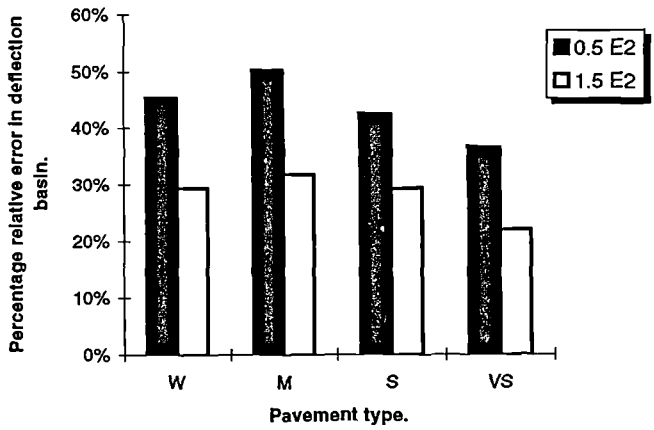


Figure 5.25, Absolute relative error in deflections basin due to the bituminous base modulus variations.

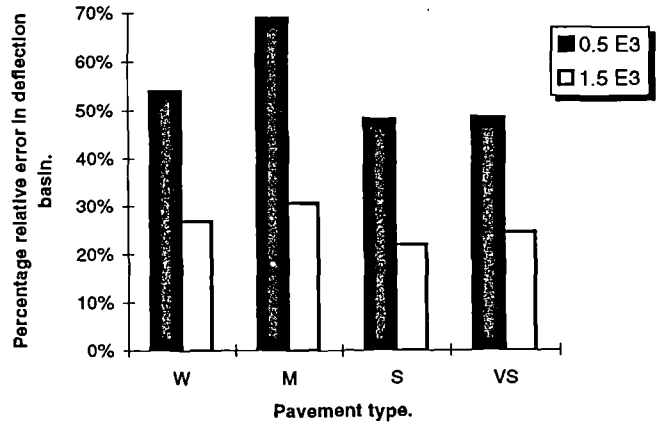


Figure 5.26, Absolute relative error in deflections basin due to the subbase modulus variations.

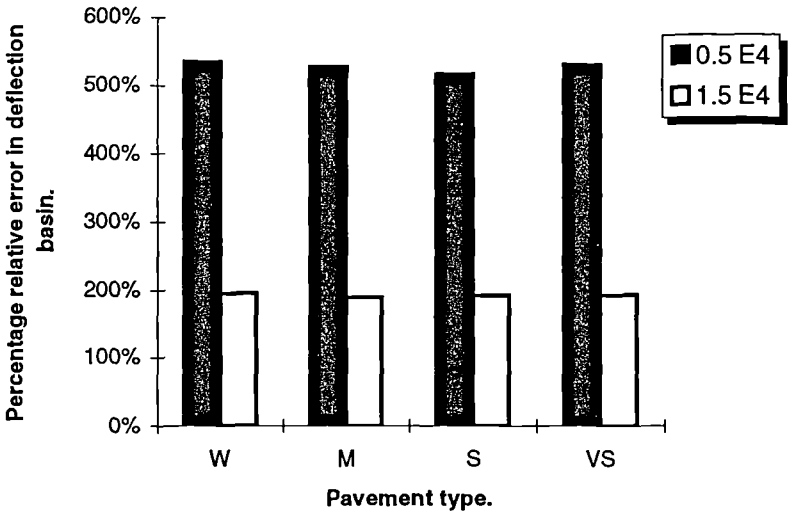


Figure 5.27, Absolute relative error in deflections basin due to the subgrade modulus variations.

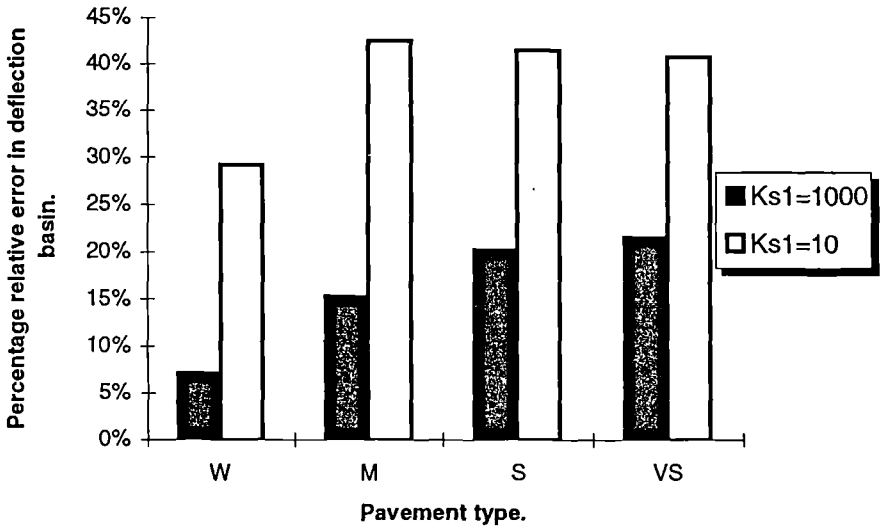


Figure 5.28, Absolute relative error in deflections basin due the interface shear reaction modulus between wearing and base courses variations.

# Chapter 6

# DEVELOPMENT OF THE BACKCALCULATION PROCEDURE

## 6.1 INTRODUCTION

In the previous chapters the need to develop the existing backcalculation procedure and the influence of the pavement parameters has been established. The development of the new model, which can backcalculate the bonding condition between the wearing course and base course in addition to the layer moduli from Falling Weight Deflectometer (FWD) test results, is detailed in this chapter.

An optimisation procedure using the common method of least squares (48) is firstly employed to try and predict the above parameters for a given hypothetical theoretical pavement. This method failed to estimate the pavement parameters accurately from the surface deflections. Hence, a two-stage backcalculation procedure is developed to overcome the limitations of the first method.

## 6.2 ASSUMPTIONS FOR THE BACKCALCULATION PROCEDURE

A simple static analysis for a layered linear elastic system, which is the most widely used due to its simplicity (12, 27, 29), is adopted for the backcalculation method. As concluded from chapter five the moduli of the bituminous base, unbound subbase and subgrade, in addition to the interface shear reaction modulus between wearing course and base course, are the only parameters to be backcalculated.

The analysis results of the previous chapters have lead to the following assumptions for the improved backcalculation procedure:

i) Assumptions inherent in the use of layered linear elastic theory are applied (16).

ii) Deflections and load measurements are accurate.

iii) The modulus of the thin wearing course is assigned as a known value in the backcalculation process.

iv) Only the interface shear reaction modulus between the wearing and base courses ($K_{s1}$) is to be backcalculated, and all other interface conditions are assumed as full adhesion.

v) Typical values of Poisson ratios for UK pavement materials are used (37). These values are assumed to be exact. This would be seen reasonable since results show that small variations in Poisson ratios do not have any significant effect on pavement response (26,58,59).

vi) All bituminous layers except the wearing course are combined into one layer and the unbound pavement layers above the subgrade are also combined. The combination of pavement layers with similar properties has been used in many backcalculation programs to reduce the number of parameters to be predicted (27,61).

vii) The thickness of each layer is assumed to be known and exact.

viii) An apparent rigid layer is assumed at a depth of 6m from the surface to represent either bedrock or the depth where the vertical deflection is negligible (27,61). However, if the shoulder boring data or other similar information indicates the depth of bedrock, then it should be included in the backcalculation procedures. This layer is used in many backcalculation procedures to simulate the stress dependent modulus of subgrade. Research has shown that the results of the backcalculation analysis can be significantly inaccurate when not including such a layer or by not locating this stiff layer near the actual depth, particularly if the actual depth is less than 4.6m. (27). The radial modulus of the pavement

at different radial distances from the load can indicate if the rigid layer exists at shallow depth (see chapter 2).

## 6.3 THEORETICAL PAVEMENT STRUCTURE

The hypothetical theoretical pavement structure is shown in figure 6.1. The BISAR program is used to compute the deflection basin under FWD load for this pavement, and this is assumed to be the measured basin. Then the pavement parameters are backcalculated and the results compared with the hypothetical values shown in figure 6.1

### 6.3.1 Backcalculating the Theoretical Pavement Parameters Using the Method of Least Squares

This method has been used in backcalculation of the four parameters of the theoretical pavement shown in figure 6.1. The method of least squares is the most widely used optimisation process for the parameters adjustment in the backcalculation procedures (12).

The initial seed parameter values have very large influence on the backcalculation results (27), the closer the seed values to the real parameters the more likely that the results will converge to the correct solution of parameters. However, the problem of a non-unique solution still needs to be overcome in many cases.

In developing the sensitivity matrix using the forward derived differences (see section 2.5.1), it was decided to consider log ($K_{s1}$) instead of ($K_{s1}$), because the latter has little influence on the deflection basin.

Table 6.1, illustrates the results of the backcalculation process using the above iterative method. Different numerical trials have been performed to backcalculate the moduli of base, subbase and subgrade ($E_j$) and the first interface shear reaction modulus ($K_{s1}$) and these include:

i) Using different seed values for the pavement parameters.

ii) Changing the rate of parameter variation in the forward derived differences necessary for the calculation of the sensitivity matrix, where one of the following combinations are varied by 5% as explained in chapter 2:

$E_j$ and $K_{s1}$ ,
$E_j$ and Log ($K_{s1}$),
Log ($E_j$) and Log ($K_{s1}$).

iii) Changing the parameters to be backcalculated. This approach will accelerate the speed of convergence of certain parameters compared with others. The parameters considered were:

$E_j$ and $K_{s1}$ ,
$E_j$ and Log ($K_{s1}$),
Log ($E_j$) and Log ($K_{s1}$),
$E_j$ and 1/ ($K_{s1}$),
$E_j$ and $\alpha_1$ (a dimensionless parameter which represents the first interface condition given by,

$$\alpha_1 = \frac{E_1 / (1 + \nu_1)(a)(K_{s1})}{1 + [E_1 / (1 + \nu_1)(a)(K_{s1})]}$$

where (a), the diameter of the loaded area by the FWD (see reference 44)).

$E^*_j$ and $K^*_{s1}$ , (rescaled parameters). Rescaling the parameters before backcalculation has been used in the ADAM program (8). After scaling, all the parameters will be between (-1 and +1). This method will convert the parameters to the same magnitude and help to eliminate some numerical problems in the backcalculation process.

Table 6.1, demonstrates acceptable results for backcalculation of $E_3$ and $E_4$ for the subbase and subgrade respectively in most cases. However, $E_2$ and $K_{s1}$ are not very accurate compared with their theoretical values shown in figure 6.1.

### 6.3.2 Possible Reasons for the Inaccurate Results

The main reason for the inaccuracy in the above results is that both $E_2$ and $K_{s1}$ influence the same portion of the deflection basin (see the deflection sensitivity analysis in chapter 4) . To study this phenomenon, the deflections of the theoretical pavement shown in figure 6.1, are computed for different combinations of $E_2$ and $K_{s1}$ using the BISAR program. $E_2$ was varied to cover a wide range from 2000 to 10000 MPa and $K_{s1}$ varied from complete debonding (10 $MN/m^3$) to a full adhesion case ($10^5$ $MN/m^3$).

Figure 6.2, shows the deflection contours in microns, at the load centre $d_0$ and at 300 and 600 mm from it, for the pavement structures. The non-uniqueness problem can be seen in that a pavement with an $E_2$ value of 4000 MPa and $K_{s1}$ of $10^5$ $MN/m^3$ can produce the same surface deflections as a pavement with an $E_2$ value of 6000 MPa and $K_{s1}$ of 10 $MN/m^3$ . In the same manner a pavement with $E_2$ of 6000 MPa and $K_{s1}$ of $10^4$ $MN/m^3$ can produce the same surface deflections as a pavement with $E_2$ of 8000 MPa and $K_{s1}$ of 10 $MN/m^3$ .

Figure 6.3, illustrates the deflection basin of the pavement shown in figure 6.1 with $E_2$ of 6000 MPa and $K_{s1}$ of $10^5$ $MN/m^3$, and the identical basins caused by reducing the first shear reaction modulus ($K_{s1}$) to 10 $MN/m^3$, or the base modulus ($E_2$ ) to 4000 MPa.

Therefore backcalculating these deflection basins may lead to convergence to either set of values. Engineering judgement and / or additional destructive testing are currently the main means to select the correct parameters.

Roque et al (54), have studied the effect of changing the FWD test configuration to discriminate between backcalculated parameters with a similar effects on deflections. They used dual-load FWD and measured the longitudinal as well as the transverse basins to backcalculate different parameters. They found that the transverse deflection basin has been influenced in different locations by changing the pavement parameters. Therefore they used the transverse basin to predict the surface modulus, and the longitudinal basin to compute the base modulus.

A similar approach has been followed in this research to discriminate between the modulus $E_2$ and shear reaction modulus $K_{s1}$ for the theoretical pavement. Figure 6.4 shows a plan of

the dual-load FWD configuration, figures 6.5 and 6.6 demonstrate the longitudinal and the transverse basins under dual-load FWD for the same pavements shown in figure 6.3. It can be seen that the deflection basins are almost identical and therefore this approach failed to discriminate between the effect of $E_2$ and $K_{s1}$ on deflections.

De Beer et al (87), used a multidepth deflectometer under dual-load FWD to validate the backcalculation results. Theoretical study of the influence of $E_2$ and $K_{s1}$ on deflections at different depth was carried out for the same pavements shown in figure 6.3. Figure 6.7, illustrates the deflections' results at different depths from the surface. Again this approach failed to discriminate between the effect of the above parameters on deflections.

The non-unique solution problem can arise from to a number of possible factors, such as:

i) Two combinations of pavement parameters producing the same deflections.

ii) Each parameter having a different influence on deflections, e.g. ($K_{s1}$) has very little influence on deflections compared with $E_4$. $K_{s1}$ has not significantly influenced the deflections in the sensitivity matrix and therefore it was kept close to its seed value after the backcalculation process.

iii) The difference in the magnitude of the pavement parameters to be backcalculated being too large.

iv) The seed values are far from the real pavement parameters. The selection of the seed values far from the real parameters will result in convergence to a local minimum rather than to a global minimum in the optimisation process.

v) The nature of the influence of ($K_{s1}$) on deflections, i.e. ($K_{s1}$) below 10 and above $10^5$ MN/m$^3$ have no effect on deflections and therefore in the backcalculation process the program will not result in any deflection's amendment after iterations beyond these limits.

The above reasons are common to all iterative backcalculation programs except the last one, since no method backcalculates ($K_{s1}$) in the analysis process. However some programs combine different layers with the same properties to reduce the number of parameters,

eliminating parameters with little influence on deflections from the backcalculation process and using a database for the initial prediction of the seed values (12).

### 6.3.3 Suggested Solutions to the Problems

To reduce the influence of the above factors on the backcalculation results, the following can be considered:

i) Reducing the number of parameters to be backcalculated, as suggested by May and Van Quintus (27).

ii) Separating the parameters in the backcalculation procedures, each parameter being predicted from the whole deflection basin.

iii) Using the database backcalculation approach to overcome the results' sensitivity to seed values. A data bank can be developed for the analysed pavement with different combinations of the parameters.

iv) A two stage backcalculation process, first predicting the parameters which have a larger influence on deflections, then the remaining parameters.

v) Using engineering judgement to discriminate between results.

vi) Carrying out physical measurements to support the backcalculation finding, such as destructive testing on cores extracted from the pavement.

Of all the above, an improved backcalculation process was developed.

### 6.3.4 The Improved Two Stages Backcalculation Procedure

The assumptions made in section 6.2 are still applicable in the improved backcalculation procedure.

If the radial moduli of the pavement structure indicate the presence of the bedrock at shallow depth (see chapter 2), the thickness of the subgrade layer can be backcalculated as a parameter in the first stage of the procedure. Otherwise, an apparent rigid layer is assumed at 6 m depth from the pavement surface.

Figure 6.8 illustrates the flow diagram for the improved method.

The surface deflections under FWD, materials' types, layers' thickness and Poisson ratios have to be known for each pavement to be analysed.

Sensitivity study has shown that $K_{sl}$ has little influence on deflections compared with the subgrade and thick bituminous moduli (see chapter 5). Therefore the backcalculation procedure involves predicting first the parameters which have significant influence on deflections, such as subgrade, subbase and bituminous base moduli, then computing the interface shear reaction modulus between wearing and base courses with little adjustment to the bituminous layer modulus. Chapter 4 has shown that changing the interface condition has the largest effect on adjacent layers. Uzan et al (67), noticed variations in the tensile strain in adjacent layers to the interface whose properties have been changed. Therefore the subbase and subgrade were kept fixed in the second stage.

The first stage involves developing a deflections database for the analysed pavement with different combination of moduli, using any forward calculation program such as BISAR (44). The deflection locations should be selected to correspond with the sensors of the FWD. Seven locations are commonly used, at the FWD load centre and at six other radial positions with 300 mm spacing. Multi-variable regression analysis (88), for each modulus as dependent variable with the deflections as independent variables was performed. Finally, statistical models for moduli prediction from measured deflections can be found. This model is unique for each case and has to be selected carefully, i.e. the model with the highest coefficient of correlation ($R^2$) should be considered.

The search technique for the best model using the multiple regression analysis is performed in a systematic manner for each dependent parameter as follows;
firstly considering that the moduli $E_j$ are the dependent parameters whereas the independent variable are all term of $d_i$ , $1/ d_i$ , $\sqrt{d_i}$ , and $Log_{10}(d_i)$ separately and collectively

( i , deflection sensor of the FWD test),
secondly considering $1/E_j$ , $\sqrt{E_j}$ , and $Log_{10}(E_j)$ as the dependent parameters respectively with all the above combinations of the independent variable ($d_i$ ).

For each case a multi-variable regression analysis is carried out using statistical software (MINITAB)(89), which predicts a model with a coefficient of correlation to describe how well this model fits the database values. Sixteen runs for each parameter are performed and the model with the highest ($R^2$) should be selected for the modulus prediction.

Each modulus has been predicted separately from the measured deflection basin. The moduli of the lower layers need to be fixed in the next stage, therefore a good match in the deflections far from the loaded area (which control these moduli) is essential for an accurate calculation.

The second stage involves developing another deflection data base with bituminous base modulus varied by 25% from the values found from the first stage, and the first interface condition varied from complete debonding to full adhesion. The 25% variation in the bituminous layer modulus is a fine tuning to reflect the error which might occur at the first stage due to the assumption of $K_{s1}$ as $10^4$ MN/m$^3$ rather than the real value (see Chapter 4). The deflection at the loaded area and the three next deflections are to be used for the data base ( i.e. $d_{0.0}$, $d_{0.3}$ , $d_{0.6}$ and $d_{0.9}$ ), since they control the moduli and parameters of the upper layers. The calculated deflection basin which has the lowest error compared with measured values is considered for parameters' prediction.

Finally the moduli of the lower layers as found from the first stage together with the modulus of the base layer and the first interface condition as found from the second stage are considered as the backcalculated parameters.

Engineering judgement and the knowledge of the deflection sensitivity to pavement parameters are still needed to direct the process to better prediction of parameters.

The above procedure has the following advantages:

i) The database approach excludes the user selection of the seed values.

ii) The two stage procedure reduces the number of backcalculated parameters to three in this case, which can be predicted accurately if the suitable model is found from the regression analysis search technique, though the base modulus is to be adjusted in the second stage. However fixing the interface condition in the first stage at any value, preferably at the most probable value of $10^4$ MN/m$^3$ (67), will not affect the results significantly since it has little influence on deflections.

iii) Fixing the predicted $E_3$ and $E_4$ and varying $E_2$ by $\pm$ 25% in addition to $K_{s1}$ , will magnify the influence of $K_{s1}$ on deflection. Therefore a suitable model can be found for computing the two parameters in the second stage. Furthermore the data base in the second stage will cover the whole range of the interface condition from complete debonding to full adhesion and hence it forces the prediction process to the correct solution.

iv) The separation in the parameter prediction will reduce the effect of their interaction in the backcalculation process. However the data base generated by the BISAR program reflects the influence of the combination of the parameters upon the deflections.

### 6.3.5 Backcalculating the Theoretical Pavement Parameters Using the Improved Procedure

The four parameters (moduli of the bituminous base, unbound subbase and subgrade in addition to the first interface shear reaction modulus) of the theoretical pavement shown in figure 6.1 were backcalculated using the improved procedure.

BISAR is used to compute the deflection basin under 40 kN surface load for the theoretical pavement and the results are assumed as the measured basin.

The measured theoretical deflections (in microns) at different radial distances are,

$d^m_{0.0} = 444$, $d^m_{0.3} = 372$, $d^m_{0.6} = 297$, $d^m_{0.9} = 231$, $d^m_{1.2} = 177$, $d^m_{1.5} = 135$
and $d^m_{1.8} = 102$ micron

A database is developed for the three pavement moduli, i.e. bituminous base subbase and subgrade, assuming all the other parameters as constant. Layers' thickness, Poisson ratios as in figure 6.1. The interface conditions were assumed as full adhesion except $K_{s1}$ was fixed as $10^2$ MN/m$^3$. The moduli were selected to cover the whole range for the type of materials as recommended in the literature (37), and the deflections for each combination are computed using the BISAR program at the seven locations. Table 6.2, illustrates the combination of moduli with their deflection database.

The resulting models from the multi-variable regression analysis search for the above pavement are,

$$\text{Log}_{10}(E_2) = 3.6402 - 0.0039499 * d_{0.0} + 0.0011255 * d_{0.6} - 0.017751 * d_{1.2} + 0.014026 * d_{1.8} + 55.65 / d_{0.0} + 101.63 / d_{0.3} - 84.4 / d_{0.6} + 105.67 / d_{0.9} - 79.44 / d_{1.2} - 26.62 / d_{1.5} + 27.03 / d_{1.8}$$

($R^2 = 96$ %)

$$\text{Log}_{10}(E_3) = 2.2887 + 0.0022259 * d_{0.0} - 0.009775 * d_{0.6} - 0.0007 * d_{1.2} + 0.01616 * d_{1.8} + 38.75 / d_{0.0} - 58.35 / d_{0.3} + 168.32 / d_{0.6} - 62.44 / d_{0.9} - 13.74 / d_{1.2} + 19.6 / d_{1.5} - 16.12 / d_{1.8}$$

($R^2 = 72.6$ %)

$$\text{Log}_{10}(E_4) = 1.99341 - 0.00014153 * d_{0.0} - 0.0001512 * d_{0.6} - 0.001466 * d_{1.2} - 0.006114 * d_{1.8} + 3.104 / d_{0.0} + 3.581 / d_{0.3} - 3.584 / d_{0.6} - 5.348 / d_{0.9} + 8.827 / d_{1.2} + 5.315 / d_{1.5} + 0.893 / d_{1.8}$$

($R^2 = 99.9$ %)

Substituting the above measured deflections in the regression equations, the first stage moduli results can be computed as,

$E_2 = 5113$ MPa

$E_3 = 108$ MPa

$E_4 = 40$ MPa.

The new deflection data base is developed for the second stage using the BISAR program for $E_2$ and $K_{s1}$ , as shown in table 6.3.

The calculated deflection basin which has the lowest error compared with the measured basin is considered and the backcalculated values for the second stage are,

$E_2 = 3835$ MPa

$K_{s1} = 10^4$ MN/m$^3$.

And the final backcalculation results using the improved method are,

$E_2 = 3835$ MPa

$E_3 = 108$ MPa

$E_4 = 40$ MPa

$K_{s1} = 10^4$ MN/m$^3$.

These results can be considered acceptable compared with their theoretical values,

$E_2 = 4000$ MPa

$E_3 = 100$ MPa

$E_4 = 40$ MPa

$K_{s1} = 10^4$ MN/m$^3$.

## 6.4 CONCLUSIONS

For the pavement considered, the improved two stage database backcalculation method yields results which compare favourably with the theoretical parameters, especially for the parameters with little influence on deflection basin such as the first interface shear reaction modulus.

However there is a clear need to validate the above method and study its robustness. Hence three different approaches were adopted, and are explained in the next chapters, i.e.

i) Theoretical validation by comparing the backcalculation results for assumed pavements with their theoretical values. Ninety pavements were selected to cover a wide range of structures in term of thickness and materials properties.

ii) Empirical validation by comparing the backcalculated moduli for real pavements tested under FWD load and physically measured moduli.

iii) Validation by comparing the backcalculated moduli with the results from other well known programs, such as WESDEF (50) and MODULUS (51), when identical pavement conditions are assumed.

Table 6.1, Pavement backcalculation results using the method of least squares.

| Test No. | Seed Values | | | | Sensitivity matrix for; | Back calculate; | Theoretical values / Backcalculated values | | | |
|---|---|---|---|---|---|---|---|---|---|---|
| | | | | | | | $E_2$ | $E_3$ | $E_4$ | $K_{s1}$ |
| | | | | | | | 4000 | 100 | 40 | $10^4$ |
| | $E_2$ (MPa) | $E_3$ (MPa) | $E_4$ (MPa) | $K_{s1}$ ($MN/m^3$) | | | $E_2$ (MPa) | $E_3$ (MPa) | $E_4$ (MPa) | $K_{s1}$ ($MN/m^3$) |
| **1** | 2500 | 150 | 70 | $10^2$ | Ej, Log($K_{s1}$) | Ej, $K_{s1}$ | 5522 | 103 | 39 | 87 |
| **2** | 2500 | 150 | 70 | $10^2$ | Ej, Log($K_{s1}$) | Ej, Log($K_{s1}$) | 5158 | 142 | 39 | 172 |
| **3** | 2500 | 150 | 70 | $10^2$ | Log Ej, Log($K_{s1}$) | Ej, $K_{s1}$ | 3537 | 193 | 40 | 63 |
| **4** | 2500 | 150 | 70 | $10^2$ | Log Ej, Log($K_{s1}$) | Ej, Log($K_{s1}$) | 5370 | 79 | 39 | 71 |
| **5** | 2500 | 150 | 70 | $10^2$ | Ej, Log($K_{s1}$) | Ej, 1/ ($K_{s1}$) | 5490 | 103 | 39 | 117 |
| **6** | 2500 | 150 | 70 | $10^2$ | Ej, Log($K_{s1}$) | Ej, $\alpha$ | 5678 | 87 | 39 | 10 |
| **7** | 2500 | 150 | 70 | $10^2$ | Ej, Log($K_{s1}$) | Ej*, Log($K^*_{s1}$) | 1000 | 63 | 116 | 478 |
| **8** | 2500 | 100 | 70 | $10^3$ | Ej, $K_{s1}$ | Ej, $K_{s1}$ | 5029 | 82 | 40 | 577 |
| **9** | 2500 | 100 | 70 | $10^3$ | Ej, Log($K_{s1}$) | Ej, $K_{s1}$ | 3784 | 99 | 40 | $3.2*10^3$ |
| **10** | 2500 | 100 | 70 | $10^4$ | Ej, Log($K_{s1}$) | Ej, $K_{s1}$ | 3578 | 122 | 40 | $1.9*10^4$ |
| **11** | 2000 | 200 | 70 | $10^5$ | Ej, Log($K_{s1}$) | Ej, $K_{s1}$ | 708 | 340 | 38 | $1.6*10^6$ |
| **12** | 6000 | 150 | 60 | $10^3$ | Ej, Log($K_{s1}$) | Ej, $K_{s1}$ | 4723 | 107 | 39 | 566 |
| **13** | 6000 | 200 | 70 | $10^2$ | Ej, Log($K_{s1}$) | Ej, $K_{s1}$ | 5371 | 113 | 39 | 120 |
| **14** | 8000 | 60 | 30 | $10^2$ | Ej, Log($K_{s1}$) | Ej, $K_{s1}$ | 6109 | 53 | 41 | 263 |

Table 6.2, Deflection database for the hypothetical theoretical pavement with different moduli combination.

| $E_2$ MPa | $E_3$ MPa | $E_4$ MPa | $d_{0.0}$ micron | $d_{0.3}$ micron | $d_{0.6}$ micron | $d_{0.9}$ micron | $d_{1.2}$ micron | $d_{1.5}$ micron | $d_{1.8}$ micron |
|---|---|---|---|---|---|---|---|---|---|
| 1000 | 50 | 40 | 852 | 602 | 393 | 259 | 176 | 124 | 90 |
| 1000 | 150 | 40 | 668 | 465 | 325 | 233 | 171 | 126 | 95 |
| 1000 | 150 | 100 | 457 | 266 | 157 | 100 | 68 | 48 | 36 |
| 1000 | 150 | 160 | 390 | 205 | 108 | 63 | 41 | 29 | 22 |
| 1000 | 250 | 40 | 589 | 410 | 300 | 224 | 169 | 128 | 97 |
| 1000 | 250 | 100 | 399 | 230 | 144 | 97 | 68 | 49 | 37 |
| 1000 | 250 | 160 | 337 | 173 | 98 | 62 | 42 | 30 | 22 |
| 1000 | 250 | 220 | 305 | 143 | 75 | 45 | 30 | 22 | 16 |
| 3000 | 50 | 40 | 592 | 478 | 357 | 258 | 186 | 134 | 98 |
| 3000 | 150 | 40 | 499 | 399 | 305 | 230 | 173 | 130 | 98 |
| 3000 | 150 | 100 | 322 | 229 | 154 | 103 | 91 | 50 | 37 |
| 3000 | 150 | 160 | 266 | 176 | 109 | 68 | 44 | 30 | 22 |
| 3000 | 250 | 40 | 453 | 362 | 282 | 218 | 168 | 129 | 99 |
| 3000 | 250 | 100 | 289 | 204 | 141 | 98 | 70 | 51 | 38 |
| 3000 | 250 | 160 | 236 | 154 | 98 | 64 | 44 | 31 | 23 |
| 3000 | 250 | 220 | 208 | 128 | 76 | 47 | 31 | 22 | 16 |
| 5000 | 50 | 40 | 497 | 418 | 329 | 249 | 187 | 138 | 103 |
| 5000 | 150 | 40 | 432 | 361 | 287 | 223 | 172 | 132 | 101 |
| 5000 | 150 | 100 | 273 | 207 | 148 | 104 | 73 | 52 | 38 |
| 5000 | 150 | 160 | 222 | 159 | 106 | 69 | 46 | 32 | 23 |
| 5000 | 250 | 40 | 399 | 333 | 268 | 212 | 166 | 130 | 101 |
| 5000 | 250 | 100 | 250 | 188 | 137 | 98 | 71 | 52 | 38 |
| 5000 | 250 | 160 | 201 | 142 | 96 | 65 | 45 | 32 | 23 |
| 5000 | 250 | 220 | 177 | 118 | 76 | 49 | 32 | 23 | 16 |
| 7000 | 50 | 40 | 441 | 380 | 308 | 241 | 185 | 140 | 106 |
| 7000 | 150 | 40 | 391 | 334 | 273 | 217 | 170 | 132 | 102 |
| 7000 | 150 | 100 | 245 | 192 | 143 | 103 | 74 | 53 | 39 |
| 7000 | 150 | 160 | 198 | 148 | 103 | 70 | 47 | 33 | 23 |
| 7000 | 250 | 40 | 365 | 311 | 256 | 206 | 164 | 130 | 102 |
| 7000 | 250 | 100 | 226 | 177 | 132 | 97 | 71 | 53 | 39 |
| 7000 | 250 | 160 | 181 | 133 | 94 | 65 | 45 | 32 | 24 |
| 7000 | 250 | 220 | 157 | 111 | 74 | 49 | 33 | 23 | 17 |
| 9000 | 50 | 40 | 403 | 352 | 291 | 232 | 182 | 140 | 107 |
| 9000 | 150 | 40 | 362 | 314 | 261 | 211 | 168 | 132 | 103 |
| 9000 | 150 | 100 | 225 | 181 | 138 | 102 | 74 | 54 | 40 |
| 9000 | 150 | 160 | 181 | 139 | 100 | 69 | 48 | 34 | 24 |
| 9000 | 250 | 40 | 340 | 294 | 247 | 201 | 162 | 129 | 102 |
| 9000 | 250 | 100 | 210 | 167 | 128 | 96 | 72 | 53 | 40 |
| 9000 | 250 | 160 | 167 | 126 | 91 | 65 | 46 | 33 | 24 |
| 9000 | 250 | 220 | 145 | 105 | 73 | 49 | 34 | 24 | 17 |

Table 6.3, Deflection database for the second stage backcalculation procedure.

| $E_2$ MPa | $K_{s1}$ MN/m$^3$ | $d_{0.0}$ micron | $d_{0.3}$ micron | $d_{0.6}$ micron | $d_{0.9}$ micron |
|---|---|---|---|---|---|
| 3835 | 10 | 500 | 410 | 317 | 239 |
| 3835 | $10^2$ | 490 | 401 | 310 | 234 |
| 3835 | $10^3$ | 465 | 382 | 299 | 230 |
| **3835** | **$10^4$** | **444** | **371** | **296** | **230** |
| 3835 | $10^5$ | 438 | 370 | 296 | 230 |
| 5110 | 10 | 457 | 383 | 304 | 234 |
| 5110 | $10^2$ | 449 | 376 | 298 | 230 |
| 5110 | $10^3$ | 428 | 360 | 288 | 226 |
| 5110 | $10^4$ | 412 | 352 | 285 | 225 |
| 5110 | $10^5$ | 407 | 350 | 285 | 255 |
| 6390 | 10 | 425 | 362 | 292 | 229 |
| 6390 | $10^2$ | 418 | 356 | 287 | 225 |
| 6390 | $10^3$ | 401 | 342 | 279 | 221 |
| 6390 | $10^4$ | 388 | 335 | 276 | 221 |
| 6390 | $10^5$ | 383 | 334 | 276 | 211 |

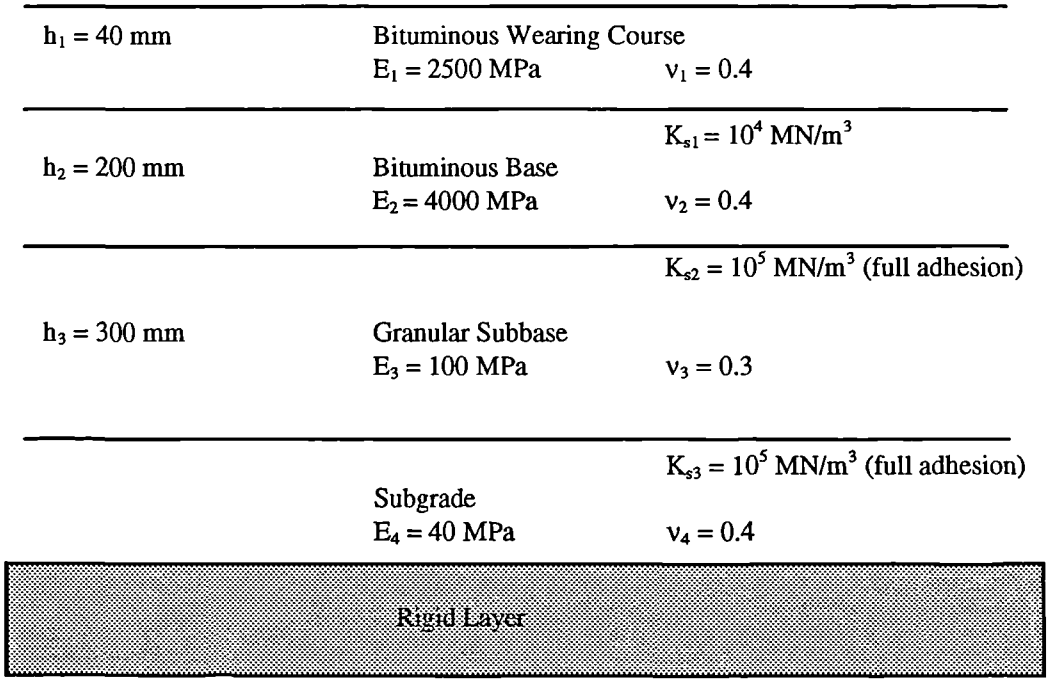


Figure 6.1, Standard pavement structure.

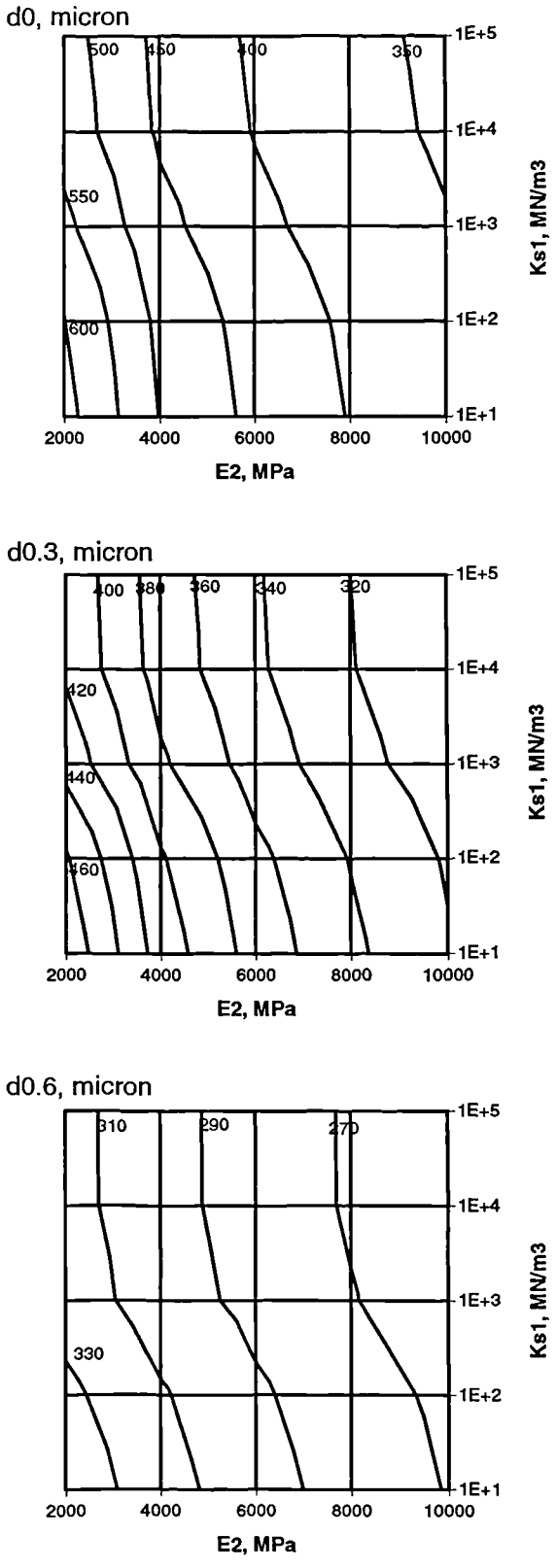


Figure 6.2, Surface deflection contours as a function of $E_2$ and $K_{s1}$.

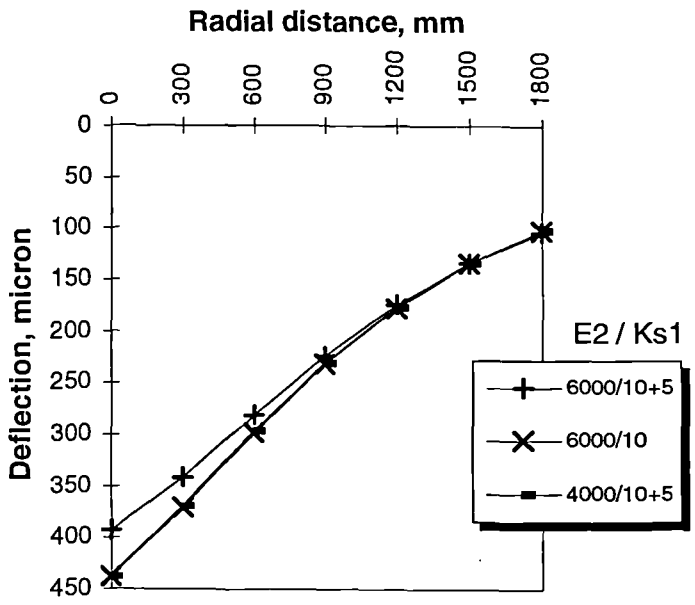


Figure 6.3, Deflection basins caused by reducing the base modulus to 4000 MPa or the first shear reaction modulus to 10 $MN/m^3$, under single load FWD.

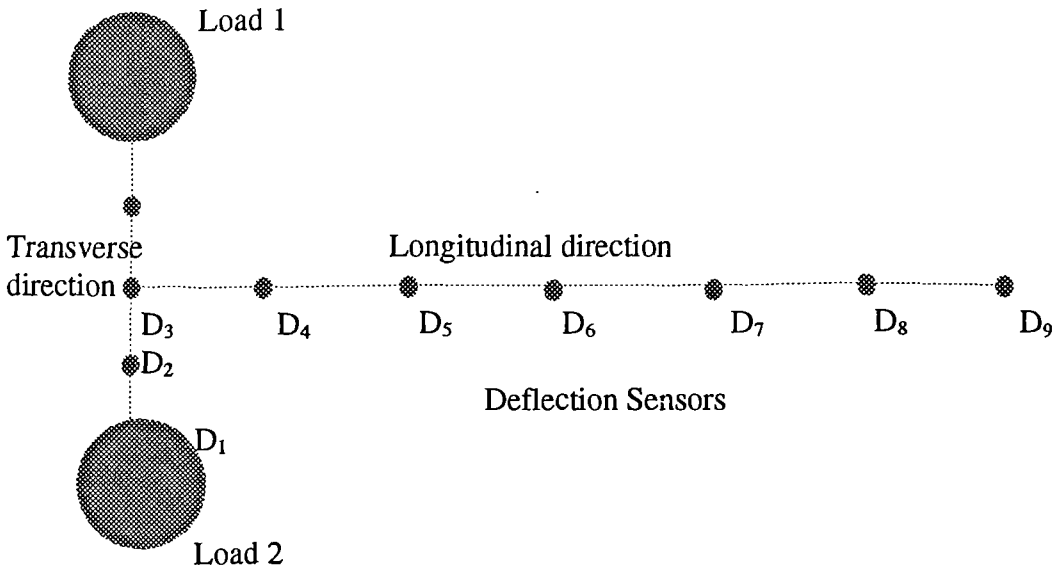


Figure 6.4, Plan view of dual load FWD system.

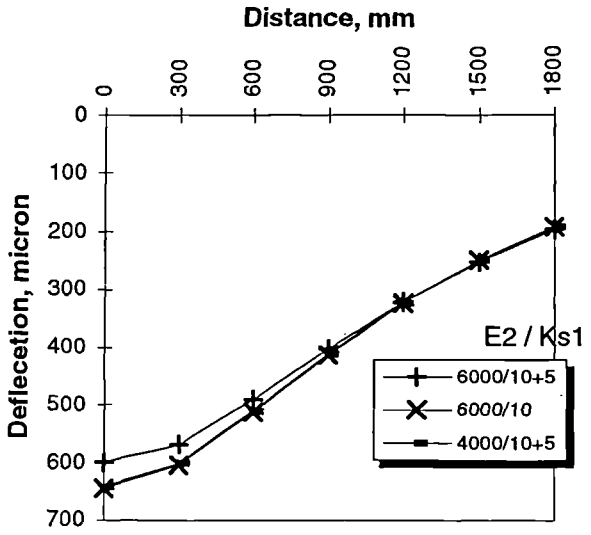


Figure 6.5, Longitudinal deflection basins caused by reducing the base modulus to 4000 MPa or the first shear reaction modulus to 10 $MN/m^3$, under dual loads FWD, (see figure 6.4).

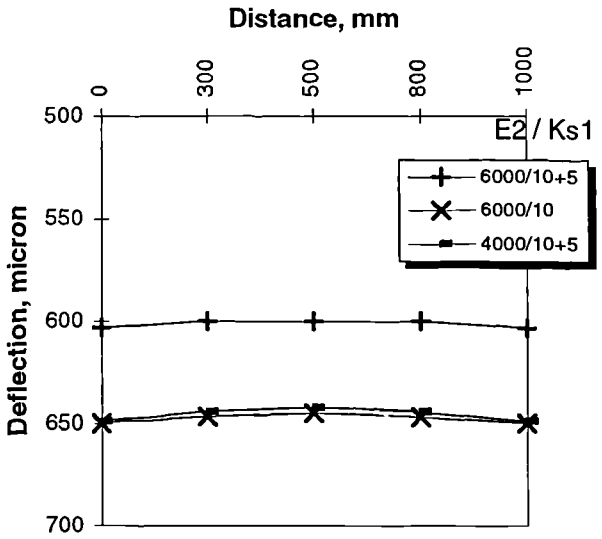


Figure 6.6, Transverse deflection basins caused by reducing the base modulus to 4000 MPa or the first shear reaction modulus to 10 MN/m$^3$, under dual loads FWD, (see figure 6.4).

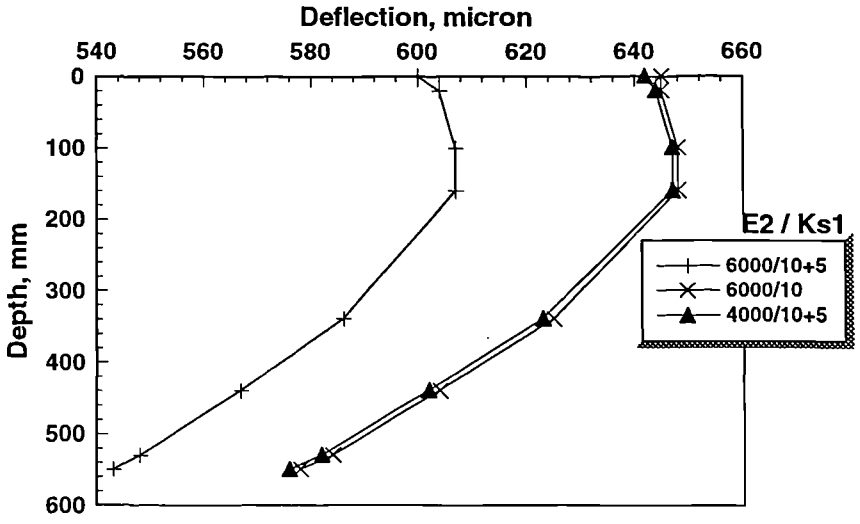


Figure 6.7, Deflection basins at different depth from the pavement surface caused by reducing the base modulus to 4000 MPa or the first shear reaction modulus to 10 MN/m$^3$, under dual loads FWD, (see figure 6.4).

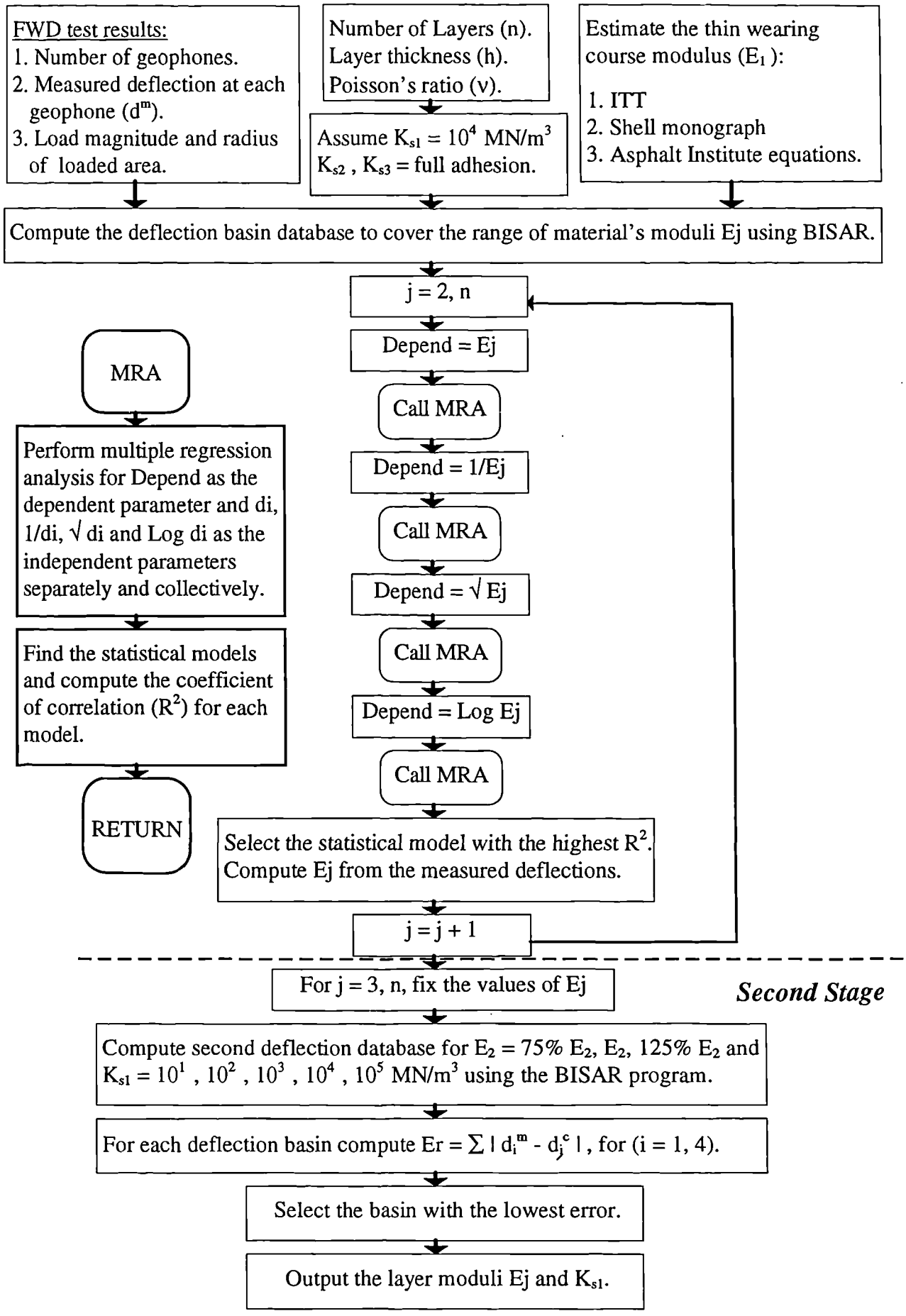


Figure 6.8, Flow chart for the improved method back-calculation procedure.

# Chapter 7

# THEORETICAL VALIDATION OF THE IMPROVED BACKCALCULATION PROCEDURE

## 7.1 INTRODUCTION

Potential errors in backcalculation are associated normally with the deflection measurement device, pavement geometry, material modelling, analysis technique and non-unique solution.

Assuming that static analysis for layered linear elastic pavement is suitable and that the FWD device can produce deflections with reasonable accuracy, the correctness of the backcalculation method depends primarily on the ability of the procedure to converge to the appropriate parameters.

The aim of this theoretical verification is to examine the capability of the inverse solution technique and the uniqueness of the solution. Therefore the improved backcalculation method is evaluated by comparing the backcalculated parameters with hypothesised values for theoretical pavements.

The pavement properties in term of layers' moduli, thickness, Poison ratios and the interface condition between layers are assumed. BISAR is used to generate a simulated deflection basin. Seven deflections are computed under a 40 kN surface load, at the load centre and at six other radial distances at 300 mm uniform spacing. This basin is considered as the measured basin under the FWD and used as input to the backcalculation procedure.

The moduli of bituminous base, subbase and subgrade in addition to the interface condition between wearing and base courses are backcalculated from this basin. The three layer moduli were computed firstly from a multiple regression analysis technique. An interface shear reaction modulus between wearing course and base is assumed as $10^4$ MN/m$^3$ in the first stage. Then a second database for the modulus of the bituminous base and the first interface condition is developed to predict the remaining two parameters, as described in Chapter 6. Finally the backcalculated parameters are compared with the theoretical assumed values to verify the backcalculation procedure.

The numerical correlations and the engineering knowledge of the materials properties are the main criteria to evaluate the success of the backcalculation methods.

## 7.2 THEORETICAL PAVEMENTS

Ninety hypothetical theoretical pavement structures are assumed to cover wide range of moduli ($E_j$), thickness ($h_j$) and the interface condition between wearing and base courses ($K_{s1}$). The thickness of wearing course, Poisson ratios, depth of bedrock and the remaining interface conditions are kept constant in all pavements as shown in table 7.1.

Nine groups of pavements are considered, each group having unique moduli values, two combinations of layers thickness and a variety of interface conditions between wearing and base courses. Two subgroups are considered according to layers' thickness, either 100 and 200 mm or 300 and 300 mm for bituminous base and granular subbase respectively. The first interface condition is changed gradually from complete debonding to full adhesion in each subgroup, with $K_{s1}$ varying as, $10^1$, $10^2$, $10^3$, $10^4$, $10^5$ MN/m$^3$ (see table 7.2).

Table 7.2 illustrates the calculation results. The four backcalculated parameters for the ninety structures are close to the theoretical assumed values from engineering point of view. However, the backcalculated moduli of the subbase are less accurate which can be explained by the fact that the contribution of this layer to the structural response of the pavement structure is small relative to that of the thick bituminous layer and subgrade (47). Therefore, it is difficult to obtain a reliable estimate of the granular layer modulus, since

even large differences in its value do not change the overall pavement load response significantly (90).

### 7.2.1 Layer Moduli Comparison

A comparison between the theoretical and backcalculated moduli is shown in figure 7.1 for the ninety pavement structures. A very high correlation of 97.7% was found between the two sets of moduli, indicating that the improved method has the capability of backcalculating the pavement parameters. However considering each layer modulus correlation individually will result in lower values. Figures 7.2 to 7.4 illustrate the correlation for base, subbase and subgrade modulus respectively.

A coefficient of correlation of 86.6% was found between the backcalculated and theoretical moduli of bituminous base, whereas the subbase moduli correlation is lower due to the reasons stated earlier, with a coefficient value of 35.7%. Figure 7.4 shows very good subgrade moduli correlation (99.9%), which is the case in most backcalculation programs due to the large influence of the subgrade on surface deflections.

### 7.2.2 Interface Bonding Condition Comparison

The theoretical interface shear reaction moduli between the wearing and base courses ($K_{s1}$) were not compared numerically with their backcalculated values. Numerical comparison for ($K_{s1}$) has some disadvantages since a large variation in the value of ($K_{s1}$) will not indicate large differences in the bonding conditions ($K_{s1}$ value of $10^5$ MN/m$^3$ is ten time bigger than $10^4$ MN/m$^3$ and they still considered as good bonding).

Therefore the range of ($K_{s1}$) was divided into three parts:

| | | |
|---|---|---|
| i) | $K_{s1} < 10^2$ MN/m$^3$ | (debonding) |
| ii) | $10^2 \leq K_{s1} \leq 10^4$ MN/m$^3$ | (intermediate case) |
| iii) | $K_{s1} > 10^4$ MN/m$^3$ | (adhesion), |

and a good estimate of the state of adhesion between wearing and base courses can be established, as weak, intermediate or strong.

Figure 7.5 presents a comparison between the theoretical and backcalculated ($K_{s1}$) on the range's basis, where the percentages of the compatibility between the estimated and theoretical values were indicated. A white space on the graph means a 'winner' case where the estimated ($K_{s1}$) has fallen within the same range part of its theoretical value. Figure 7.5 shows 62% of the ninety pavement structures as 'winners'.

Some values were predicted outside their ranges, however they can still be considered as good estimates since they are close to their theoretical values. These cases occur when the ($K_{s1}$) theoretical value is $10^5$ and predicted as $10^4$ MN/m$^3$ or the theoretical value is 10 and predicted as $10^2$ MN/m$^3$. These cases have been named as 'semi-winners' and presented as grey areas in figure 7.5. The dark spaces represent the 'losers' where the estimated results are very far from their theoretical values, (e.g. when the theoretical value of $K_{s1}$ is $10^5$ MN/m$^3$ and predicted as $10^2$ or as 10 MN/m$^3$ ). No 'loser' from the ninety analysed pavements was recorded in figure 7.5.

However, from a practical point of view, the maintenance engineer needs to know if the interface between the wearing and base courses exhibits good adhesion or poor bonding. This can established by dividing the ($K_{s1}$) range into two separate sections:

i) $K_{s1} < 10^4$ MN/m$^3$ (poor bonding)

ii) $K_{s1} \geq 10^4$ MN/m$^3$ (good bonding).

Figure 7.6, demonstrates a comparison between the predicted and the theoretical bonding condition for the ninety pavements, where 80% of the estimated results agree with their hypothetical values..

## 7.3 COMPARISON WITH OTHER BACKCALCULATION PROGRAMS

The aim of this section is;

i) to study the errors which might evolve by assuming the interface conditions as full adhesion,
ii) to verify the improved backcalculation procedure by comparing it with other programs when identical pavement conditions are assumed in the analysis process,
iii) to show the improvement in the moduli prediction result from including the first shear reaction modulus in the backcalculation process.

The same ninety deflection basins for the theoretical pavements are used to backcalculate the moduli of bituminous base, granular subbase and subgrade using different backcalculation programs. WESDEF (50) and MODULUS (51) are used assuming full adhesion between pavement layers, as is commonly found in backcalculation procedures.

These moduli should carry some errors to compensate for modelling the first interface condition as full adhesion rather than the actual value.

Table 7.3, illustrates the comparison between the theoretical and backcalculated moduli using the improved, WESDEF and MODULUS programs for the ninety pavements.

Figures 7.7, 7.8 and 7.9, demonstrate the relative error in predicting the moduli of bituminous base, subbase and subgrade respectively, using the improved and WESDEF programs for the ninety structures.

Table 7.3 and figure 7.7 show that the backcalculated modulus of bituminous base is most affected by first interface condition modelling errors. The weaker the pavement the larger the reduction in the modulus values, and the closer the real interface condition to the assumed values ( full adhesion with $K_{s1} = 10^5$ MN/m$^3$) , the lower the effect on backcalculated base modulus. Up to 60% reduction in base modulus was recorded in the extreme cases using the WESDEF program to compensate the modelling error. Therefore an improvement of up to 40% was observed in base modulus when complete debonding occurs.

The estimated moduli of subbase and subgrade have not been affected by the above modelling error (see figures 7.8 and 7.9), however the results show some scattered values for subbase moduli in all backcalculation programs. This conclusion will validate the

assumption made in the improved backcalculation procedure, of fixing the moduli of lower layers in the second stage and tuning only the base modulus and the interface condition (see chapter 6).

The backcalculated results of the theoretical pavements having full adhesion between wearing and base courses ($K_{s1} = 10^5$ MN/m$^3$), i.e. pavement's number with their last digit as a (5), are compared for different backcalculation methods. Figure 7.10, illustrates a comparison between the improved method and WESDEF moduli for the eighteen pavements with full adhesion between layers. Similarly figure 7.11 shows the comparison between the improved procedure and MODULUS moduli.

Very good correlation between the improved method and both WESDEF and MODULUS results can be seen in figures 7.10 and 7.11 for the eighteen pavements. Coefficients of correlation of more than 97% were observed for both cases, hence the improved backcalculation method has been validated by comparing its results with other known programs.

Table 7.3 also presents the improvement in the backcalculated moduli over the conventional methods, when the interface condition between wearing and base courses is considered in the backcalculation process. This improvement was mostly noticed when complete debonding occurs between wearing and base courses.

Figures 7.12 to 7.15 demonstrate the relationship between the hypothetical moduli and the WESDEF backcalculated values for the three layers together, the bituminous base, subbase and subgrade respectively. In the same manner the comparisons were presented for the ninety structures using MODULUS program in figure 7.16 to 7.19.

Coefficients of correlation of 86.5% and 85.8% for all the moduli were recorded for WEDDEF and MODULUS program respectively, compared with 97.7% using the improved method.

Considering each modulus relationship individually, coefficient values of 42.7% and 41.3% were found for bituminous base using WESDEF and MODULUS respectively, compared

with 84.6% for the improved method. These low values are mainly due to the first interface condition modelling error which affects mostly the adjacent layers.

Coefficients of 35.9% and 23.2% were predicted for subbase modulus relationship whereas 99.8% and 99.4% were found for subgrade moduli using WESDEF and MODULUS respectively. On the other hand the improved method coefficients of 35.7% and 99.9% were presented in figure 7.3 and 7.4 for subbase and subgrade respectively.

No improvement was noticed for both the subbase and subgrade since ($K_{s1}$) has no influence on lower layer moduli. The poor agreement between the backcalculated moduli of subbase and their theoretical values using the three procedures is explained earlier in this chapter.

Therefore the improved method has advantages in predicting the layers moduli if the bonding conditions were not perfect between the wearing and base courses. The improvement was mainly noticed in the estimation of bituminous modulus, where up to 40% improvement was recorded. The subbase and subgrade moduli were predicted with the same accuracy as the conventional methods.

## 7.4 SUMMARY

Flexible pavement's evaluation using the FWD and backcalculation of moduli, assuming full adhesion between layers may cause some errors in the predicted moduli.

The backcalculated modulus of the bituminous base was most affected by the first interface condition modelling errors, the modulus of subbase was not significantly influenced, whereas the subgrade was not affected by the above errors.

The improved backcalculation procedure has been verified by comparing the backcalculated parameters with hypothesised values for theoretical pavements.

The improved backcalculation method has been also validated by comparing the backcalculated moduli with other programs' results, i.e. WESDEF and MODULUS.

Employing the improved method will result in a better moduli prediction compared with the conventional programs. Moreover, the ability of this method to detect poor bonding between the wearing and base course can demonstrate the improvement achieved by the developed procedure.

Table 7.1, Properties of hypothetical theoretical pavement structures.

| Layer | Category | Properties |
|---|---|---|
| Bituminous wearing course | Modulus (MPa)<br>Thickness (mm)<br>Poisson ratio<br>$K_{s1}$ ($MN/m^3$) | 2500, 5000, 7500<br>40<br>0.4<br>10, $10^2$, $10^3$, $10^4$, $10^5$ |
| Bituminous base | Modulus (MPa)<br>Thickness (mm)<br>Poisson ratio<br>$K_{s2}$ ($MN/m^3$) | 4000, 7000, 10000<br>100, 300<br>0.4<br>$10^5$ |
| Granular subbase | Modulus (MPa)<br>Thickness (mm)<br>Poisson ratio<br>$K_{s3}$ ($MN/m^3$) | 100, 150, 200<br>200, 300<br>0.3<br>$10^5$ |
| Subgrade | Modulus (MPa)<br>Thickness (mm)<br>Poisson ratio | 40, 80, 120, 160<br>6000 - (pavement thickness)<br>0.4 |

Table 7.2, Theoretical and backcalculated parameters for structures 2, 3 and 4.

| | | | Theoretical Parameters | | | | | Backcalculated Parameters | | | |
|---|---|---|---|---|---|---|---|---|---|---|---|
| St.No. | $h_2$ mm | $h_3$ mm | $E_1$ MPa | $E_2$ MPa | $E_3$ MPa | $E_4$ MPa | $K_{s1}$ MN/m$^3$ | $E_2$ MPa | $E_3$ MPa | $E_4$ MPa | $K_{s1}$ MN/m$^3$ |
| 2A-1 | 100 | 200 | 2500 | 4000 | 100 | 40 | $10^1$ | 3340 | 65 | 40 | $10^3$ |
| 2A-2 | | | | | | | $10^2$ | 3970 | 68 | 40 | $10^3$ |
| 2A-3 | | | | | | | $10^3$ | 4040 | 87 | 40 | $10^3$ |
| 2A-4 | | | | | | | $10^4$ | 4900 | 77 | 40 | $10^4$ |
| 2A-5 | | | | | | | $10^5$ | 6235 | 73 | 40 | $10^4$ |
| 2B-1 | 300 | 300 | 2500 | 4000 | 100 | 40 | $10^1$ | 4010 | 96 | 41 | $10^1$ |
| 2B-2 | | | | | | | $10^2$ | 4010 | 111 | 41 | $10^1$ |
| 2B-3 | | | | | | | $10^3$ | 4350 | 130 | 39 | $10^2$ |
| 2B-4 | | | | | | | $10^4$ | 4125 | 123 | 40 | $10^3$ |
| 2B-5 | | | | | | | $10^5$ | 3650 | 114 | 40 | $10^5$ |
| 3A-1 | 100 | 200 | 5000 | 7000 | 150 | 40 | $10^1$ | 6350 | 66 | 41 | $10^3$ |
| 3A-2 | | | | | | | $10^2$ | 6390 | 75 | 41 | $10^3$ |
| 3A-3 | | | | | | | $10^3$ | 4050 | 129 | 40 | $10^4$ |
| 3A-4 | | | | | | | $10^4$ | 6455 | 155 | 40 | $10^4$ |
| 3A-5 | | | | | | | $10^5$ | 8160 | 145 | 40 | $10^4$ |
| 3B-1 | 300 | 300 | 5000 | 7000 | 150 | 40 | $10^1$ | 6790 | 114 | 40 | $10^2$ |
| 3B-2 | | | | | | | $10^2$ | 7930 | 106 | 41 | $10^1$ |
| 3B-3 | | | | | | | $10^3$ | 6160 | 147 | 40 | $10^5$ |
| 3B-4 | | | | | | | $10^4$ | 6740 | 151 | 40 | $10^5$ |
| 3B-5 | | | | | | | $10^5$ | 7630 | 147 | 40 | $10^3$ |
| 4A-1 | 100 | 200 | 7500 | 10000 | 200 | 40 | $10^1$ | 9865 | 91 | 41 | $10^3$ |
| 4A-2 | | | | | | | $10^2$ | 9590 | 118 | 41 | $10^3$ |
| 4A-3 | | | | | | | $10^3$ | 9835 | 226 | 40 | $10^3$ |
| 4A-4 | | | | | | | $10^4$ | 11795 | 171 | 40 | $10^4$ |
| 4A-5 | | | | | | | $10^5$ | 10390 | 180 | 40 | $10^5$ |
| 4B-1 | 300 | 300 | 7500 | 10000 | 200 | 40 | $10^1$ | 10230 | 100 | 40 | $10^2$ |
| 4B-2 | | | | | | | $10^2$ | 10435 | 101 | 41 | $10^2$ |
| 4B-3 | | | | | | | $10^3$ | 9035 | 141 | 41 | $10^4$ |
| 4B-4 | | | | | | | $10^4$ | 11590 | 180 | 40 | $10^3$ |
| 4B-5 | | | | | | | $10^5$ | 11330 | 151 | 41 | $10^3$ |

Table 7.2 ( cont.), Theoretical and backcalculated parameters for structures 5, 6 and 7.

| | | | Theoretical Parameters | | | | | Backcalculated Parameters | | | |
|---|---|---|---|---|---|---|---|---|---|---|---|
| St.No. | $h_2$ mm | $h_3$ mm | $E_1$ MPa | $E_2$ MPa | $E_3$ MPa | $E_4$ MPa | $K_{s1}$ MN/m$^3$ | $E_2$ MPa | $E_3$ MPa | $E_4$ MPa | $K_{s1}$ MN/m$^3$ |
| 5A-1 | 100 | 200 | 2500 | 4000 | 100 | 80 | $10^1$ | 3175 | 90 | 80 | $10^3$ |
| 5A-2 | | | | | | | $10^2$ | 3250 | 92 | 80 | $10^3$ |
| 5A-3 | | | | | | | $10^3$ | 4210 | 99 | 80 | $10^3$ |
| 5A-4 | | | | | | | $10^4$ | 3570 | 94 | 80 | $10^5$ |
| 5A-5 | | | | | | | $10^5$ | 4675 | 95 | 80 | $10^5$ |
| 5B-1 | 300 | 300 | 2500 | 4000 | 100 | 80 | $10^1$ | 3925 | 95 | 80 | $10^2$ |
| 5B-2 | | | | | | | $10^2$ | 3840 | 110 | 80 | $10^2$ |
| 5B-3 | | | | | | | $10^3$ | 4150 | 145 | 78 | $10^2$ |
| 5B-4 | | | | | | | $10^4$ | 4250 | 125 | 79 | $10^3$ |
| 5B-5 | | | | | | | $10^5$ | 4600 | 107 | 79 | $10^3$ |
| 6A-1 | 100 | 200 | 5000 | 7000 | 150 | 80 | $10^1$ | 6420 | 93 | 81 | $10^3$ |
| 6A-2 | | | | | | | $10^2$ | 6360 | 100 | 81 | $10^3$ |
| 6A-3 | | | | | | | $10^3$ | 5150 | 131 | 81 | $10^4$ |
| 6A-4 | | | | | | | $10^4$ | 6570 | 159 | 80 | $10^4$ |
| 6A-5 | | | | | | | $10^5$ | 6996 | 150 | 80 | $10^5$ |
| 6B-1 | 300 | 300 | 5000 | 7000 | 150 | 80 | $10^1$ | 6540 | 98 | 81 | $10^3$ |
| 6B-2 | | | | | | | $10^2$ | 6640 | 101 | 82 | $10^3$ |
| 6B-3 | | | | | | | $10^3$ | 6040 | 141 | 82 | $10^4$ |
| 6B-4 | | | | | | | $10^4$ | 8630 | 162 | 80 | $10^2$ |
| 6B-5 | | | | | | | $10^5$ | 6785 | 134 | 82 | $10^5$ |
| 7A-1 | 100 | 200 | 7500 | 10000 | 200 | 80 | $10^1$ | 8230 | 144 | 82 | $10^3$ |
| 7A-2 | | | | | | | $10^2$ | 9710 | 163 | 82 | $10^2$ |
| 7A-3 | | | | | | | $10^3$ | 9650 | 208 | 82 | $10^3$ |
| 7A-4 | | | | | | | $10^4$ | 9515 | 182 | 81 | $10^4$ |
| 7A-5 | | | | | | | $10^5$ | 10885 | 157 | 82 | $10^5$ |
| 7B-1 | 300 | 300 | 7500 | 10000 | 200 | 80 | $10^1$ | 10345 | 127 | 81 | $10^2$ |
| 7B-2 | | | | | | | $10^2$ | 10895 | 111 | 83 | $10^2$ |
| 7B-3 | | | | | | | $10^3$ | 11105 | 167 | 82 | $10^2$ |
| 7B-4 | | | | | | | $10^4$ | 8290 | 197 | 81 | $10^5$ |
| 7B-5 | | | | | | | $10^5$ | 11585 | 176 | 82 | $10^3$ |

Table 7.2 (cont.), Theoretical and backcalculated parameters for structures 8, 9 and 10.

| | | | Theoretical Parameters | | | | | Backcalculated Parameters | | | |
|---|---|---|---|---|---|---|---|---|---|---|---|
| St.No. | $h_2$ mm | $h_3$ mm | $E_1$ MPa | $E_2$ MPa | $E_3$ MPa | $E_4$ MPa | $K_{s1}$ MN/m$^3$ | $E_2$ MPa | $E_3$ MPa | $E_4$ MPa | $K_{s1}$ MN/m$^3$ |
| 8A-1 | 100 | 200 | 5000 | 7000 | 150 | 120 | $10^1$ | 6610 | 102 | 121 | $10^3$ |
| 8A-2 | | | | | | | $10^2$ | 6625 | 110 | 121 | $10^3$ |
| 8A-3 | | | | | | | $10^3$ | 6590 | 140 | 119 | $10^3$ |
| 8A-4 | | | | | | | $10^4$ | 6875 | 165 | 121 | $10^4$ |
| 8A-5 | | | | | | | $10^5$ | 7540 | 157 | 120 | $10^5$ |
| 8B-1 | 300 | 300 | 5000 | 7000 | 150 | 120 | $10^1$ | 8400 | 65 | 122 | $10^3$ |
| 8B-2 | | | | | | | $10^2$ | 7446 | 89 | 122 | $10^3$ |
| 8B-3 | | | | | | | $10^3$ | 5995 | 174 | 119 | $10^4$ |
| 8B-4 | | | | | | | $10^4$ | 6940 | 171 | 118 | $10^4$ |
| 8B-5 | | | | | | | $10^5$ | 8265 | 132 | 121 | $10^3$ |
| 9A-1 | 100 | 200 | 7500 | 10000 | 200 | 120 | $10^1$ | 10145 | 177 | 120 | $10^2$ |
| 9A-2 | | | | | | | $10^2$ | 8000 | 183 | 121 | $10^3$ |
| 9A-3 | | | | | | | $10^3$ | 9710 | 189 | 122 | $10^3$ |
| 9A-4 | | | | | | | $10^4$ | 8370 | 226 | 121 | $10^4$ |
| 9A-5 | | | | | | | $10^5$ | 12150 | 197 | 121 | $10^4$ |
| 9B-1 | 300 | 300 | 7500 | 10000 | 200 | 120 | $10^1$ | 10210 | 118 | 123 | $10^3$ |
| 9B-2 | | | | | | | $10^2$ | 9845 | 145 | 121 | $10^3$ |
| 9B-3 | | | | | | | $10^3$ | 10400 | 190 | 120 | $10^3$ |
| 9B-4 | | | | | | | $10^4$ | 10055 | 195 | 122 | $10^4$ |
| 9B-5 | | | | | | | $10^5$ | 11205 | 176 | 120 | $10^4$ |
| 10A-1 | 100 | 200 | 7500 | 10000 | 200 | 160 | $10^1$ | 7965 | 109 | 161 | $10^4$ |
| 10A-2 | | | | | | | $10^2$ | 8070 | 119 | 162 | $10^4$ |
| 10A-3 | | | | | | | $10^3$ | 9835 | 215 | 158 | $10^4$ |
| 10A-4 | | | | | | | $10^4$ | 10475 | 200 | 160 | $10^4$ |
| 10A-5 | | | | | | | $10^5$ | 12960 | 188 | 162 | $10^4$ |
| 10B-1 | 300 | 300 | 7500 | 10000 | 200 | 160 | $10^1$ | 10175 | 122 | 160 | $10^3$ |
| 10B-2 | | | | | | | $10^2$ | 9810 | 152 | 161 | $10^3$ |
| 10B-3 | | | | | | | $10^3$ | 8265 | 215 | 160 | $10^4$ |
| 10B-4 | | | | | | | $10^4$ | 10480 | 179 | 161 | $10^4$ |
| 10B-5 | | | | | | | $10^5$ | 11730 | 162 | 162 | $10^3$ |

Table 7.3, Comparison between theoretical and backcalculated moduli using different programs ( Improved, WESDEF and MODULUS ), for structures 2,3 and 4.

| | $E_2$ (MPa) | | | | $E_3$ (MPa) | | | | $E_4$ (MPa) | | | |
|---|---|---|---|---|---|---|---|---|---|---|---|---|
| St. No. | Theo. | Imp. | WES. | MOD. | Theo. | Imp. | WES. | MOD. | Theo. | Imp. | WES. | MOD |
| 2A-1 | 4000 | 3340 | 1321 | 1686 | 100 | 65 | 76 | 69 | 40 | 40 | 40 | 41 |
| 2A-2 | 4000 | 3970 | 1622 | 1662 | 100 | 68 | 77 | 77 | 40 | 40 | 40 | 41 |
| 2A-3 | 4000 | 4040 | 1641 | 1784 | 100 | 87 | 115 | 109 | 40 | 40 | 40 | 40 |
| 2A-4 | 4000 | 4900 | 2782 | 2865 | 100 | 77 | 122 | 122 | 40 | 40 | 40 | 39 |
| 2A-5 | 4000 | 6235 | 3738 | 3865 | 100 | 73 | 109 | 122 | 40 | 40 | 40 | 39 |
| 2B-1 | 4000 | 4010 | 3064 | 3316 | 100 | 96 | 74 | 44 | 40 | 41 | 40 | 43 |
| 2B-2 | 4000 | 4010 | 3022 | 3473 | 100 | 111 | 101 | 48 | 40 | 41 | 40 | 43 |
| 2B-3 | 4000 | 4350 | 3128 | 3219 | 100 | 130 | 180 | 146 | 40 | 39 | 38 | 39 |
| 2B-4 | 4000 | 4125 | 3550 | 3752 | 100 | 123 | 162 | 115 | 40 | 40 | 39 | 39 |
| 2B-5 | 4000 | 3650 | 3803 | 4458 | 100 | 114 | 135 | 46 | 40 | 40 | 39 | 42 |
| 3A-1 | 7000 | 6350 | 2630 | 2923 | 150 | 66 | 100 | 83 | 40 | 41 | 40 | 41 |
| 3A-2 | 7000 | 6390 | 2677 | 2923 | 150 | 75 | 111 | 90 | 40 | 41 | 40 | 41 |
| 3A-3 | 7000 | 4050 | 2475 | 2892 | 150 | 129 | 176 | 142 | 40 | 40 | 40 | 41 |
| 3A-4 | 7000 | 6455 | 4031 | 4068 | 150 | 155 | 214 | 199 | 40 | 40 | 40 | 39 |
| 3A-5 | 7000 | 8160 | 6373 | 7005 | 150 | 145 | 174 | 139 | 40 | 40 | 40 | 40 |
| 3B-1 | 7000 | 6790 | 5252 | 5783 | 150 | 114 | 124 | 45 | 40 | 40 | 40 | 43 |
| 3B-2 | 7000 | 7930 | 5315 | 6181 | 150 | 106 | 152 | 38 | 40 | 41 | 40 | 44 |
| 3B-3 | 7000 | 6160 | 5392 | 5945 | 150 | 147 | 253 | 139 | 40 | 40 | 40 | 41 |
| 3B-4 | 7000 | 6740 | 6105 | 6581 | 150 | 151 | 265 | 152 | 40 | 40 | 39 | 40 |
| 3B-5 | 7000 | 7630 | 6825 | 6448 | 150 | 147 | 181 | 205 | 40 | 40 | 40 | 39 |
| 4A-1 | 10000 | 9865 | 3894 | 3940 | 200 | 91 | 105 | 106 | 40 | 41 | 40 | 41 |
| 4A-2 | 10000 | 9590 | 3769 | 4023 | 200 | 118 | 118 | 109 | 40 | 41 | 41 | 41 |
| 4A-3 | 10000 | 9835 | 3420 | 3968 | 200 | 226 | 204 | 172 | 40 | 40 | 40 | 41 |
| 4A-4 | 10000 | 11795 | 5419 | 5400 | 200 | 171 | 274 | 269 | 40 | 40 | 40 | 40 |
| 4A-5 | 10000 | 10390 | 8842 | 10214 | 200 | 180 | 234 | 178 | 40 | 40 | 40 | 40 |
| 4B-1 | 10000 | 10230 | 7447 | 7577 | 200 | 100 | 145 | 104 | 40 | 40 | 40 | 41 |
| 4B-2 | 10000 | 10435 | 7667 | 7324 | 200 | 101 | 154 | 109 | 40 | 41 | 41 | 41 |
| 4B-3 | 10000 | 9035 | 7734 | 8613 | 200 | 141 | 260 | 119 | 40 | 41 | 41 | 42 |
| 4B-4 | 10000 | 11590 | 8313 | 10808 | 200 | 180 | 353 | 43 | 40 | 40 | 40 | 44 |
| 4B-5 | 10000 | 11330 | 9667 | 9151 | 200 | 151 | 244 | 266 | 40 | 41 | 40 | 39 |

Table 7.3 (cont.), Comparison between theoretical and backcalculated moduli using different programs ( Improved, WESDEF and MODULUS ), for structures 5,6 and 7.

| | $E_2$ (MPa) | | | | $E_3$ (MPa) | | | | $E_4$ (MPa) | | | |
|---|---|---|---|---|---|---|---|---|---|---|---|---|
| St. No. | Theo. | Imp. | WES. | MOD. | Theo. | Imp. | WES. | MOD. | Theo. | Imp. | WES. | MOD. |
| 5A-1 | 4000 | 3175 | 1621 | 1693 | 100 | 90 | 76 | 75 | 80 | 80 | 83 | 82 |
| 5A-2 | 4000 | 3250 | 1642 | 1694 | 100 | 92 | 79 | 79 | 80 | 80 | 83 | 82 |
| 5A-3 | 4000 | 4210 | 1781 | 1807 | 100 | 99 | 104 | 106 | 80 | 80 | 81 | 80 |
| 5A-4 | 4000 | 3570 | 3017 | 2922 | 100 | 94 | 107 | 118 | 80 | 80 | 81 | 79 |
| 5A-5 | 4000 | 4675 | 3842 | 3855 | 100 | 95 | 102 | 108 | 80 | 80 | 80 | 79 |
| 5B-1 | 4000 | 3925 | 3079 | 3108 | 100 | 95 | 80 | 74 | 80 | 80 | 83 | 84 |
| 5B-2 | 4000 | 3840 | 3033 | 2986 | 100 | 110 | 101 | 104 | 80 | 80 | 81 | 82 |
| 5B-3 | 4000 | 4150 | 3114 | 3212 | 100 | 145 | 143 | 132 | 80 | 78 | 79 | 80 |
| 5B-4 | 4000 | 4250 | 3737 | 3900 | 100 | 125 | 114 | 99 | 80 | 79 | 80 | 82 |
| 5B-5 | 4000 | 4600 | 4031 | 4172 | 100 | 107 | 94 | 72 | 80 | 79 | 81 | 85 |
| 6A-1 | 7000 | 6420 | 2765 | 2953 | 150 | 93 | 105 | 92 | 80 | 81 | 80 | 82 |
| 6A-2 | 7000 | 6360 | 2718 | 2880 | 150 | 100 | 112 | 100 | 80 | 81 | 80 | 82 |
| 6A-3 | 7000 | 5150 | 2695 | 952 | 150 | 131 | 165 | 95 | 80 | 81 | 79 | 317 |
| 6A-4 | 7000 | 6570 | 4162 | 4294 | 150 | 159 | 206 | 191 | 80 | 80 | 79 | 79 |
| 6A-5 | 7000 | 6996 | 6398 | 6446 | 150 | 150 | 172 | 163 | 80 | 80 | 79 | 79 |
| 6B-1 | 7000 | 6540 | 5405 | 5683 | 150 | 98 | 112 | 74 | 80 | 81 | 80 | 86 |
| 6B-2 | 7000 | 6640 | 5153 | 5384 | 150 | 101 | 162 | 124 | 80 | 82 | 80 | 82 |
| 6B-3 | 7000 | 6040 | 5444 | 5714 | 150 | 141 | 227 | 177 | 80 | 82 | 79 | 80 |
| 6B-4 | 7000 | 8630 | 5979 | 6341 | 150 | 162 | 258 | 188 | 80 | 80 | 78 | 79 |
| 6B-5 | 7000 | 6785 | 6754 | 7610 | 150 | 134 | 200 | 81 | 80 | 82 | 78 | 85 |
| 7A-1 | 10000 | 8230 | 3792 | 3986 | 200 | 144 | 125 | 122 | 80 | 82 | 81 | 81 |
| 7A-2 | 10000 | 9710 | 3868 | 4070 | 200 | 163 | 128 | 123 | 80 | 82 | 81 | 82 |
| 7A-3 | 10000 | 9650 | 3705 | 4083 | 200 | 208 | 189 | 71 | 80 | 82 | 81 | 81 |
| 7A-4 | 10000 | 9515 | 5357 | 5357 | 200 | 182 | 259 | 267 | 80 | 81 | 80 | 79 |
| 7A-5 | 10000 | 10885 | 8878 | 8813 | 200 | 157 | 238 | 226 | 80 | 82 | 80 | 79 |
| 7B-1 | 10000 | 10345 | 7503 | 8037 | 200 | 127 | 183 | 98 | 80 | 81 | 79 | 83 |
| 7B-2 | 10000 | 10895 | 7869 | 8259 | 200 | 111 | 154 | 86 | 80 | 83 | 81 | 85 |
| 7B-3 | 10000 | 11105 | 7451 | 7896 | 200 | 167 | 337 | 243 | 80 | 82 | 79 | 79 |
| 7B-4 | 10000 | 8290 | 8161 | 9658 | 200 | 197 | 415 | 117 | 80 | 81 | 78 | 81 |
| 7B-5 | 10000 | 11585 | 9405 | 10928 | 200 | 176 | 297 | 92 | 80 | 82 | 78 | 84 |

Table 7.3 (cont.), Comparison between theoretical and backcalculated moduli using different programs ( Improved, WESDEF and MODULUS ), for structures 8, 9 and 10.

| | $E_2$ (MPa) | | | | $E_3$ (MPa) | | | | $E_4$ (MPa) | | | |
|---|---|---|---|---|---|---|---|---|---|---|---|---|
| St. No. | Theo. | Imp. | WES. | MOD. | Theo. | Imp. | WES. | MOD. | Theo. | Imp. | WES. | MOD |
| 8A-1 | 7000 | 6610 | 2814 | 2763 | 150 | 102 | 108 | 111 | 120 | 121 | 119 | 123 |
| 8A-2 | 7000 | 6625 | 2801 | 2809 | 150 | 110 | 114 | 113 | 120 | 121 | 120 | 123 |
| 8A-3 | 7000 | 6590 | 2873 | 2988 | 150 | 140 | 151 | 139 | 120 | 119 | 119 | 122 |
| 8A-4 | 7000 | 6875 | 4525 | 4250 | 150 | 165 | 180 | 186 | 120 | 121 | 117 | 118 |
| 8A-5 | 7000 | 7540 | 6925 | 6514 | 150 | 157 | 155 | 165 | 120 | 120 | 117 | 119 |
| 8B-1 | 7000 | 8400 | 5430 | 5696 | 150 | 65 | 117 | 79 | 120 | 122 | 119 | 134 |
| 8B-2 | 7000 | 7446 | 5296 | 5465 | 150 | 89 | 158 | 106 | 120 | 122 | 116 | 128 |
| 8B-3 | 7000 | 5995 | 5449 | 5874 | 150 | 174 | 205 | 129 | 120 | 119 | 117 | 125 |
| 8B-4 | 7000 | 6940 | 5914 | 6021 | 150 | 171 | 272 | 230 | 120 | 118 | 114 | 117 |
| 8B-5 | 7000 | 8265 | 6792 | 7138 | 150 | 132 | 190 | 125 | 120 | 121 | 116 | 123 |
| 9A-1 | 10000 | 10145 | 3723 | 3999 | 200 | 177 | 140 | 127 | 120 | 120 | 121 | 123 |
| 9A-2 | 10000 | 8000 | 3686 | 3970 | 200 | 183 | 149 | 135 | 120 | 121 | 121 | 123 |
| 9A-3 | 10000 | 9710 | 3951 | 4114 | 200 | 189 | 184 | 174 | 120 | 122 | 120 | 117 |
| 9A-4 | 10000 | 8370 | 5795 | 5591 | 200 | 226 | 243 | 252 | 120 | 121 | 118 | 119 |
| 9A-5 | 10000 | 12150 | 9303 | 8754 | 200 | 197 | 209 | 234 | 120 | 121 | 118 | 118 |
| 9B-1 | 10000 | 10210 | 7600 | 8069 | 200 | 118 | 160 | 92 | 120 | 123 | 119 | 132 |
| 9B-2 | 10000 | 9845 | 7542 | 7220 | 200 | 145 | 209 | 209 | 120 | 121 | 116 | 119 |
| 9B-3 | 10000 | 10400 | 7851 | 7813 | 200 | 190 | 249 | 236 | 120 | 120 | 118 | 120 |
| 9B-4 | 10000 | 10055 | 8899 | 8484 | 200 | 195 | 326 | 297 | 120 | 122 | 114 | 118 |
| 9B-5 | 10000 | 11205 | 9605 | 9272 | 200 | 176 | 314 | 290 | 120 | 120 | 114 | 116 |
| 10A-1 | 10000 | 7965 | 3730 | 3986 | 200 | 109 | 148 | 139 | 160 | 161 | 163 | 166 |
| 10A-2 | 10000 | 8070 | 3725 | 3971 | 200 | 119 | 152 | 142 | 160 | 162 | 163 | 166 |
| 10A-3 | 10000 | 9835 | 3748 | 4148 | 200 | 215 | 194 | 172 | 160 | 158 | 160 | 163 |
| 10A-4 | 10000 | 10475 | 5668 | 5468 | 200 | 200 | 249 | 259 | 160 | 160 | 158 | 157 |
| 10A-5 | 10000 | 12960 | 8699 | 8888 | 200 | 188 | 220 | 224 | 160 | 162 | 159 | 158 |
| 10B-1 | 10000 | 10175 | 7576 | 7895 | 200 | 122 | 159 | 122 | 160 | 160 | 158 | 170 |
| 10B-2 | 10000 | 9810 | 7278 | 7557 | 200 | 152 | 216 | 163 | 160 | 161 | 156 | 163 |
| 10B-3 | 10000 | 8265 | 7627 | 7949 | 200 | 215 | 257 | 193 | 160 | 160 | 157 | 164 |
| 10B-4 | 10000 | 10480 | 8555 | 8718 | 200 | 179 | 332 | 290 | 160 | 161 | 152 | 155 |
| 10B-5 | 10000 | 11730 | 9587 | 10158 | 200 | 162 | 260 | 174 | 160 | 162 | 154 | 162 |

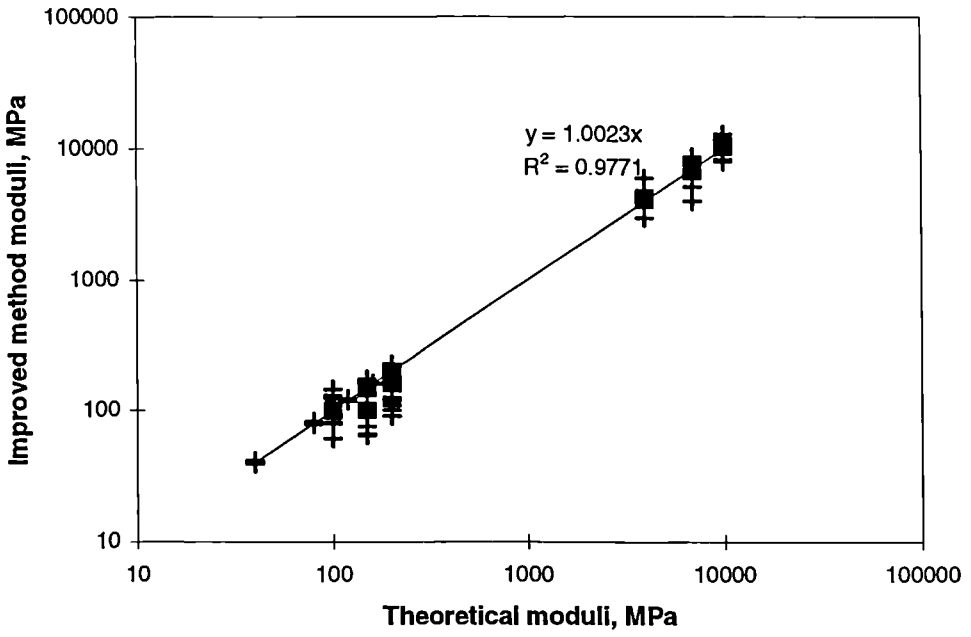


Figure 7.1, Comparison between the improved method backcalculated and theoretical moduli for the 90 structures.

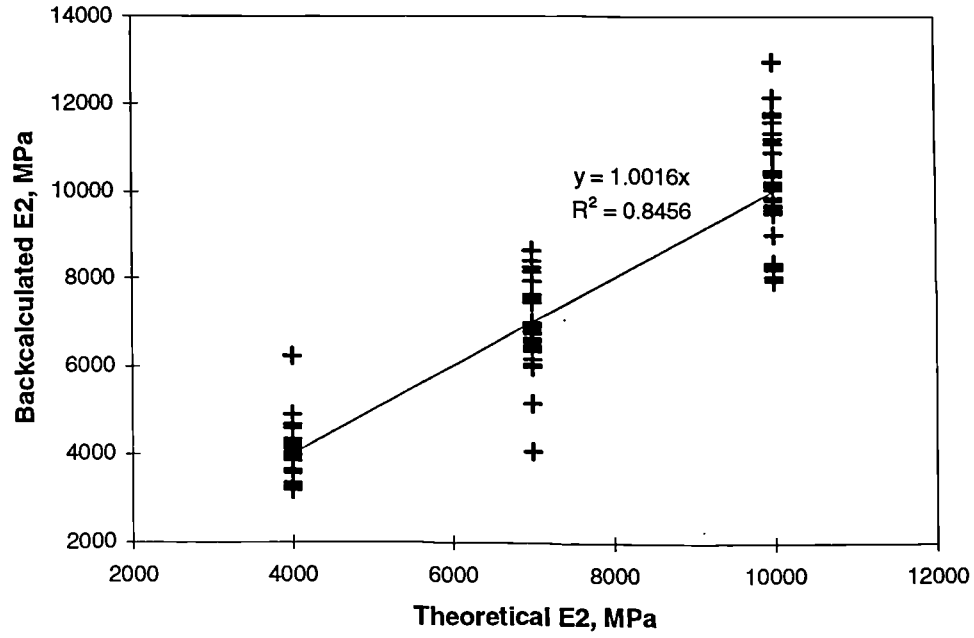


Figure 7.2, Comparison between the improved method backcalculated and theoretical moduli of bituminous base for the 90 structures.

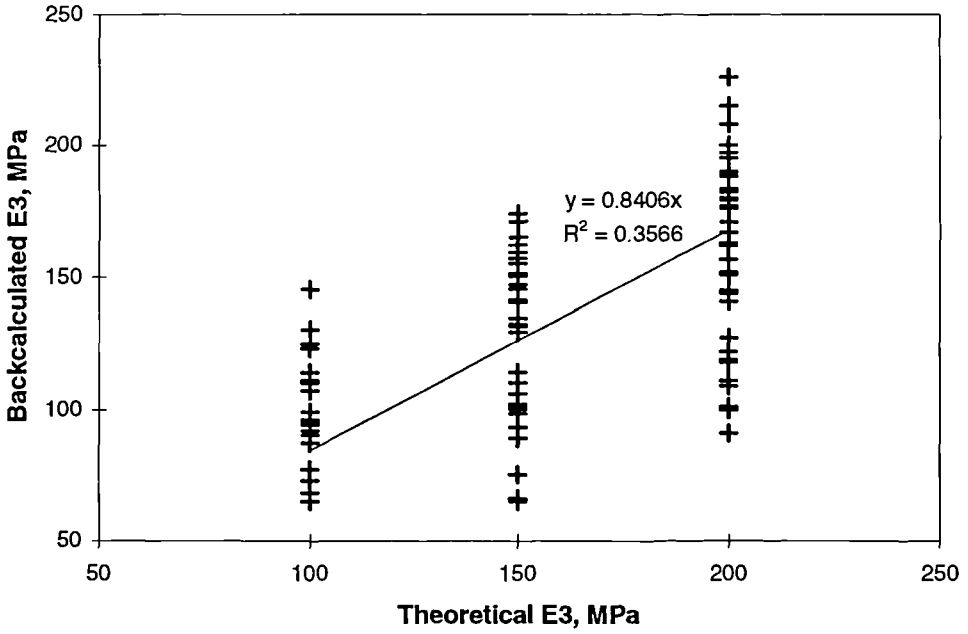


Figure 7.3, Comparison between the improved method backcalculated and theoretical moduli of unbound subbase for the 90 structures.

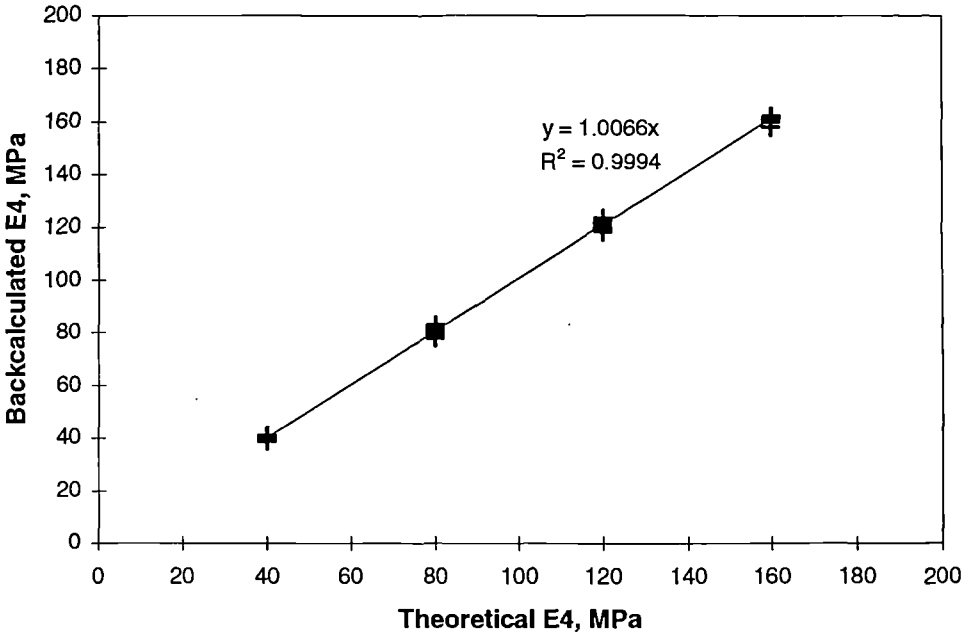


Figure 7.4, Comparison between the improved method backcalculated and theoretical moduli of subgrade for the 90 structures.

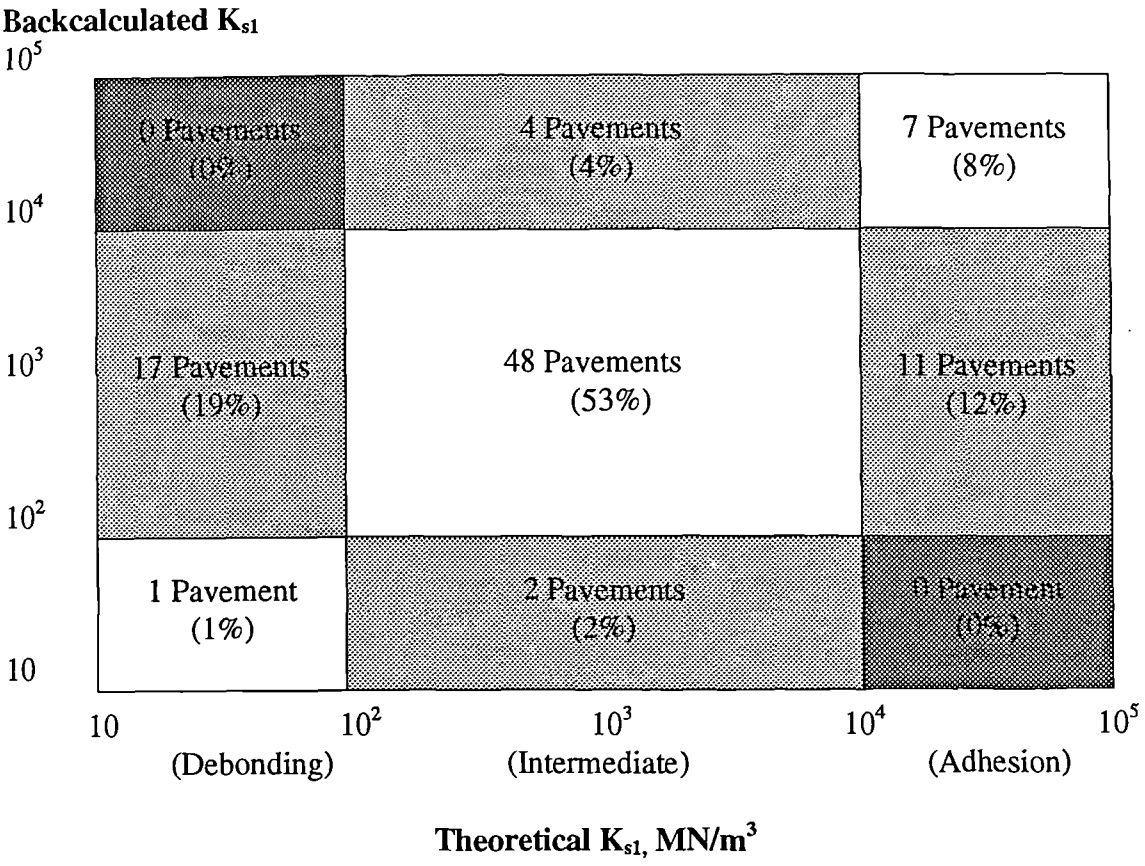


Figure 7.5, Comparison between backcalculated and theoretical bonding condition between wearing and base courses for the 90 structures on the ranges basis.

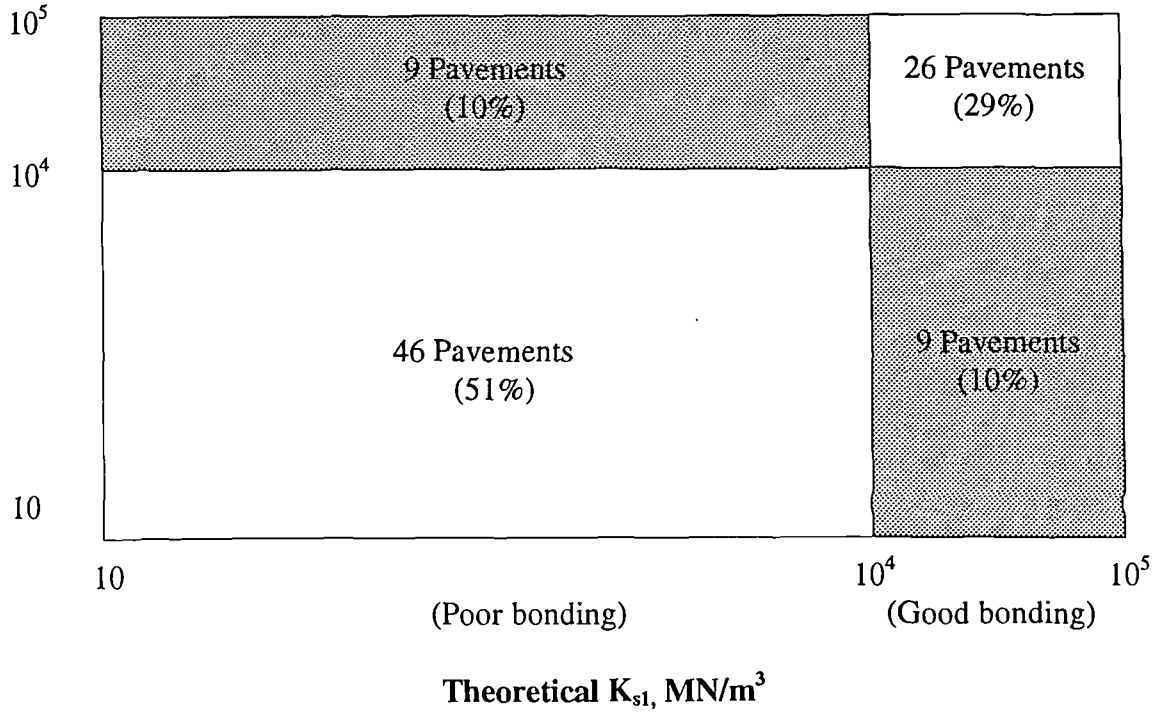


Figure 7.6, Comparison between backcalculated and theoretical bonding condition between wearing and base courses for the 90 structures for practical use.

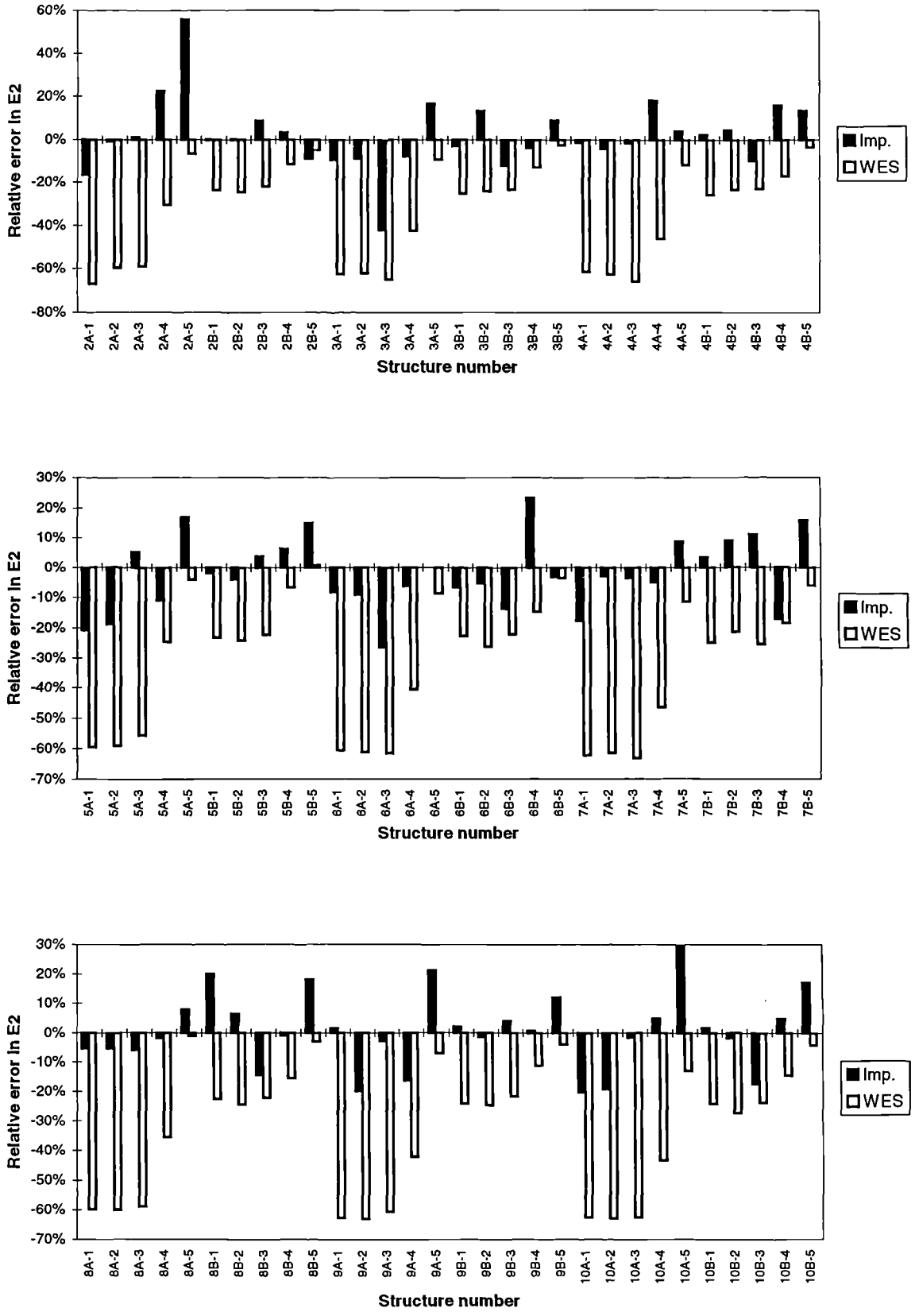


Figure 7.7, Relative error in predicting the modulus of bituminous base using the improved and the WESDEF programs for the 90 structures.

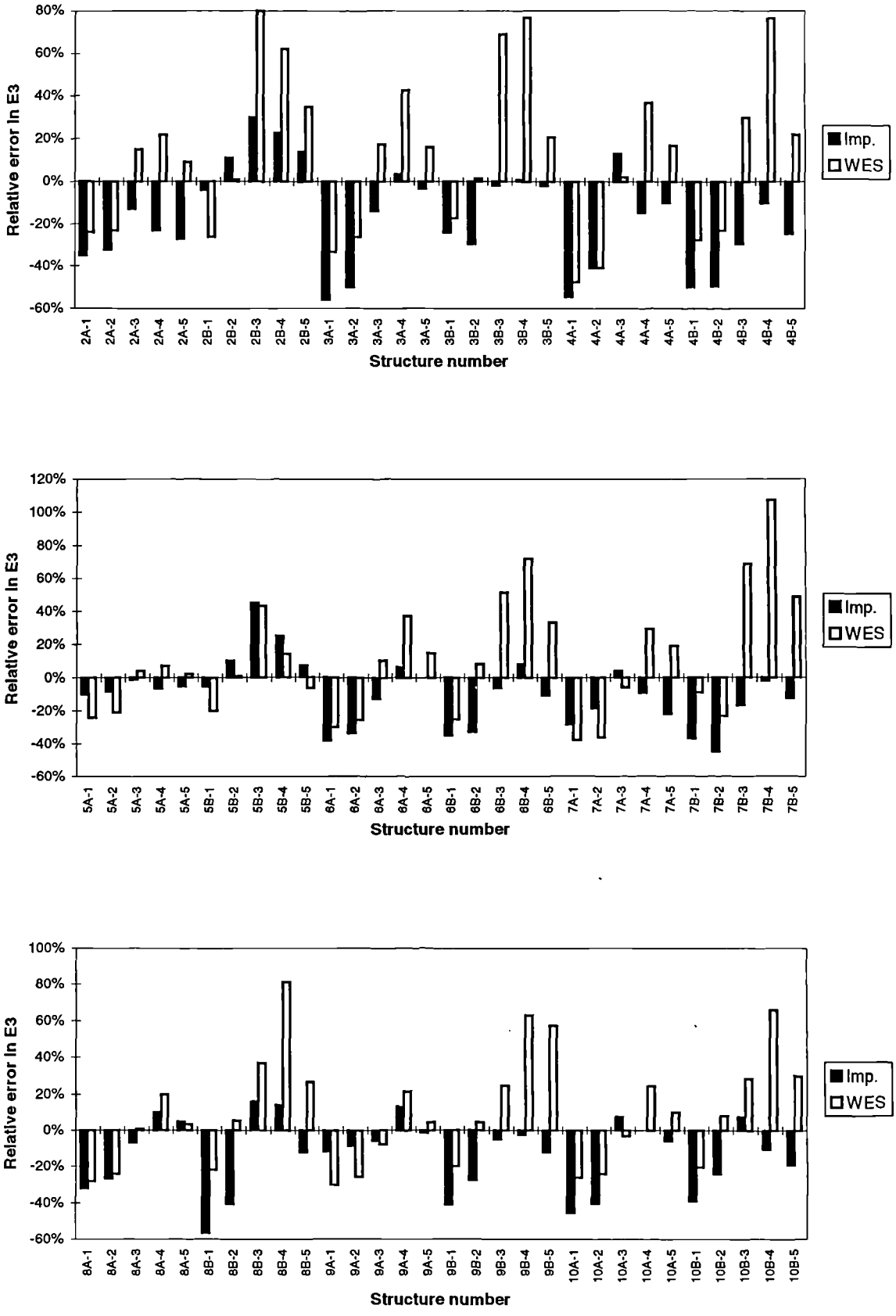


Figure 7.8, Relative error in predicting the modulus of unbound subbase using the improved and the WESDEF programs for the 90 structures.

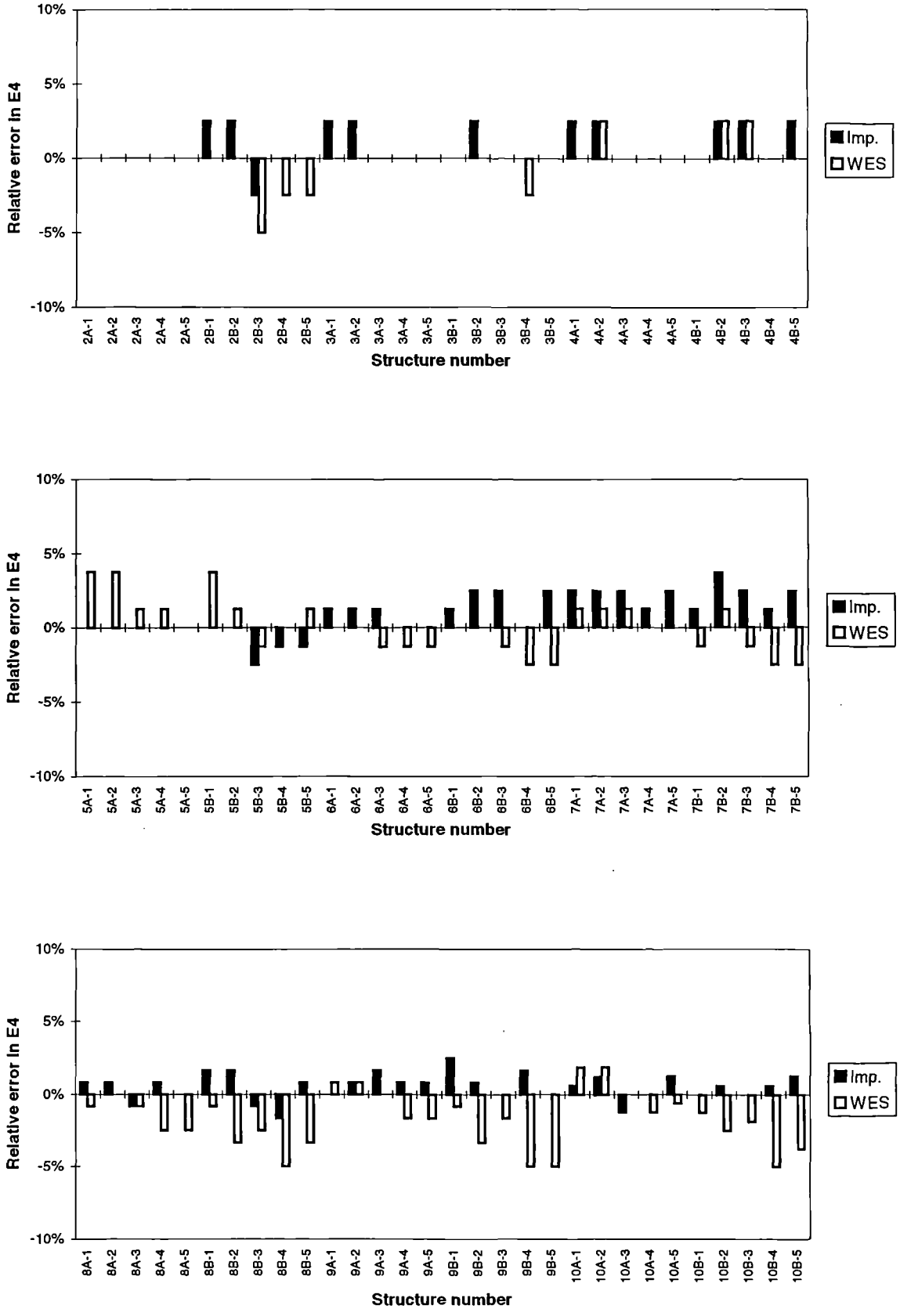


Figure 7.9, Relative error in predicting the modulus of subgrade using the improved and the WESDEF programs for the 90 structures.

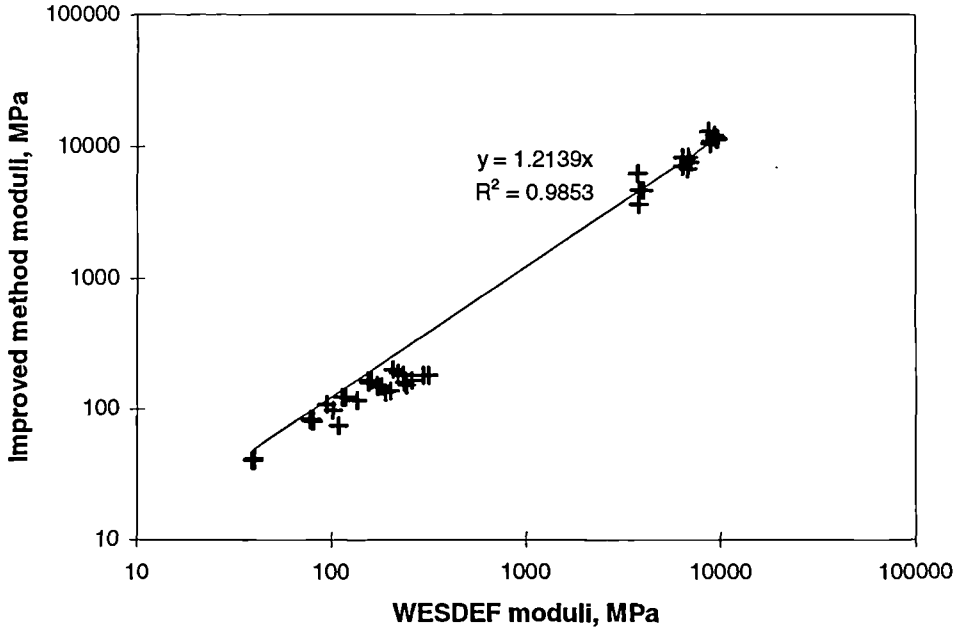


Figure 7.10, Comparison between backcalculated moduli using the improved method and WESDEF program for the 18 structures with full adhesion.

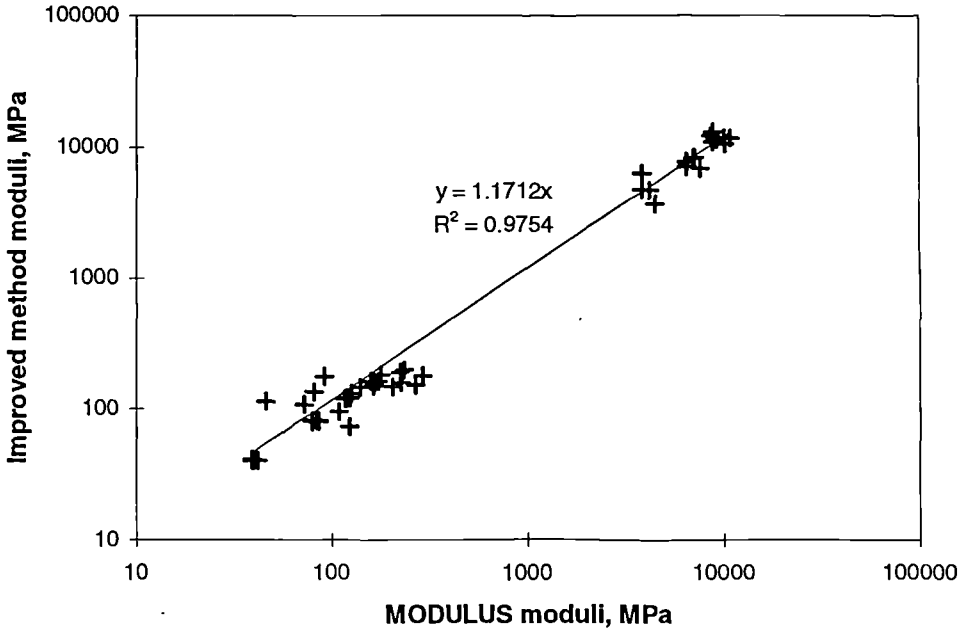


Figure 7.11, Comparison between backcalculated moduli using the improved method and MODULUS program for the 18 structures with full adhesion.

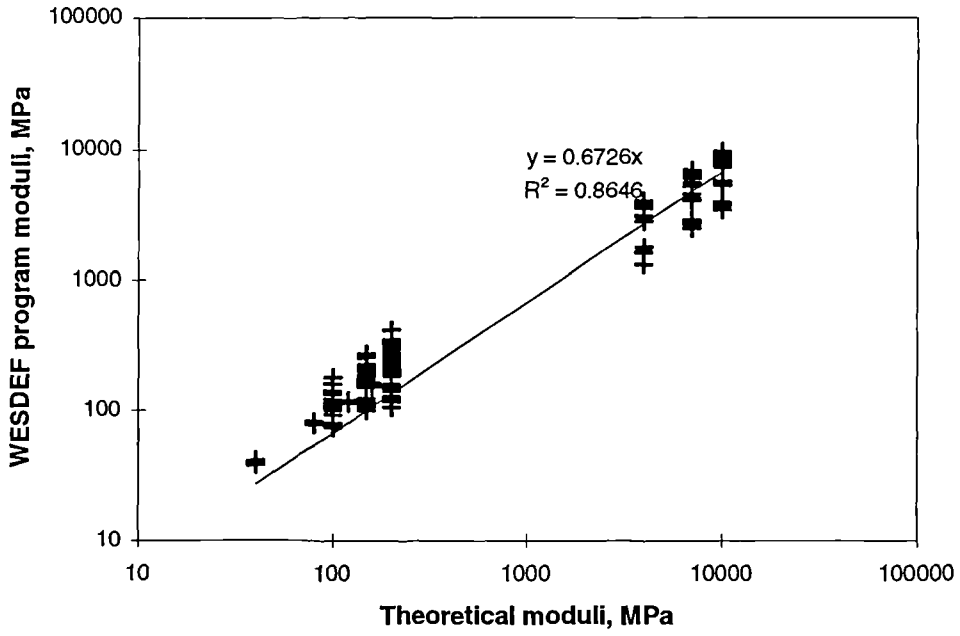


Figure 7.12, Comparison between WESDEF backcalculated and theoretical moduli for the 90 structures.

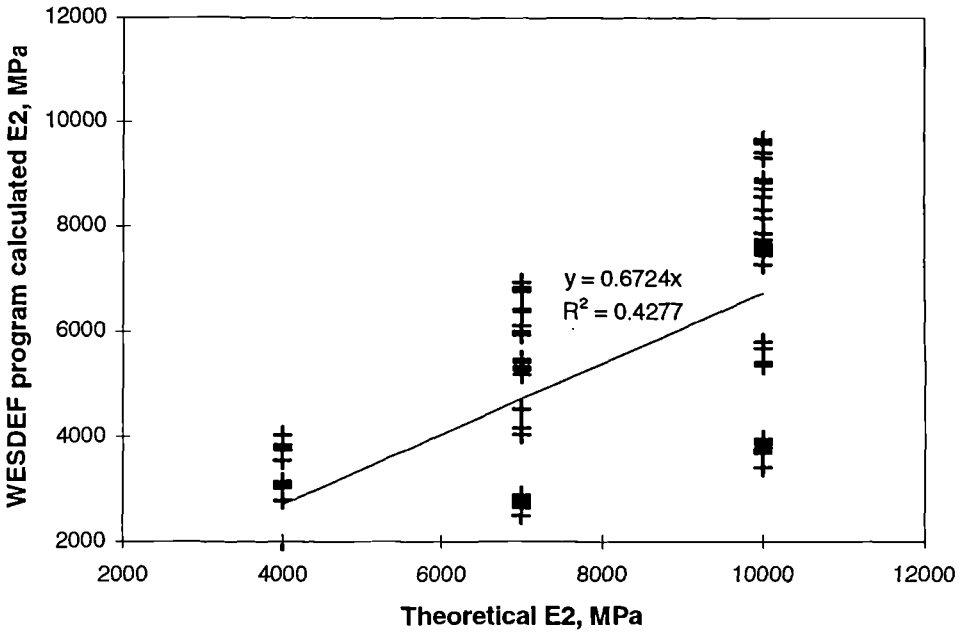


Figure 7.13, Comparison between WESDEF backcalculated and theoretical moduli of bituminous base for the 90 structures.

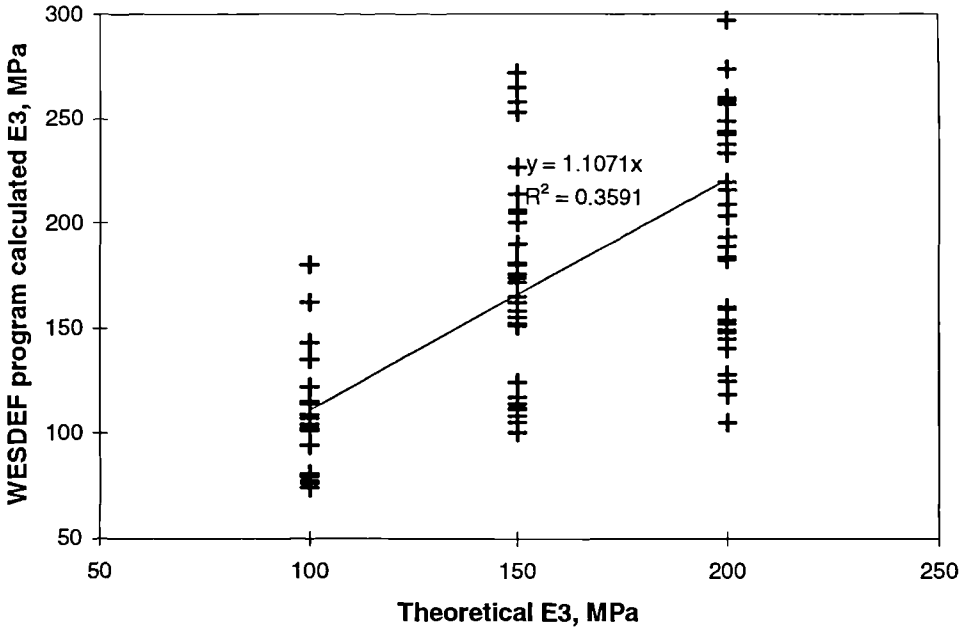


Figure 7.14, Comparison between WESDEF backcalculated and theoretical moduli of unbound subbase for the 90 structures.

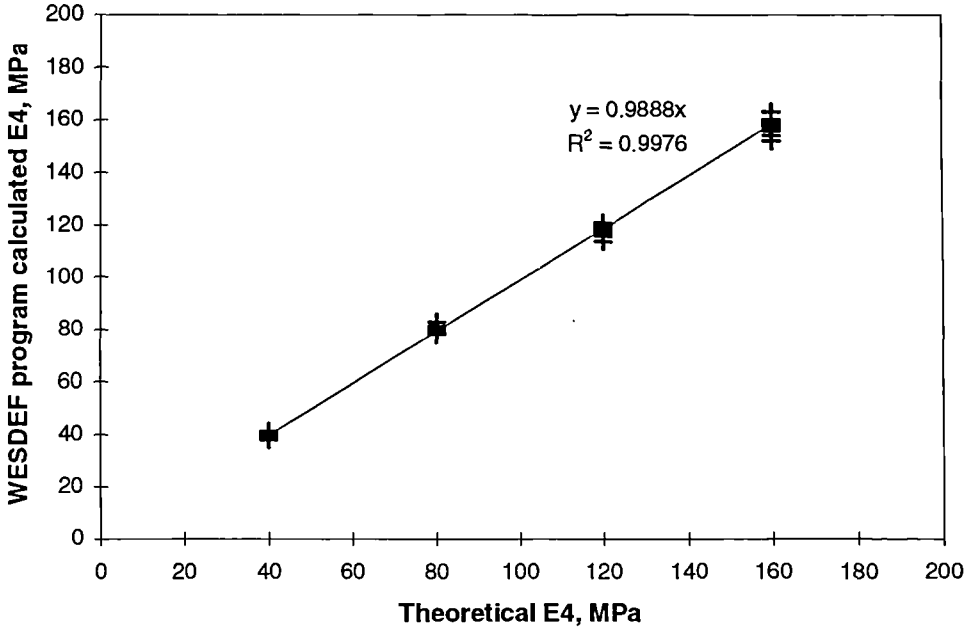


Figure 7.15, Comparison between WESDEF backcalculated and theoretical moduli of subgrade for the 90 structures.

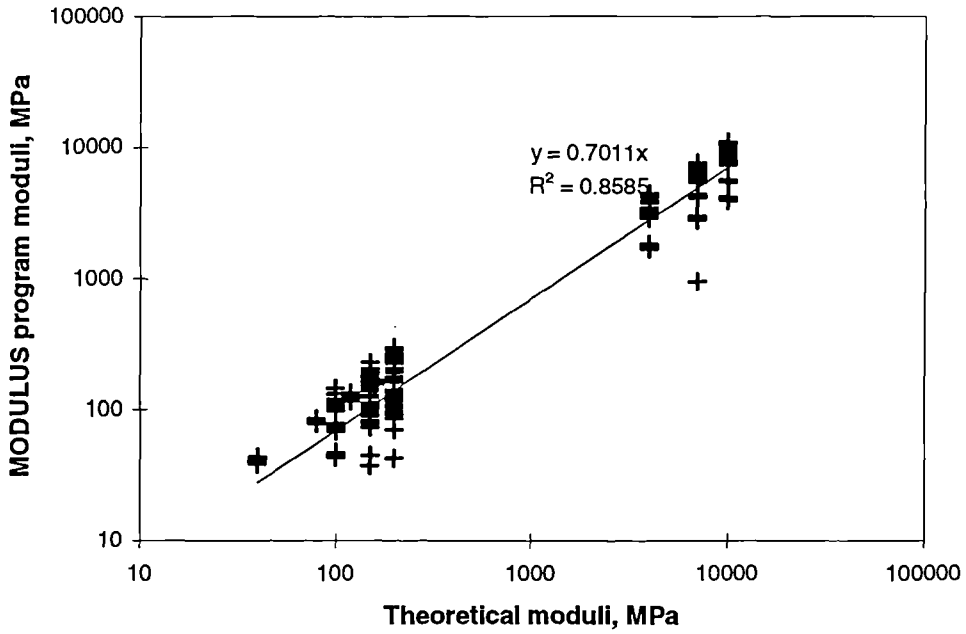


Figure 7.16, Comparison between MODULUS backcalculated and theoretical moduli for the 90 structures.

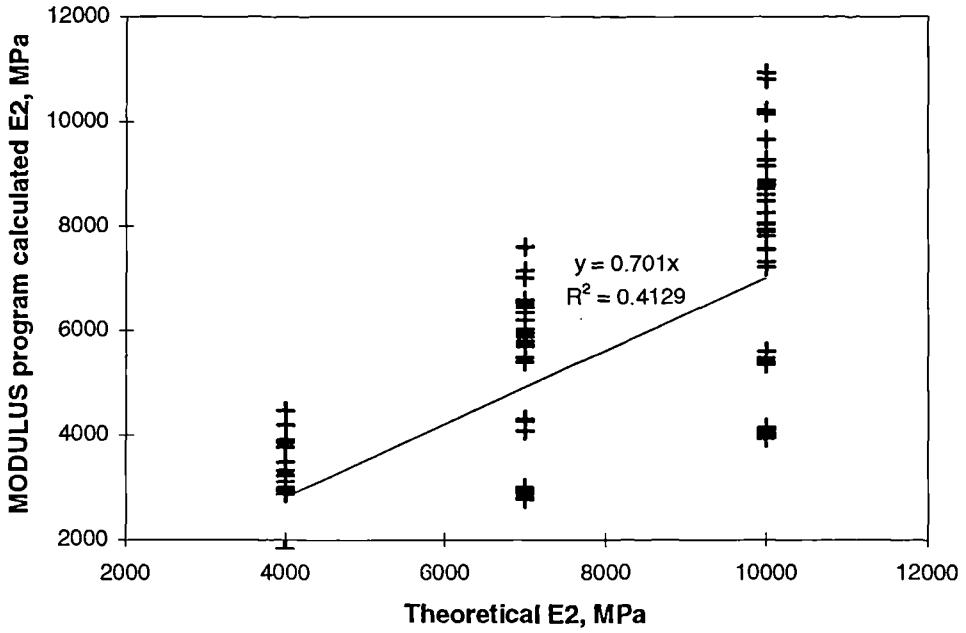


Figure 7.17, Comparison between MODULUS backcalculated and theoretical moduli of bituminous base for the 90 structures.

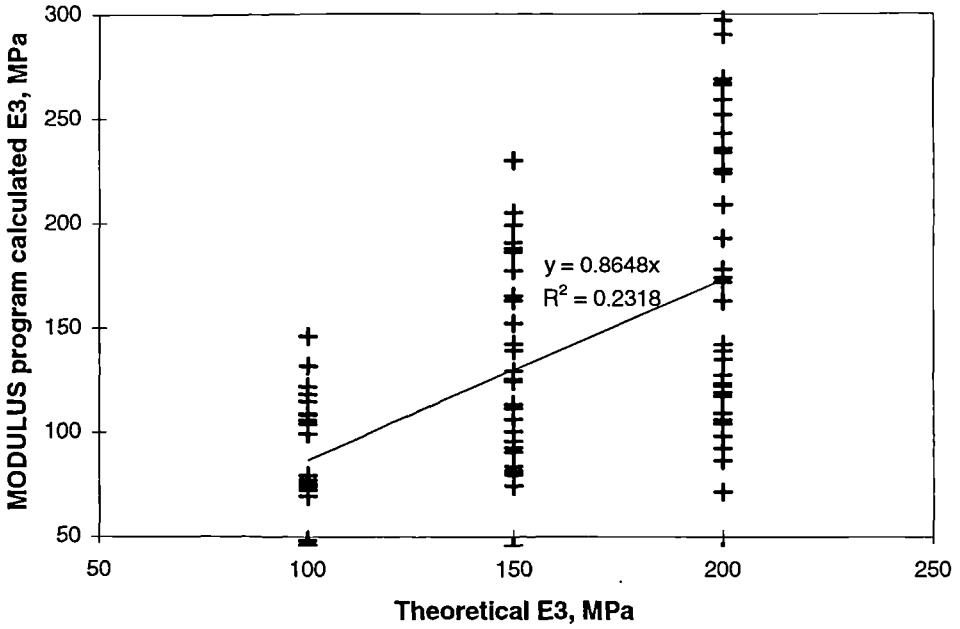


Figure 7.18, Comparison between MODULUS backcalculated and theoretical moduli of unbound subbase for the 90 structures.

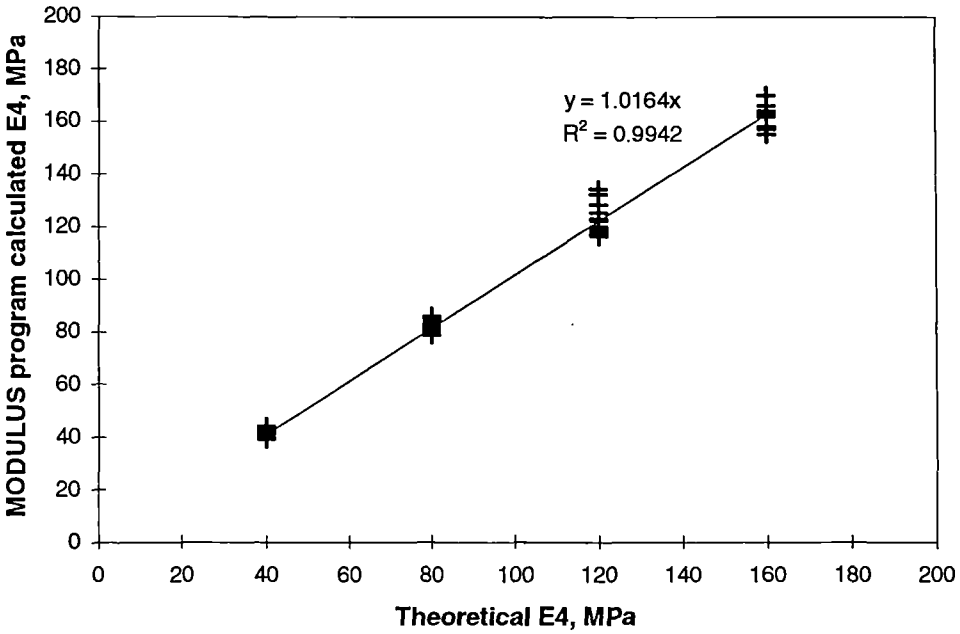


Figure 7.19, Comparison between MODULUS backcalculated and theoretical moduli of subgrade for the 90 structures.

# Chapter 8

# FULL SCALE TESTING OF PAVEMENTS - A34 HANDFORTH-WILMSLOW BYPASS

## 8.1 INTRODUCTION

Any empirical validation of the backcalculation procedure is very difficult because no reference point is available for mechanistic pavement analysis. Mechanistic properties have normally been determined by standard laboratory tests (30). However since neither backcalculation nor laboratory test methods provide a reference modulus, backcalculation results have been verified through an examination of the compatibility of the two methods.

Many researchers validate their backcalculation programs by comparing the moduli results with physically measured properties either in the laboratory or insitu (6,30,47,91,92,93).

An Indirect Tensile Test (ITT) for resilient modulus of bituminous mixes on cores extracted from the pavements using the Nottingham Asphalt Tester NAT (35) was used. The unbound layers and subgrade soil properties were predicted from the Dynamic Cone Penetrometer (DCP) tests (40). However, where the subbase and capping layers are very thick, as was most often the case, the construction records of the Standard Penetration Test (SPT) (39) for subgrade were used to validate the backcalculation results.

Testing new uncracked pavements will result in a better agreement between laboratory and backcalculated moduli. Hossain et al (94), verified this statement by comparing backcalculated asphalt concrete moduli from FWD test results on a new pavement section with the resilient moduli determined in the laboratory.

Although a laboratory test defined the physical properties of individual material, the difficulties of creating the same pavement stresses and environmental conditions in the laboratory make the results not very representative. The surface deflections under the FWD reflect the real insitu pavement condition and therefore the backcalculated parameters can more realistically represent the insitu material properties (43,94). A reliable estimate of the pavement material moduli from FWD and backcalculation procedure is essential for comparison with measured properties.

Uzan and Lytton (95) stated that the measured deflection basins under FWD can be separated into the following components:

i) the true deflection,
ii) the systematic error due to modelling,
iii) the random error due to the measuring devices and
iv) the random error due to intrinsic variability of the materials.

In order to achieve reliable results, both the systematic error and the random errors due to measuring devices must be eliminated. The former can be minimised by using better modelling such as nonlinear material behaviour. The latter can also be minimised through repeating the test several times at the same location (95).

The following measures have been employed in this empirical analysis to make the comparison as realistic as possible.

i) New untrafficked pavement sections were selected for the FWD tests, in order to avoid the effect of cracks, voids and other pavement defects on backcalculated moduli.
ii) Four load levels were conducted using the FWD test at each location to study the pavement material nonlinearity.
iii) At each load level four drops were performed and the average deflection basins were considered for backcalculation, to eliminate the random errors due to measuring devices.
iv) Core extractions for laboratory tests and DCP measurements were carried out at the same FWD test locations to overcome the pavement and subgrade variation with distance.

v) Layer thicknesses were measured from the cores and construction drawings.

vi) The pavement's temperature was measured according to ASTM (96). Laboratory testing for bituminous layers were performed at the same field temperature.

vii) A "radial modulus at different radial distance" method (61) was used to detect any bedrock at shallow depth.

However, some variation should be expected between the measured and backcalculated moduli due to the following reasons (43,47,90,91,94).

i) The combining of different layers with the same properties into one structural layer in the backcalculation procedure.

ii) The stress state for the limited sized bituminous material cores in the laboratory can differ significantly from that in the field.

iii) Different material volumes were tested in the field and the laboratory.

iv) FWD test has a different loading time compared with the laboratory experiments.

v) The insitu DCP test for unbound materials is empirical and its result usually correlated with an analytical parameter such as modulus of elasticity. This correlation may not hold for a wide range of materials.

## 8.2 TESTING METHODOLOGY

Four full scale untrafficked pavements were selected for testing from the A34 Handforth-Wilmslow Bypass in the Greater Manchester area. Prestbury link (Pres), Handforth Bypass (HBP), Hypermarket slip road (Hyp) and Manchester Airport Eastern link road (MAE) are the four sites provided by Cheshire County Council and tested (October 1st 1995).

Radial modulus analysis indicates the absence of stiff bedrock at shallow depth for the tested pavements.

The pavements were simplified as four layer systems with an apparent stiff layer at 6m depth from the surface as shown in figure 8.1. All bituminous layers except the wearing course were combined into one layer, whereas the granular subbase and the capping layers were combined as layer 3 which is imposed on the subgrade soil.

The average thickness of each layer, as measured from cores for bituminous materials or from construction drawing for unbound layers, is illustrated in figure 8.1 for each pavement.

The investigation of the pavement structures involved the following procedure, the details of which are explained later in this chapter.

i) FWD tests were performed.
ii) Cores were extracted from the full depth of bituminous layers.
iii) DCP tests were conducted.
iv) ITT's for resilient modulus were carried out on the cores for different bituminous layers.
v) The surface deflections under the FWD were analysed to backcalculate the moduli of bituminous base, unbound layer and subgrade in addition to the shear reaction modulus between the wearing and base courses using the improved method.
vi) The same deflections were used to backcalculate the moduli of the same layers using WESDEF and MODULUS programs.
vii) A comparison between the backcalculated moduli using the improved method and the measured values was carried out.
viii) Finally, the backcalculated moduli using the improved method and both WESDEF and MODULUS programs were compared attempt to verify the performance of the new procedure.

### 8.2.1 FWD Testing

FWD tests were performed at five locations at 25 m intervals for each pavement, except for the Handforth Bypass (HBP) where only three locations were tested. At each location four load levels were carried out, where 25, 40, 65 and 80 kN loads on a 300 mm diameter circular plate were applied.

Four drops at each load level were performed and the average basins were determined to eliminate the likelihood of random errors due to the measuring devices.

The average pavements' temperatures were measured according to the ASTM standard (96) as follows;

A small hole was drilled to 100 mm depth in the bituminous layer, water was filled in the hole and then the temperature was measured with a thermometer set in the water after the reading was stabilised. The average pavements' temperature was 12 °C which was used for the laboratory test for bituminous materials.

Therefore all the backcalculated properties are for a field temperature of 12 °C.

### 8.2.2 Core Extraction

Seven 150 mm diameter cores were cut from the four pavements to the full depth of the bituminous layers as shown in figure 8.2. The selection of the cores' locations was mainly made due to access restriction on the new pavements. Two cores were extracted from each pavement except the MAE pavement where one core was cut. Second and third locations were selected for coring from the Prestbury link road, whereas first and third locations were chosen from the HBP pavement. The Hypermarket slip road was cored at the second and fifth places and only one core was extracted at the forth location from MAE pavement. Figures 8.3 and 8.4 show the core specimens.

The objectives of the coring are firstly to obtain the actual thickness of bituminous layers for the backcalculation procedure and secondly to determine the bituminous moduli in the laboratory using the Nottingham Asphalt Tester.

### 8.2.3 Dynamic Cone Penetrometer (DCP) Tests

Dynamic Cone Penetrometer, (figure 8.5) considered in this research was based on a design used in South Africa and extensively studied by Klein et al (40) and others (97,98,99). It consists of a 16 mm diameter steel bar with a 60° cone at one end. The impact is provided by means of an 8 kg sliding hammer falling 575 mm.

The DCP test was performed in the core hole, where the coned end of the bar penetrated the unbound materials under the action of the falling hammer. The penetration depth and the

number of blows of the weight were recorded and plotted later in a graph. The slope of the regression line in mm/blow was used to calculate the California Bearing Ratio (CBR) and modulus value using the TRL equations (4,100);

$$Log_{10}(CBR) = 2.48 - 1.057\ Log_{10}(\text{DCP slope in mm/blow})$$

$$E = 17.6\ (CBR)^{0.64}$$

All the four investigated pavements have thick unbound layers above the subgrade which make it difficult to reach the subgrade and measure its properties with the DCP. Therefore the Standard Penetration Test (SPT) (39) results, as found in the geotechnical report for the pavement location, were used to predict the CBR values of the subgrade. The following equation was used in the calculation (101);

$$Log_{10}(CBR) = -5.13 + 6.55\ (Log_{10}\ SPT)^{-026}$$

where, SPT is the penetration in mm/blow.

Table 8.1 presents the testing results for unbound materials with their computed moduli from the above equations. The detail results of the DCP tests can be found in the following sections for each pavement. These moduli are not very reliable, since the formulae are empirical and do not necessary accommodate different unbound material types (61,102). However they can still be used as a good indication for the compatibility comparison with the backcalculated moduli.

### 8.2.4 Indirect Tensile Tests (ITT)

A repeated load indirect tensile test (35) was performed on the wearing course, base course and road base for each core at 12 °C. These tests were carried out at the University of Uslter in Northern Ireland. Two or three tests were conducted and the average moduli were computed (see table 8.2). The combined modulus of base course (bc) and road base (rb) was calculated for comparison purposes with the backcalculated value for the second layer using the following equation (102);

$$E_2 = \left[ \left( \frac{h_{bc}}{h_{bc} + h_{rb}} \right) E_{bc}^{1/3} + \left( \frac{h_{rb}}{h_{bc} + h_{rb}} \right) E_{rb}^{1/3} \right]^3$$

where,

$h_{bc}$, $h_{rb}$ are the thickness of base course and road base respectively

$E_{bc}$, $E_{rb}$ are the moduli of base course and road base respectively.

### 8.2.5 Backcalculation

Deflection basins under a 40 kN load were analysed for each location to predict the pavement properties.

The laboratory indirect tensile test modulus for the thin wearing course was assigned as a known value in the backcalculation procedure (see chapter 6). All other bituminous layers are combined into one base layer, whereas the subbase and capping layers are combined and assumed as layer 3 for backcalculation purposes.

Typical values for Poisson's ratio of 0.35 for bituminous layers, 0.3 for unbound layers and 0.4 for the subgrade were adopted. The average layer's thickness for each pavement is presented in figure 8.1.

Radial moduli were computed using Rada's equation (61) (see chapter 2). The radial moduli as a function of radial distances were plotted to detect any shallow bedrock at each location. A stiff layer at 6 m depth was assumed in the backcalculation procedure for all the pavements. This assumption was supported by calculating the rigid layer depth using both WESDEF and MODULUS programs, where approximately 6 m depth was found.

Average deflections as a function of the FWD load level were plotted for each location. A linear analysis was assumed appropriate for the studied pavements.

The deflection basins were used to backcalculate;

i) the moduli of second, third and fourth layers in addition to the shear reaction modulus between wearing and base courses using the improved procedure, and

ii) the moduli of second, third and fourth layers using WESDEF and MODULUS programs, assuming full adhesion between pavement layers.

Table 8.3 presents the backcalculation results for the analysed pavements using the three programs. The discussion of these results is detailed in the following sections for each pavement.

## 8.3 PRESTBURY LINK ROAD PAVEMENT ANALYSIS

Deflection basins under a 40 kN FWD load were drawn in figure 8.6 for the five locations. Low deflection values were recorded which indicate very stiff subgrade and a strong pavement.

Radial moduli were plotted for each location in figure 8.7. Some irregularities were noticed in the graphs due to deflection measurement errors, however an apparent rigid layer at 6 m depth can be considered appropriate for the pavement analysis.

Figure 8.8 shows the deflections at the load centre, 300, 600 and at 1800 mm radial distances as a function of FWD load. The surface deflections have a linear relationship with the loads due to the stiff pavement structure, therefore the linear analysis assumption can be considered acceptable for backcalculation purposes.

Figures 8.9 and 8.10, illustrate the DCP test result for the two cores at 25 and 50 m locations. The slopes of the regression line of 2.37 and 3.09 mm/blow for the second and third location respectively were recorded. The variations of CBR values were also plotted along the depth of the unbound layer.

The surface deflection and the backcalculated moduli using the improved method, were drawn along the longitudinal distance of the road in figures 8.11 and 8.12 respectively. An average modulus of the bituminous base of 15000 MPa and very strong unbound layer

modulus of 1000 MPa was calculated, probably due to some cementing action. A stiff subgrade with modulus of 200 and up to 400 MPa for the last location was predicted using the improved procedure. Good bonding with shear reaction modulus between wearing and base course of $10^5$ MN/m$^3$ was computed, which is normal for the new untrafficked pavement (see table 8.3).

Figure 8.13 demonstrates the comparison between the measured and backcalculated moduli using the improved, WESDEF and MODULUS programs. The measured moduli are usually lower than the predicted values due to the reasons explained earlier in this chapter. However, generally good agreement was noticed between the measured and calculated moduli using the improved method and the calculated results of different programs. Quantifying the relationships will be carried out later in this chapter for all the pavements, where the correlation coefficients will be calculated.

## 8.4 HANDFORTH BYPASS PAVEMENT ANALYSIS

Three locations only were considered for this pavement at 25 m intervals. Surface deflections were plotted in figure 8.14, whereas the radial moduli were drawn in figure 8.15. Figure 8.16 illustrates the deflections as a function of FWD loads. The above assumption of linear pavement materials and the location of stiff layer at 6 m depth can be considered appropriate for this pavement.

DCP results for the first and last locations were shown in figures 8.17 and 8.18 respectively. The slope value of 3.64 mm/blow was found for the first location, whereas 2.88 mm/blow was calculated for the last location.

Surface deflections along the pavement were plotted in figure 8.19 to describe the regularity of the pavement materials with longitudinal distance. Figure 8.20 demonstrates the improved method predicted moduli. Calculated moduli of around 11000 MPa for bituminous base and 500 MPa unbound materials were found. A uniform subgrade modulus of 140 MPa was predicted. The adhesion state between the wearing and base courses was found acceptable with an average value of $10^4$ MN/m$^3$ (see table 8.3).

The comparison between the measured and backcalculated moduli using different methods is shown in figure 8.21. Good agreement was observed between the moduli values. However a low modulus value for the unbound layer of the second location was predicted using the MODULUS program, which might be explained as a nonunique solution problem.

## 8.5 HYPERMARKET SLIP ROAD PAVEMENT ANALYSIS

Higher deflections were recorded for this pavement as shown in figure 8.22, which can be explained as thinner pavement and weaker subgrade soil compared with previous structures.

Figure 8.23 presents the radial moduli for the five locations. Modulus stiffening was recorded with radial distance for the second location which indicates nonlinear subgrade behaviour. However an apparent rigid layer at 6 m depth can simulate the subgrade stiffening effect. The pavement materials can be assumed as having linear properties as concluded from figure 8.24.

Figures 8.25 and 8.26 demonstrate the DCP test analysis results. A regression line's slope of 2.59 and 4.33 mm/blow was found for the second and fifth pavement location respectively.

Figure 8.27 shows the longitudinal deflections. The last two locations exhibit lower deflection values, which imply stronger pavement and subgrade for these places. The backcalculated parameters are presented in figure 8.28 and table 8.3. Lower moduli values were predicted compared with previous pavements, as expected. An average 6000 MPa for bituminous base and 450 MPa for unbound layer were calculated, whereas the subgrade moduli from 110 to 180 MPa for the last location was found. Again good adhesion was found between wearing and base courses with average shear reaction modulus of $10^4$ MN/m$^3$.

Close agreements were found between the measured and backcalculated moduli as shown in figure 8.29. specially for bituminous base where only about 5% relative difference was recorded.

## 8.6 MANCHESTER AIRPORT EASTERN LINK PAVEMENT ANALYSIS

Surface deflections under 40 kN load, radial moduli and deflection variation with FWD load were plotted in figures 8.30, 8.31 and 8.32 respectively for the five locations. The pavement materials and subgrade soil exhibit linear behaviour as shown in the graphs. The DCP test was carried out only at the fourth location where the core was extracted. A slope value of the regression line of 4.73 mm/blow was recorded in figure 8.33, which is equal to 58% CBR value for the unbound materials.

Figure 8.34 shows the deflections' variation along the pavement distances and figure 8.35 illustrates the backcalculated moduli using the improved method. Table 8.3 demonstrates average moduli of 15000 MPa for the base layer, 300 MPa for unbound layer and 200 MPa for subgrade. Acceptable bonding between wearing and base courses of $10^4$ MN/m$^3$ was computed.

However the second location improved method backcalculated moduli were unacceptable, with high bituminous modulus (more than 15000 MPa) and very low subbase modulus (around 70 MPa). These results might be due to deflection measurement error, construction defects or nonunique backcalculation solution. The predicted values using the WESDEF and MODULUS programs revealed similar results to the improved method for the second location as shown in table 8.3, which exclude the failure of the improved procedure parameter prediction.

Close agreements were found between the backcalculated moduli using different programs as presented in figure 8.36. The measured moduli were lower than the computed values for the only location tested.

## 8.7 DISCUSSION AND CONCLUSIONS

The aim of this chapter was to verify empirically the improved method by testing full scale pavement structures.

The improved method backcalculated moduli were compared firstly with measured values and secondly with computed moduli using WESDEF and MODULUS programs.

Figure 8.37 shows the comparison between the improved method calculated and measured moduli for the bituminous base, unbound layer and subgrade at the seven cored locations. A correlation coefficient of 79% was found, indicating good compatibility considering the expected variation between the moduli values explained in section 8.1.

Figures 8.38 and 8.39 illustrate the comparison between the improved procedure moduli and WESDEF and MODULUS values respectively. The eighteen tested deflection locations were considered as shown in table 8.3, the three moduli for each location were included in the graphs. Coefficients of correlation of more than 90% were found for both cases, which indicate satisfactory performance of the improved procedure. This good agreement between the improved and the conventional methods, which assumed full adhesion between the pavement layers, is due to the existence of good bonding in most cases.

The predicted adhesion properties between the wearing and base courses were satisfactory with average shear reaction modulus ($K_{s1}$) of $10^4$ MN/m$^3$. This interface condition was expected for the new untrafficked pavements.

Finally the improved procedure demonstrates similar moduli results compared with other backcalculation programs. However backcalculating the interface condition between wearing and base courses can be considered as an improvement to the existing procedures.

Table 8.1, Measured unbound materials properties.

| | Unbound materials (layer 3) | | | Subgrade (layer 4) | | |
|---|---|---|---|---|---|---|
| | DCP (mm/blow) | CBR (%) | $E_3$ (MPa) | STP mm/blow) | CBR (%) | $E_4$ (MPa) |
| **Pres. 2** | 2.37 | 121 | 380 | 20 | 9.5 | 75 |
| **Pres. 3** | 3.09 | 92 | 317 | 20 | 9.5 | 75 |
| **HBP 1** | 3.64 | 77 | 284 | 18.75 | 10.5 | 80 |
| **HBP 3** | 2.88 | 99 | 332 | 18.75 | 10.5 | 80 |
| **Hyp. 2** | 2.59 | 110 | 357 | 18.75 | 10.5 | 80 |
| **Hyp. 5** | 4.33 | 64 | 252 | 18.75 | 10.5 | 80 |
| **MAE 4** | 4.73 | 58 | 238 | 20 | 9.5 | 75 |

Table 8.2, Indirect Tensile Test Modulus results for bituminous materials at 12°C.

| | ITT $E_{wc} = E_1$ (MPa) | | | | ITT $E_{bc}$ (MPa) | | | | ITT $E_{rb}$ (MPa) | | | $E_2$ (MPa) |
|---|---|---|---|---|---|---|---|---|---|---|---|---|
| | Test 1 | Test 2 | Test 3 | $E_1$ Av. | Test 1 | Test 2 | Test 3 | $E_{bc}$ Av. | Test 1 | Test 2 | $E_{rb}$ Av. | $E_{bc}$ & $E_{rb}$ |
| **Pres. 2** | 3101 | 3011 | | **3056** | 5537 | 5581 | | 5559 | 6170 | 6146 | 6158 | **5554** |
| **Pres. 3** | 3111 | 2850 | | **2981** | 4861 | 4736 | | 4799 | 8836 | 9224 | 9030 | **7420** |
| **HBP 1** | 3081 | 2694 | 3375 | **3050** | 4346 | 3805 | 3921 | 4024 | 8411 | 7706 | 8059 | **7158** |
| **HBP 3** | 3224 | 3254 | | **3239** | 3568 | 3356 | | 3462 | 8241 | 7667 | 7954 | **6919** |
| **Hyp. 2** | 3833 | 4442 | 4440 | **4238** | 5156 | 5124 | | 5140 | 8220 | 8767 | 8494 | **7283** |
| **Hyp. 5** | 3002 | 2989 | | **2996** | 4326 | 4523 | | 4425 | 8614 | 8505 | 8560 | **7019** |
| **MAE 4** | 3579 | 4155 | 3983 | **3906** | 7993 | 7264 | | 7629 | 5696 | 5961 | 5829 | **6933** |

Table 8.3, Backcalculated parameters from Falling Weight Deflectometer test result at 12°C using different programs (Improved, WESDEF and MODULUS).

| | $E_2$ (MPa) | | | $E_3$ (MPa) | | | $E_4$ (MPa) | | | $K_{s1}$ MN/m$^3$ |
|---|---|---|---|---|---|---|---|---|---|---|
| | **Imp.** | **WES.** | **MOD.** | **Imp.** | **WES.** | **MOD.** | **Imp.** | **WES.** | **MOD.** | **Imp.** |
| **Pres1** | 14365 | 15000 | 15000 | 1186 | 1034 | 474 | 189 | 195 | 340 | $10^5$ |
| **Pres2** | 18940 | 15000 | 15000 | 1313 | 1034 | 1034 | 197 | 236 | 216 | $10^5$ |
| **Pres3** | 10640 | 10551 | 13490 | 800 | 798 | 622 | 255 | 264 | 282 | $10^5$ |
| **Pres4** | 18750 | 15000 | 15000 | 1507 | 1034 | 1034 | 300 | 345 | 399 | $10^5$ |
| **Pres5** | 16810 | 12740 | 11896 | 944 | 1034 | 868 | 409 | 345 | 429 | $10^3$ |
| **HBP1** | 11060 | 9343 | 10336 | 646 | 788 | 659 | 160 | 154 | 164 | $10^5$ |
| **HBP2** | 14445 | 14444 | 15000 | 281 | 260 | 81 | 136 | 132 | 216 | $10^4$ |
| **HBP3** | 10960 | 12241 | 12302 | 542 | 273 | 258 | 139 | 144 | 149 | $10^3$ |
| **Hyp1** | 6860 | 5964 | 6724 | 454 | 356 | 308 | 107 | 115 | 123 | $10^3$ |
| **Hyp2** | 6870 | 6222 | 7068 | 382 | 337 | 284 | 110 | 115 | 124 | $10^4$ |
| **Hyp3** | 4590 | 4383 | 4435 | 526 | 456 | 455 | 108 | 114 | 114 | $10^4$ |
| **Hyp4** | 7320 | 7368 | 7458 | 723 | 644 | 644 | 130 | 137 | 138 | $10^5$ |
| **Hyp5** | 7340 | 6727 | 6652 | 429 | 424 | 424 | 180 | 184 | 184 | $10^5$ |
| **MAE1** | 15055 | 13642 | 15000 | 336 | 242 | 112 | 210 | 231 | 321 | $10^4$ |
| **MAE2** | 27360 | 15000 | 14574 | 49 | 79 | 93 | 232 | 345 | 310 | $10^5$ |
| **MAE3** | 13545 | 11441 | 11624 | 431 | 428 | 398 | 206 | 211 | 220 | $10^4$ |
| **MAE4** | 13770 | 12026 | 11962 | 360 | 338 | 338 | 227 | 226 | 233 | $10^4$ |
| **MAE5** | 16385 | 15000 | 15000 | 139 | 149 | 92 | 171 | 195 | 255 | $10^4$ |

| | | |
|---|---|---|
| $h_1$ | Bituminous Wearing Course<br>Layer 1 | $\nu_1 = 0.35$<br>$K_{s1}$= variable |
| $h_2$ | Bituminous Base<br>Layer 2 | $\nu_2 = 0.35$<br>$K_{s2}$ = full adhesion |
| $h_3$ | Granular Subbase + Capping layer<br>Layer 3 | $\nu_3 = 0.3$<br>$K_{s3}$ = full adhesion |
| $h_4$ | Subgrade<br>Layer 4 | $\nu_4 = 0.4$ |
| | Rigid Layer | |

| Pavement Location | $h_1$ (mm) | $h_2$ (mm) | $h_3$ (mm) | $h_4$ (mm) |
|---|---|---|---|---|
| **Prestbury link road (Pres)** | 40 | 180 | 825 | 4955 |
| **Handforth Bypass (HBP)** | 45 | 320 | 600 | 5035 |
| **Hypermarket slip road (Hyp)** | 45 | 185 | 600 | 5170 |
| **Manchester Airport Eastern Road (MAE)** | 50 | 410 | 600 | 4940 |

Figure 8.1, Summary of A34 pavement structures.

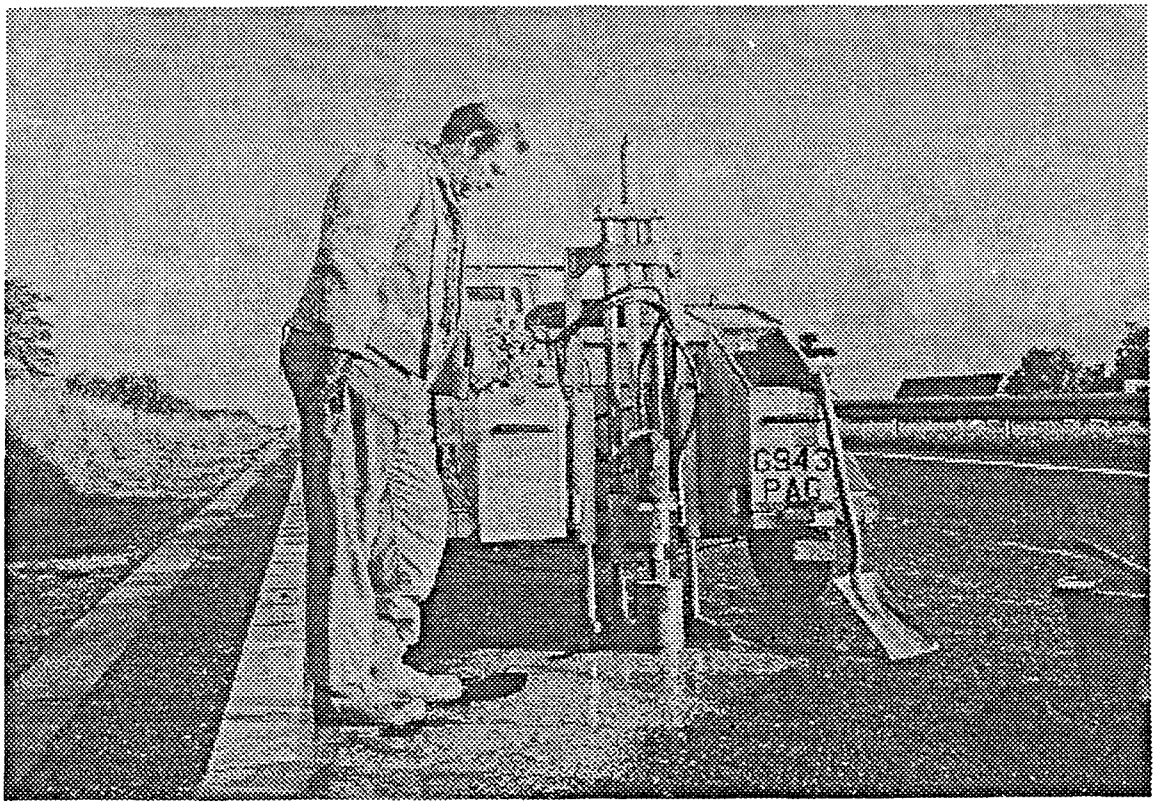


Figure 8.2, Core extraction from the pavement.

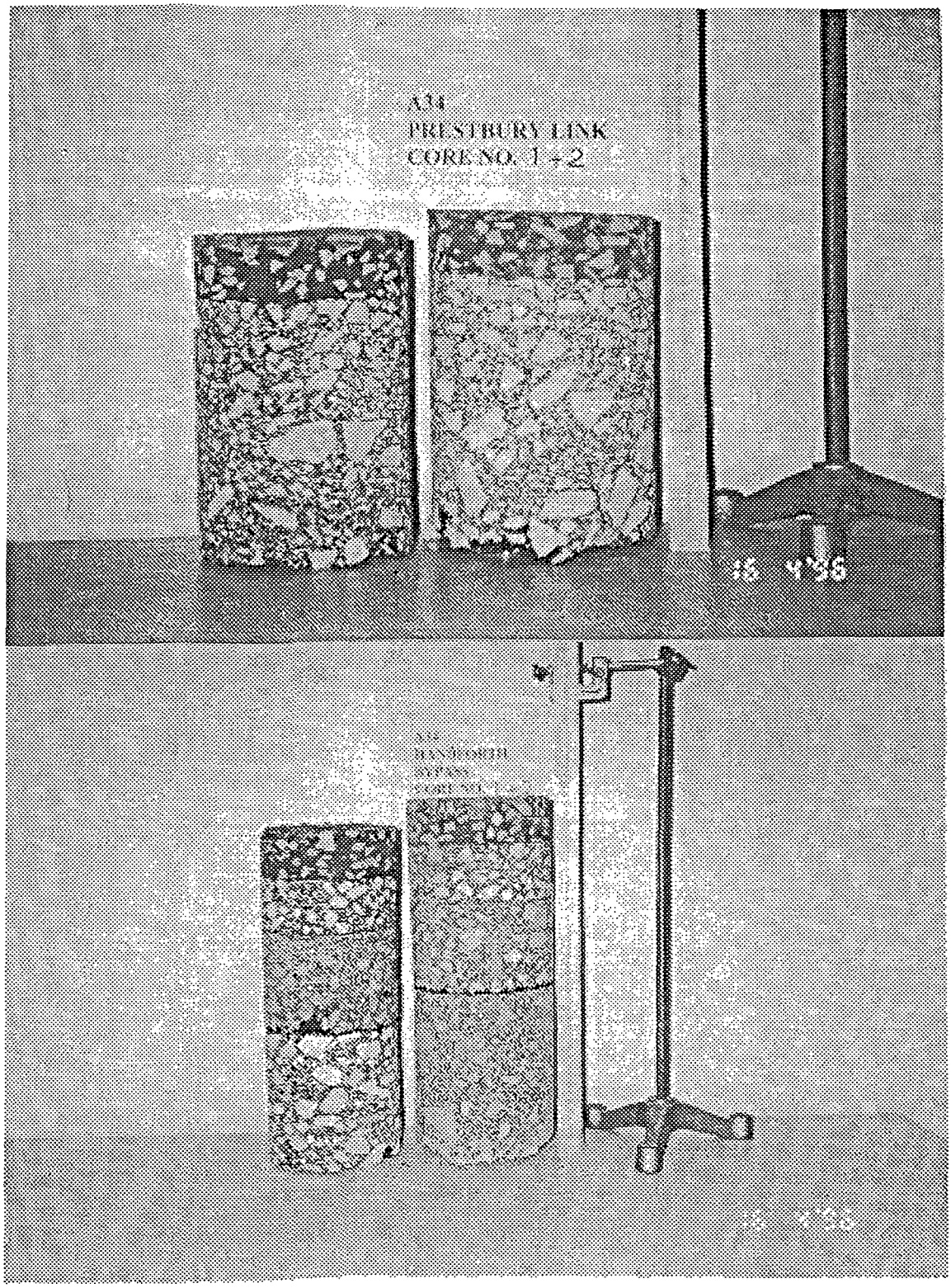


Figure 8.3, Prestbury link road and Handforth Bypass cores.

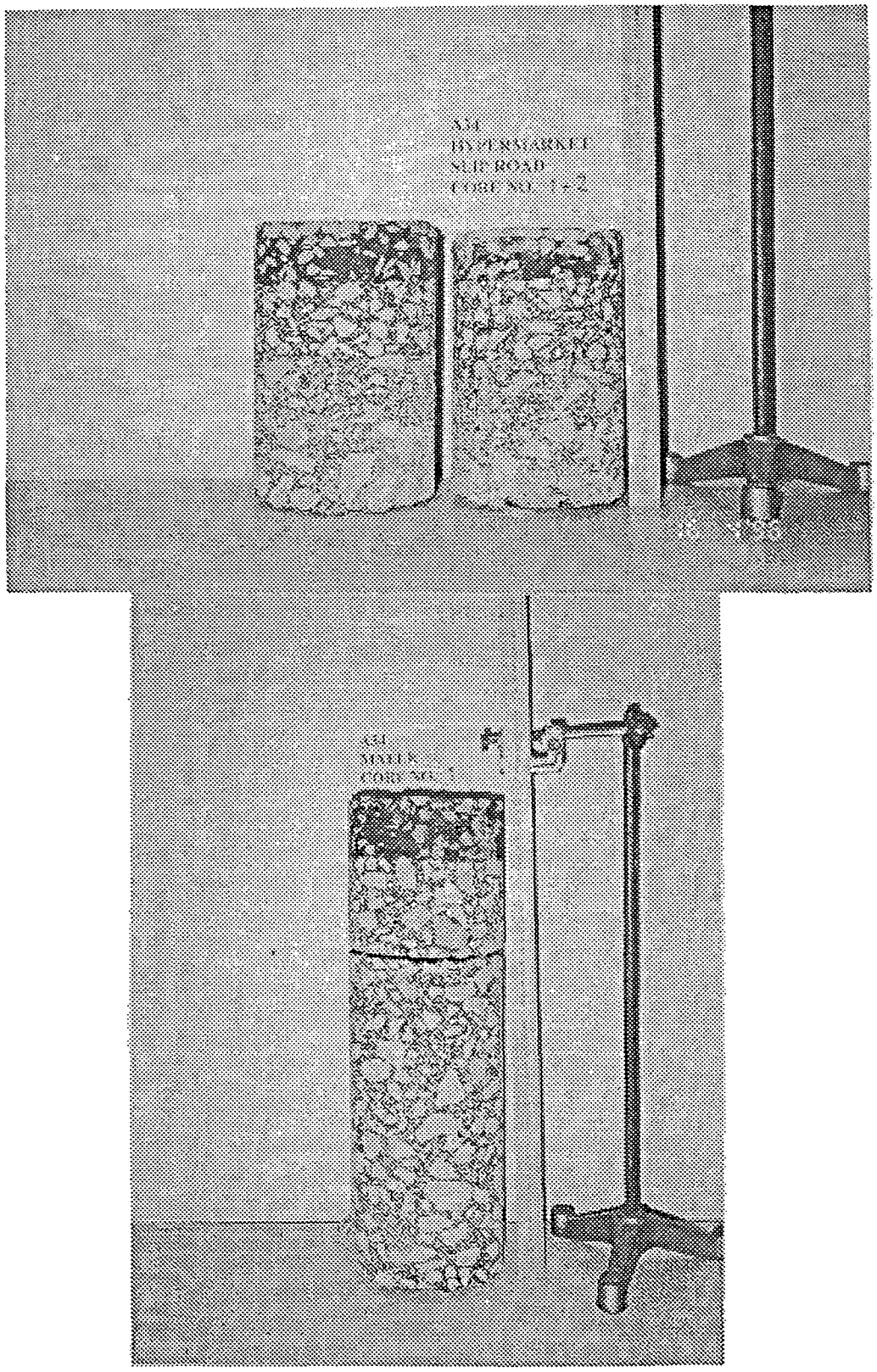

Figure 8.4, Hypermarket slip road and Manchester Airport Eastern link road cores.

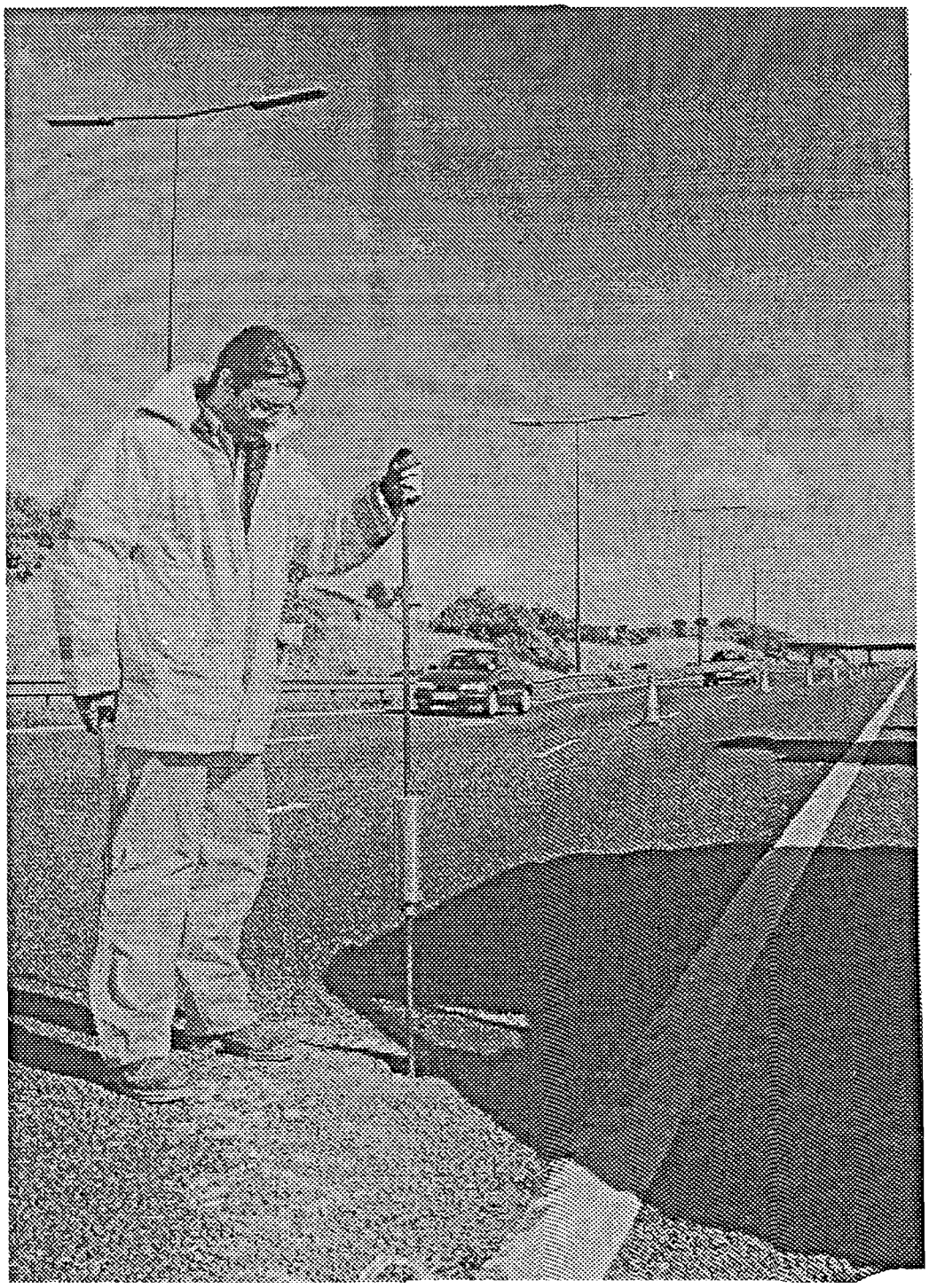

Figure 8.5, Dynamic Cone Penetrometer (DCP) testing.

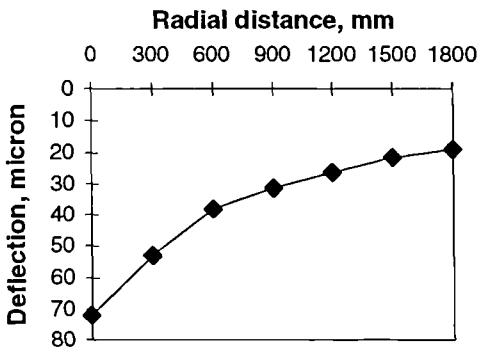


(Chainage 0)

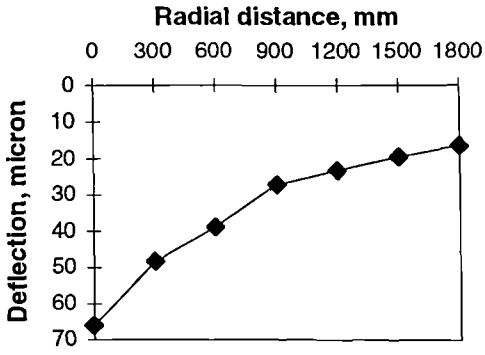


(Chainage 25)

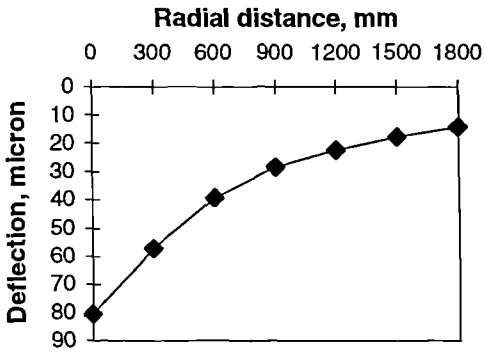


(Chainage 50)

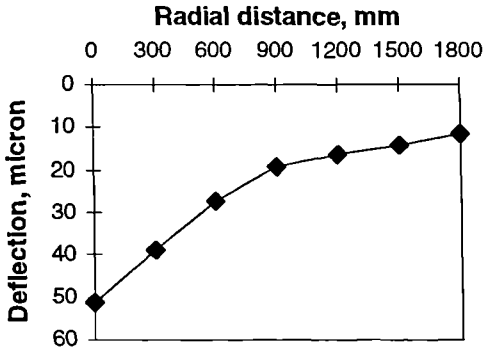


(Chainage 75)

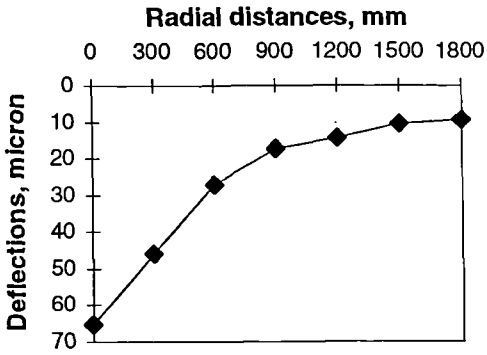


(Chainage 100)

Figure 8.6, Surface deflections for Prestbury link road.

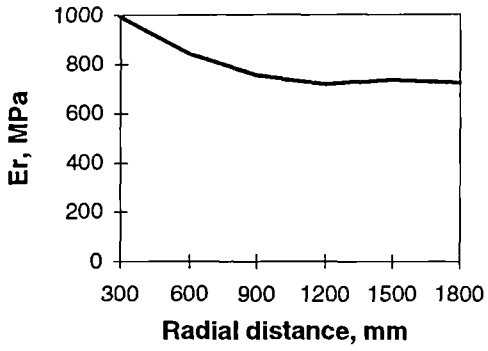


(Chainage 0)

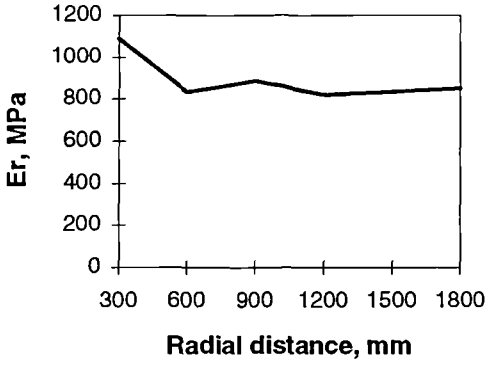


(Chainage 25)

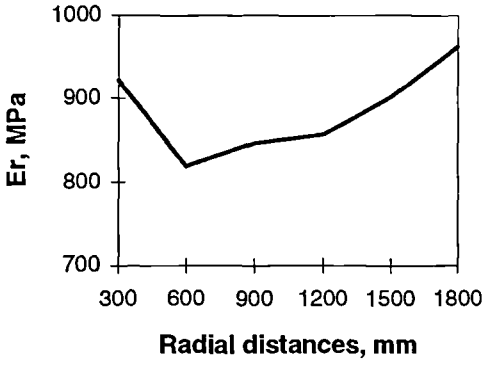


(Chainage 50)

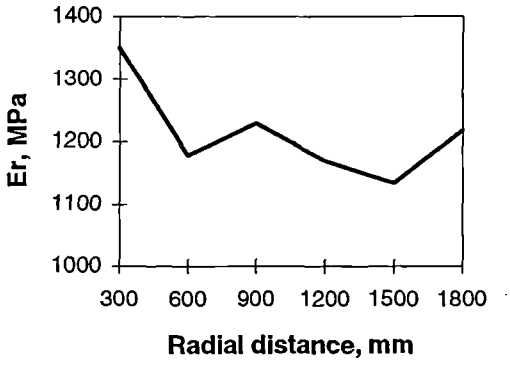


(Chainage 75)

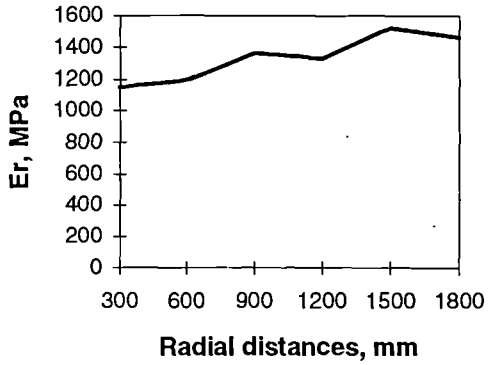


(Chainage 100)

Figure 8.7, Radial moduli for Prestbury link road.

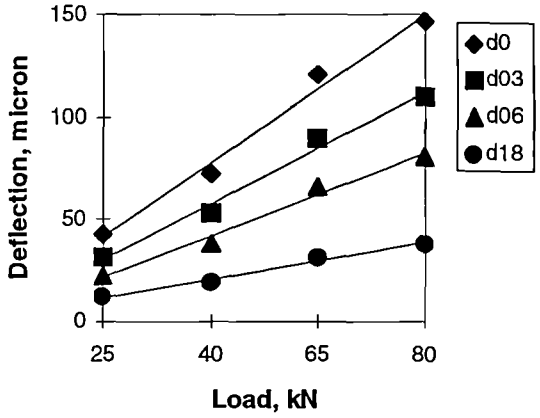


(Chainage 0)

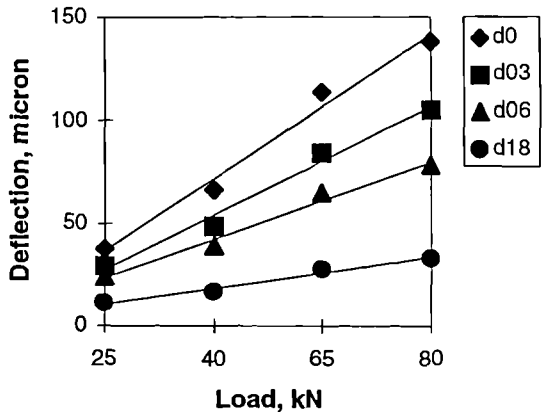


(Chainage 25)

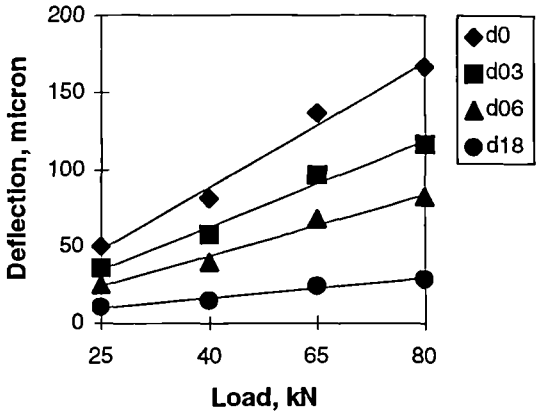


(Chainage 50)

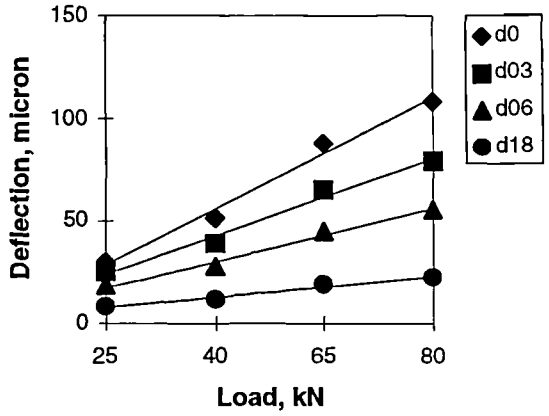


(Chainage 75)

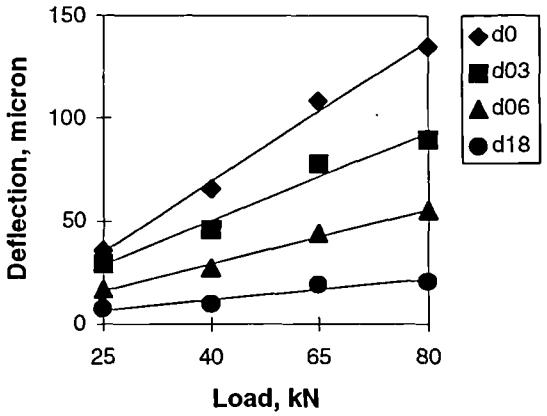


(Chainage 100)

Figure 8.8, Surface deflections as a function of FWD load, Prestbury link road.

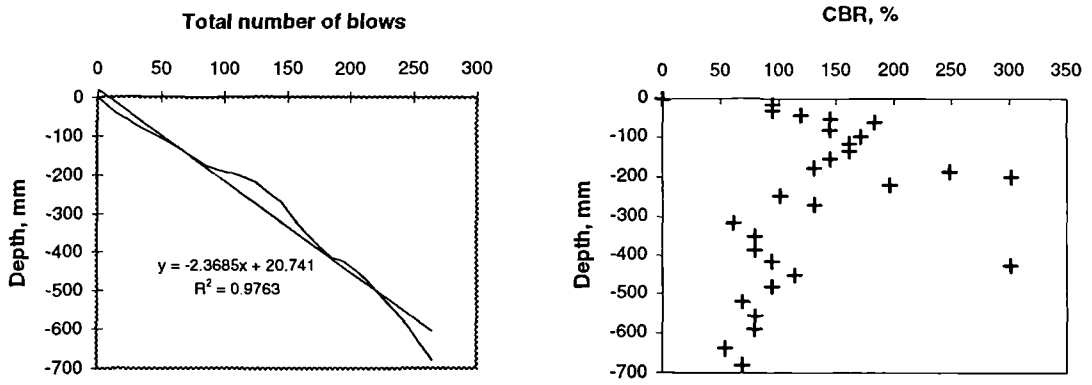


Figure 8.9, DCP test results for Prestbury link road (Chainage 25).

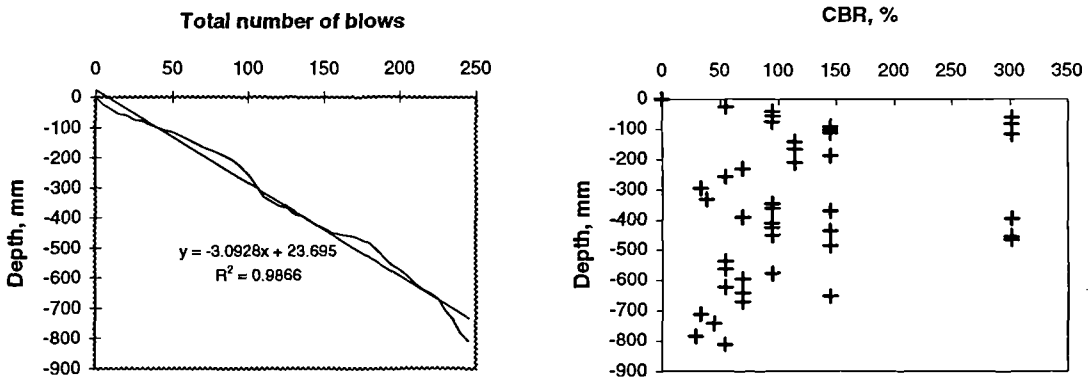


Figure 8.10, DCP test results for Prestbury link road (Chainage 50).

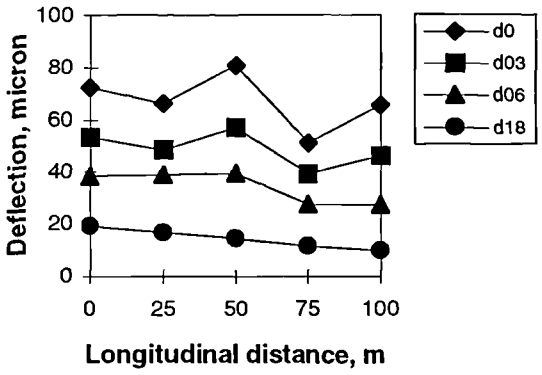


Figure 8.11, Deflections of Prestbury link road.

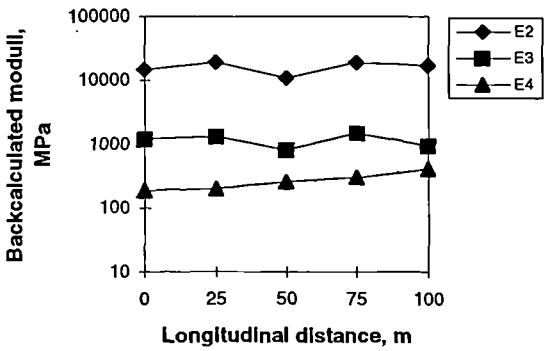


Figure 8.12, Backcalculated moduli for Prestbury link road.

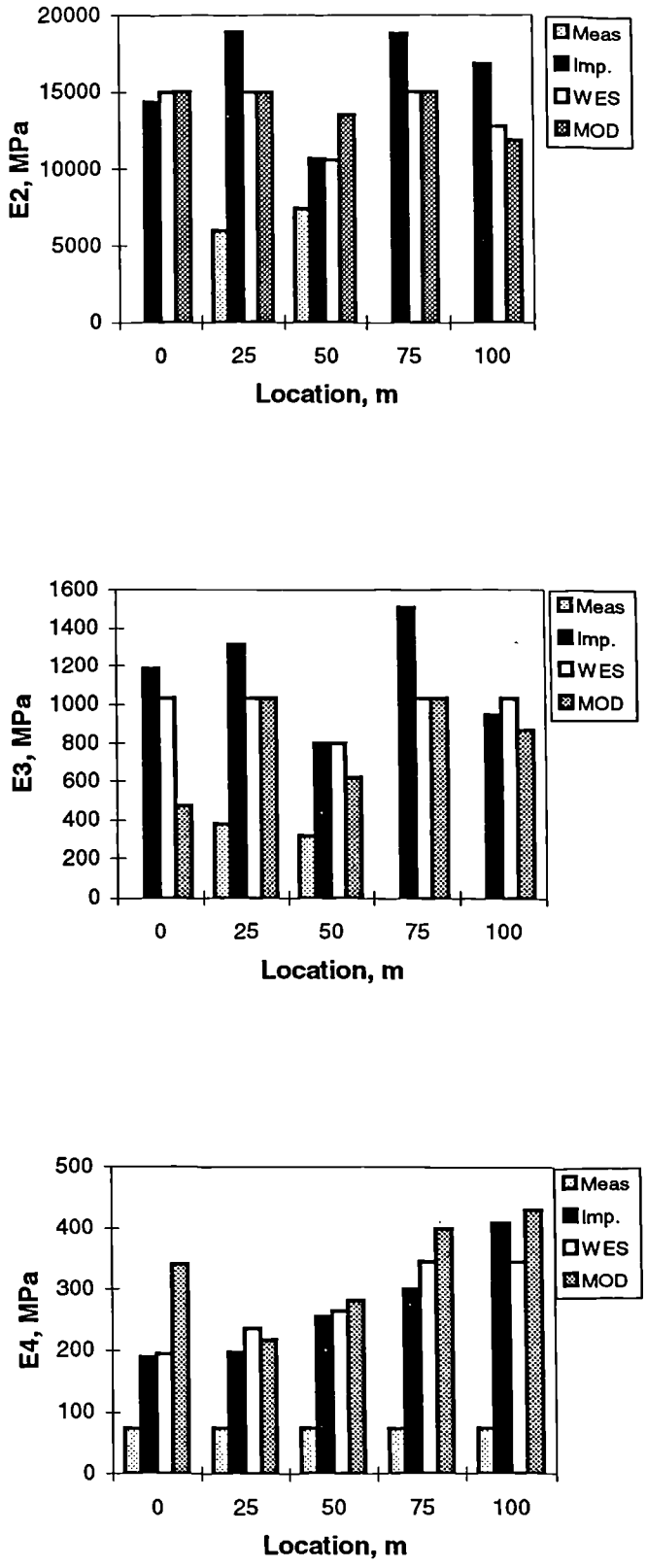


Figure 8.13, Comparison between measured and backcalculated moduli using different programs (Improved, WESDEF and MODULUS) for Prestbury link road.

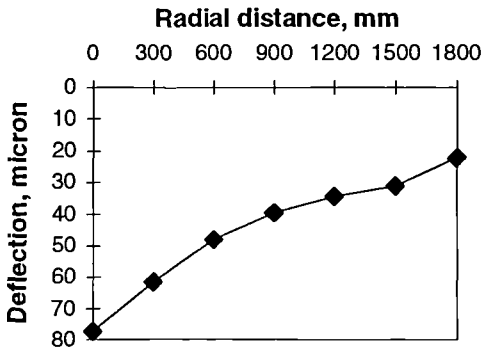


(Chainage 0)

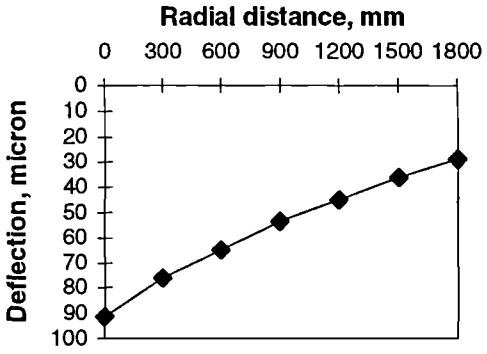


(Chainage 25)

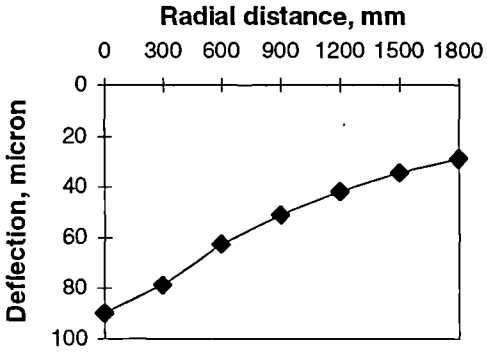


(Chainage 50)

Figure 8.14, Surface deflections for Handforth Bypass.

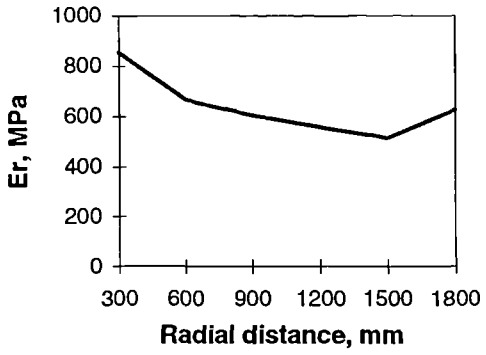


(Chainage 0)

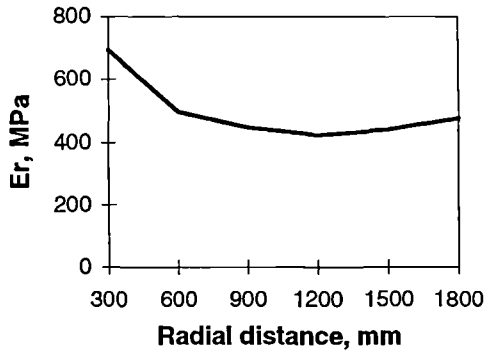


(Chainage 25)

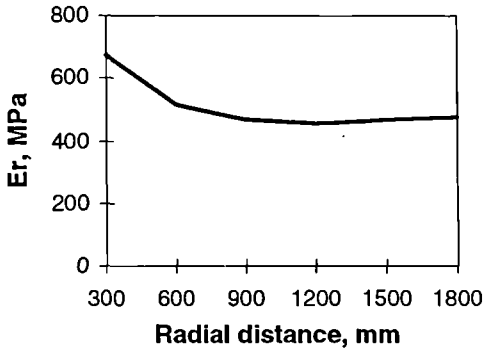


(Chainage 50)

Figure 8.15, Radial moduli for Handforth Bypass.

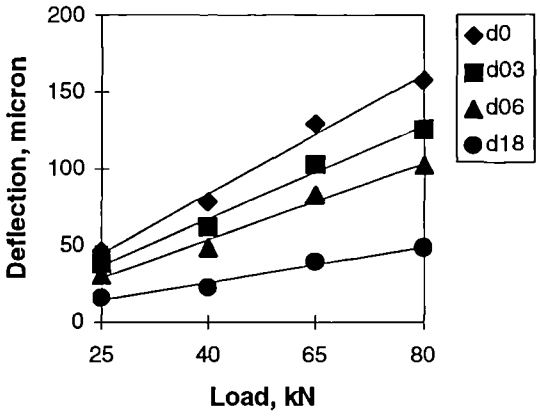


(Chainage 0)

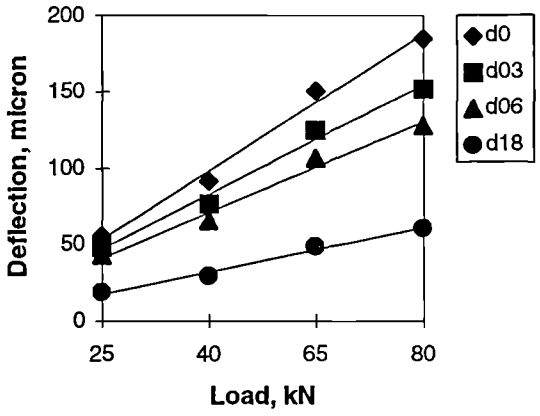


(Chainage 25)

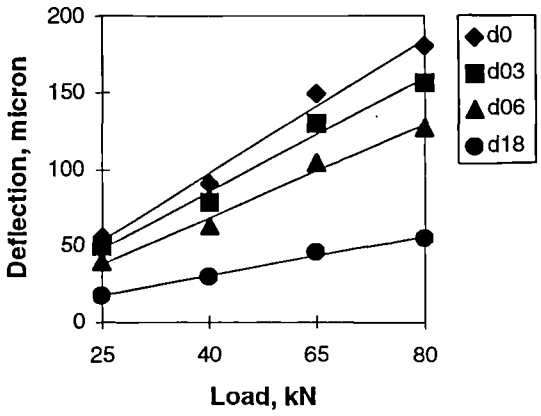


(Chainage 50)

Figure 8.16, Surface deflections as a function of FWD load, Handforth Bypass.

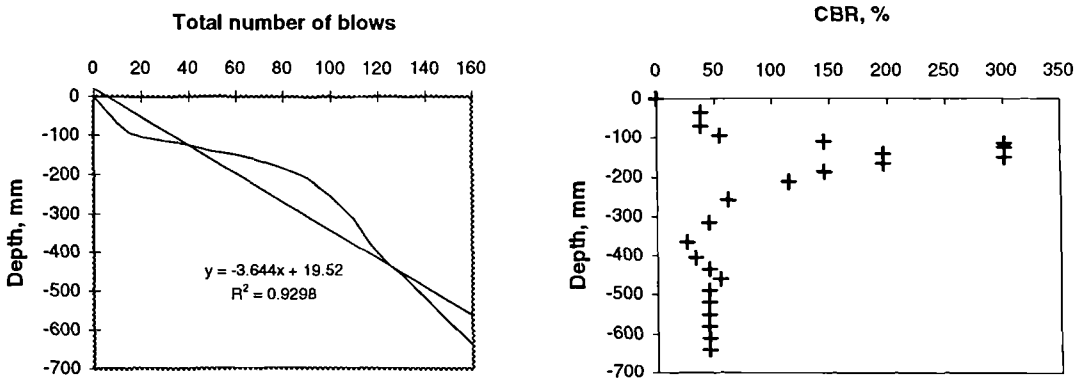


Figure 8.17, DCP test results for Handforth Bypass (Chainage 0).

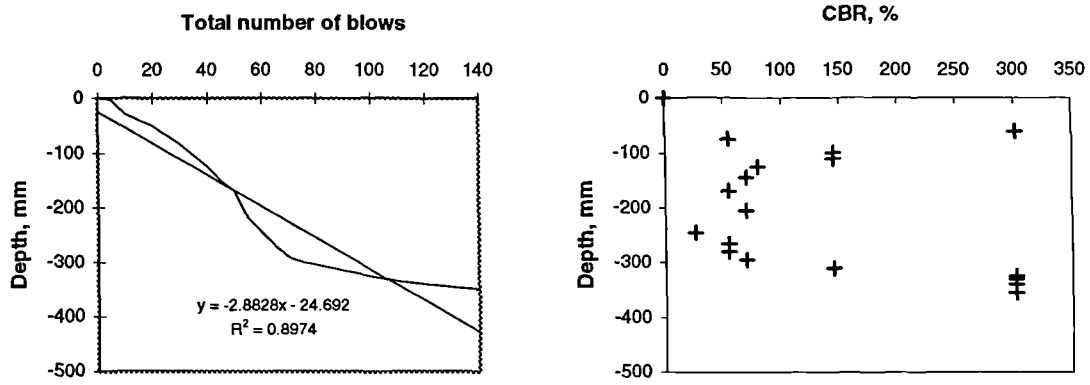


Figure 8.18, DCP test results for Handforth Bypass (Chainage 50).

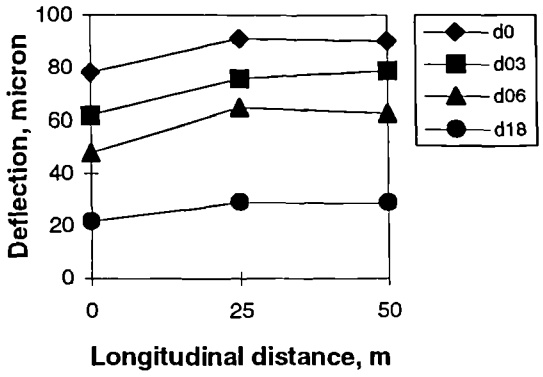


Figure 8.19, Deflections of Handforth Bypass

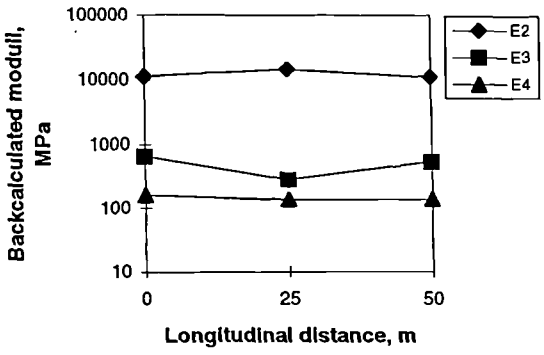


Figure 8.20, Backcalculated moduli for Handforth Bypass.

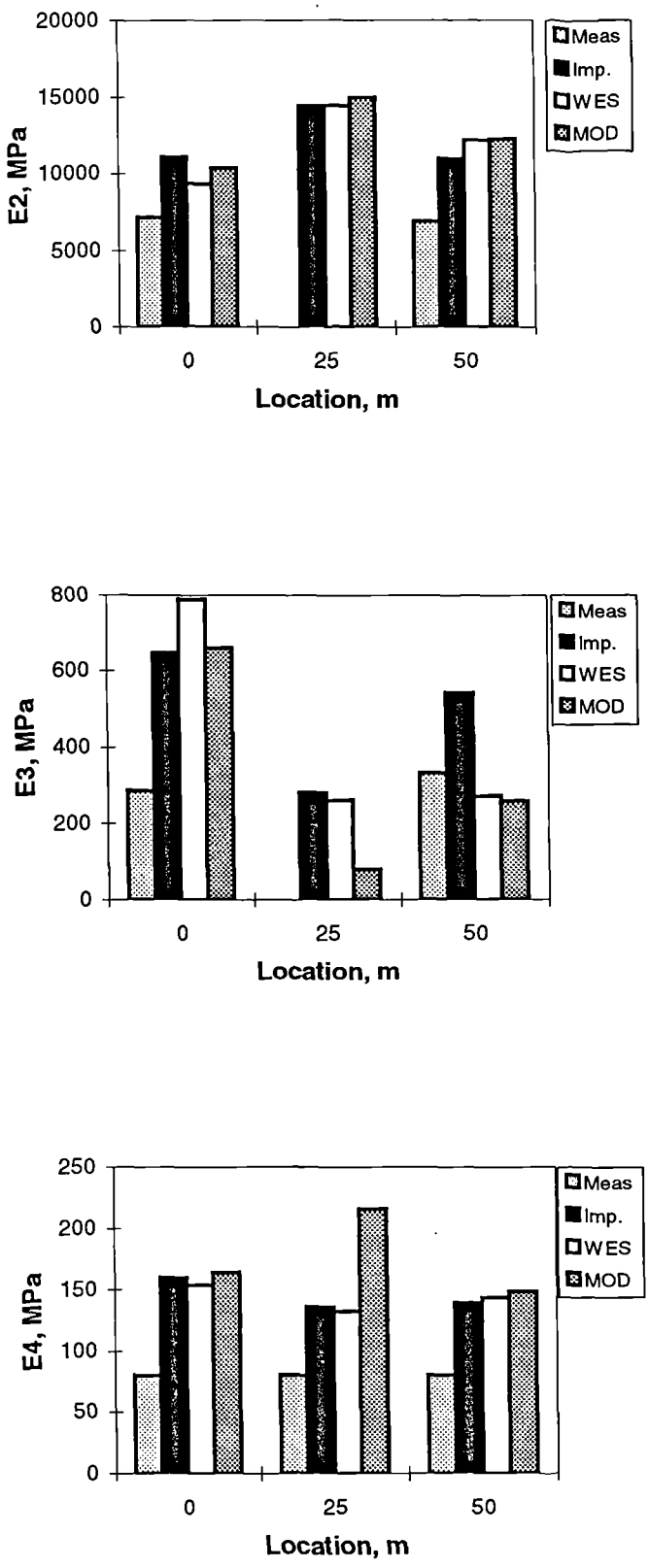


Figure 8.21, Comparison between measured and backcalculated moduli using different programs (Improved, WESDEF and MODULUS) for Handforth Bypass.

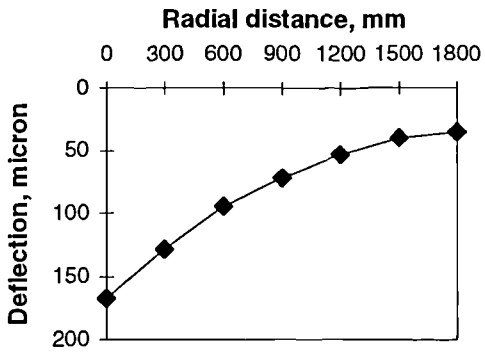


(Chainage 0)

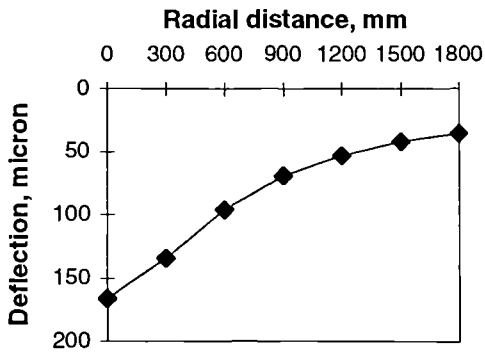


(Chainage 25)

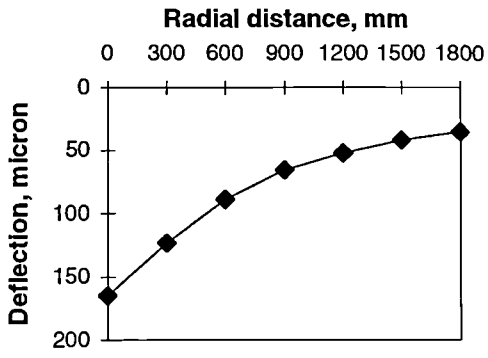


(Chainage 50)

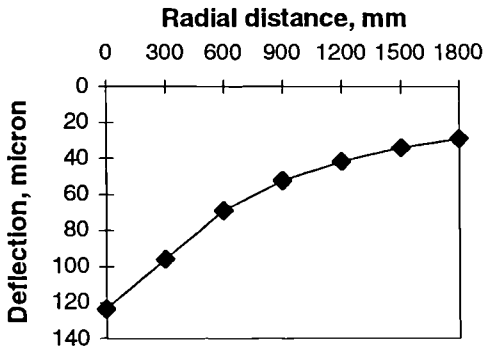


(Chainage 75)

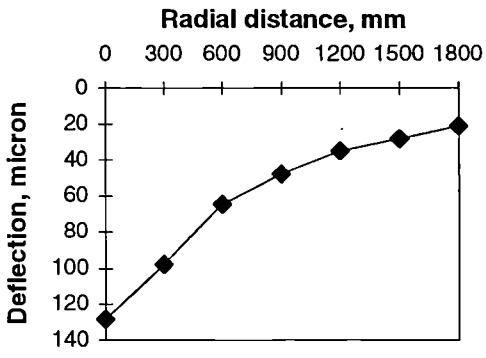


(Chainage 100)

Figure 8.22, Surface deflections for Hypermarket link road.

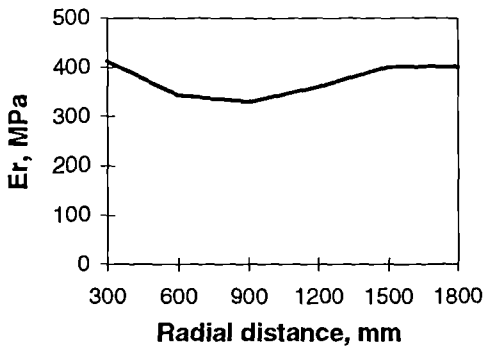


(Chainage 0)

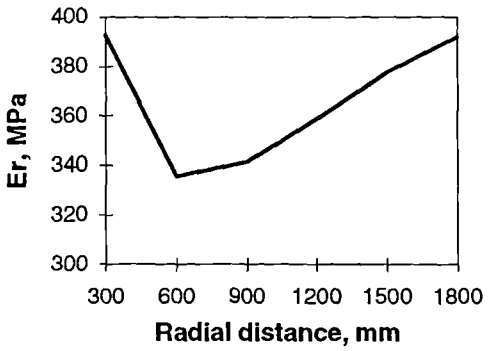


(Chainage 25)

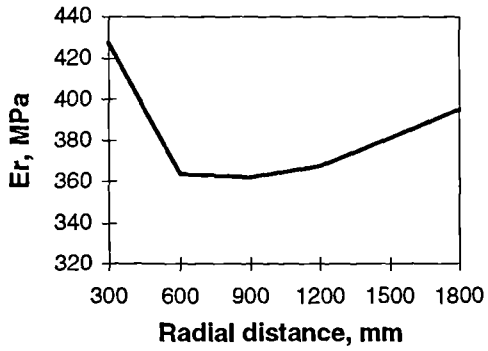


(Chainage 50)

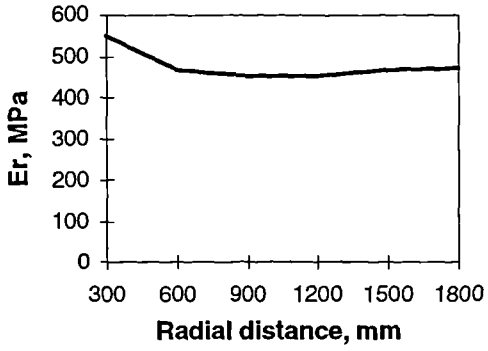


(Chainage 75)

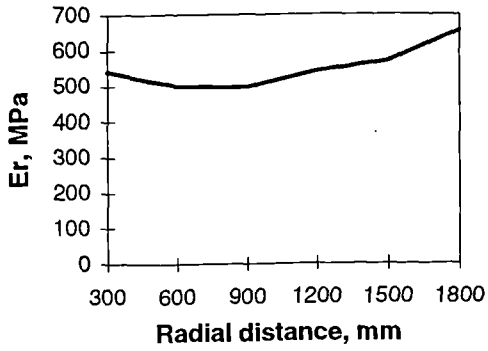


(Chainage 100)

Figure 8.23, Radial moduli for Hypermarket link road.

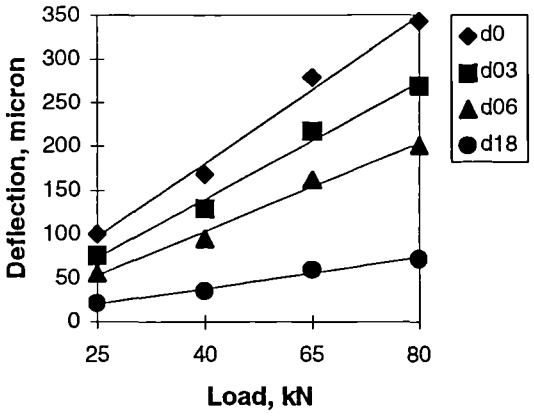


(Chainage 0)

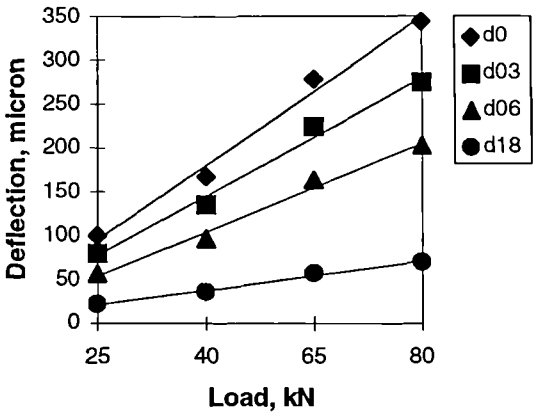


(Chainage 25)

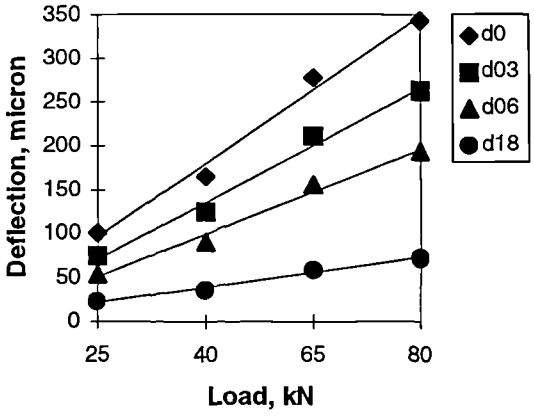


(Chainage 50)

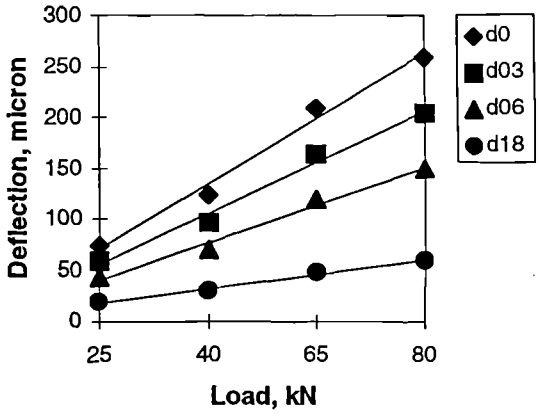


(Chainage 75)

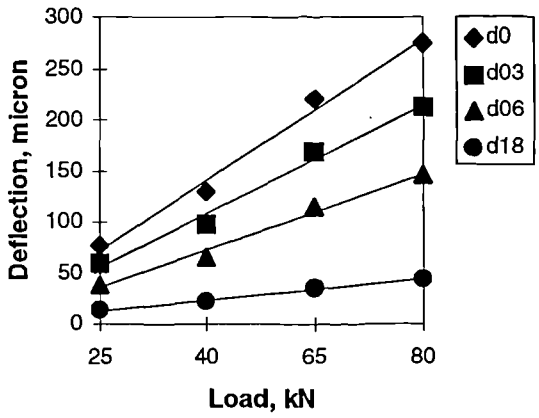


(Chainage 100)

Figure 8.24, Surface deflections as a function of FWD load, Hypermarket link road.

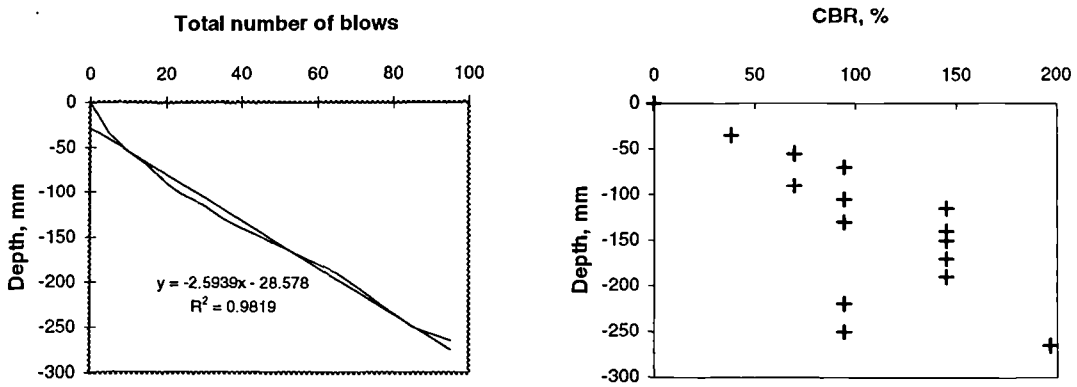


Figure 8.25, DCP test results for Hypermarket link road (Chainage 25).

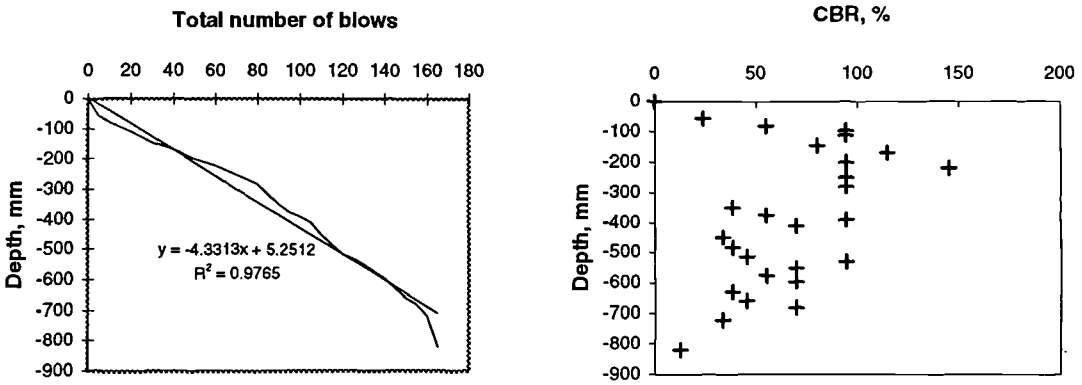


Figure 8.26, DCP test results for Hypermarket link road (Chainage 100).

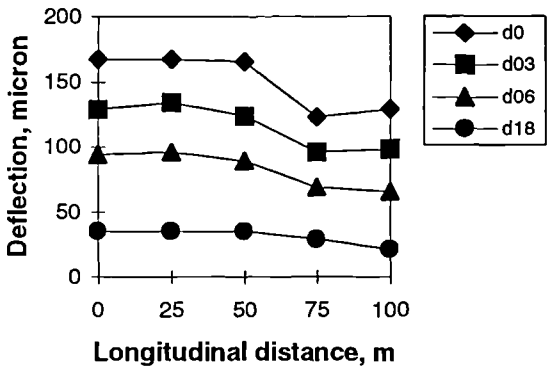


Figure 8.27, Deflections of Hypermarket link road.

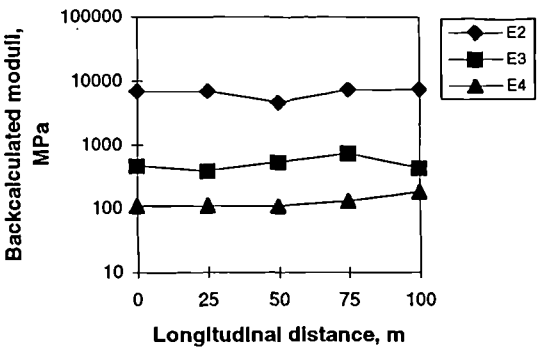


Figure 8.28, Backcalculated moduli for Hypermarket road.

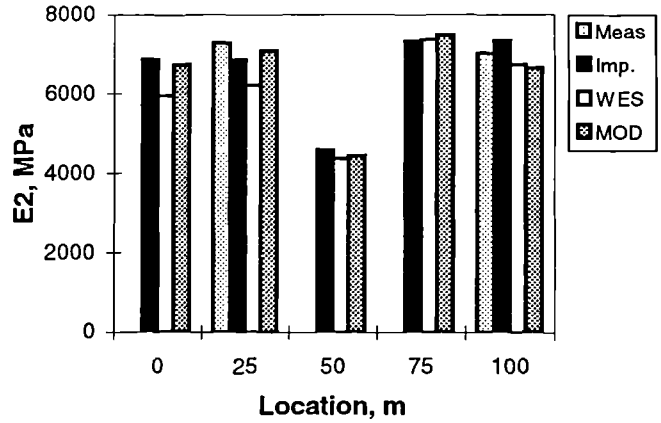


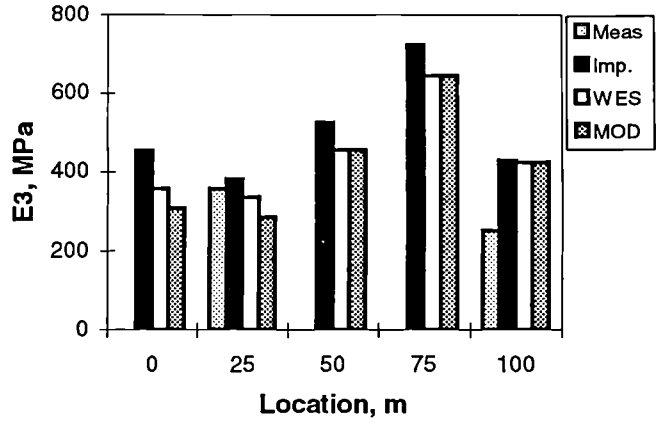


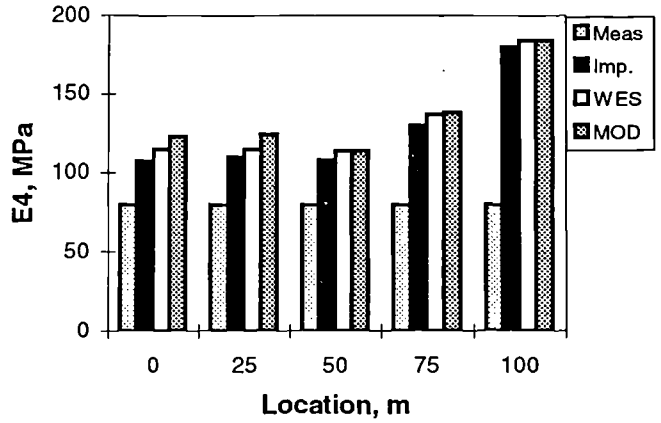


Figure 8.29, Comparison between measured and backcalculated moduli using different programs (Improved, WESDEF and MODULUS) for Hypermarket link road.

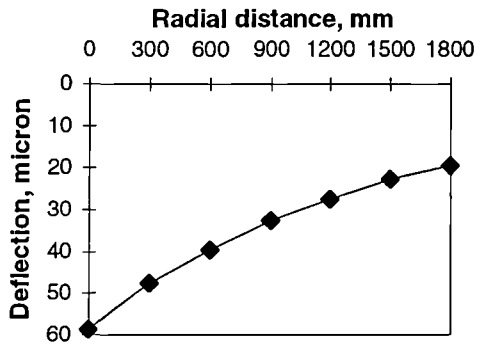


(Chainage 0)

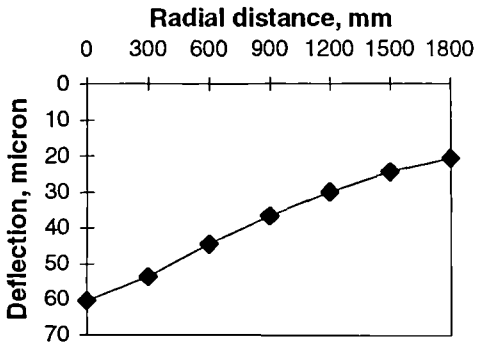


(Chainage 25)

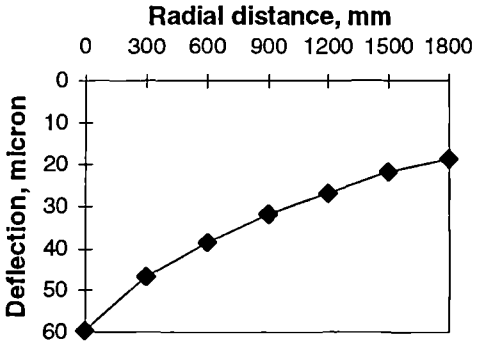


(Chainage 50)

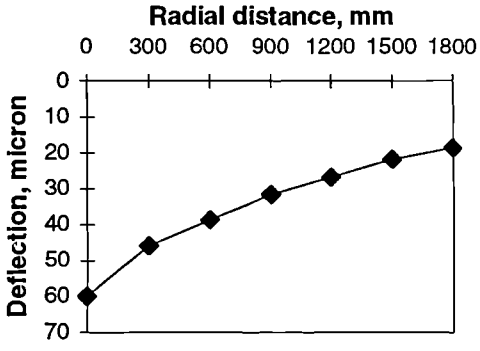


(Chainage 75)

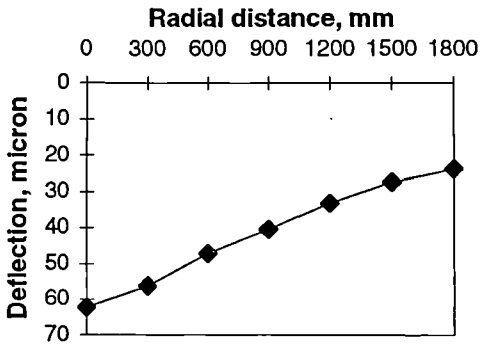


(Chainage 100)

Figure 8.30, Surface deflections for Manchester airport eastern link road.

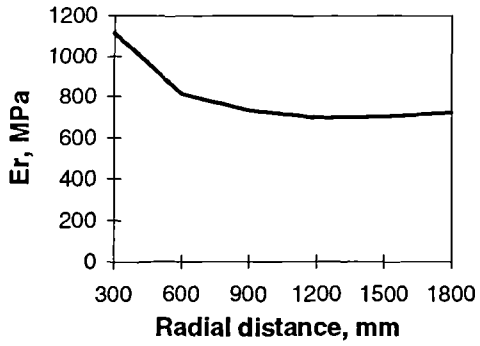


(Chainage 0)

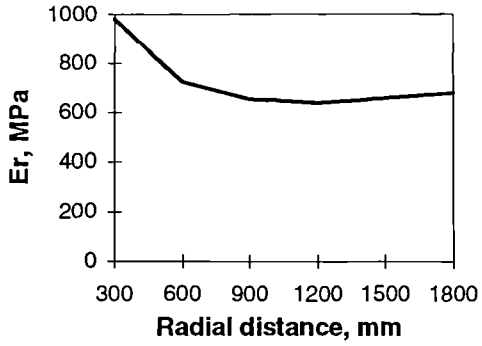


(Chainage 25)

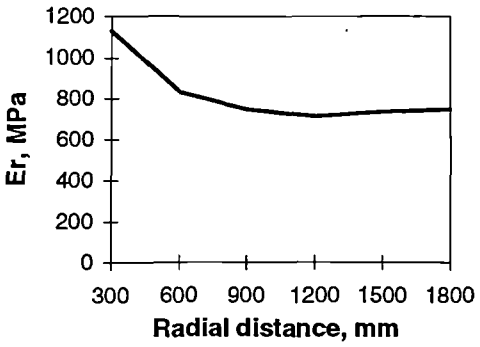


(Chainage 50)

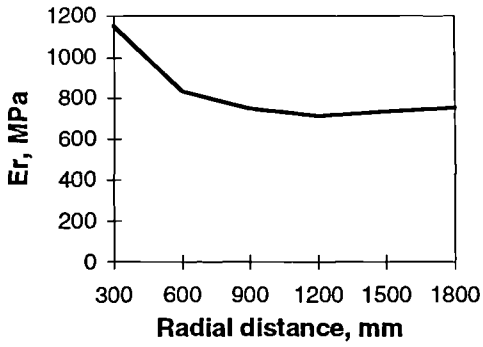


(Chainage 75)

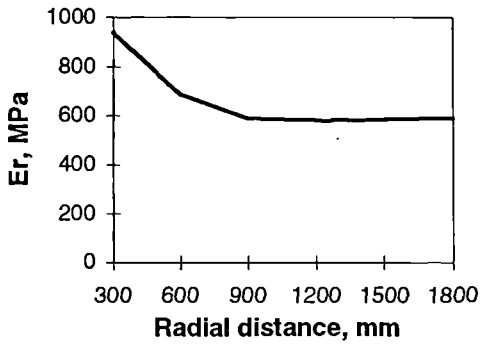


(Chainage 100)

Figure 8.31, Radial moduli for Manchester airport eastern link road.

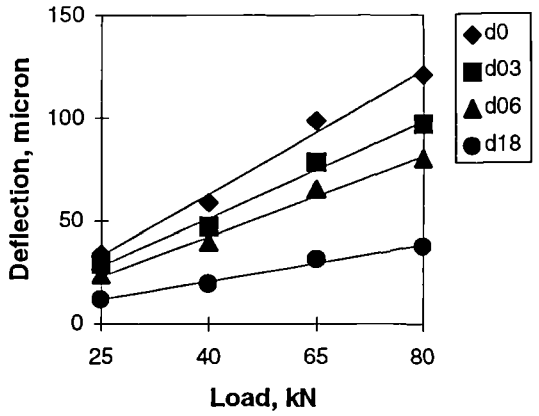


(Chainage 0)

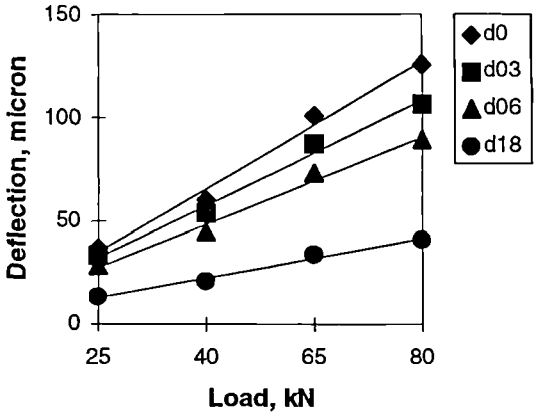


(Chainage 25)

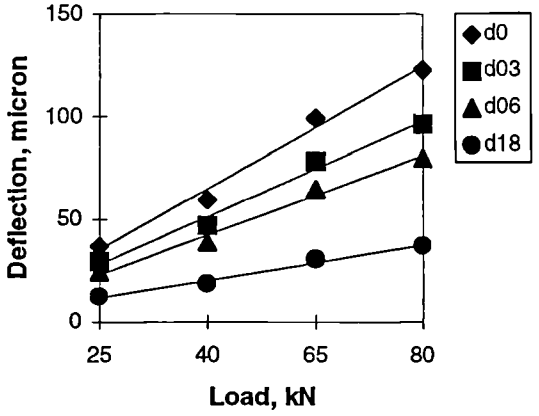


(Chainage 50)

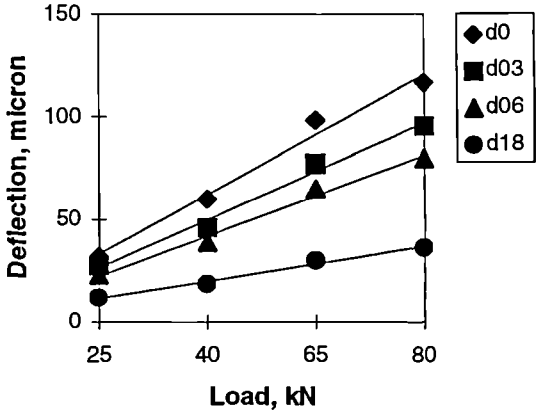


(Chainage 75)

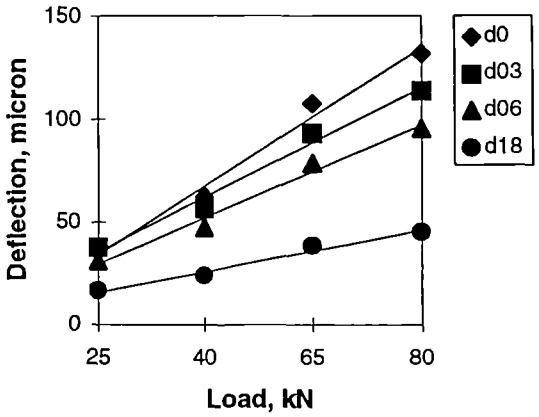


(Chainage 100)

Figure 8.32, Surface deflections as a function of FWD load, Manchester airport eastern link road.

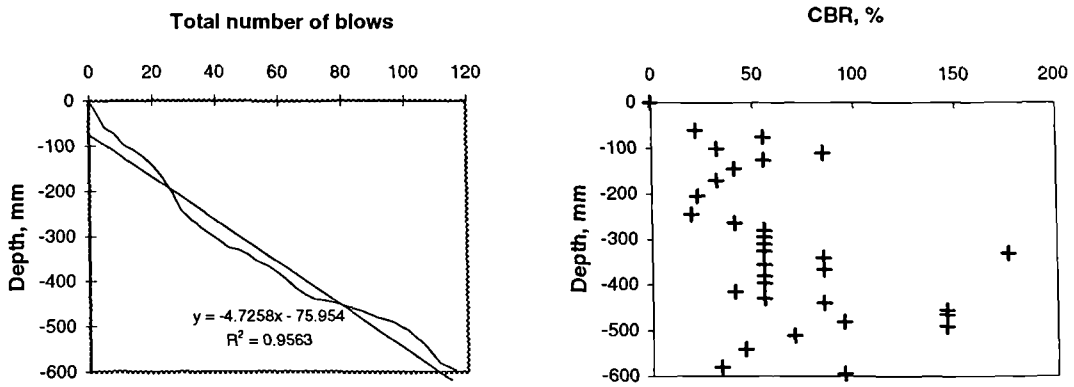


Figure 8.33, DCP test results for Manchester airport eastern link road (Chainage 75).

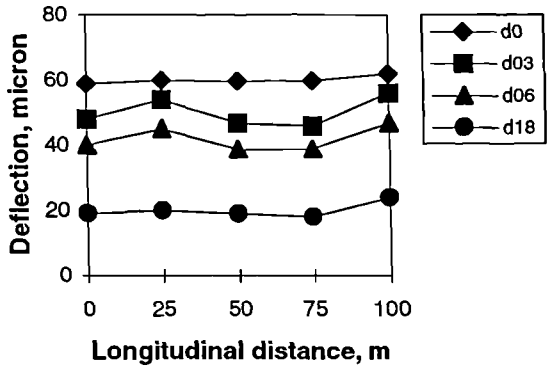


Figure 8.34, Deflections of Manchester airport eastern link road

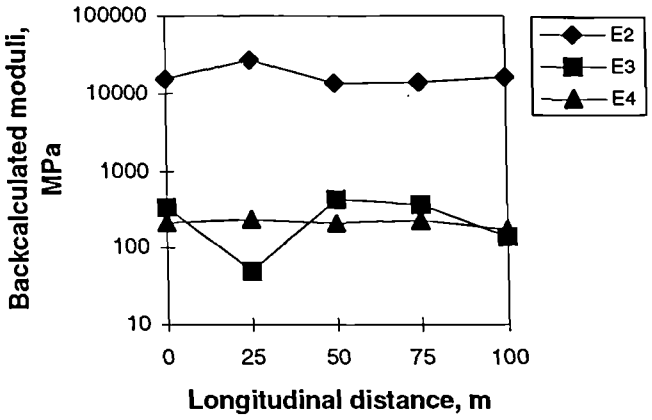


Figure 8.35, Backcalculated moduli for Manchester airport eastern link road.

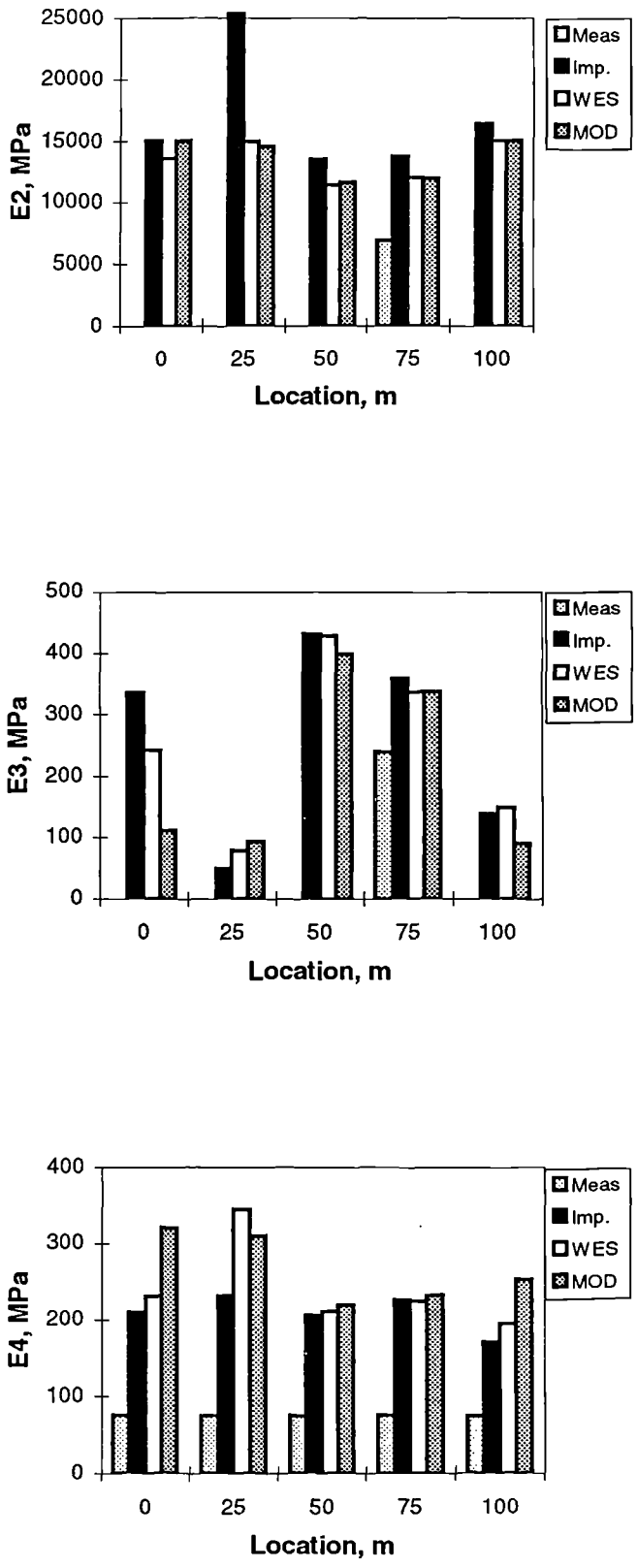


Figure 8.36, Comparison between measured and backcalculated moduli using different programs (Improved, WESDEF and MODULUS) for Manchester airport eastern link road.

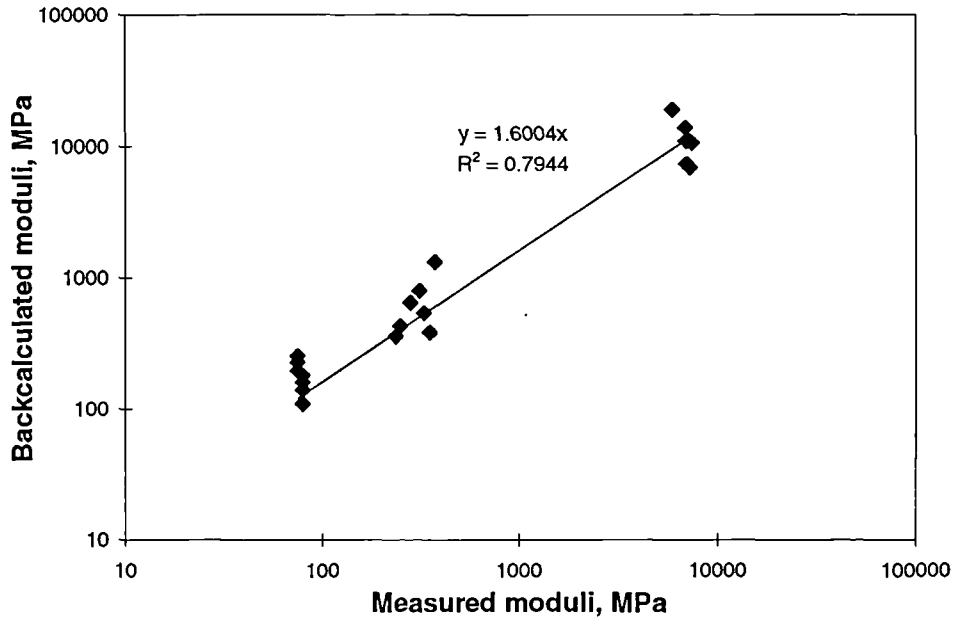


Figure 8.37, Comparison between the improved method backcalculated and measured moduli for A34 roads.

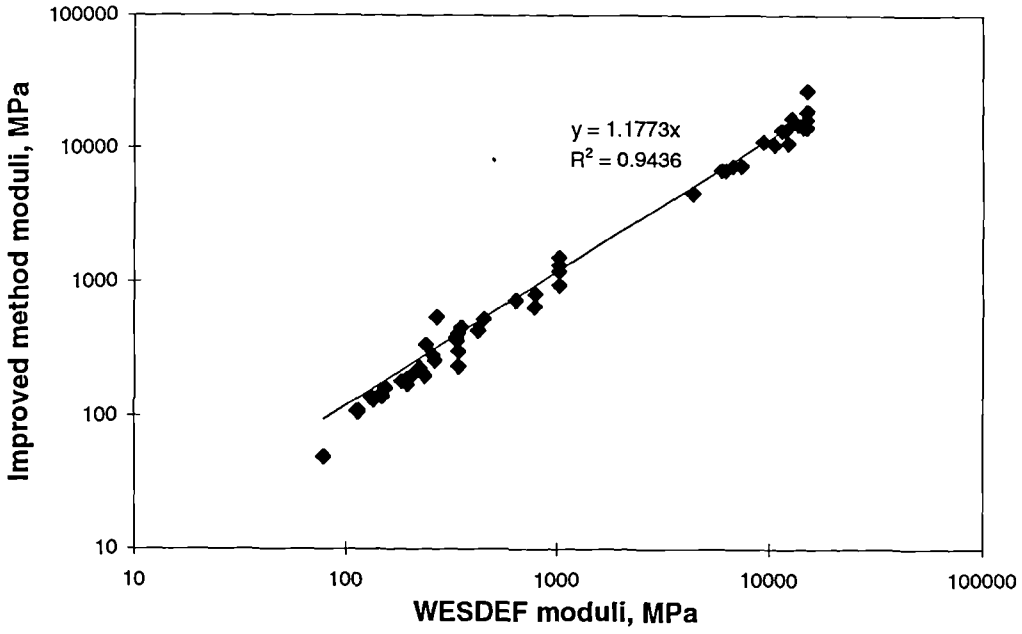


Figure 8.38, Comparison between backcalculated moduli using the improved procedures and WESDEF program for A34 roads.

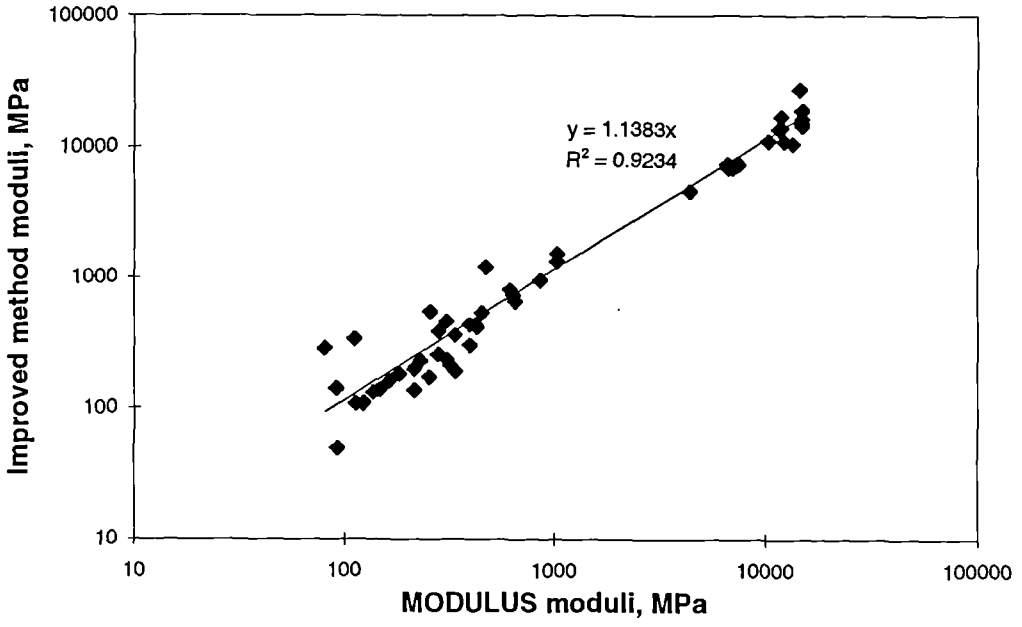


Figure 8.39, Comparison between backcalculated moduli using the improved procedures and MODULUS program for A34 roads.

# Chapter 9

# FULL SCALE TESTING OF PAVEMENT - A41 ROAD PAVEMENT ANALYSIS

## 9.1 INTRODUCTION

The same methodology for the A34 road pavements was adopted in this chapter for the empirical verification of the improved procedure.

The A41 road section (Aylesbury) test results were provided by SWK Pavement Engineering Ltd. Falling Weight Deflectometer (FWD) tests, layers' thickness, Indirect Tensile Test (ITT) (35) for bituminous mixtures and Dynamic Cone Penetrometer (DCP) tests (40) for unbound materials for the eight selected locations, were made available for the validation procedure.

The investigation of the A41 road section in a separate chapter was mainly made for to the following reasons:

i) the road had been subjected to traffic for more than 20 years,

ii) the results were supplied for analysis only and no control was made on the type and configuration of the tests,

iii) only one load magnitude was performed using the FWD, therefore the study of the pavement materials non-linearity was not feasible.

The pavement was simplified for backcalculation purposes as a three layer system with additional rigid layer at certain depth as shown in figure 9.1. The first layer represents the bituminous wearing course whereas the remaining bituminous materials were combined to form layer two. Due to the lack of information about the subbase thickness, the unbound layers including the subgrade were assumed as layer three. Figure 9.1 shows large variations

in the layer thickness from one location to another due to repair and overlay construction during the pavement life.

To make more realistic comparison between the laboratory measured moduli and the backcalculated values, only the deflection basins at the core locations were analysed. Therefore the comparison results were considered for each location independently and no reference was made to the average deflection and thickness to predict the overall road pavement conditions.

The rigid layer was assumed at 6 m depth from the pavement surface except for cores 5 and 12, where the radial moduli details indicate possible bedrock at shallow depth. The detail of the bedrock depth calculation is outlined later in this chapter.

## 9.2 PAVEMENT TESTING

Deflection basins under 50 kN FWD load for the eight cores' locations are illustrated in figure 9.2. Seven deflection sensors were used at the load centre, 300, 600, 900, 1200, 1500 and at 2100 mm radial distance.

Deflection magnitude varied between locations due to the variations in layer's thickness and subgrade stiffness. The stronger the pavement, the lower the deflection values. Deflections far from the load centre are influenced mainly by the lower layers' properties as explained in Chapter Five. Figure 9.2 demonstrates very low deflections at the 2100 mm radial distance for the core numbers 5 and 12, which indicate very stiff subgrade or bedrock presence at a shallow depth.

A radial modulus shown in figure 9.3 was used for detecting the presence of the rigid layer as explained in previous chapters. Both cores 5 and 12 locations revealed shallow bedrock beneath the pavement, as indicated by the large increase in the radial modulus away from the load centre. Therefore it was decided to backcalculate the depth of rigid layer for these locations in addition to the normal parameters in the improved method. An apparent stiff layer at 6 m depth was assumed in the remaining core locations as shown in figure 9.1.

Table 9.1 presents the measured moduli for the eight locations. ITT was used to predict the moduli of bituminous layers and DCP test results were used for unbound materials. The TRL (4,100) empirical relationships for calculating the unbound materials moduli from DCP test results were applied (see Chapter 8). A large variation in subgrade modulus along the pavement length was noticed.

## 9.3 BACKCALCULATION RESULTS

The deflection basin for each core location was analysed. Apparent stiff layer was assumed at 6 m depth to represent the bedrock. However the bedrock depth for cores 5 and 12 was backcalculated using the improved method due to the strong indication of its presence at shallow depth (see figure 9.3). Subgrade thicknesses of 2475 and 3525 mm were computed for the core locations 5 and 12 respectively. This has been done by considering the subgrade thickness as an unknown parameter in the first stage backcalculation procedure. WESDEF program predicts approximately subgrade thickness of 2.5 m for the two locations to support these values.The layer thickness and the Poisson's ratios are presented in figure 9.1.

The modulus of the wearing course was fixed in the backcalculation process as found from the ITT results. The modulus of the bituminous base ($E_2$) and the modulus of the subgrade ($E_3$) in addition to the shear reaction modulus between the wearing and base courses ($K_{s1}$) were predicted using the improved method.

The same deflection basins were used to backcalculate the moduli of the bituminous base and subgrade soil using the following programs, WESDEF(50), SID (49) and MODULUS (51). The above assumptions were made in the backcalculation process except that full adhesion was assumed at the interface between the pavement's layers. The depth of the bedrock for location 5 and 12 were assumed in these backcalculation programs as predicted by the improved method.

Table 9.2 presents the backcalculation results for the eight cores using the improved, WESDEF, SID and MODULUS programs. Some variations were noticed between the backcalculated moduli at different locations, specially for the subgrade moduli. However, comparing the backcalculated results using different programs for each core location

independently revealed good agreement. The adhesion properties between wearing and base courses, as computed from the improved method were acceptable. Shear reaction modulus was found to vary between $10^4$ and $10^5$ MN/m$^3$ , except a value of $10^3$ MN/m$^3$ for core C3 to indicate intermediate bonding condition.

## 9.4 COMPARISON BETWEEN MEASURED AND CALCULATED MODULI

Figure 9.4 shows the comparison between the measured moduli and the calculated values using the improved, WESDEF, SID and MODULUS programs, for the eight studied cores.

Lower values (up to 50% ) for measured bituminous base moduli compared with the calculated values were found, due to the reasons explained in previous chapters. Very good agreement for the subgrade foundation was noticed.

The comparison between the improved method computed moduli and the measured values was carried out in figure 9.5. A high coefficient of correlation of 79.8% was found which validate the improved procedure.

Figures 9.6, 9.7 and 9.8 demonstrate the comparison between the improved method predicted moduli on one hand and WESDEF, SID and MODULUS programs moduli respectively on the other hand.

Very high coefficients of correlation of 96.4%, 84.1% and 96% for WESDEF, SID and MODULUS were found respectively. These values support the previous conclusion of the satisfactory performance of the improved procedure.

## 9.5 CONCLUSIONS

The new improved method for backcalculating the layer moduli and the shear reaction modulus between the wearing and base courses, has been empirically validated using the A41 road testing results.

Good correlation (79.8%) was found between the predicted and measured moduli. Furthermore the comparison with other well known backcalculation programs results revealed good agreement (more than 84%) when the same simplifications were used.

Acceptable adhesion was predicted between the wearing and base courses for most of the pavement locations.

Therefore, the use of the improved method in pavement assessment is recommended since it predicts the state of adhesion between the wearing and base courses in addition to the layers moduli.

Table 9.1, Measured pavement layer moduli for A41 road.

| Core number | ITT $E_1$ (MPa) | ITT $E_2$ (MPa) | DCP $E_3$ (MPa) |
|---|---|---|---|
| C1 | NA | NA | 100 |
| C3 | NA | 5500 | 162 |
| C4 | 4500 | 5450 | 354 |
| C5 | 3450 | 6650 | 267 |
| C12 | NA | 2100 | 168 |
| C14 | NA | 8750 | NA |
| C15 | 7400 | 6650 | 138 |
| C16 | NA | NA | 75 |

Table 9.2, Backcalculated parameters from Falling Weight Deflectometer test result using different programs (Improved, WESDEF, SID and MODULUS), for A41 road.

| Core number | $E_2$ (MPa) | | | | $E_3$ (MPa) | | | | $K_{s1}$ MN/m$^3$ |
|---|---|---|---|---|---|---|---|---|---|
| | Imp. | WES. | SID | MOD. | Imp. | WES. | SID | MOD. | Imp. |
| C1 | 14780 | 15000 | 19039 | 15000 | 92 | 87 | 76 | 91 | $10^4$ |
| C3 | 19835 | 15000 | 10677 | 14741 | 151 | 171 | 171 | 169 | $10^3$ |
| C4 | 14540 | 15000 | 16925 | 15000 | 282 | 273 | 265 | 280 | $10^5$ |
| C5 | 13440 | 11975 | 11216 | 13622 | 184 | 185 | 188 | 177 | $10^4$ |
| C12 | 8880 | 5332 | 5146 | 6850 | 101 | 119 | 122 | 110 | $10^5$ |
| C14 | 12150 | 12165 | 12120 | 12804 | 201 | 191 | 196 | 188 | $10^5$ |
| C15 | 14605 | 13180 | 11924 | 11353 | 104 | 107 | 107 | 115 | $10^5$ |
| C16 | 13650 | 13460 | 12527 | 13665 | 95 | 98 | 97 | 95 | $10^4$ |

| | | |
|---|---|---|
| $h_1$ | Bituminous Wearing Course<br>Layer 1 | $\nu_1 = 0.35$<br>$K_{s1}$= variable |
| $h_2$ | Bituminous Base<br>Layer 2 | $\nu_2 = 0.35$<br>$K_{s2}$ = full adhesion |
| $h_3$ | Subgrade<br>Layer 3 | $\nu_4 = 0.4$ |

Rigid Layer

| Core number | $h_1$ (mm) | $h_2$ (mm) | $h_3$ (mm) |
|---|---|---|---|
| **C1** | 40 | 165 | 5795 |
| **C3** | 60 | 210 | 5730 |
| **C4** | 55 | 255 | 5690 |
| **C5** | 55 | 110 | To be backcalculatd |
| **C12** | 55 | 145 | To be backcalculatd |
| **C14** | 55 | 255 | 5690 |
| **C15** | 60 | 195 | 5745 |
| **C16** | 50 | 305 | 5645 |

Figure 9.1, Summary of A41 pavement structure for the eight selected locations.

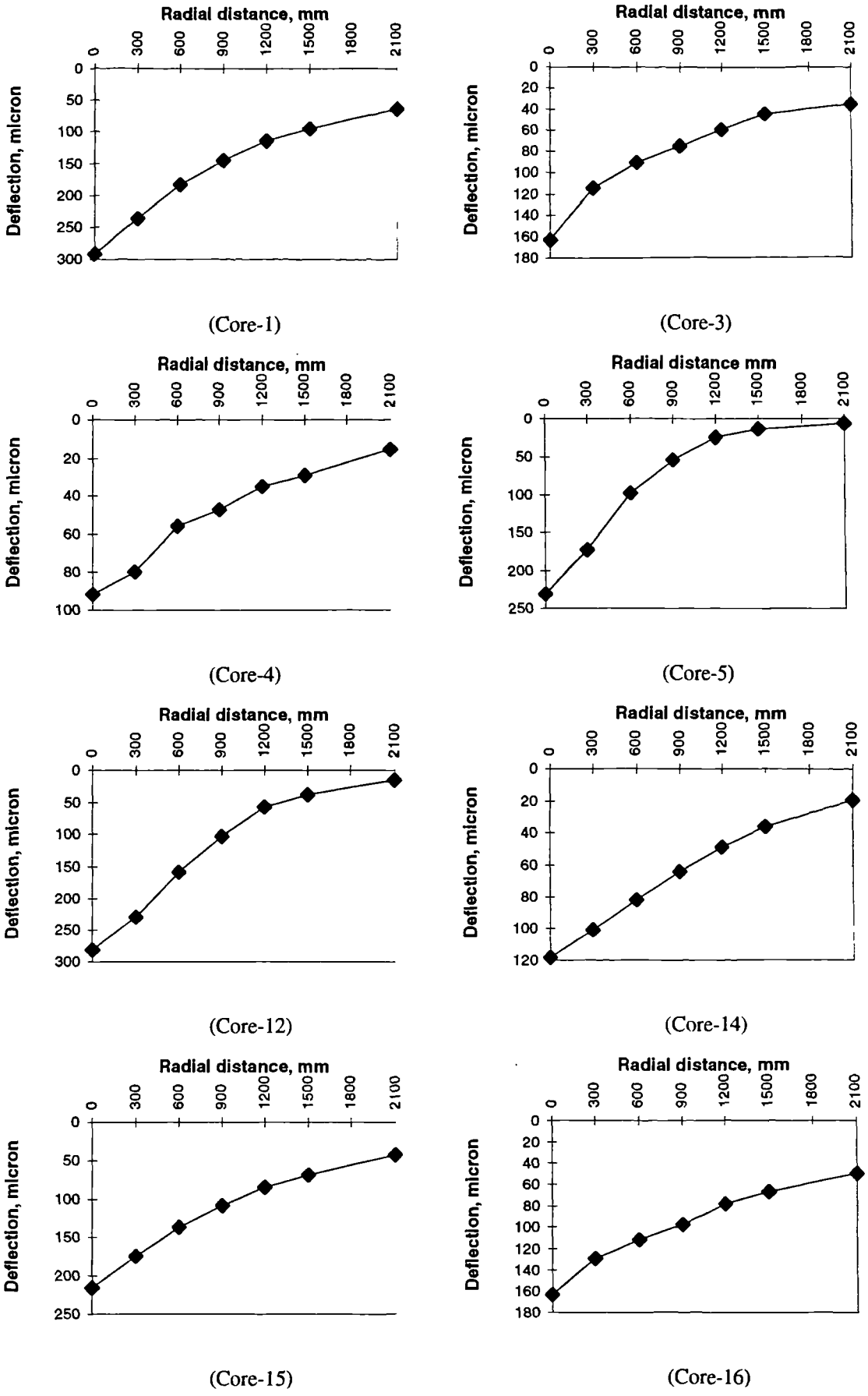


Figure 9.2, Surface deflections for A41 road.

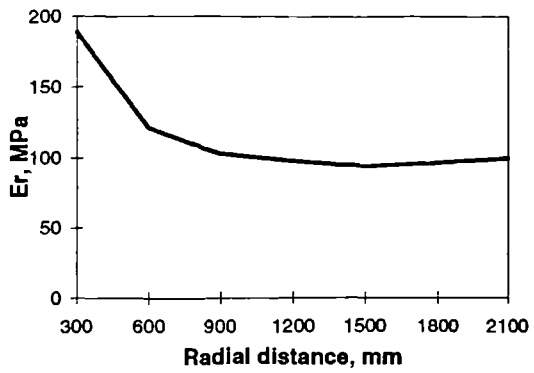


(Core-1)

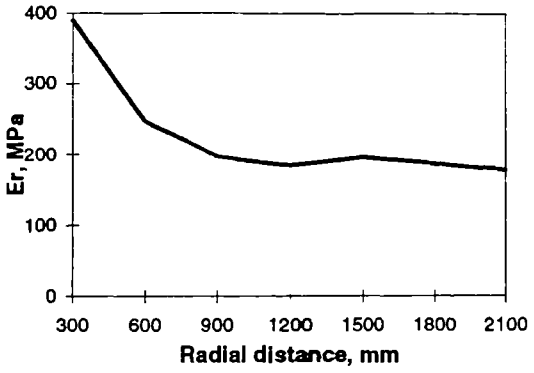


(Core-3)

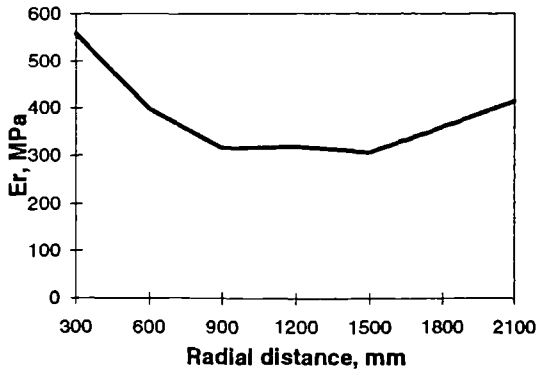


(Core-4)

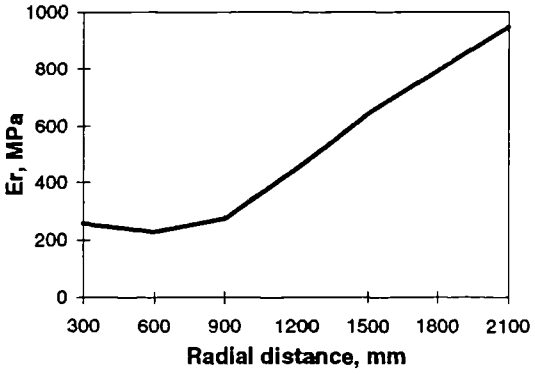


(Core-5)

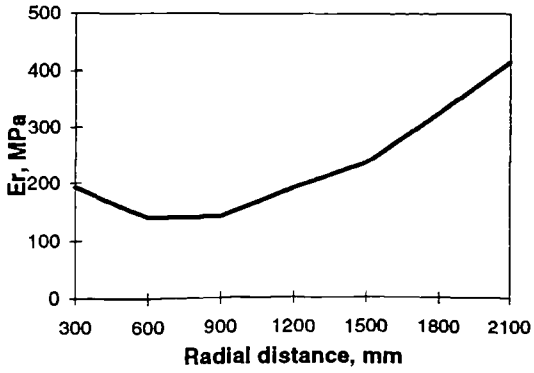


(Core-12)

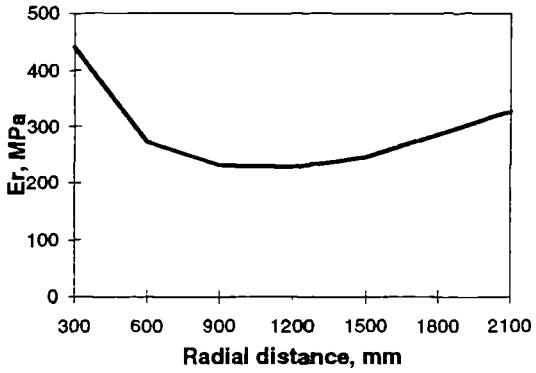


(Core-14)

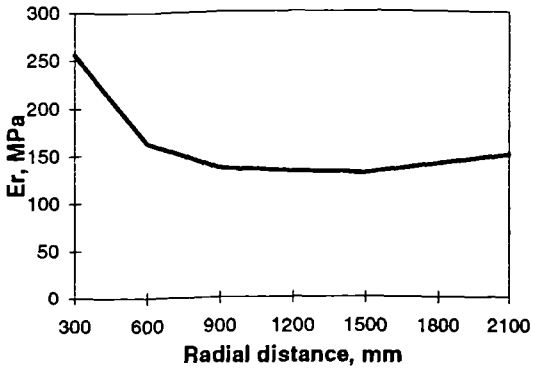


(Core-15)

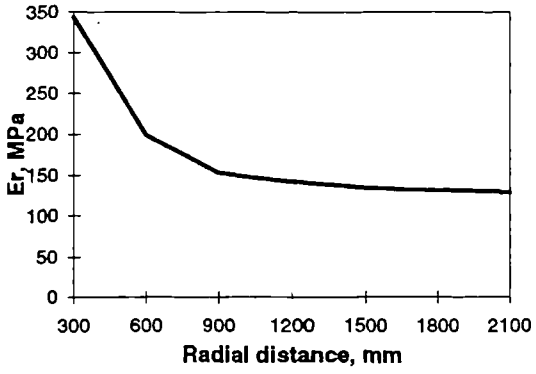


(Core-16)

Figure 9.3, Radial moduli for A41 road.

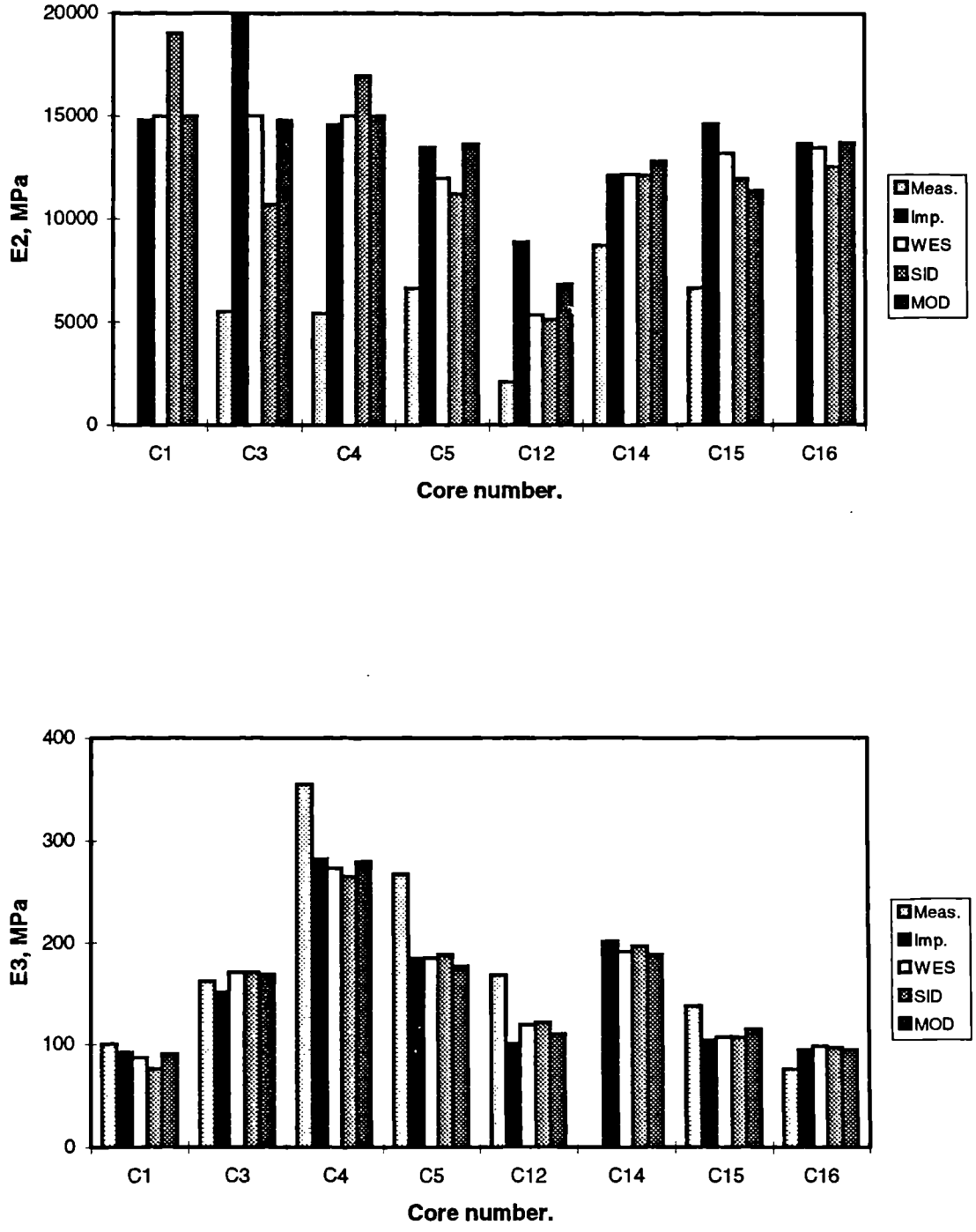


Figure 9.4, Comparison between measured and backcalculated moduli using different programs (Improved, WESDEF, SID and MODULUS) for A41 road.

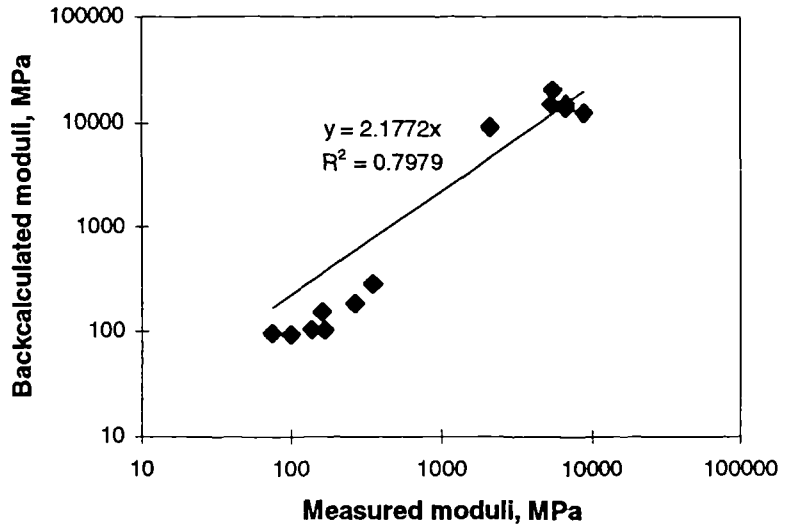


Figure 9.5, Comparison between the improved method backcalculated and measured moduli for A41 road.

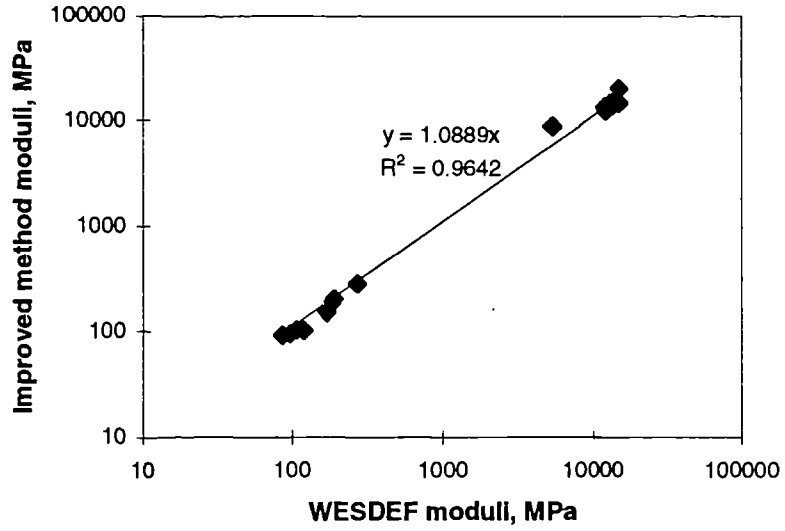


Figure 9.6, Comparison between backcalculated moduli using the improved method and WEDDEF program for A41 road.

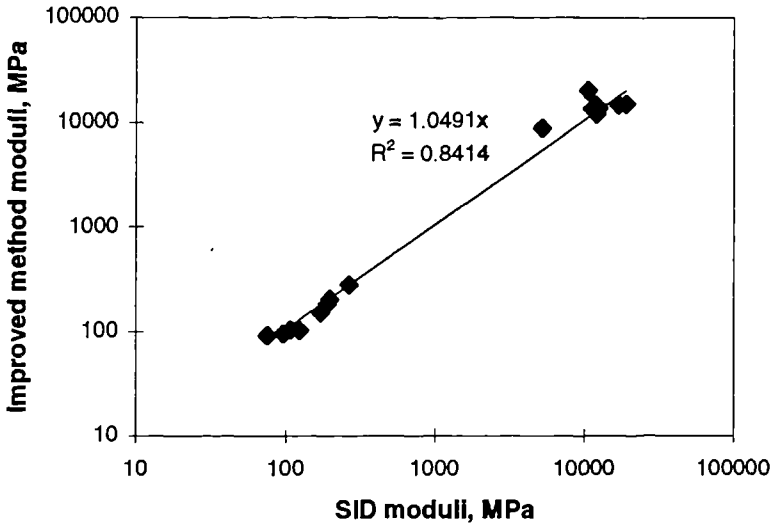


Figure 9.7, Comparison between backcalculated moduli using the improved method and SID program for A41 road.

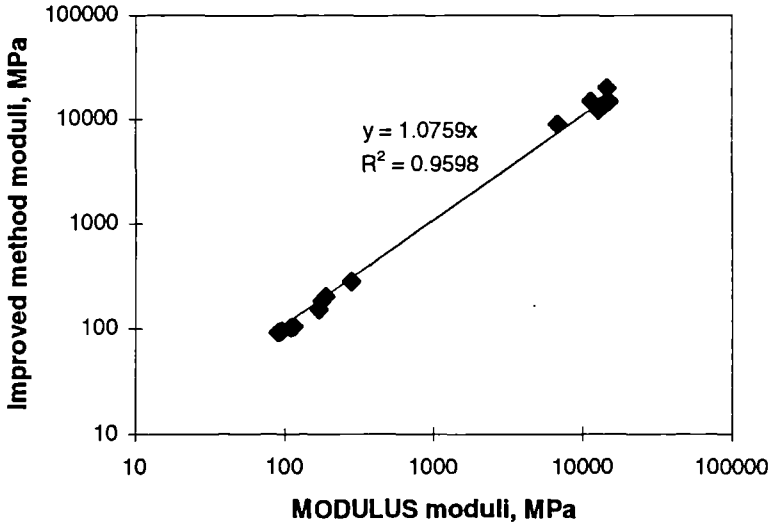


Figure 9.8, Comparison between backcalculated moduli using the improved method and MODULUS program for A41 road.

# Chapter 10

# CONCLUSIONS AND RECOMMENDATIONS FOR FURTHER STUDY

## 10.1 CONCLUSIONS

Most structural evaluation methods for flexible pavements have assumed that full adhesion exists between the pavement layers. However, practical evidence of debonding failure has been reported between the wearing and the base courses both in the UK and Europe.

The testing procedures reported in the literature for assessing the adhesion properties between the bituminous layers are either destructive on samples extracted from the pavement, hence do not represent the insitu condition within the pavement structure, or their results can not be incorporated into the structural analysis model for multilayer structure, and therefore predicting the pavement response to load is not feasible.

The BISAR program includes Goodman's constitutive law to represent the interface condition between layers ($K_s$) in a fundamental form. Numerical analysis using the BISAR program to identify the range of $K_{s1}$ for flexible pavements has been carried out. The results show that $K_{s1}$ varies from 10 MN/m$^3$ (complete debonding) to $10^5$ MN/m$^3$ (full adhesion), and beyond these two limits there is no significant change in pavement response such as stresses, strains and displacements.

Many analytical procedures have been developed to predict the pavement layer properties using the measured surface deflection under the FWD and employing the multilayered elastic system method. Normally, the thickness and Poisson's ratios of each layer in addition to the interface condition between the pavement layers are assumed or known, and the layer moduli are estimated.

Backcalculated layer moduli of hypothetical pavements assuming full adhesion between the wearing and base courses rather than the real value, resulted in some errors in the predicted moduli.

From the practical evidence and deflection sensitivity to pavement parameters, a two-stage improved backcalculation procedure has been developed. This method can predict the shear reaction modulus at the interface between the wearing and base courses ($K_{s1}$) in addition to the layer moduli. However, the thin wearing course moduli is to be assigned a fixed value as recommended in the literature. The first stage estimates the layer moduli using the best models from the multiple regression analysis, and the second stage predicts the interface condition ($K_{s1}$) with little adjustment to the base modulus.

Analysing ninety theoretical pavement structures using both the improved method and the conventional method, which assumed full adhesion between the pavement layer, has shown the following;

i) The new method provides up to 40 % improvement in bituminous base modulus prediction in the extreme cases, when the interface condition between the wearing and base courses is included in the analysis process.
ii) The moduli of the subbase and subgrade were not improved significantly using the new method
iii) The improved method backcalculated moduli can be considered acceptable compared with their hypothetical values.
iv) Considering the three ranges of the interface conditions as poor, partial and good bonding, the backcalculated ($K_{s1}$) range compared well with their hypothetical values.

Therefore, the improved backcalculation procedure has been validated using the theoretical pavement structures.

The improved method has been also validated by comparing the backcalculated moduli with other well known programs, such as WESDEF and MODULUS, when identical pavement conditions are assumed.

The new method has been further verified using the empirical approach, where the backcalculated moduli for real pavement tested under the FWD load and physically measured moduli correlated well. These tests were performed on four different flexible pavements in this research, in addition to analysing other road pavement data obtained from different sources.

Finally, the improved method can be used to predict the causes of pavement failure, such as debonding or materials, and as a quality control to assess the state of adhesion between the pavement layers after construction and overlaying.

## 10.2 RECOMMENDATIONS FOR FURTHER WORKS

This research provides an improvement in the existing backcalculation methods by estimating the interface condition in addition to the layer moduli. The new two stage database process overcomes some limitations of the conventional methods in predicting the pavement parameters which have little influence on surface deflections. However, further studies are needed to improve and validate the theoretical procedure such as:

i) Developing a structural analysis program to calculate the pavement response using the numerical integration approximation or finite element analysis. This program can replace BISAR in developing the deflection database and overcome its copyright limitation. Hence a complete software package employing the knowledge base system for pavement structural evaluation can be developed.

ii) The existing methods employ static analysis for a multilayered elastic system, with the subgrade non-linearity accounted for by placing an apparent rigid layer at certain depth. Although these assumptions are considered acceptable in the literature due to their simplicity and the calculation time and space required, the non-linear materials representation using the constitutive relationships and dynamic analysis of the deflection results could provide a more realistic representation.

iii) Although full scale pavement validation has been carried out, no control and little information were known about the existing interface condition. Hence constructing a full-scale experimental pavement with variable interface adhesion properties can provide a sound proof of the improved method in detecting the bonding conditions.

iv) Correlating the backcalculated interface condition from the experimental pavement with other testing devices such as, the French impedance method, the Austrian splitting wedge method or the shear box test.

v) Correlating the calculated strains using the predicted pavement parameters with the measured values from strain guages installed within the experimental pavements.

vi) This research mainly focused on the predicting the interface condition between the wearing and base courses in flexible pavements, due to the practical evidence of slippage failure. However, in principle the bonding condition between any two layers can be investigated. The research can be applied to analyse rigid and composite pavements.

Furthermore, the improved method can be implemented to investigate the initiation and development of slippage between the layers and the effect of traffic and environment on the interface behaviour. This work can be carried out by testing and backcalculating the experimental pavement properties at different times during its life.

Finally, the mode of flexible pavement failure by fatigue cracking may be altered when debonding exists between the bituminous layers. Consequently, the pavement's critical and failure condition due to fatigue may change. Hence, the investigation of the crack's initiation locations and possible propagation should be carried out, using laboratory beams and full scale pavements.

# REFERENCES


1. Molenaar, A.A.A. "State of the Art of Pavement Evaluation", Proc. 4th Inter. Conf. on the Bearing Capacity of Roads and Airfields, Vol. 2, Minneapolis, USA, 1994, pp 1781-1801.

2. Ullidtz, P. "Pavement Analysis", Elsevier, Amsterdam, 1987.

3. Brown, S.F. and Peattie, K.R. "The Structural Design of Bituminous Pavements for Heavy Traffic", Proc. Instn. Civ. Engns. Vol. 57, March 1974, pp 83-97.

4. Powell, W.D. Potter, J.F. Mayhew, H.C. and Nunn, M.E. "The Structural Design of Bituminous Roads", Transport and Road Research Laboratory, Report LR 1132, 1984.

5. Kennedy, C.K. and Lister, N.W. "Prediction of Pavement Performance for the Design of Overlays", Transport and Road Research Laboratory, Report LR833, 1978.

6. Ali, N.A. and Khosla, N.P. "Determining Layer Moduli Using a Falling Weight Deflectometer", Transportation Research Board, Record 1117, Washington, DC, 1987, pp 1-10.

7. Elfino, M.K. Choubane, B. and McQueen, R.D. "Pavement Evaluation in Virginia: State of the Practice", Transportation Research Board, Record 1505, Washington DC, 1995, pp 84-94.

8. Hossain, M. Zaniewski, J. and Rajan, S. "Estimation of Pavement Layer Moduli Using Nonlinear Optimization Technique", J. of Transportation Engineering, ASCE, Vol. 120, No. 3, May/June 1994, pp 376-393.

9. Kennedy, C.K. and Lister, N.W. "Experimental Studies of Slippage", The Performance of Rolled Asphalt Road Surfacing, The Institution of Civil Engineers, London, 1980, pp 31-56.

10. Peattie, K.R. "The Incidence and Investigation of Slippage Failures", The Performance of Rolled Asphalt Road Surfacing, The Institution of Civil Engineers, London, 1980, pp 3-15.

11. Lepert, P.H. Poilane, J.P. and Bats-Villard, M. "Evaluation of Various Field Measurement Techniques for the Assessment of Pavement Interface Condition", Proc. of the 7th Int. Conf. on Asphalt Pavements, Vol. 3, Nottingham, 1992, pp 224-237.

12. Uzan, J. "Advanced Backcalculation Techniques", Nondestructive Testing of Pavement and Backcalculation of Moduli (Second Volume), ASTM STP 1198, Harold L. Von Quintus, Albert J. Bush III and Gilbert Y. Baladi, Eds, ASTM, Philadelphia. 1994, pp 3-37.

13. Boussinesq, J. "Aplication des Potentiels a L'etude D'equilibrium et du Movement des Solides Elastic", Gauthier Villars, Paris, 1885.

14. Zhou, H. Hicks, R.G. and Bell, C.A. "BOUSDEF: A Backcalculation Program for Determining Moduli of Pavement Structure", Transportation Research Board, Record 1260. Washington DC, 1990, pp 166-179.

15. Peattie, K,R. and Ullidtz, P. "Simplified Computing Technique for Analysing Flexible Pavements", Proc. Instn. Civ. Engrs., Part 2, Vol. 71, March 1981, pp 185-196.

16. Burmister, D.M. "The General Theory of Stresses and Displacements in Layered Soil System", J. Appl. Phys., 1945, Vol. 16, No. 2, pp 89-96, No. 3, pp 126-127, No. 5, pp 296-302.

17. Acum, W.E.A. and Fox, L. "Computation of Load Stresses in Three-layer Elastic System", Geotechnique, Vol. 2, No. 4, 1951. pp 293-300.

18. Peattie, K.R. "Stresses and Strain Factors for Three-layer Elastic System", Highway Research Board, Bulletin 342, 1962.

19. De Almeida, J.R. "Analytical Techniques for the Structural Evaluation of Pavements", PhD Thesis, University of Nottingham, 1993.

20. Mamlouk, M.S. Houston, W.N. Houston, S.L. and Saniewski, J.P. "Rational Characterization of Pavement Structures Using Deflection Analysis", Report FHWA-A-A287-254, Vol. 1, Centre for Advanced Research in Transportation, Arizona State University, Tempe, 1988.

21. Kilareski, W.P. and Anani, B. "Evaluation of Insitu Moduli and Pavement Life from Deflection Basins", Proc. of the 5th Int. Conf. on the Struct. Design of Asphalt Pavements, Vol. 1, 1982, pp 349-366.

22. Chen, D. Zaman, M.M. and Laguros, J.G. "Resilient Moduli of Aggregate Materials: Variability Due to Testing Procedure and Aggregate Type", Transportation Research Board, Record 1462. Washington DC, 1994, pp 57-64.

23. Kennedy, C.K. "Analytical Flexible Pavement Design: A Critical State of the Art Review 1984", Proc. Instn. Civ. Engrs., Part 1, Vol. 78, Aug. 1985, pp 897-917.

24. Uddin, W. and McCullough, B.F. "Insitu Material Properties from Dynamic Deflection Equipment", Nondestructive Testing of Pavement and Backcalculation of Moduli, ASTM STP 1026, A. J. Bush III and G. Y. Baladi, Eds, ASTM, Philadelphia, 1989, pp 278-290.

25. Siddharthan, R. Norris, G.M. and Epps, J.A. "Use of FWD Data for Pavement Material Characterization and Performance". J. of Transportation Engineering, ASCE, Vol. 117, No. 6, Nov./Dec. 1991, pp 660-678.

26. Rohde, G. T. Smith, R.E. and Scullion, T. "Pavement Deflection Analysis on Sections Where Subgrade Vary in Stiffness with Depth", Proc. of the 7th Int. Conf. on Asphalt Pavements, Vol. 3, Nottingham, 1992, pp 280-295.

27. May, R. W. and Von Quintus, H.L. "The Quest for a Standard Guide to NDT Backcalculation", Nondestructive Testing of Pavement and Backcalculation of Moduli (Second Volume), ASTM STP1198, Harlod L. Von Quintus, Albert J. Bush III and Gilbert Y. Baladi, Eds, ASTM, Philadelphia, 1994, pp 505-520.

28. Meier, R.W. and Rix, G.J. "Backcalculation of Flexible Pavement Moduli Using Artificial Neural Networks", Transportation Research Board, Record 1448, Washington DC, 1994, pp 75-82.

29. Ullidtz, P. and Ceotzee, N.F. "Analytical Procedures in Nondestructive Testing Pavement Evaluation", Transportation Research Board, Record 1482, Washington DC, 1995, pp 61-66.

30. Lee, S.W. "Backcalculation of Pavement Moduli by Use of Pavement Surface Deflections", PhD thesis, University of Washington, 1988.

31. Santha, B.L. "Resilient Modulus of Subgrade Soil: Comparison of Two Constitutive Equations", Transportation Research Board, Record 1462, Washington DC. 1994, pp 79-90.

32. Van Der Poel, C. J. "A General System Describing the Visco-Elastic Properties of Bitumens and its Relation to Routine Test Data", J. of Appl. Chemistry, No. 4, 1954, pp 221-236.

33. Yoder, E.J. and Witczak, N.W. "Principles of Pavement Design", Second Edition, John Wiley and Sons, New York, 1975.

34. Mamlouk, M.S. and Sarofim, R.T. "Modulus of Asphalt Mixture- An unresolved Dilemma", Transportation Research Board, Record 1117, Washington DC, 1987, pp 193-198.

35. Cooper, K.E. and Brown, S. F. "Development of a Simple Apparatus for the Measurement of the Mechanical Properties of Asphalt Mixes", Proc. Eurobitume Symp., Madrid, 1989, pp 494-498

36. Nunn, M.E. "Towards a Performance Specification for Bituminous Roadbase", Proc. of the 7th Int. Conf. on Asphalt Pavements, Vol. 3, Nottingham, 1992, pp 260-279.

37. Brunton, J. M. Armitage, R.J. and Brown, S.F. "Seven Years Experience of Pavement Evaluation", Proc. 7th Int. Conf. on Asphalt Pavements, Vol. 3 , Nottingham, 1992, pp 17-30.

38. Heulkelam, W. and Klomp, A. J. G. "Dynamic Testing as a Means of Controlling Pavements During and After Construction", Proc. 1st Int. Conf. on Struct. Design of Asphalt Pavements, Ann Arbor, 1962, pp 667-679.

39. British Standard Institution, BS 1377:1975, "Method of Test for Soil for Civil Engineering Purposes, Test 19, Standard Penetration Test", 1975.

40. Kleyn, E. Maree, J.H. and Savage, P.F. "The Application of Pavement DCP to Determine the Insitu Bearing Properties of Road Pavement Layers and Subgrades in South Africa", Proc. 2nd European Symposium on Penetrometer Testing , Amsterdam, May 1982.

41. Brown, S.F. and Pappin, J.W. "Modelling of Granular Materials in Pavements", Transportation Research Board, Record 1022, Washington DC, 1985, pp 45-51.

42. Brown, S. F. Tam, W.S. and Brunton, J.M. "Structural Evaluation and Overlay Design: Analysis and Implementation", Proc. of the 6th Int. Conf. on the Struct. Design of Asphalt Pavements. Vol. 1, Ann Arbor, 1987, pp 1013-1028.

43. Houston, W. and Mamlouk, M. "Laboratory Versus Nondestructive Testing for Pavement Design", J. of Transportation Engineering, ASCE, Vol. 118, No. 2, March/April 1992, pp 207-222.

44. De Jong, D. L. Peutz, M.G. F. and Korswagen, A.R. "Computer Program, BISAR, Layered Systems Under Normal and Tangential Loads", Royal/Shell Laboratory, External Report AMSR 0006.73, Amsterdam, 1973.

45. Tenison, J.H. "Proposed New Mexico State Highway Department Elastic Layer Overlay Evaluation and Design Procedures for Asphalt Concrete Pavements", Proc. AAPT, Vol. 53, 1984, pp 381-414.

46. Irwin, L.H. "Users Guide to MODCOMP2", Report No. 83-8, Cornell University Local Road Program, Cornell University, Ithaca, NY, Nov. 1983.

47. De Almeida, J.R. Brown, S.F. and Thom, N.H. "A Pavement Evaluation Procedure Incorporating Material Nonlinearity", Nondestructive Testing of Pavement and Backcalculation of Moduli (Second Volume), ASTM STP 1198, Harold L. Von Quintus, Albert J. Bush III and Gilbert Y. Baladi, Eds, ASTM, Philadelphia, 1994, pp 218-232.

48. Hou, Y.T. "Evaluation of Layered Materials Properties from Measured Surface Deflections", PhD Thesis, University of Utah, USA, 1977.

49. Wang, F. and Lytton, R.L. "System Identification Method for Backcalculating Pavement Layer Properties", Transportation Research Board, Record 1384, Washington, DC, 1993. pp 1-7.

50. Van Cauwelaert, F.J. Alexander, D.R. White, T.D. and Baker, W.R. "Multilayer Elastic Program for Backcalculating Layer Moduli in Pavement Evaluation", Nondestructive Testing of Pavement and Backcalculation of Moduli, ASTM STP 1026, A. J. Bush III and G. Y. Baladi, Eds, ASTM, Philadelphia, 1989, pp 171-188.

51. Scullion, T. and Michalak, C. "MODULUS 4.0: User Manual", Research Report 1123-4F, Texas Transportation Institute, 1990.

52. Hall, K.T. and Mohseni, A. "Backcalculation of Asphalt Concrete-Overlaid Portland Cement Concrete Pavement Layer Moduli", Transportation Research Board, Record 1293, Washington DC, 1991, pp 112-123.

53. Wolfe, R.K. Randolph, B.W. and Colony, D.C. "Standarised Elastic Moduli of Pavement Layers for Overlay Design", J. of Transportation Engineering, ASCE, Vol. 121, No. 2, March/April 1995, pp 221-232.

54. Roque, R. Romero, P. And Ruth, B. "Evaluation of Dual-Load Nondestructive Testing System to Better Discriminate Near-Surface Layer Moduli", Transportation Research Board, Record 1355, Washington DC, 1992, pp 52-58.

55. Uzan, J. Lytton, R.L. and Germann, F.P. "General Procedure for Backcalculating Layer Moduli", Nondestructive Testing of Pavement and Backcalculation of Moduli, ASTM STP 1026, A. J. Bush III and G. Y. Baladi, Eds, ASTM, Philadelphia, 1989, pp 217-228.

56. Maser, K. R. Scullion, T. Roddis, W. M. K. and Fernando. E. "Radar for Pavement Thickness Evaluation", Nondestructive Testing of Pavement and Backcalculation of Moduli (Second Volume), ASTM STP 1198, Harold L. Von Quintus, Albert J. Bush III and Gilbert Y. Baladi, Eds, ASTM, Philadelphia, 1994, pp 343-360.

57. Sivaneswaran, N. Kamer, S.L. and Mahomey, J.P. "Advanced Backcalculation Using a Nonlinear Least Squares Optimisation Technique", Transportation Research Board, Record 1293, Washington, DC, 1991, pp 93-102.

58. Matsui, K. Inoue, T. and Sampei, T. "Reflection of Model and Measurement Errors on Stiffness Estimates", Proc. of the 7th Int. Conf. on Asphalt Pavements, Vol. 2, Nottingham, 1992. pp 263-276.

59. Maestas, J.M. and Mamlouk, M. "Comparison of Pavement Deflection Analysis Methods Using Overlay Design", Transportation Research Board, Record 1377, Washington, DC, 1992, pp 17-25.

60. Al Hakim, B. Al-Nageim, H. and Pountney, D.C. "Reflection of the Interface Condition Modelling Error on Backcalculated Moduli and Pavement Remaining Life", Proc. 1st Eurasphalt & Eurobitume Congress, Paper E&E 8.215, Strasbourgh, France, 1996.

61. Rada, G.R. Witczak, M.W. and Rabinow, S.D. "Comparison of AASHTO Structural Evaluation Techniques Using Nondestructive Deflection Testing", Transportation Research Board, Record 1207, Washington DC, 1988, pp 134-144.

62. Hossain, M. And Zaniewski, J.P. "Detection and Determination of Depth of Rigid Bottom in Backcalculation of Layer Moduli from Falling Weight Deflectometer Data", Transportation Research Board, Record 1293. Washington DC, 1991, pp 124-135.

63. Davies, T.G. and Mamlouk, M.S. "Theoretical response of Multi-Layered Pavement Systems to Dynamic Non-Destructive Testing", Transportation Research Board, Record 1022, Washington, DC, 1985, pp 1-7.

64. Zaghloul, S.M. White, T.D. Drnevich, V.P. and Coree, B. "Dynamic Analysis of FWD Loading and Pavement Response Using a Three-Dimensional Dynamic Finite Element Program", Nondestructive Testing of Pavement and Backcalculation of Moduli (Second Volume), ASTM STP 1198, Harold L. Von Quintus, Albert J. Bush III and Gilbert Y. Baladi, Eds, ASTM, Philadelphia, 1994, pp 125-138.

65. Shaat, A.A. "Investigation into Slippage of Bituminous Layer in Overlaid Pavement in Northern Ireland", Consultancy Report Submitted for the DOE in N. Ireland, 1992.

66. Brown, S. F. and Brunton, J. M. "The Influence of Bonding Between Bituminous Layers", Highways and Transportation, Vol. 31, No. 5, May 1984, p 16-17.

67. Uzan, J. Livneh, M. and Eshed, Y. "Investigation of Adhesion Properties Between Asphalt Concrete Layers", Proc. AAPT, Vol. 47, 1978, pp 495-521.

68. Brown, S. F. and Pell, P.S. "The Potential for a Theoretically Based Approach to Flexible Pavement Design", Proc. of the Seminars on Road Design and Highway Maintenance, Annual Meeting of PTRC, July 1976, pp 9-20.

69. Pell, P.S. "Discussion on Slippage of Rolled Asphalt Wearing Courses", The performance of Rolled Asphalt Road Surfacing, The Institution of Civil Engineers, London, 1980, pp 64-65.

70. Irwin, L.H. "Report of the Discussion Group on Practical Limitations and What Can Be Done to Overcome Them", Transportation Research Board, Record 1377, Washington DC, 1992, pp 1-2.

71. Schuab, J. "Catalogue of Deficiencies on Asphalt Pavements", Ed. Gyorgy Foder, Budapest, 1984.

72. Goodman, R. E. Taylor, R. L. and Brekke, T. L. "A Model for the Mechanics of Jointed Rocks", J. of Soil Mechanics and Foundation Division, ASCE, Vol. 94, No. SM3, 1968, pp 637-659.

73. Romain, J. E. "Contraines, Deformations et Deflections dans les Systemes Multicouches Elastiques", Rapport de Recherche No. 147/JER/1968, CRR, Bruxelles, 1968.

74. Vergne, A. Lemaire, M. Caperaa, S. and Nouailles, A. "Modele Multicouche de Comportement d'une Structure Routiere", Annales de L'institut Technique du Batiment et des Traveaux Publics, Vol. 390, 1981, pp 2-15, In French.

75. Shahin, M.Y. Kirchner, K. Blackman, E.W. and Tomito, H. "Effect of Layer Slippage on Performance of Asphalt-Concrete Pavements", Transportation Research Board, Record 1095, Washington DC, 1986, pp 79-85.

76. O'flaherty, C.A. "Highway Engineering". Vol. 2, 3rd Ed., Edward Arnold Ltd, London, 1985.

77. Woodside, A.R. Woodward, W.D.H. and Clements, H.W. "Inhibiting Reflective Cracking", Proc. 2nd National Conf. On Asphaltic Mixtures and Pavements, Thessaloniki, 1996, pp 116-128.

78. Woodside, A.R. and Clements, H.W. "Development of a Pavement Model to Optimize the Properties of Stress Absorbing Membrane Interlays", Proc. 1st Eurasphalt & Eurobitume Congress, Paper E&E 1.220, Strasbourgh, France, 1996.

79. Tschegg, E.K. Kroyer, G. Tan, D.M. Stanzl-Tschegg, S.E. and Litzka, J. "Investigation of Bonding Between Asphalt Layers on Road Construction", J. of Transportation Engineering, ASCE, Vol. 121, No. 4, July/Aug. 1995, pp 309-316.

80. Gerritsen, A.H. and Koole, R.C. "Seven Years' Experience With the Structural Aspects of the Shell Pavement Design Manual", Proc. of the 6th Int. Conf. on the Struct. Design of Asphalt Pavements, Vol. 1, Ann Arbor, 1987, pp 94-106.

81. Briggs, R.C. and Nazarian, S. "Effect of Unknown Rigid Subgrade Layer on Backcalculation of Pavement Moduli and Projections of Pavement Performance". Transportation Research Board, Record 1227, Washington DC, 1989, pp 183-193.

82. Uddin, W. Meyer, A.H. and Hudson, W.R. "A Flexible Pavement Structural Evaluation System Based on Dynamic Deflections", Proc. AAPT, Vol. 54, 1985. pp 432-453.

83. Asphalt Institute, "Research and Development of the Asphalt Institute's Thickness Design Manual (MS-1) Ninth Edition", Research Report No. 82-2, 1982.

84. Shell International, "Shell Pavement Design Manual", Shell International Petroleum Company Ltd, 1978.

85. Alexander, D.R. Kohn, S.D. and Grogon, W.P. "Nondestructive Testing Techniques and Evaluation Procedures for Airfield Pavements", Nondestructive Testing of Pavement and Backcalculation of Moduli, ASTM STP 1026, A. J. Bush III and G. Y. Baladi, Eds, ASTM, Philadelphia, 1989, pp 502-524.

86. Department of Transport "Design Manual for Roads and Bridges: Vol. 7. Pavement Design and Maintenance", HMSO, London, 1994.

87. De Beer, M. Horak, E. and Visser, A.T. "The Multidepth Deflectometer (MDD) System for Determining the effective Elastic Moduli of Pavement Layers". Nondestructive Testing of Pavement and Backcalculation of Moduli, ASTM STP 1026, A. J. Bush III and G. Y. Baladi, Eds, ASTM, Philadelphia, 1989, pp 70-89.

88. Kennedy J.B. and Neville, A.M. "Basic Statistical Method for Engineers and Scientists", third edition, Happer and Row Publisher, New York, 1986.

89. Minitab Inc., "MINITAB for Windows Release 9.2: User Manual", State College, USA, 1993.

90. Newcomb, D.E. "Comparisons of Field and Laboratory Estimated Resilient Moduli of Pavement Materials", Proc. AAPT, Vol. 56, 1987, pp 91-110.

91. Scullion, T. Uzan, J. and Paredes, M. "MODULUS: A Microcomputer-Based Backcalculation System", Transportation Research Board, Record 1260, Washington DC, 1990, pp 180-191.

92. Anderson, M. "A Data Base Method for Backcalculation of Composite Pavement Layer Moduli", Nondestructive Testing of Pavement and Backcalculation of Moduli, ASTM STP 1026, A. J. Bush III and G. Y. Baladi, Eds, ASTM, Philadelphia, 1989, pp 201-216.

93. Akram, T. Scullion, T. and Smith, R.E. "Comparing Laboratory and Backcalculated Moduli on Instrumented Pavement Sections", Nondestructive Testing of Pavement and Backcalculation of Moduli (Second Volume), ASTM STP 1198, Harold L. Von

Quintus, Albert J. Bush III and Gilbert Y. Baladi, Eds, ASTM, Philadelphia, 1994, pp 170-202.

94. Hossain, M. And Scofield, L.A. "Correlation Between Backcalculated and Laboratory Determined Asphalt Concrete Moduli", Transportation Research Board, Record 1377, Washington DC, 1992, pp 67-76.

95. Uzan, J. and Lytton, R. "Experimental Design Approach to Nondestructive Testing of Pavements", J. of Transportation Engineering, ASCE, Vol 115, No. 5, Sep. 1989, pp 505-520.

96. ASTM, "Standard Guide for General Pavement Deflection Measurements D4695-87", 1987.

97. Harison, J.A. "Correlation of CBR and Dynamic Cone Penetrometer Strength Measurement of Soils", Proc. ARR, Vol. 16, No. 2, June 1986, pp 130-136.

98. Livneh, M. And Ishai, I. "Pavement and Material Evaluation by Dynamic Cone Penetrometer" Proc. of the 6th Int. Conf. on the Struct. Design of Asphalt Pavements, Vol. 1, Ann Arbor, 1987, pp 665-676.

99. Chua, K.M. "Determination of CBR and Elastic Modulus of Soils Using a Portable Pavement Dynamic Cone Penetrometer", Proc. Of Penetration Testing, 1988, pp 407-414.

100. Transport and Road Research Laboratory "Overseas Road Note 8. A user Manual for a Program to Analyse Dynamic Cone Penetrometer Data", TRRL, Crowthorne, UK, 1990.

101. Livneh, M. "Validation of Correlation Between a Number of Penetration Tests and Insitu California Bearing Ratio Tests", Transportation Research Board, Record 1219, Washington DC, 1989. pp 56-67.

102. Brown , S.F. Selig, E.T. "The Design of Pavement and Rail Track Foundation, Chapter 6: Cyclic Loading of Soil From Theory to Design", Edited by M.P.O. O'Reilly and S.F. Brown, Blackies, 1991, pp 249-305.

# APPENDIX

# PUBLICATIONS

1. The Influence of the Interface Friction Coefficient on Composite Concrete Pavement Performance, Proceedings 7th International Symposium on Concrete Roads, Vol. 1, Vienna, Austria, 1994, pp 37-42.

2. The Relevance of the Interface Friction Coefficient to Pavement Performance, SCI Lecture Papers, Symposium on the Fundamental Properties of Bituminous Materials, Paper No. 55, London, United Kingdom, 1994.

3. Reflection of Interface Condition Modelling Error on Backcalculated Moduli and Pavement Remaining Life, Proc. 1st Eurasphalt & Eurobitume Congress, Paper E&E 8.215, Strasbourg, France, 1996.

4. The Development of an Improved Pavement Backcalculation. Accepted for publication at the International Conference on Rehabilitation and Development of Civil Engineering Infrastructure Systems, American University of Beirut, Lebanon. June 1997.

# THE INFLUENCE OF THE INTERFACE FRICTION COEFFICIENT ON COMPOSITE CONCRETE PAVEMENT PERFORMANCE

# INFLUENCE DU COEFFICIENT DE FROTTEMENT ENTRE COUCHES SUR LES PERFORMANCES DES CHAUSSEES COMPOSITES EN BETON

# DER EINFLUß DER REIBUNG IN DEN GRENZFLÄCHEN AUF DAS VERHALTEN VON DECKEN IN MISCHBAUWEISE

**B. AL HAKIM**, BSc MSc, Research Assistant, Liverpool John Moores University, U.K.
**H. AL NAGEIM**, BSc MSc PhD MIHT, Senior Lecturer, Liverpool John Moores University, U.K.
**D.C. POUNTNEY**, BSc PhD, Principal Lecturer, Liverpool John Moores University, U.K.

## SUMMARY

The paper discusses the role of non-destructive testing in pavement evaluation and the importance of bonding between its layers on back-calculated properties. Rigid composite pavement structures were analysed using the BISAR programme under different bonding coefficients ($k_s$) between the asphalt and the concrete layers. The results indicate that:

a) A small amount of debonding reduced the back-calculated moduli of the top and second layers in average by 20% and 8% of full adhesion case respectively.

b) Deflections are very sensitive to the interface condition for the values of $k_s$ between $10^4$ and $10^2$ m³/MN.

Therefore the use of the interface friction coefficient in a fundamental back-analysis method allows for a more accurate calculation of the remaining life of the pavement, analysis of the causes of its failure, and more importantly, can be used as a quality control during construction and overlaying.

## RESUME

Ce rapport décrit le rôle des essais non destructifs dans l'évaluation des chaussées et l'importance de l'adhérence entre les différentes couches, pour les propriétés calculées en retour. Les structures de chaussées composites rigides ont été analysées au moyen du programme BISAR pour différents coefficients d'adhérence ($k_s$) entre les couches d'asphalte et de béton. Les résultats montrent que:

a) une faible diminution de l'adhérence a réduit en moyenne les valeurs des modules calculés en retour de la couche supérieure et de la deuxième couche de 20% a 8% respectivement par rapport à des valeurs d'adhérence totale;

b) les déflexions sont très sensibles à l'état des couches à l'interface pour des valeurs de $k_s$ comprises entre $10^4$ et $10^{-2}$ m³/MN.

Par conséquent, l'utilisation du coefficient de frottement à l'interface dans une méthode fondamentale d'analyse en retour permet de calculer avec une précision très grande la durée de vie résiduelle de la chaussée, d'analyser les causes de sa défaillance et surtout peut servir de contrôle de qualité lors des opérations de construction et de recouvrement.

## ZUSAMMENFASSUNG

Dieser Beitrag berichtet über die Rolle zerstörungsfreier Prüfverfahren bei der Beurteilungvon Fahrbahndecken und über die Beduetung des Verbunds zwischen den Schichten für die rückermittelten Eigenschaften. Es wurden Strukturen von steifen Verbunddecken in Mischbauweise mit Hilfe des BISAR Programmes, und mit verschiedenen Verbundkoeffizienten ($k_s$) zwischen den Asphalt- und den Betonschichten analysiert. Die Ergebnisse zeigen, daß:

a) ein geringer Verbundsverlust die rückerrechneten Moduli der obersten und der zweiten Schicht im Schnitt jeweils um 20% und 8% des vollen Verbunds senkt ;

b) Deflektionen reagieren stark auf den Zustand der Grenzfläche für die Werte von $k_s$ zwischen $10^4$ und $10^{-2}$ m³/MN.

Deshalb erlaubt die Anwendung eines Koeffizienten für die Reibung in der Grenzfläche eine genauere Berrechnung der Lebensdauer der Fahrbahn, die Analyse der Ermüdungsgründe und, was noch wichtiger ist, dadurch können während des Baus und Hocheinbaus Qualitätsanalysen durchgeführt werden.

## 1. INTRODUCTION

In recent years a number of non destructive testing techniques have been developed to evaluate the mechanical properties of existing pavement structures. The Falling Weight Deflectometer (FWD) has been considered as the most effective device due to its ability to simulate insitu conditions of the pavement under traffic load.

Layers' moduli of the pavement structure are the most common property to be evaluated from the FWD test results. These moduli are used in assessing the pavement integrity and the its residual life. The remaining life, in term of millions of standard axles, is compared with the future traffic requirement and the selection of remedial work, such as overlay, partial or complete reconstruction may be decided.

The analysis of the data from the FWD surveys generally involves the use of backcalculation techniques, to estimate the moduli of the various layers of the pavement structure. The conventional backcalculation methods seek to define the layers' moduli on the basis that all the other parameters influencing the surface deflection are assumed to be accurately known. The degree of bonding between the pavement layers and poisson ratio of each layer are amongst these parameters.

The report of the discussion group on practical limitations of pavement nondestructive testing using the FWD and back calculation techniques (1), stated that the methodology is not sensitive to the degree of bonding between pavement layers.

The ways to overcome the above limitations fell into two major categories: improvement of the equipment and improvement of the analytical models.

This paper describes the importance of including the friction coefficient in the backcalculation procedures to allow the determination of more accurate values for the pavement properties.

## 2. THE INTERFACE CONDITIONS BETWEEN PAVEMENT LAYERS

Pavement damage due to the effect of debonding is hardly a new phenomenon in road structures. Early work (2,3,4) suggested that a slip plane may develop between pavement layers due to lack of binder coat, pollution of the base before spreading of the binder, surfacing or overlaying in cold weather, and construction in stages. Furthermore in composite pavement the difference in thermal expansion of the concrete and asphalt materials may contribute to the layers debonding.

The condition of the bonding between various layers influences the pavement performance through its impact on the stress distribution within the structure. Thus it can undermine the structural integrity and ability of the pavement to carry traffic loads.

Some researchers demonstrated theoretically the effect of the interface condition between layers on overall pavement performance, (2,5,6,7,8). Van Cauwelaert et al (9), indicated that partial friction is the best representation of the in situ interface conditions between pavement layers, and no experimental data to quantify this parameter has been reported.

Conventional interpretation of the FWD results involves the backclaculation of layers moduli using either the full rough (perfect adhesion) or the full smooth case (adhesion free) between the pavement layers, which are the extreme conditions.

## 3. FALLING WEIGHT DEFLECTOMETER AND BACKCALCULATION TECHNIQUES

The principle of the FWD is that a given load is applied to a pavement surface by a falling weight and the pavement deflections are measured at different distances from the weight. Subsequently linear elastic layered or finite element analysis is used to match theoretical deflection basins to those measured in the FWD survey. Finally the moduli for each layer are evaluated from the back calculation analysis.

Back calculation technique follows two radically different methods, the iterative approach and the data base approach. The iterative approach programs aim to determine a set of layer moduli, in an iterative manner, that minimise the error between the calculated and measured deflections using a suitable convergence criterion. On the other hand the data base approach is a forward calculation to build a data base for different pavement structures, from which the layer moduli can be determined using an appropriate search technique.

A deflection basin is an output of the falling weight imposed on the pavement surface. The

shape of that basin is a function of several variables including, thickness, modulus and poisson ratio of each layer in addition to the bonding condition between pavement layers.

By assuming perfect measuring equipment, the deflection basin produced by the FWD represents the actual response of the pavement properties. These properties can be found from the back calculation procedures, therefore a small change in surface deflection will result in variations in the prediction of pavement properties.

## 4. INFLUENCE OF FRICTION BETWEEN LAYERS ON SURFACE DEFLECTIONS

A rigid composite pavement structure, Figure 1, was analysed using the BISAR program (10) to demonstrate the effects of friction between pavement layers on surface deflection. The pavement properties were chosen to represent a typical composite pavement structure.

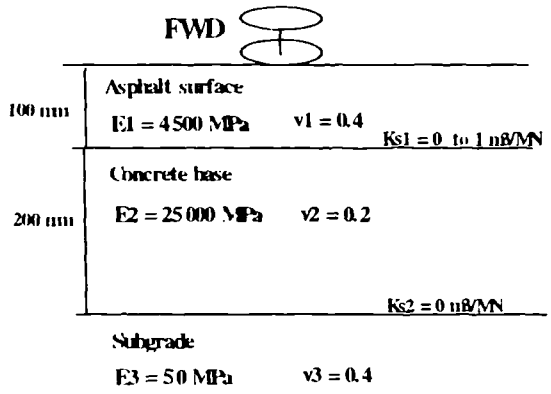


Figure 1, Pavement properties.

The ability of the BISAR program to model the layer interface coefficient made the investigation of the layers' friction possible. The program sets the interface conditions as $K_S$ factor, which can be changed from 0 (full adhesion) to 1 $m^3$/MN (adhesion free)

The first interface coefficient, *Ks1*, was changed gradually between the asphalt and concrete layers from the full adhesion to the full smooth case. The deflection basins were drawn in figure 2, which illustrates the variations in the surface deflections. A 3°₀ and 1% increases in the calculated deflection were recorded at d0 and d0.3 respectively due to the inclusion of friction $K_{S1}$ = $10^{-4}$ $m^3$/MN instead of $k_{S1}$ = 0 (full adhesion) (d0 represents the deflection at the location of the falling weight centre whereas d0.3 at a distance of 300 mm from it). Further increase in d0 and d0.3 of 20% and 18% were recorded respectively when the smooth condition $k_{S1}$ = 1 $m^3$/MN was used.

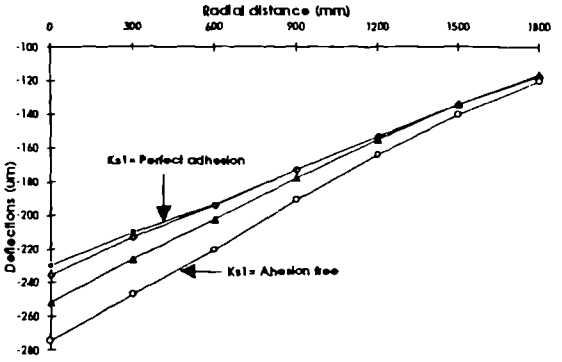


Figure 2. Effect of the interface conditions on deflection basin (pavement figure 1).

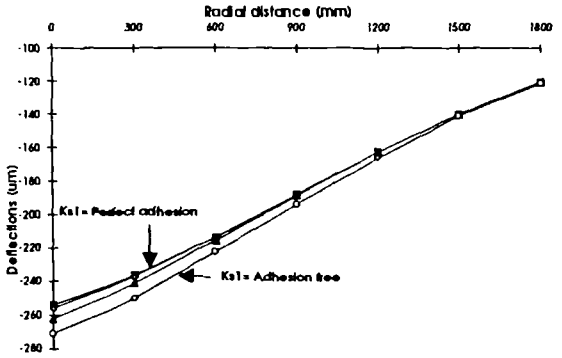


Figure 3, Effect of interface conditions on deflection basin (pavement with 40mm surface).

Figure 3. demonstrates the effect of the asphalt layer thickness on the calculated deflection. In this case the same pavement was analysed using surface thickness of 40 mm instead of 100 mm. It can be seen that the influence of changing the values of $K_{S1}$ on surface deflection is still significant for the thin surface layer.

To exhibit the sensitivity of the deflection at the load centre using different bonding conditions between the first and the second layer, contour lines were plotted (figure 4 and 5). Figure 4 shows the results for d0 as a function of $E_1$ (modulus of the top layer) and $K_{S1}$. In this case the pavement structure shown in figure 1, was analysed by varying $E_1$ values to cover a wide range from a weak surface to new asphalt material moduli.

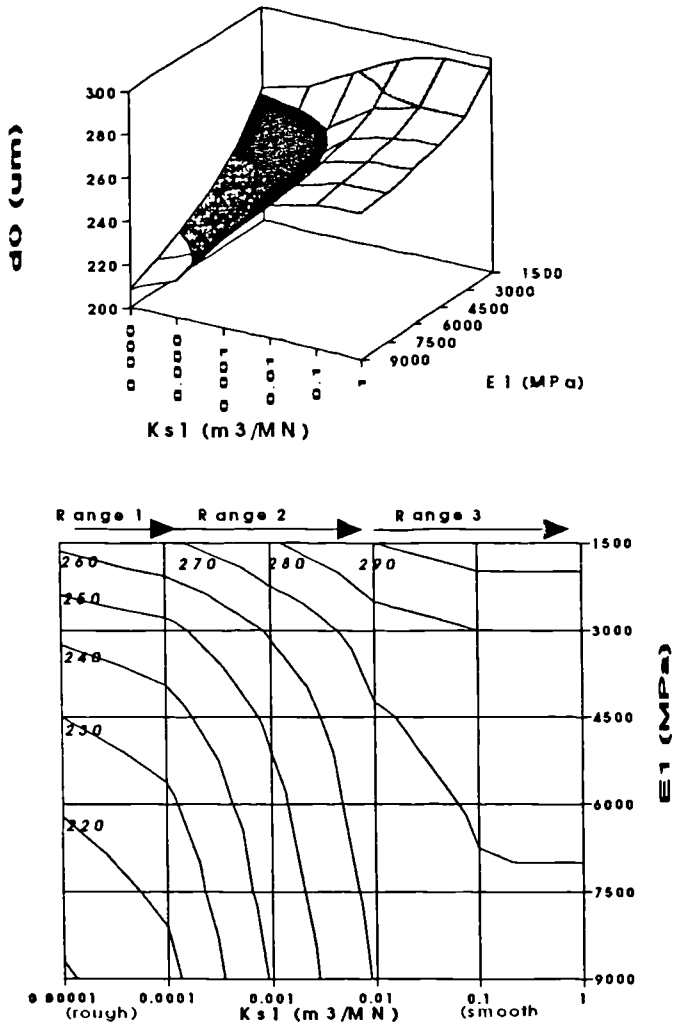


Figure 4, Deflection contours at the load centre as a function of E1 and Ks1.

The contour curves show that the higher the slope of the curves (range 2) the higher the influence of $K_{S1}$ and the lower the influence of $E_1$ on d0. Figure 4, also demonstrates that a small change in $K_{S1}$ from $10^{-4}$ to $10^{-3}$ $m^3$/MN is associated with a very large variation in $E_1$ in order to achieve the same deflection. This information is very valuable to quality control and construction engineers.

Figure 5, Shows the interrelation between the deflections' d0.2 , the first interface conditions, $K_{S1}$, and the modulus of the second layer $E_2$.

Again the same ranges of sensitivity were noted in figure 5,

1. $0 < K_{S1} < 10^{-4} m^3$/MN, (range 1)
   d is sensitive to both E and $K_{S1}$.

2. $10^{-4} < K_{S1} < 10^{-2} m^3$/MN, (range 2)
   d is very sensitive to $K_{S1}$.

3. $10^{-2} < K_{S1} < 1 m^3$/MN, (range 3)
   d is sensitive to E.

These finding support the conclusion that a small change in the friction coefficient between pavement layers can produce strains in the pavement that approach those of the free slippage case.

## 5. INFLUENCE OF FRICTION ON BACK CALCULATED LAYER MODULI

For the structure shown in figure 1, three deflection basins were plotted assuming $k_{S1} = 0$ (full adhesion), $k_{S1} = 10^{-4}$ $m^3$/MN (case in between) and $k_{S1} = 1$ $m^3$/MN (adhesion free). Then the moduli of the first and second layer

were back-calculated from these basins using full adhesion between pavement layers, as adopted by other researchers. The results indicate that a small slip between the asphalt and concrete layers, ($k_{S1}$ = $10^{-4}$ $m^3$/MN), has reduced in average $E_1$ by 20% and $E_2$ by 8% as a ratio of the full adhesion case.

These results have been found from the simple assumption that each deflection location will affect only one layer modulus, which is not always the case since the whole pavement will contribute the deflection basin.

However the findings indicate that the interface conditions between the asphalt and concrete layers will influence significantly the deflection basins (see figures 2 and 3), and therefore the whole backcalculated pavement properties will be affected.

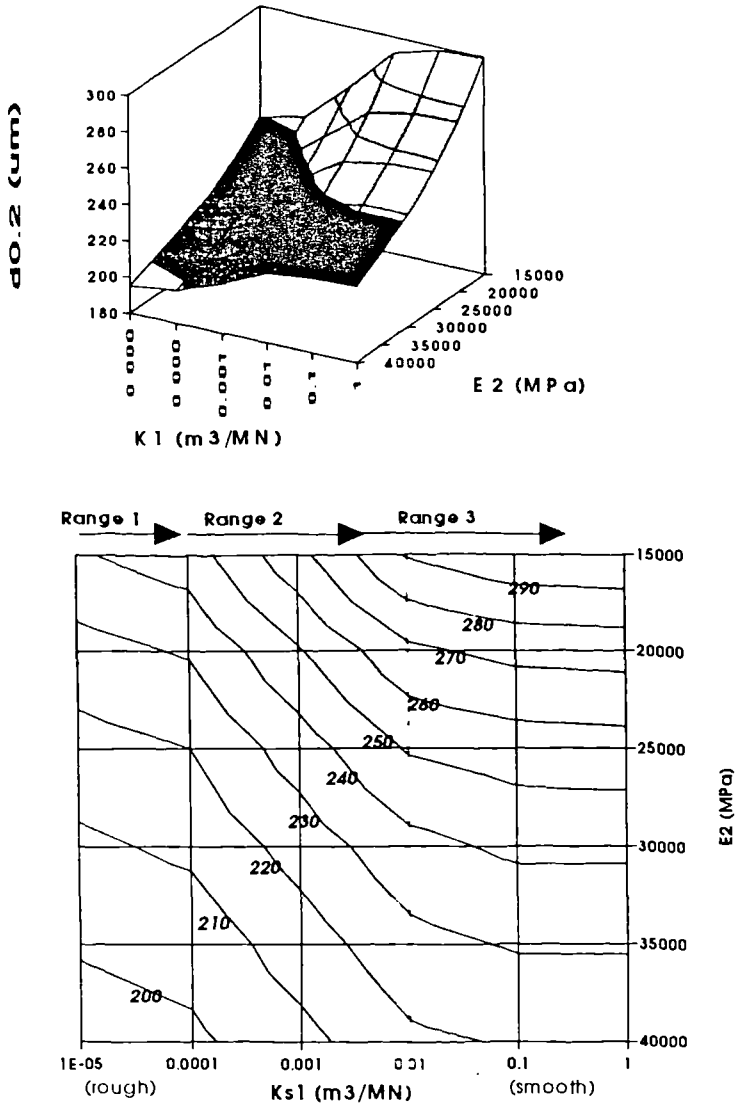


Figure 5, Deflection contours at 200 mm from the load centre as a function of E2 and Ks1

## 6. CONCLUSION

1. Pavement nondestructive deflection testing using the FWD and the back calculation of its properties has some limitations.

2. Many parameters affect the back calculated pavement properties from the deflection basin. One of the prominent factors which has not been included in the existing models is the interface condition between the various layers.

3. For the analysed pavements the deflections are found to be sensitive to the change in layers' moduli and to the interface conditions between them. However the deflection values at d0 and

d0.2 are very sensitive to $K_{S1}$ values in the range between $10^{-4}$ to $10^{-2}$ $m^3/MN$.

4. Including a friction coefficient of $10^{-4}$ $m^3/MN$, between the first top two layers instead of full adhesion has resulted in reduction of 20% and 8% in the back calculated layer moduli of the first and second layer respectively.

5. Cracks and damage in the pavement materials in addition to the interface condition between its layers will reduce the layers' moduli. Therefore the existing back calculated moduli are effective moduli that reflect the pavement's behaviour and are not unique material properties.

6. Due to the above findings and all the practical evidence of debonding failures, a more fundamental back calculation method for pavement properties is required, This method is currently under development by the authors at Liverpool John Moores University. The new method would be useful not only in assessing the pavement's remaining life according to both back calculated moduli and interface conditions, but also to analyse the causes of pavement failure.

7. The new method will be used also as a quality control to assess the state of adhesion between pavement layers after construction and overlaying using the FWD.

## REFERENCES


1. Irwin, L.H., (1992), Report of the Discussion Group on Practical Limitations and What Can Be Done To Overcome Them, Transportation Research Board, Record 1377, Washington, DC, pp 1-2.

2. Uzan, J. Livneh, M. and Eshed, Y., (1978), Investigation of Adhesion Properties Between Asphalt Concrete Layers, Proc. AAPT, Vol. 47, pp 495-521.

3. Brown, S.F. and Pell, P.S., (1976), The Potential for a Theoretically Based Approach to Flexible Pavement Design, Proc. of the Seminars on Road Design and Highway Maintenance, Annual Meeting of PTRC, pp 9-20.

4. Lepert, P.H. Poilane, J.P. and Bats-Villard, M., (1992), Evaluation of Various Field Measurement Techniques for the Assessment of Pavement Interface Condition, Proc. of the 7th Int. Conf. on Asphalt Pavements, Vol. 3. Nottingham, pp 224-237.

5. Vergne, A. Lemaire, M. Caperaa, S. and Nouailles, A., (1981). Modèle Multicouche de Comportement d'une Structure Routière, Annales de L'institut Technique du Batiment et des Travaux Publics, Vol. 390, pp 2-15, In French.

6. Shahin, M.Y. Kirchner, K. Blackmon, E.W. and Tomita, H., (1986), Effect of Layer Slippage on Performance of Asphalt Concrete Pavements, Transportation Research Board, Record 1095, Washington D.C., pp 79-85.

7. Ameri-Gaznon, M. and Little, D.N., (1990), Octahedral Shear Stress Analyses of an ACP Overlay on a Rigid Base, Proc. AAPT, Vol. 59. pp 443-479.

8. Rollings, R.S. and Witczak, M.W., (1990), Design of Rigid Overlays for Airfields, Journal of Transportation Engineering, Vol. 116, No. 4, pp 492-506.

9. Van Cauwelaert, F.J. Alexander, D.R. White, T.D. and Barker, W.R., (1989), Multilayer Elastic Program for Backcalculating Layer Moduli In Pavement Evaluation, Nondestructive Testing of Pavement and Backcalculation of Moduli. ASTM STP 1026, A.J. Bush III and G.Y. Baladi, Eds, ASTM, Philadelphia, pp 171-188.

10. De Jong, D. L. et al, (1973), Computer Program BISAR, Royal/Shell Laboratory, External Report AMSR 0006.73, Amsterdam.

SCI LECTURE PAPERS SERIES

PAPER No 0055

ISSN 1353-114X

Al Hakim B, Al Nageim H and Morley D

# RELEVANCE OF THE INTERFACE FRICTION COEFFICIENT TO PAVEMENT PERFORMANCE

From the Construction Materials Group symposium *Fundamental Properties of Bituminous Materials* held jointly with the Institute of Asphalt Technology and the Institution of Highways and Transportation in London on 27 October 1994

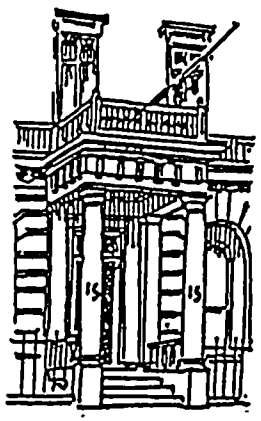



## THE RELEVANCE OF THE INTERFACE FRICTION COEFFICIENT TO PAVEMENT PERFORMANCE.

B. Al Hakim, BSc MSc, Research Assistant, Liverpool John Moores University.
H. Al Nageim, BSc MSc PhD MIHT, Senior Lecturer, Liverpool John Moores University
D. Morley, BSc MA, Principal Lecturer, Liverpool John Moores University

### ABSTRACT

The design and rehabilitation of pavement structures depend upon the accurate characterisation of the mechanical properties of the materials that compose them and the friction coefficient between their individual layers. Pavements which do not exhibit slippage failure may have had a limited amount of bonding provided whilst the layer was being placed. However, no fundamental measure of surface friction between the individual layers of pavement under traffic and environmental conditions yet exists.

The paper discusses the importance of bonding between pavement layers on back-calculated moduli using non-destructive testing techniques.

The interaction among surface deflection, bonding conditions between pavement layers and the layer moduli were studied for two flexible pavement structures using the BISAR program. The condition of bonding ($k_s$) between the top two layers was gradually changed from full adhesion ($k_s$=0m$^3$/MN) to full slippage ($k_s$=1m$^3$/MN). The results indicate that:

a) A small amount of slippage ($k_s$=10$^{-4}$m$^3$/MN) reduced the back-calculated moduli of the first layer in a range of 10 to 40% and the second layer by 8 to 30% as ratio of full adhesion case.

b) Deflections are very sensitive to the interface condition for the values of $k_s$ between 10$^{-4}$ and 10$^{-3}$ m$^3$/MN.

The results revealed that the use of the interface friction coefficient in the back-analysis technique allows for a more accurate calculation of the mechanical properties of the pavement, analysis of the causes of pavement failure, and, more importantly, can be used as a quality control to assess the state of adhesion between pavement layers after construction and overlaying using the falling weight deflectometer.

B Al Hakim H Al Nageim D Morley
Liverpool John Moore's University Clarence Street Liverpool Merseyside L3 5UG

## 1. INTRODUCTION

The use of nondestructive testing techniques ( NDT) in the field of highway and airport pavements has received a considerable attention due to increased interest in their ability to predict the pavement remaining life and the degree of strengthening required. Of many static, impulse, vehicular and vibration nondestructive testing devices, the falling weight deflectometer (FWD) has been considered as the most widely used device for pavement evaluation (1,2).

In the FWD test, a mass is dropped from a given height into a base plate placed on the pavement surface, which to some degree simulates actual traffic loading action on pavement. Pavement reaction to the falling weight is then measured in terms of deflections through a series of velocity transducers at defined distances from the centre of the base plate. The deflection basin produced by the FWD can be used as input parameter to an elastic layered system model, like BISAR program (3), to backcalculate the stress - strain characteristics of the materials used in the various layers of the pavement structure in terms of the materials moduli. These data can then be used to determine the bearing capacity, estimate the remaining life and decide the suitable overlay technique to restore the integrity of the pavement over the desire design life.

The conventional backcalculation methods seek to define the layers' moduli on the basis that all the other parameters influencing the surface deflection are assumed to be accurately known. The degree of bonding between the pavement layers and poisson's ratio of each layer are amongst these parameters.

The report of the discussion group on practical limitations of pavement nondestructive testing using the FWD and back calculation techniques (4), stated that " the methodology is not sensitive to the degree of bonding between pavement layers. The ways to overcome the above limitations fell into two major categories: improvement of the equipment and improvement of the analytical models. " However no fundamental method yet exist to incorporate the bonding between pavement layers in the analysis process.

The data presented in this paper is an outcome of a simplified elastic layered approach currently undertaken by the authors to determine both the moduli of pavement layers and the bonding coefficient between its layers from a given surface deflection. The new approach is based on a nondestructive full scale testing to represent the insitu condition of the pavement under traffic loading and real interaction between its layers.

## 2. THE INTERFACE CONDITIONS BETWEEN PAVEMENT LAYERS

Pavement damage due to the effect of debonding is hardly a new phenomenon in road structures. Early work (5,6,7,8) suggested that a slip plane may develop between pavement layers due to lack of binder coat, pollution of the base before spreading of the binder, surfacing or overlaying in cold weather, and construction in stages.

The condition of the bonding between various layers influences the pavement performance through its impact on the stress distribution within the pavement structure. Thus it can undermine the structural integrity and ability of the pavement to carry traffic loads.



In the UK a large number of debonding failure has been reported in road pavements (5,9). Most of the cases occurred between the wearing course and base course and associated with low stiffness base (10,11). Whereas in France, a 1986 study showed that slippage failure affects 5% of the French highway network (7).

Some researchers demonstrated theoretically the effect of the interface condition between layers on overall pavement performance, (6,12,13,14,15). Van Cauwelaert et al (16), indicated that partial friction is the best representation of the in situ interface conditions between pavement layers, and no experimental data to quantify this parameter has been reported.

Conventional interpretation of the FWD results involves the backcalculation of layers moduli using either the full rough (perfect adhesion) or the full smooth case (adhesion free) between the pavement layers, which are the extreme conditions

This paper describes the importance of including the friction coefficient in the backcalculation procedures to allow the determination of more accurate values for the pavement properties.

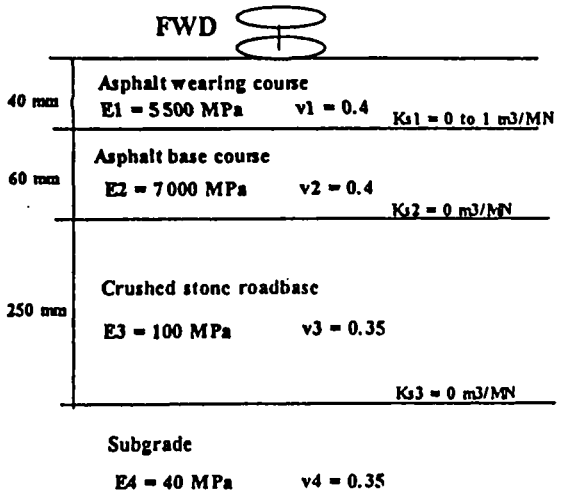


Figure 1 Pavement with crushed stone roadbase.

## 3. INFLUENCE OF FRICTION BETWEEN LAYERS ON SURFACE DEFLECTIONS

A flexible pavement structure, Figure 1, was analysed using the BISAR program (3) to demonstrate the effects of friction between pavement layers on surface deflection. The pavement properties were chosen to represent a typical flexible pavement structure with crushed stone base.

The BISAR program is based on a set of linear elastic equations which incorporate the influence of bonding between the pavement layers in addition to the layer mechanical properties on the calculated deflections under the action of traffic load. The program sets the interface conditions as $K_S$ factor, which can be changed from 0 (full adhesion) to 1 m³/MN (adhesion free)

The value of, *Ks1*, (figure 1) was changed gradually between the top two layers from the full adhesion to the full smooth case and the deflection basins were calculated and drawn at the specified radial distances under the FWD load. Figure 2, illustrates a significant variation in the surface deflections starting from the centre of the loaded base plate and up to 600 mm radial position. A 7% and 1% increases in the calculated deflection were recorded at d0 and d0.3 respectively due to the inclusion of friction $K_{S1}$ = $10^{-4}$ m³/MN instead of $k_{S1}$ = 0 (full adhesion) (d0 represents the deflection at the location of the falling weight centre whereas d0.3 at a distance of 300 mm from it). Further increase in d0 and d0.3 of 32% and 15% were recorded respectively when the smooth condition $k_{S1}$ = 1 m³/MN was used.

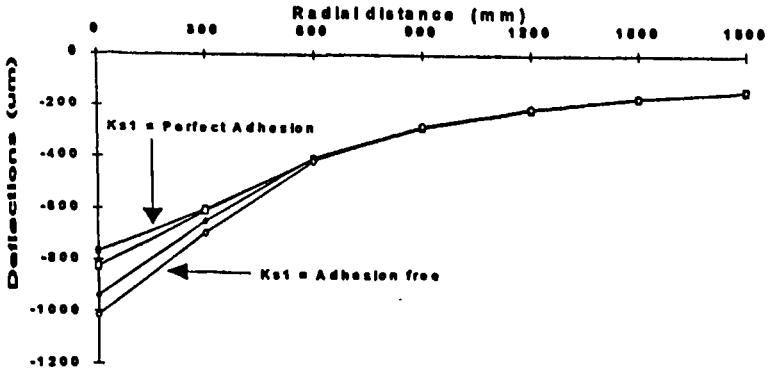


Figure 2 Effect of the first interface coefficient on deflection basin ( Pavement with crushed stone base).

Flexible pavement with asphalt road base, figure 3, was also analysed and the deflection basins were drawn in figure 4 for different friction coefficients. Significant increases in surface deflection were recorded throughout when debonding between the top two layers was introduced. It can be seen from this figure that lower surface deflections were recorded in comparison with the values reported in figure 2. This is due to the fact that this pavement represents a strong structure with high asphalt base modulus, and thus it can carry more traffic loads.

To exhibit the sensitivity of the deflection using different bonding conditions between the first and the second layer, contour lines were plotted in figures 5 to 8. The moduli of the first and second layer (E1) and (E2) were changed respectively to cover a wide range from weak to a strong asphalt layer.



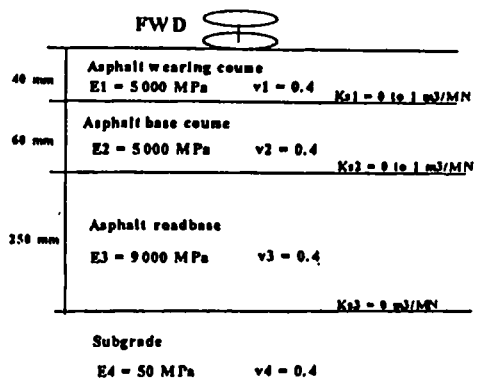


Figure 3 Pavement with asphalt roadbase.

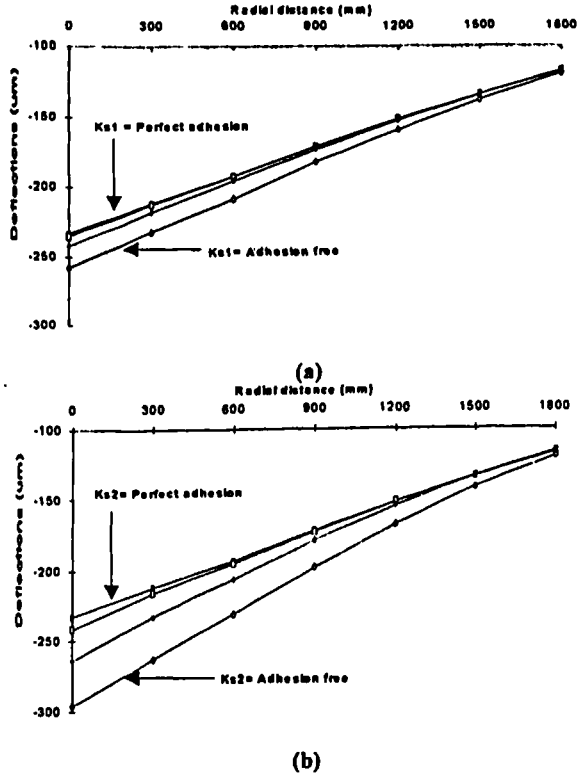


Figure 4 Effect of the first interface coefficient (a) and the second interface coefficient (b) on deflection basin. (Pavement with asphalt base).

The results for the pavement with crushed stone road base are recorded in figures 5 and 6 whereas figures 7 and 8 show the results for the pavement with asphalt road base. Figure 5 shows the relationship between the deflection at the load centre (d0), $E_1$ (modulus of the top layer) and $K_{s1}$ (the first interface coefficient), whereas the results for d0.2 (deflection at 200 mm from the load centre) as a function of E2 and $K_{s1}$ were illustrated in figure 6.

The contour curves illustrate the sensitivity of deflection on both E and $K_{s1}$. The higher the slope of the curves the higher the influence of $K_{s1}$ and the lower the influence of E upon d. Figures 5 to 8, also demonstrate that a small change in $K_{s1}$ from $10^{-4}$ to $10^{-2}$ m³/MN is associated with a very large variation in E in order to achieve the same deflection. This information is very valuable to quality control and construction engineers.

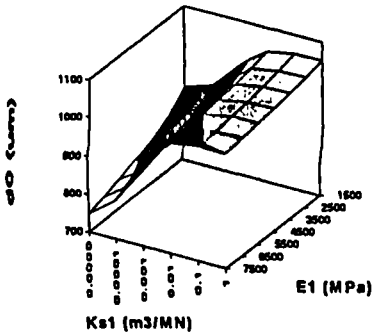


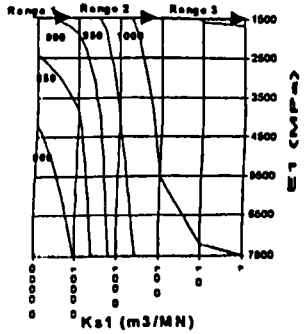


Figure 5 Deflection contours at the load centre as a function of E1 and Ks1 (Pavement with crushed stone base).

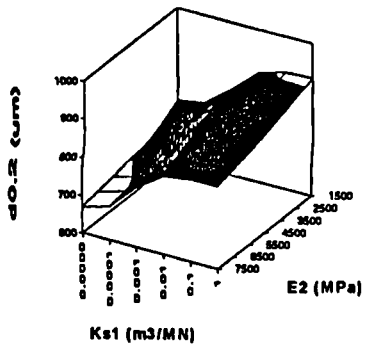


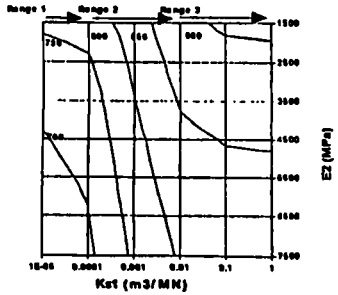


Figure 6 Deflection contours at 200 mm from the load centre as a function of E2 and Ks1 (Pavement with crushed stone base).



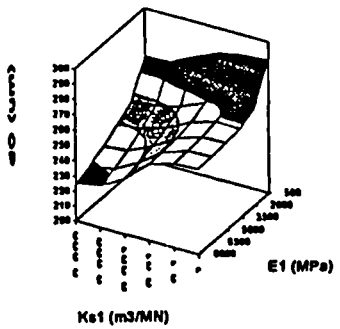


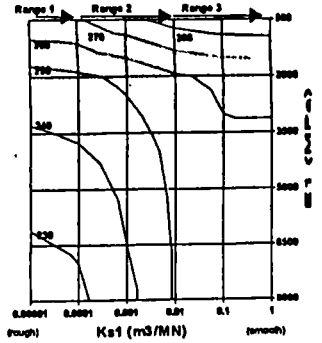


Figure 7 Deflection contours at the load centre as a function of E1 and Ks1 (Pavement with asphalt base).

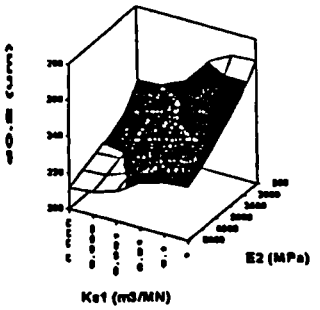


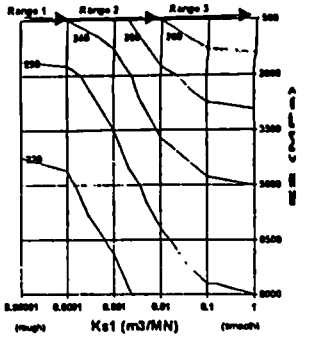


Figure 8 Deflection contours at 200 mm from the load centre as a function of E2 and Ks1 (Pavement with asphalt base).

Three ranges of sensitivity were noted from the contours' lines,

1. $0 < K_{s1} < 10^{-4}$m³/MN, (range 1) d is sensitive to both E and $K_{s1}$,
2. $10^{-4} < K_{s1} < 10^{-2}$m³/MN, (range 2) d is very sensitive to $K_{s1}$,
3. $10^{-2} < K_{s1} < 1$m³/MN, (range 3) d is sensitive to E.

## 4. INFLUENCE OF FRICTION ON BACK CALCULATED LAYER MODULI

Four deflection basins were plotted for each pavement structure as shown in figures 2 and 4a, assuming $k_{s1} = 0$ (full adhesion), $k_{s1} = 10^{-4}$ m³/MN, $k_{s1} = 10^{-3}$ m³/MN and $k_{s1} = 1$ m³/MN (adhesion free). Then the moduli of the first and second layer were back-calculated from these basins as if they are the measured deflections from the FWD test results, full adhesion between pavement layers was used in the backcalculation as adopted by other researchers. The results for the case of full adhesion and $k_{s1} = 10^{-4}$ m³/MN are compared in table 1, which indicates that a small slip between the first and the second layers for pavement 1, ( $k_{s1} = 10^{-4}$ m³/MN), has reduced in average $E_1$ by 40% and $E_2$ by 31% as a ratio of the full adhesion case.

These results have been found from the simple assumption that each deflection location will affect only one layer modulus, which is not always the case since the whole pavement will contribute the deflection basin.

However the findings indicate that the interface conditions between the wearing course and base course will influence significantly the deflection basins (figures 2 and 4), and therefore the whole backcalculated pavement properties will be affected.

Table 1. The reduction in back calculated moduli due to inclusion of slip between the top two layers as a percentage of perfect adhesion case.

| Pavement 1, (crushed stone road base) | | |
|---|---|---|
| Ks1 (m³/MN) | 0 | $10^{-4}$ |
| E1 | 100 | 35-45 |
| E2 | 100 | 30-35 |
| **Pavement 2, (asphalt road base)** | | |
| E1 | 100 | 7-14 |
| E2 | 100 | 6- 9 |

## 5. CONCLUSION

1. Pavement nondestructive deflection testing using the FWD and the back calculation of its properties has some limitations.

2. One of the prominent factors which affect the back calculated pavement properties and has not been included in the existing backcalculation methods is the interface condition between the various layers.



3. The deflections for the flexible pavements analysed in this study are found to be sensitive to the change in layers' moduli and to the interface conditions between them. However the deflection values at d0 and d0.2 are very sensitive to $K_{s1}$ values in the range among $10^{-4}$ to $10^{-3}$ m³/MN.

4. Changing the friction coefficient form 0 (full adhesion) to $10^{-4}$ m³/MN between the first top two layers has resulted in reduction of 40% and 31% in the back calculated layer moduli of the first and second layer respectively.

5. Cracks and damage in the pavement materials in addition to the interface condition between its layers will reduce the layers' moduli. Therefore the existing back calculated moduli are effective moduli that reflect the pavement's behaviour and are not unique material properties.

6. Due to the above findings and all the practical evidence of debonding failures, a more fundamental back calculation method for pavement properties is required, This method is currently under development by the authors at Liverpool John Moores University. The new method would be useful not only in assessing the pavement's remaining life according to both back calculated moduli and interface conditions, but also to analyse the causes of pavement failure.

7. The new method will be used also as a quality control to assess the state of adhesion between pavement layers after construction and overlaying using the FWD.

## REFERENCES


1. Wang, F. and Lytton, R.L., (1993)," System Identification Method for Backcalculating Pavement Layer Properties ", Transportation Research Board, Record 1384, Washington, DC, pp 1-7.

2. Shaat, A.A., (1993), " A Mechanistic Method for Estimation of Concrete Pavement Parameters ", Presented at Concrete 2000, University of Dundee, Scotland, pp 1211-1222.

3. De Jong, D. L. et al, (1973)," Computer Program, BISAR ", Royal/Shell Laboratory, External Report AMSR 0006.73, Amsterdam.

4. Irwin, L.H., (1992)," Report of the Discussion Group on Practical Limitations and What Can Be Done To Overcome Them ", Transportation Research Board, Record 1377, Washington, DC, pp 1-2.

5. Brown, S.F. and Pell, P.S., (1976)," The Potential for a Theoretically Based Approach to Flexible Pavement Design ", Proc. of the Seminars on Road Design and Highway Maintenance, Annual Meeting of PTRC, pp 9-20.

6. Uzan, J. Livneh, M. and Eshed, Y., (1978)," Investigation of Adhesion Properties Between Asphalt Concrete Layers ", Proc. AAPT, Vol. 47, pp 495-521.

7. Lepert, P.H. Pollane, J.P. and Bats-Villard, M., (1992),"Evaluation of Various Field Measurement Techniques for the Assessment of Pavement Interface Condition ", Proc. of the 7th Int. Conf. on Asphalt Pavements, Vol. 3, Nottingham, pp 224-237.

8. Al Hakim, B. Al Nageim, H. and Pountney, D.C., (1994), " The Influence of the Interface Friction Coefficient on Composite Concrete Pavement Performance ", Proc. 7th Intr. Symposium on Concrete Roads, Vol. 1, Vienna, pp 37-42.

9. Brunton, J.M. and Brown, S.F. (1984), " The Influence of Bonding Between Bituminous Layers", Highways and Transportation, Vol.31, No. 5, pp 16-17.

10. Peatties, K.R. (1980), " The Incidence and Investigation of Slippage Failures ", The Performance of Rolled Asphalt Surfacing, The Institution of Civil Engineers, London, pp 3-15.

11. Kennedey, C.K. and Lister, N.W. (1980), " Experimental Studies of Slippage ", The Performance of Rolled Asphalt Surfacing, The Institution of Civil Engineers, London, pp 31-56.

12. Vergne, A. Lemaire, M. Caperaa, S. and Nouailles, A., (1981)," Modèle Multicouche de Comportement d'une Structure Routière" Annales de L'insttut Technique du Batiment et des Travaux Publics, Vol. 390, pp 2-15, In French.

13. Shahin, M.Y. Kirchner, K. Blackmon, E.W. and Tomita, H., (1986), " Effect of Layer Slippage on Performance of Asphalt Concrete Pavements ", Transportation Research Board, Record 1095, Washington D.C., pp 79-85.

14. Ameri-Gaznon, M. and Little, D.N., (1990)," Octahedral Shear Stress Analyses of an ACP Overlay on a Rigid Base ", Proc. AAPT, Vol. 59, pp 443-479.

15. Rollings, R.S. and Witczak, M.W., (1990)," Design of Rigid Overlays for Airfields ", Journal of Transportation Engineering, Vol. 116, No. 4, pp 492-506.

16. Van Cauwelaert, F.J. Alexander, D.R. White, T.D. and Barker, W.R., (1989), " Multilayer Elastic Program for Backcalculating Layer Moduli In Pavement Evaluation ", Nondestructive Testing of Pavement and Backcalculation of Moduli, ASTM STP 1026, A.J. Bush III and G.Y. Baladi, Eds, ASTM, Philadelphia, pp 171-188.

# REFLECTION OF INTERFACE CONDITION MODELLING ERROR ON BACKCALCULATED MODULI AND PAVEMENT REMAINING LIFE

BACHAR AL HAKIM, BSc MSc, Researcher, School of the Built Environment, Liverpool John Moores University, UK.
HASSAN AL NAGEIM, BSc MSc PhD MIHT, Senior Lecturer, School of the Built Environment, Liverpool John Moores University, UK.
DAVID C. POUNTNEY, BSc PhD, Principal Lecturer, School of Computing and Mathematics, Liverpool John Moores University, UK.

## Summary

Pavement evaluation using non destructive testing techniques, such as the Falling Weight Deflectometer (FWD), and backcalculation of the layers' moduli, has become widely used. This is due to their ability to simulate the insitu pavement condition under traffic load.

Conventional backcalculation programs for flexible pavements assume full adhesion exists between pavement layers in the analysis process. However, practical evidence of slippage failure has been reported in the UK. This paper investigates the influence of the error in modelling the interface condition between bituminous layers as full adhesion instead of using the real bonding condition on backcalculated moduli and pavement remaining life.

A wide range of flexible pavement structures were analysed in this study, where the interface conditions between bituminous layers varied from full bonding to complete slippage. The surface deflections were calculated at seven locations, using the BISAR program. These deflections were assumed as the measured deflections produced by FWD and were utilised to backcalculate the layer moduii assuming full adhesion between pavement layers. Comparisons were carried out between both the actual and backcalculated moduli, and the actual and predicted pavement remaining life for each case.

The results indicate that modelling errors of the interface condition between bituminous layers, a) reduces the backcalculated moduli of the bituminous base and the unbound subbase on average by 40% and 30% respectively, when complete debonding exists, b) does not affect the subgrade modulus, and c) changes the pavement residual life by up to 40% in extreme conditions.

# L'EFFET DE LA MODELISATION DE L'ERREUR DE LA CONDITION DE L'INTERFACE SUR LES MODULES CALCULES EN RETOUR ET LA DUREE DE VIE RESIDUELLE DE LA CHAUSSEE

BACHAR AL HAKIM, BSc MSc, Researcher, School of the Built Environment, Liverpool John Moores University, UK.
HASSAN AL NAGEIM, BSc MSc PhD MIHT, Senior Lecturer, School of the Built Environment, Liverpool John Moores University, UK.
DAVID C. POUNTNEY, BSc PhD, Principal Lecturer, School of Computing and Mathematics, Liverpool John Moores University, UK.

## Résumé

L'évaluation de la chaussée par les techniques d'essai non destructif, comme la FWD, et le calcul en retour des modules de couches, est devenue très courante. Ceci est du a leur capacités de stimuler l'in-situ condition de la chaussée sous la charge du trafic.

Les programmes conventionnels de calcul en retour pour les chaussées flexibles supposent l'existence d'une adhérence parfaite entre les couches de la chaussée dans le processus d'analyse. Mais en pratique il a été reporté l'existence de glissement au Royaume Unie. Cette recherche étudie l'influence de l'erreur dans la modélisation de la condition de l'interface des couche bitumineuse comme parfaite adhérence au lieu d'utiliser la condition d'adhérence réelle sur les modules calculées en retour et sur la durée de vie résiduelle de la chaussée.

Une grande variété de chaussées flexibles a été analysée dans cette étude, où la condition d'interface entre les couche bitumineuse varie d'une adhérence totale au glissement complet. Les déflexions sur la surface on été calculées, en utilisant le programme BISAR, dans sept endroits. Il est suppose que ces déflexions sont mesurées grâce au FWD, et on été utilise pour calculer les modules des couche en supposant une totale adhésion entre les couches de la chaussée. Une étude comparative entre les modules actuels et modules calculées en retour et aussi entre la durée de vie résiduelle de la chaussée actuelle et prédît pour chaque cas.

Les résultats indiquent que le modélisation des erreurs de la condition d'interface entre les couches bitumineuse, a) réduit les calculs en retour de modules de la base bitumineuse et la sous base d'au moins 40% et 30% respectivement dans le cas du glissement libre, b) n'a pas d'effet sur le module du sol, et c) change la durée de vie résiduelle de la chaussée de 40% dans les condition extrêmes.

# REFLEXION DES FEHLERS IN DER MODELLIERUNG DES GRENZFLACHENZUSTANDS AUF DIE RUCKERRECHNETEN MODULI UND DIE VERBLEIBENDE LEBENSDAUER VON FAHRBAHNDECKEN

BACHAR AL HAKIM, BSc MSc, Researcher, School of the Built Environment, Liverpool John Moores University, UK.
HASSAN AL NAGEIM, BSc MSc PhD MIHT, Senior Lecturer, School of the Built Environment, Liverpool John Moores University, UK.
DAVID C. POUNTNEY, BSc PhD, Principal Lecturer, School of Computing and Mathematics, Liverpool John Moores University, UK.

## Zusammenfassung

Die Bewertung von Fahrbahndecken unter Benutzung zerstörungsfreier Prüfverfahren wie dem Fallgewicht-Deflektometer (FWD) und der Rückberechnung der Moduli einer Schicht findet weite Anwendung. Der Grund hierfür liegt in ihrer Fähigkeit, den Zustand der Fahrbahndecke an Ort und Stelle unter Verkehrslast zu simulierren.

Herkömmliche Rückberechnungsprogrmme für flexible Fahrbahndecken gehen davon aus, daß im Analyseprozeß eine vollständige Adhäsion zwischen den Schichten der Fahrbahhndecke gegeben ist. Wie auch immer, im Vereiningten Königreich wurde über praktische Beweise von Schlupfversagen berichter. Dieser Beitrag untersucht den Einfluß des Fehlers, den Zustand der Grenzflächen zwischen bituminösen Schiten als vollständige Adhäsion zu modellieren, anstatt den tatsächlichen Verbundzustand auf rückberechnete Moduli und verbleibende Lebensdauer der Fahrbahndecke anzuwenden.

In dieser Studie wurde ein weiter Bereich flexibler Fahrbahndeckenstrukturen analysiert, wobei die Grenzflächenzustände zwischen den bituminösen Schichten von vollständigem Verbund bis zu völligem Schlupf variierten. Die Oberflächendeflektionen wurden - unter Anwendung des BISAR-programmes- an sieben Stellen berechnet. Diese Deflektionen wurden als die gemessenen, und vom FWD produzierten Deflextionen vorausgesetzt, und sie wurden dazu nutzbar gemacht, die Schichtmoduli-unter Annahme vollständiger Adhäsion zwischen den Fahrbanschichten-rückzuberechnen. Für jeden Fall wurden Vergleiche angestellt zwiscen beidem, den tatsächlichen und den rückberechneten Moduli, und der tatsächlichen und der vorausgesagten verbleibenden Lebensdauer.

Die Ergebnisse zeigen, daß die Fehler in der Modellierung des Grenzflächenzustands zwischen bituminösen Schichten, a) die rückberechneten Moduli der bituminösen Basis und der ungebundenen Sauberkeitsschicht im Durchschnitt um 40% bzw. 30% reduzieren, wenn vollständiger Verbundsverlust gegeben ist, b) den Untergrund-Modulus nicht beeinflussen, und c) das Restleben der Fahrbahndecke unter extremen Umständen um bis zu 40% verändern.

# REFLECTION OF INTERFACE CONDITON MODELLING ERROR ON BACKCALCULATED MODULI AND PAVEMENT REMAINING LIFE

BACHAR AL HAKIM, BSc MSc, Researcher, School of the Built Environment, Liverpool John Moores University, UK.
HASSAN AL NAGEIM, BSc MSc PhD MIHT, Senior Lecturer, School of the Built Environment, Liverpool John Moores University, UK.
DAVID C. POUNTNEY, BSc PhD, Principal Lecturer, School of Computing and Mathematics, Liverpool John Moores University, UK.

## INTRODUCTION

The Falling Weight Deflectometer (FWD) has been in use for many years for pavement evaluation, due to its economical and environmental advantages and its reliability in representing the insitu pavement structural conditions.

The pavement is modelled as a layered linear elastic system and therefore its response due to external loads can be calculated numerically, using the values of material properties and pavement geometry, by employing a structural analysis model such as BISAR (1). Pavement assessment involves measuring the surface deflections under the FWD at predetermined locations. These deflections can be used to estimate the layers' moduli employing the inverse solution which has been termed as backcalculation. The backcalculation technique is an iterative method that modifies the pavement moduli and calculates the deflections until a good match between the measured and the calculated deflections occur. The backcalculated moduli resulting from the best fit deflections are used to evaluate the pavement remaining life. The residual life is then compared with future traffic requirements to decide the pavement rehabilitation procedures.

However, some errors are involved in the layer moduli prediction due to the pavement modelling, material modelling and measurements' accuracy. Quantifying these errors is important for the accurate prediction of layer moduli and therefore the estimation of existing pavement life.

## DEFLECTIONS CALCULATION AND OBJECTIVE OF THIS STUDY

The aim of the backcalculation procedure is to minimise the difference between the measured and calculated deflections in an iterative manner to predict the pavement insitu mechanical properties. A square sum of the difference can be expressed as,

$$\varepsilon^2 = \sum_{i=1}^{n} ( d_i^c - d_i^m )^2 \qquad [1]$$

where,

$d_i^m$, measured deflection at the specified location i under the FWD load,

$d_i^c$, calculated deflection at the specified location i,

n , number of deflections.

The calculated deflections are functions of pavement parameters, i.e.

$$d_i^c = f_i ( E_j, \upsilon_j, h_j, k_{sj} ) \qquad [2]$$

where,

$E_j$, $\upsilon_j$, $h_j$, modulus, Poisson ratio and thickness of layer j
$k_{sj}$ , interface condition between layers j and j +1

Most backcalculation techniques seek to define layer moduli $E_j$ on the basis that all other pavement parameters are assumed or known. The surface deflections under the falling weight reflect the real insitu pavement conditions in term of layer moduli, thicknesses, Poisson ratios and the interface condition between the individual layers. Therefore any errors in assuming one parameter will affect the backcalculated moduli, and this error depends on the sensitivity of surface deflections to this parameter.

Layer thicknesses can be measured from cores extracted from the pavement. However some computer programs can backcalculate the thicknesses in addition to the moduli (2,3). Poisson ratios appear to have insignificant effect in predicting the pavement moduli (4).

The objective of this study is to investigate the theoretical influence of errors in assuming the interface condition between bituminous layers, for a range of flexible pavements, on backcalculated moduli and the remaining life of the pavement.

## THE INTERFACE CONDITION BETWEEN PAVEMENT LAYERS

Numerical solution of a multilayered system requires the knowledge of the boundary conditions between layers in order to predict the structural responses to surface loading. These conditions can be either full bonding, with the same shear stresses on both sides of the interface, or complete debonding where no shear stress will transfer between layers. A general fundamental model for the interface, assuming that the shear stress of the layer above the interface is a function of the difference in horizontal displacements of the layers above and below the interface, is to be used, i.e.

$$\tau \cdot k_s = ( u_2 - u_1 ) \qquad [3]$$

where,

$\tau$ , shear stress
$u_1$, $u_2$ , horizontal displacement on both sides of the interface
$k_s$ , horizontal shear reaction modulus at the interface.

This equation represents Goodman's constitutive law to describe the interface behaviour (5).

Numerical analysis using the BISAR program to identify the range of $k_s$ for flexible pavements has been carried out. The results show that $k_s$ varies from $10^{-1}$ $m^3/MN$ (complete debonding) to $10^{-5}$ $m^3/MN$ (full adhesion), and beyond these two limits there is no significant change in pavement response such as stresses, strains and displacements.

The study of Van Cauwelaert et al (6) indicated that, partial friction is the best representation of the insitu interface condition between pavement layers, and no experimental data to quantify this parameter has been reported.

## METHODOLOGY

Most of the procedures followed in this paper is based on the methodology proposed by Biggs and Nazarian (7), in studying the effects of unknown rigid layer on backcalculated moduli.

Four theoretical structures were investigated in this study to represent a wide range of flexible pavements in term of strength. The moduli and Poisson ratios were fixed in all pavements whereas the thickness of base and subbase were varied as shown in figure 1. The pavements consist of four layer systems with an additional rigid layer at 6m depth, to represent either bedrock or the depth where the vertical deflection is negligible.

Figure 1. Pavement Structures

For each pavement structure the interface condition between the bituminous layers was changed gradually from full adhesion to complete debonding, with $k_{s1}$ varying as, $10^{-5}$, $10^{-4}$, $10^{-3}$, $10^{-2}$, $10^{-1}$ $m^3/MN$. All other interface conditions were kept constant and assumed as full adhesion. The investigation of the impact of the first interface for this study is due to the practical evidence of slippage failure which has been reported between bituminous layers (8,9). However, in principle the interface condition between any two layers of the pavement can be studied.

The horizontal strain at the bottom of the bituminous base and the vertical strain at the top of the subgrade were calculated under 40KN load using the BISAR program. These values were used for the assessment of the actual life of the pavement structures. Also the surface deflections were calculated and named as the measured deflection basins.

The twenty deflection basins were used to backcalculate the layer moduli. The pavement parameters assumed in the backcalculation process were identical to those in the theoretical structures except the first interface condition was fixed as full adhesion as is commonly found in most backcalculation programs.

The moduli of the second, third and fourth layers were backcalculated using manual fitting deflections, and the modulus of the 40mm wearing course was fixed as recommended by May and Van Quintus (10), in describing the proposed ASTM standard for backcalculation. These backcalculated moduli should carry some errors to compensate for modelling the interface conditions as full adhesion rather than the actual values.

The resulting backcalculated moduli were input into BISAR to calculate the strains at the same locations as in the theoretical pavements. These strains were used to predict the new remaining life of the pavements.

Finally, the actual remaining life of the pavements, as calculated for the theoretical structures, were compared with the new remaining life as predicted from the backcalculated moduli, to demonstrate the influence of the interface condition modelling errors.

## REMAINING LIFE PREDICTION

The final aim of pavement assessment is the estimation of the remaining life to decide the rehabilitation requirement, therefore the impact of assuming full bonding interface on prediction of remaining life was performed.

Most of the analytical design procedures for flexible pavement adopt the concept of limiting the horizontal tensile strain at the bottom of bituminous layer to control fatigue cracking and the vertical compressive strain at the top of subgrade to control permanent deformation. In this study the semi-empirical relationship developed by TRL (11), between the above strains and the pavement life in terms of number of standard axle load of 80 KN was used, namely

$$\text{Log } N_t = - 9.38 - 4.16 \text{ Log } \varepsilon_t \qquad [4]$$

$$\text{Log } N_z = - 7.21 - 3.95 \text{ Log } \varepsilon_z \qquad [5]$$

where,

$N_t$ , is the number of standard axle load to cause fatigue cracking

$N_z$ , is the number of standard axle load to cause permanent deformation

$\varepsilon_t$ , is the horizontal tensile strain at the bottom of bituminous layer

$\varepsilon_z$ , is the vertical compressive strain at the top of subgrade

The final pavement remaining life is the smallest of the fatigue and deformation lives. These equations were used to predict the remaining life for each of the twenty structures using the actual and the backcalculated moduli.

## RESULTS AND DISCUSSIONS

### Influence of Modelling $k_{s1}$ on Backcalculated $E_2$

Figure 2, illustrates the ratio of backcalculated to actual modulus of the layer 2 versus the ratio of actual to assumed interface condition between bituminous layers, (note that log $k_{s1}$ was used in the graphs). The above moduli ratio of layer 2 has decreased on average by 40% for full adhesion assumption instead of complete debonding in the backcalculation procedures. However, the weaker the structure the higher the reduction in the moduli ratio.

Figure 2. Influence of the interface condition modelling error on backcalculated modulus of layer 2.

Figure 3. Influence of the interface condition modelling error on backcalculated modulus of layer 3.

### Influence of Modelling $k_{s1}$ on Backcalculated $E_3$

Figure 3, shows the ratio of backcalculated to actual modulus of the layer 3 versus the ratio of actual to assumed interface condition between bituminous layers. The ratio of backcalculated to actual subbase modulus varied between 70% and 140%. These results may be interpreted not only as error in modelling $k_{s1}$, but also as error in deflections fitting in the backcalculation procedures.

### Influence of Modelling $k_{s1}$ on Backcalculated $E_4$

Figure 4, demonstrates the ratio of backcalculated to actual modulus of the layer 4 versus the ratio of actual to assumed interface condition between bituminous layers. It is apparent that by modelling the interface condition as full adhesion instead of the real cases, there is no significant effect on backcalculated $E_4$.

Figure 4, Influence of the interface condition modelling error on backcalculated modulus of layer 4.

### Influence of modelling $k_{s1}$ on Pavement Remaining Life

Figures 5, 6 and 7, demonstrate the influence of error in modelling the interface condition $k_{s1}$, on estimation of pavement remaining life. Figure 5, shows that the ratio varied in a range of 50% for fatigue life, when using full adhesion instead of full slippage between bituminous layers. The deformation life varied between 60% and 140%, when using full adhesion rather than the actual $k_{s1}$ as shown in figure 6. Figure 7, illustrates the error of modelling $k_{s1}$on predicting the final pavement remaining life, again the ratio varied between 60% and 140%.

However, one of the main problem in the backcalculation technique, is that two combinations of pavement moduli may result in the same deflections. Therefore, by fitting the measured and calculated deflections a convergence may occur to a different set of moduli. This problem can cause some errors in pavement residual life prediction to contribute or compensate for pavement modelling errors.

Figure 5. Influence of the interface condition modelling error on fatigue life.

Figure 6, Influence of the interface condition modelling error on deformation life.

Figure 7, Influence of the interface condition modelling error on pavement remaining life.

## CONCLUSIONS

1. Flexible pavement evaluation using the FWD and backcalculation of moduli, assuming full adhesion between bituminous layers may cause some errors in moduli and life prediction.

2. For the analysed structures, the backcalculated moduli of second and third layers are most affected by first interface condition modelling errors. Average reductions of 40 and 30% in the backcalculated moduli for layer 2 and 3 respectively, were recorded (when complete debonding exists). In contrast the backcalculated modulus of subgrade was not influenced by the above error.

3. The prediction of pavement remaining life was affected by the interface condition between bituminous layers modelling errors by up to 40%. However the problem of non unique backcalculated moduli in the deflection fitting may contribute to the above errors.

4. Due to the practical evidence of slippage failure and the finding of this study, an advanced backcalculation procedure has been developed by the authors. The new method can backcalculate the first interface condition in addition to the layer moduli to obtain more accurate data for pavement assessment. For further details see reference 12.

## REFERENCES


1. De Jong, D. L. et al " Computer Program, BISAR ", Royal/Shell Laboratory, External Report AMSR 0006.73, Amsterdam, 1973.

2. Sivaneswaran, N. Karmer, S.L. and Mahomey, J.P." Advanced Backcalculation Using a Nonlinear Least Squares Optimisation Technique ", Transportation Research Board, Record 1293, Washington, DC, 1991, pp 93-102.

3. Wang, F. and Lytton R.L. " System Identification Method for Backcalculating Pavement Layer Properties ", Transportation Research Board, Record 1384, Washington, DC, 1993, pp1-7.

4. Matsui, K. Inoue, T. and Sampei, T. " Reflection of Model and Measurement Errors on Stiffness Estimates ", Proc. of the 7th Int. Conf. on Asphalt Pavements, Vol. 2, Nottingham, 1992, pp 263-276.

5. Goodman, R.E. Taylor, R.L. and Brekke, T.R. "A Model for the Mechanics of Jointed Rock", Journal of the Soil Mechanics and Foundations Division, ASCE, Vol. 94, No. SM3, May 1968, pp 637-659.

6. Van Cauwelaert, F.J. Alexander, D.R. White, T.D. and Barker, W.R. " Multilayer Elastic Program for Backcalculating Layer Moduli In Pavement Evaluation ", Nondestructive Testing of Pavement and Backcalculation of Moduli, ASTM STP 1026, A.J. Bush III and G.Y. Baladi, Eds, ASTM, Philadelphia, 1989, pp 171-188.

7. Biggs, R.C. and Nazarian, S. " Effect of Unknown Rigid Subgrade Layer on Backcalculation of Pavement Moduli and Projections of Pavement Performance ", Transportation Research Board, Record 1227, Washington, DC, 1989, pp 183-193.

8. Kennedy, C.K. and Lister, N.W. " Experimental Studies of Slippage ", The Performance of Rolled Asphalt Road Surfacing, The Institution of Civil Engineers, London. 1980, pp 31-56.
9. Peattie, K.R. " The Incidence and investigation of slippage failures ", The Performance of Rolled Asphalt Road Surfacing, The Institution of Civil Engineers, London, 1980, pp 3-15.

10. May R.W. and Von Quintas, H.L. " The Quest for a Standard Guide to NDT Backcalculation ", Nondestructive Testing of Pavement and Backcalculation of Moduli (Second Volume), ASTM STP 1198, Harold L. Von Quintas, Albert J. Bush III and Gilbert Y. Baladi, Eds. ASTM, Philadelphia, 1994, pp 505-520.

11. Powell, W.D. Potter, J.F. Mayhew, H.C. and Nunn, M.E. " The structural Design of Bituminous Roads ", Transport and Road Research Laboratory Report LR1132, 1984.

12. Al Hakim, B. Al Nageim, H. and Pountney, D.C. " Advanced Backcalculation Procedures for Pavement Parameters ", In preperation.

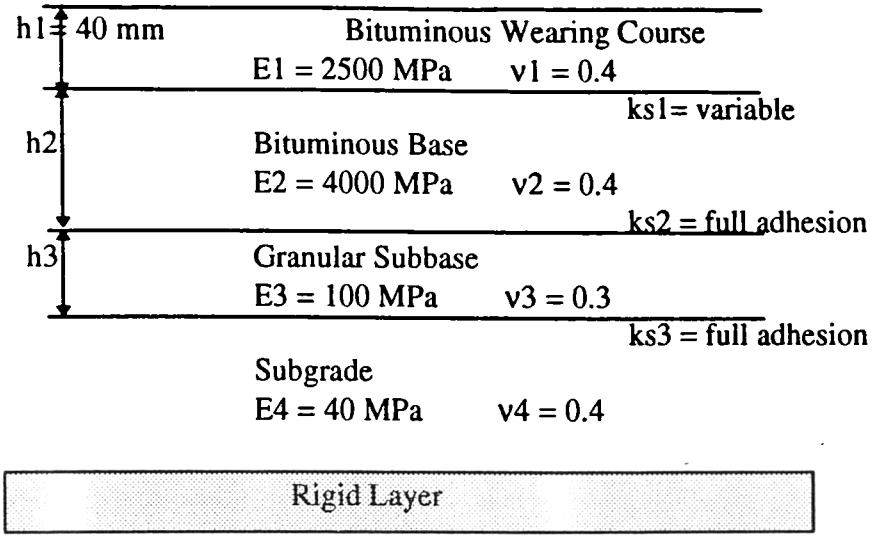


| | Structure 10 | Structure 11 | Structure 12 | Structure 13 |
|---|---|---|---|---|
| h2, mm | 250 | 200 | 150 | 100 |
| h3, mm | 400 | 300 | 200 | 200 |

Figure 1, Pavement Structures

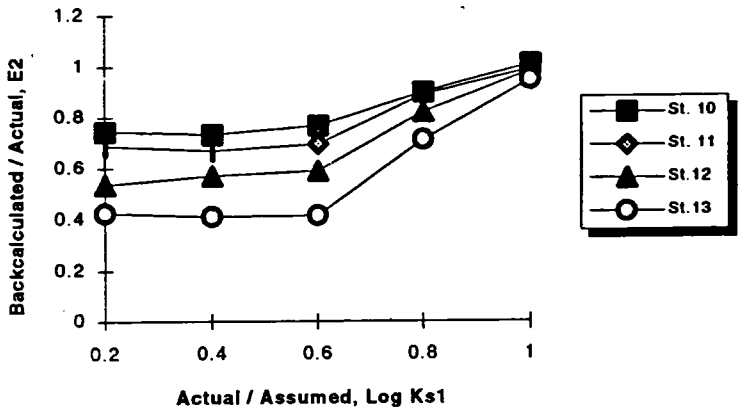


Figure 2, Influence of the interface condition modelling error on backcalculated modulus of layer 2.

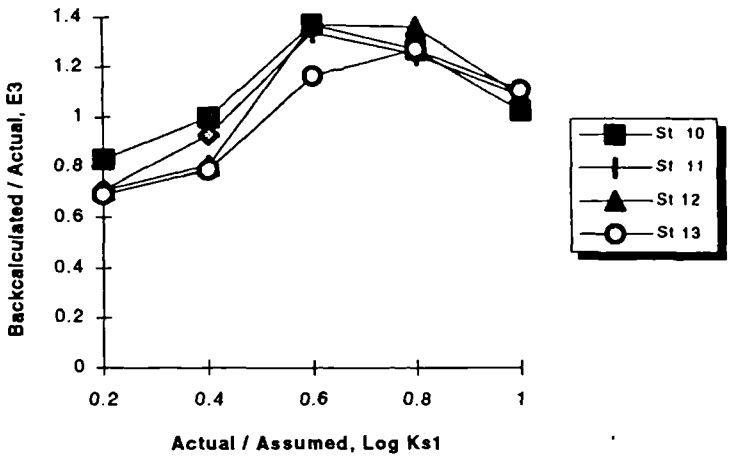


Figure 3, Influence of the interface condition modelling error on backcalculated modulus of layer 3.

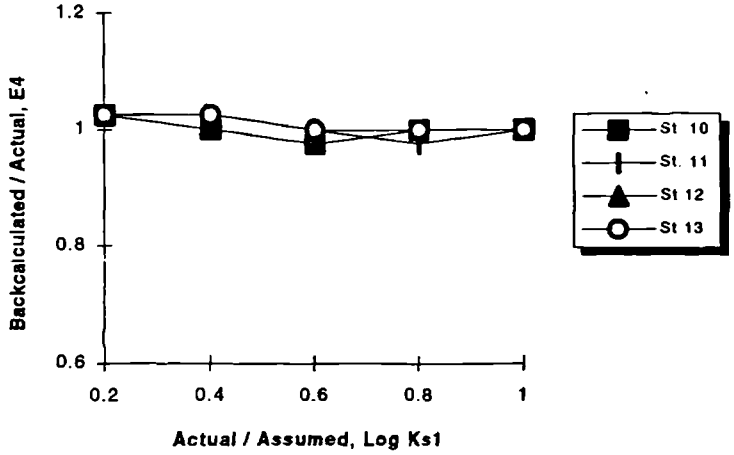


Figure 4, Influence of the interface condition modelling error on backcalculated modulus of layer 4

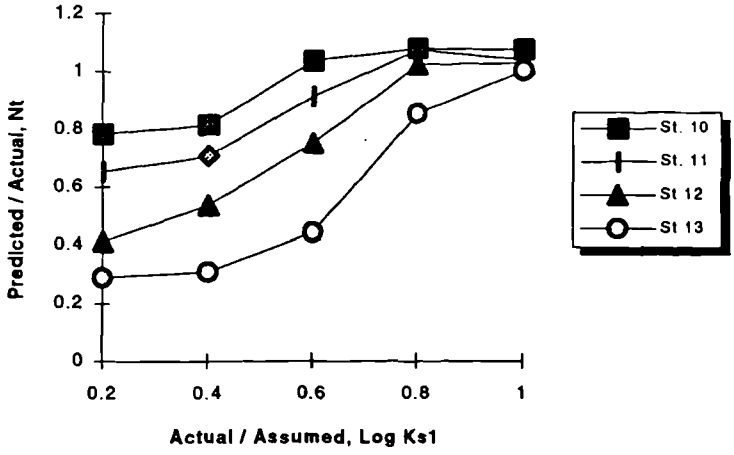


Figure 5, Influence of the interface condition modelling error on fatigue life.

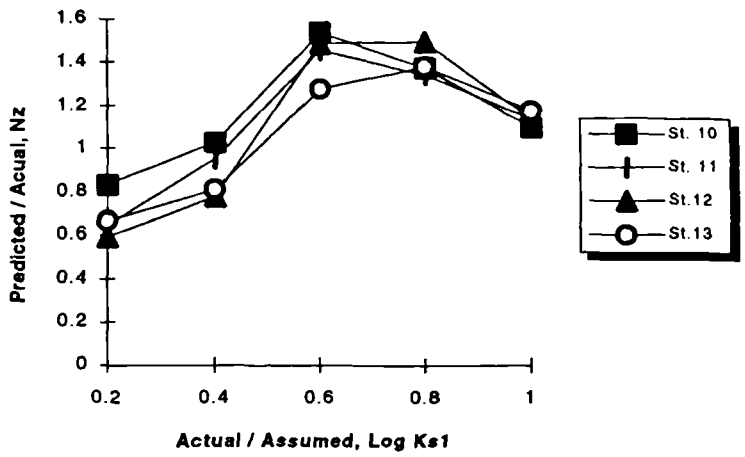


Figure 6, Influence of the interface condition modelling error on deformation life.

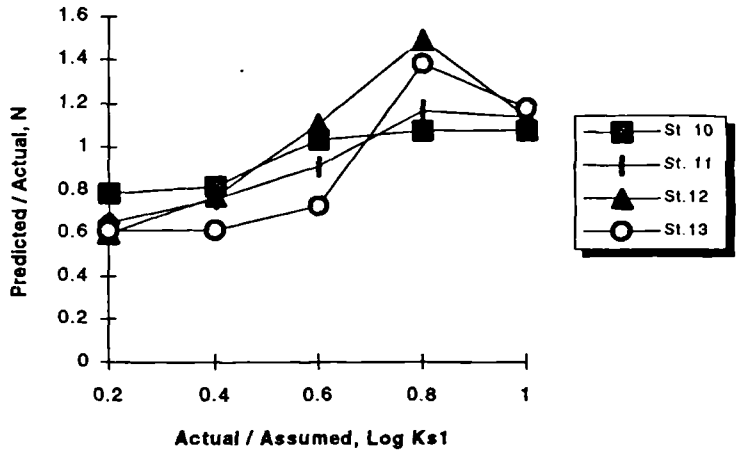


Figure 7, Influence of the interface condition modelling error on pavement remaining life.

# THE DEVELOPMENT OF AN IMPROVED PAVEMENT BACKCALCULATION

**B. Al Hakim[1], H. Al Nageim[2], D. Pountney[3] and L. Lesley[4]**

## ABSTRACT

This paper describes the development of an improved flexible pavement evaluation method using the Falling Weight Deflectometer (FWD) test results.

Practical evidence of debonding failure between the wearing course and base course has been reported in flexible pavements. Therefore an improvement in the current assessment methods, which assume full adhesion between the pavement layers in the analysis process, is needed.

The new procedure can predict the interface condition between the wearing and base courses in addition to the pavement layers' moduli from the measured surface deflections.

Comparisons between the conventional method and this improved method are carried out for ninety pavement structures. The results reveal a significant improvement in the bituminous base modulus prediction, where up to 40% reduction in relative error was recorded for the extreme cases including the bonding condition.

**KEYWORDS:** Flexible Pavement, Evaluation, FWD, Backcalculation, Interface Condition.

## INTRODUCTION

Cost-effective pavement rehabilitation process requires the accurate knowledge of its existing structural and functional properties. *Therefore non-destructive testing* such as the Falling Weight Deflectometer (FWD) has become widely used for pavement evaluation [1]. The principal of the FWD is that an impact load is applied to a pavement surface and the deflections are measured at seven locations to represent the pavement strength. However, due to the lack of an analytical method for direct estimation of the pavement properties, many backcalculation programs have been developed to predict these parameters from the measured deflection basin under FWD.

The pavement is modelled as a layered linear elastic system, therefore its deflections due to surface load can be calculated numerically using a structural analysis program such as BISAR [2]. The backcalculation technique is an iterative method that modifies the pavement parameters and calculates the deflections until a good match between the measured and the calculated deflections occur. The parameters resulting from the best fit deflections are used to evaluate the pavement remaining life.

[1]Researcher, School of the Built Environment, Liverpool John Moores University, UK.
[2]Senior Lecturer, School of the Built Environment, Liverpool John Moores University, UK.
[3]Principal Lecturer, School of Computing and Mathematics, Liverpool John Moores University, UK.
[4]Professor of Transport Science, School of the Built Environment, Liverpool John Moores University, UK.

Most backcalculation techniques seek to define the moduli of pavement layers on the basis that all other pavement parameters, such as layers' thickness, Poisson ratios and the interface conditions, are assumed or known.

Layer thicknesses can be measured from cores extracted from the pavement or from ground penetrating-radar tests [3]. Poisson ratios appear to have insignificant effect in predicting the pavement moduli [4]. Full adhesion between pavement layers is assumed in the conventional analysis for flexible pavements. However, practical evidence of debonding failure has been reported between wearing course and base course in the UK and Europe [5,6,7].

Previous work [8], demonstrated the influence of the interface condition between wearing and base courses modelling error on backcalculated layers' moduli and remaining life prediction for flexible pavements.

This paper describes the development of a new backcalculation procedure for the prediction of the interface shear reaction modulus between wearing and base courses in addition to the layer moduli from FWD test results.

## DEVELOPMENT OF AN IMPROVED BACKCALCULATION PROCEDURE

### Assumptions

A simple static analysis for the pavement as a linear elastic system is adopted for the backcalculation method with the following assumptions (see figure 1):

i) Deflections and load measurements are accurate.

ii) The modulus of the thin wearing course ($E_1$) is assigned as a known value in the backcalculation process, as recommended by May and Van Quintus in describing the proposed ASTM standard for backcalculation [9].

iii) Only the interface shear reaction modulus between the wearing and base courses ($K_{s1}$) is to be backcalculated, and all other interface conditions are assumed as full adhesion.

iv) Typical values of Poisson ratios for UK pavement materials are used, these values assumed to be exact.

v) The thickness of each layer is assumed to be known and exact.

vi) An apparent rigid layer is assumed at a depth of 6m from the surface to represent either bedrock or the depth where the vertical deflection is negligible. However, if the shoulder boring data or other similar information indicates the depth of bedrock, then it should be included in the backcalculation procedures. This layer is used in many backcalculation programs to simulate the stress-dependent subgrade modulus.

## Method of Least Squares

Firstly, the method of least squares [10] is used to predict assumed hypothetical pavement parameters from surface deflections. The backcalculated layer moduli ($E_i$) and the interface shear reaction modulus between wearing and base courses ($K_{s1}$) were not satisfactory predicted due to many factors, such as:

i) Non-unique solution, where two or more combination of pavement parameters produce the same deflections.

ii) Each parameter has a different influence on deflections, e.g. ($K_{s1}$) has very little influence on deflections compared with thick layers and subgrade moduli.

iii) The results are very sensitive to the initial estimate of parameters.

iv) The nature of the influence of ($K_{s1}$) on deflections. ($K_{s1}$) values below 10 MN/m$^3$ (complete debonding) and above $10^5$ MN/m$^3$ (full adhesion) have no effect on deflections and therefore, in the backcalculation process, the program will not deliver any deflections' amendment after iterations beyond these limits.

Therefore a two-stage backcalculation process has been developed to overcome some of the above limitations.

## The Improved Two Stage Backcalculation Procedure

The surface deflections under FWD, materials' types, layers' thickness and Poisson ratios have to be known for the analysed pavement.

Sensitivity study has shown that ($K_{s1}$) has little influence on deflections compared with the subgrade and thick bituminous moduli [11]. Therefore, the backcalculation procedure involves predicting first the parameters which have large influence on deflections, such as subgrade, subbase and bituminous base moduli, then computing the interface shear reaction modulus between wearing and base courses with little adjustment to the bituminous layer modulus. Variation in the interface condition has the largest effect on adjacent layers [12], therefore the subbase and subgrade were kept fixed in the second stage. Figure 2 shows the flow diagram for the two stage backcalculation procedure.

The first stage involves developing a deflections' database for the analysed pavement with different combination of moduli, using the BISAR program [2]. The deflection locations should be selected to correspond the sensors of the FWD.

The search technique for the best model using multiple regression analysis is performed for each modulus as dependent variable with the deflections as independent variables. The models with the highest coefficient of correlation ($R^2$) are employed to predict the layers' moduli from the measured deflections.

The moduli of the lower layers need to be fixed in the next stage and therefore a good match in the deflections far from the loaded area, which control these moduli, is essential for an accurate calculation.

The second stage involves developing other deflection database with a bituminous base modulus varied by 25% from the value found from the first stage, and the first interface condition varied from complete debonding to full adhesion. The deflection at the loaded area and the three next deflections are to be used for the database, since they control the moduli and parameters of the upper layers. The calculated deflection basin which has the lowest error compared with measured values is considered for parameters' prediction.

Finally the moduli of the lower layers as found from the first stage, together with the modulus of base layer and the first interface condition as found from the second stage are taken as the backcalculated parameters.

## THEORETICAL PAVEMENT BACKCALCULATION RESULTS

Ninety theoretical pavement structures were chosen to cover a wide range of moduli ($E_j$), thickness ($h_j$) and interface condition between wearing and base courses ($K_{s1}$). The thickness of wearing course, Poisson ratios ($v_j$), depth of bedrock and the remaining interface conditions were kept constant in all pavements as shown in figure 1.

The surface deflections were calculated for each structure, under a 40 kN load using the BISAR program and named as the measured deflections. Each deflection basin was used to backcalculate;

i) the moduli of the second, third and fourth layers using the WESDEF [13] program and assuming full adhesion between pavement layers, as is commonly found in most evaluation techniques,

and

ii) the moduli of the second, third and fourth layers in addition to the interface condition between the wearing and base courses using the improved procedure reported here.

Figures 3, 4, and 5, demonstrate the relative error in predicting the moduli of bituminous base, subbase and subgrade respectively, using the improved and WESDEF programs for the ninety structures.

Figure 3, shows that the backcalculated modulus of bituminous base is most affected by first interface condition modelling errors. The weaker the pavement the larger the reduction in the modulus values, and the closer the real interface condition to the assumed values (full adhesion with $K_{s1} = 10^5$ MN/m$^3$) , the lower the effect on backcalculated base modulus. Up to 60% reduction in base modulus was recorded in the extreme cases using the WESDEF program to compensate the modelling error. The estimated moduli of subbase and subgrade have not been affected by the above modelling error (see figures 4 and 5), however the results show some scattered values for subbase moduli in the two backcalculation procedures. This conclusion validates the assumption made in the improved backcalculation procedure, of fixing the moduli of lower layers in the second stage and tuning only the base modulus and the interface condition.

## CONCLUSIONS AND SUGGESTED FURTHER WORKS

Flexible pavement's evaluation using the FWD and backcalculation of moduli, assuming full adhesion between layers, may cause some errors in the predicted moduli.

The backcalculated modulus of the bituminous base was most affected by the first interface condition modelling errors. The modulus of subbase was not significantly influenced and the subgrade was not affected by these errors.

For the analysed pavements, the new method provides up to 40% improvement in base modulus prediction in some cases, when the interface conditions between the wearing and base courses were included in the analysis process.

Even allowing for this promising improvement, the improved backcalculation procedure can be further verified using three different approaches:

i) Theoretical validation by comparing the backcalculated results of the ninety structures with their hypothesised values.

ii) Empirical validation by comparing the backcalculated moduli for real pavements tested under FWD load and physically measured moduli.

iii) Validation by comparing the backcalculated moduli with other well known programs, such as WESDEF [13] and MODULUS [14], when identical pavement conditions are assumed.

Such validation is in process and will be reported elsewhere [11].

## REFERENCES

[1] Uzan, J. "Advanced Backcalculation Techniques", Nondestructive Testing of Pavement and Backcalculation of Moduli (Second Volume), ASTM STP 1198, Harold L. Von Quintus, Albert J. Bush III and Gilbert Y. Baladi, Eds, ASTM, Philadelphia, 1994, pp 3-37.

[2] De Jong, D. L. et al "Computer Program, BISAR", Royal/Shell Laboratory, External Report AMSR 0006.73, Amsterdam, 1973.

[3] Maser, K. R. Scullion, T. Roddis, W. M. K. And Fernando, E. "Radar for Pavement Thickness Evaluation", Nondestructive Testing of Pavement and Backcalculation of Moduli (Second Volume), ASTM STP 1198, Harold L. Von Quintus, Albert J. Bush III and Gilbert Y. Baladi, Eds, ASTM, Philadelphia, 1994, pp 343-360.

[4] Matsui, K. Inoue, T. and Sampei, T. "Reflection of Model and Measurement Errors on Stiffness Estimates", Proc. of the 7th Int. Conf. on Asphalt Pavements, Vol. 2, Nottingham, 1992, pp 263-276.

[5] Kennedy, C.K. and Lister, N.W. "Experimental Studies of Slippage", The Performance of Rolled Asphalt Road Surfacing, The Institution of Civil Engineers, London, 1980, pp 31-56.

[6] Peattie, K.R. "The Incidence and investigation of slippage failures", The Performance of Rolled Asphalt Road Surfacing, The Institution of Civil Engineers, London, 1980, pp 3-15.

[7] Lepert, P.H. Poilane, J.P. and Bats-Villard, M. "Evaluation of Various Field Measurement Techniques for the Assessment of Pavement Interface Condition", Proc. of the 7th Int. Conf. on Asphalt Pavements, Vol. 3, Nottingham, 1992, pp 224-237.

[8] Al Hakim, B. Al Nageim, H. and Pountney, D.C. "Reflection of the Interface Condition Modelling Error on Backcalculated Moduli and Pavement Remaining Life", Proc. 1st Eurasphalt & Eurobitume Congress, Paper E&E 8.215, Strasbourg, France, 1996.

[9] May R.W. and Von Quintus, H.L. " The Quest for a Standard Guide to NDT Backcalculation", Nondestructive Testing of Pavement and Backcalculation of Moduli (Second Volume). ASTM STP 1198, Harold L. Von Quintus, Albert J. Bush III and Gilbert Y. Baladi, Eds, ASTM, Philadelphia, 1994, pp 505-520.

[10] Sivaneswaran, N. Karmer, S.L. and Mahomey, J.P. "Advanced Backcalculation Using a Nonlinear Least Squares Optimisation Technique", Transportation Research Board, Record 1293, Washington, DC, 1991, pp 93-102.

[11] Al Hakim, B. "An Improved Flexible Pavement Backcalculation Procedure", In preparation.

[12] Uzan, J. Livneh, M. And Eshed, Y. "Investigation of Adhesion Properties Between Asphalt Concrete Layers", Proc. AAPT, Vol. 47, 1978, pp 495-521.

[13] Van Cauwelaert, F.J. Alexander, D.R. White, T.D. and Barker, W.R. "Multilayer Elastic Program for Backcalculating Layer Moduli in Pavement Evaluation", Nondestructive Testing of Pavement and Backcalculation of Moduli, ASTM STP 1026, A.J. Bush III and G.Y. Baladi, Eds, ASTM, Philadelphia. 1989, pp 171-188.

[14] Scullion, T. and Michalak, C. "MODULUS 4.0: User Manual", Research Report 1123-4F, Texas Transportation Institute, 1990.

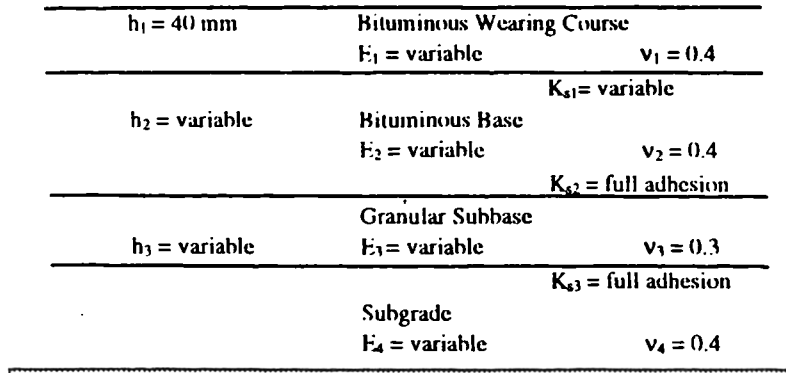


| ST. | $E_1$ MPa | $E_2$ MPa | $E_3$ MPa | $E_4$ MPa | $h_2$ mm | $h_3$ mm | $K_{s1}$ MN/m³ |
|---|---|---|---|---|---|---|---|
| 2A1 | 2500 | 4000 | 100 | 40 | 100 | 200 | $10^1$ |
| 2A2 | | | | | | | $10^2$ |
| 2A3 | | | | | | | $10^3$ |
| 2A4 | | | | | | | $10^4$ |
| 2A5 | | | | | | | $10^5$ |
| 2B1 | 2500 | 4000 | 100 | 40 | 300 | 300 | $10^1$ |
| 2B2 | | | | | | | $10^2$ |
| 2B3 | | | | | | | $10^3$ |
| 2B4 | | | | | | | $10^4$ |
| 2B5 | | | | | | | $10^5$ |
| 3A1 | 5000 | 7000 | 150 | 40 | 100 | 200 | $10^1$ |
| 3A2 | | | | | | | $10^2$ |
| 3A3 | | | | | | | $10^3$ |
| 3A4 | | | | | | | $10^4$ |
| 3A5 | | | | | | | $10^5$ |
| 3B1 | 5000 | 7000 | 150 | 40 | 300 | 300 | $10^1$ |
| 3B2 | | | | | | | $10^2$ |
| 3B3 | | | | | | | $10^3$ |
| 3B4 | | | | | | | $10^4$ |
| 3B5 | | | | | | | $10^5$ |
| 4A1 | 7500 | 10000 | 200 | 40 | 100 | 200 | $10^1$ |
| 4A2 | | | | | | | $10^2$ |
| 4A3 | | | | | | | $10^3$ |
| 4A4 | | | | | | | $10^4$ |
| 4A5 | | | | | | | $10^5$ |
| 4B1 | 7500 | 10000 | 200 | 40 | 300 | 300 | $10^1$ |
| 4B2 | | | | | | | $10^2$ |
| 4B3 | | | | | | | $10^3$ |
| 4B4 | | | | | | | $10^4$ |
| 4B5 | | | | | | | $10^5$ |
| 5A1 | 2500 | 4000 | 100 | 80 | 100 | 200 | $10^1$ |
| 5A2 | | | | | | | $10^2$ |
| 5A3 | | | | | | | $10^3$ |
| 5A4 | | | | | | | $10^4$ |
| 5A5 | | | | | | | $10^5$ |
| 5B1 | 2500 | 4000 | 100 | 80 | 300 | 300 | $10^1$ |
| 5B2 | | | | | | | $10^2$ |
| 5B3 | | | | | | | $10^3$ |
| 5B4 | | | | | | | $10^4$ |
| 5B5 | | | | | | | $10^5$ |
| 6A1 | 5000 | 7000 | 150 | 80 | 100 | 200 | $10^1$ |
| 6A2 | | | | | | | $10^2$ |
| 6A3 | | | | | | | $10^3$ |
| 6A4 | | | | | | | $10^4$ |
| 6A5 | | | | | | | $10^5$ |

| ST. | $E_1$ MPa | $E_2$ MPa | $E_3$ MPa | $E_4$ MPa | $h_2$ mm | $h_3$ mm | $K_{s1}$ MN/m³ |
|---|---|---|---|---|---|---|---|
| 6B1 | 5000 | 7000 | 150 | 80 | 300 | 300 | $10^1$ |
| 6B2 | | | | | | | $10^2$ |
| 6B3 | | | | | | | $10^3$ |
| 6B4 | | | | | | | $10^4$ |
| 6B5 | | | | | | | $10^5$ |
| 7A1 | 7500 | 10000 | 200 | 80 | 100 | 200 | $10^1$ |
| 7A2 | | | | | | | $10^2$ |
| 7A3 | | | | | | | $10^3$ |
| 7A4 | | | | | | | $10^4$ |
| 7A5 | | | | | | | $10^5$ |
| 7B1 | 7500 | 10000 | 200 | 80 | 300 | 300 | $10^1$ |
| 7B2 | | | | | | | $10^2$ |
| 7B3 | | | | | | | $10^3$ |
| 7B4 | | | | | | | $10^4$ |
| 7B5 | | | | | | | $10^5$ |
| 8A1 | 5000 | 7000 | 150 | 120 | 100 | 200 | $10^1$ |
| 8A2 | | | | | | | $10^2$ |
| 8A3 | | | | | | | $10^3$ |
| 8A4 | | | | | | | $10^4$ |
| 8A5 | | | | | | | $10^5$ |
| 8B1 | 5000 | 7000 | 150 | 120 | 300 | 300 | $10^1$ |
| 8B2 | | | | | | | $10^2$ |
| 8B3 | | | | | | | $10^3$ |
| 8B4 | | | | | | | $10^4$ |
| 8B5 | | | | | | | $10^5$ |
| 9A1 | 7500 | 10000 | 200 | 120 | 100 | 200 | $10^1$ |
| 9A2 | | | | | | | $10^2$ |
| 9A3 | | | | | | | $10^3$ |
| 9A4 | | | | | | | $10^4$ |
| 9A5 | | | | | | | $10^5$ |
| 9B1 | 7500 | 10000 | 200 | 120 | 300 | 300 | $10^1$ |
| 9B2 | | | | | | | $10^2$ |
| 9B3 | | | | | | | $10^3$ |
| 9B4 | | | | | | | $10^4$ |
| 9B5 | | | | | | | $10^5$ |
| 10A1 | 7500 | 10000 | 200 | 160 | 100 | 200 | $10^1$ |
| 10A2 | | | | | | | $10^2$ |
| 10A3 | | | | | | | $10^3$ |
| 10A4 | | | | | | | $10^4$ |
| 10A5 | | | | | | | $10^5$ |
| 10B1 | 7500 | 10000 | 200 | 160 | 300 | 300 | $10^1$ |
| 10B2 | | | | | | | $10^2$ |
| 10B3 | | | | | | | $10^3$ |
| 10B4 | | | | | | | $10^4$ |
| 10B5 | | | | | | | $10^5$ |

Figure 1, The theoretical properties of the ninety pavement structures.

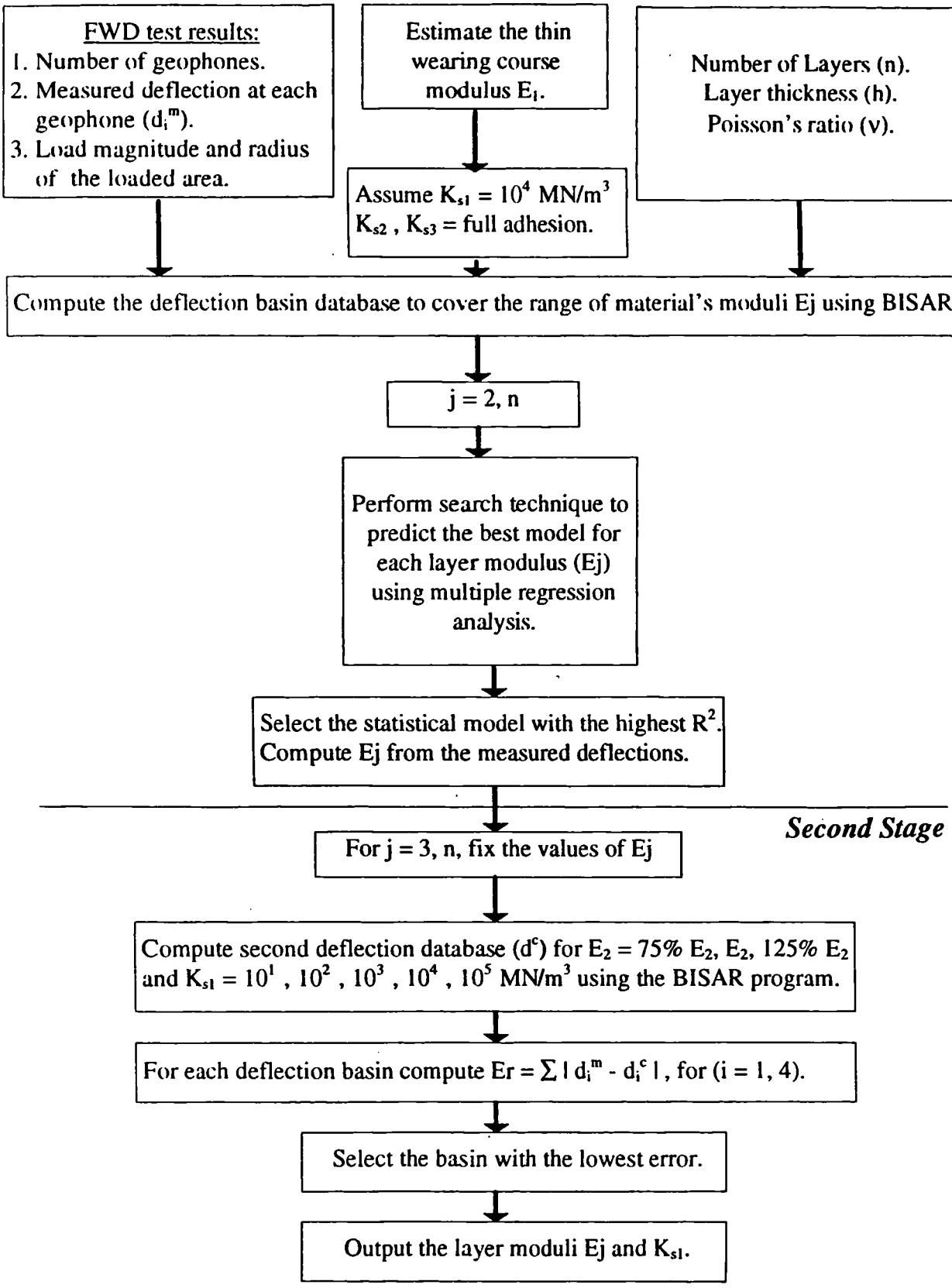


Figure 2, Flow chart for the improved method backcalculation procedure.

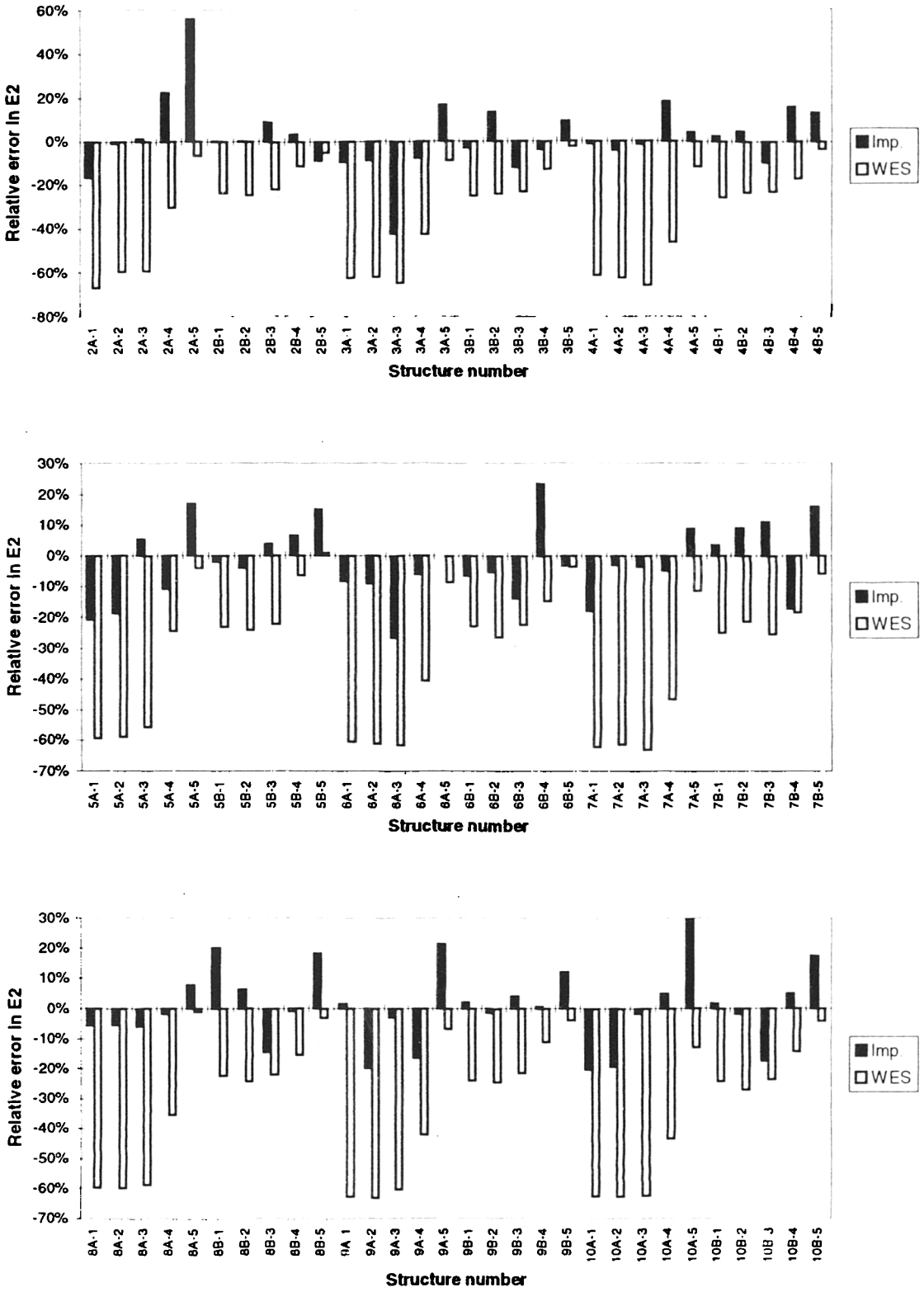


Figure 3, Relative error in predicting the modulus of bituminous base using the improved and the WESDEF programs for the 90 pavement structures.

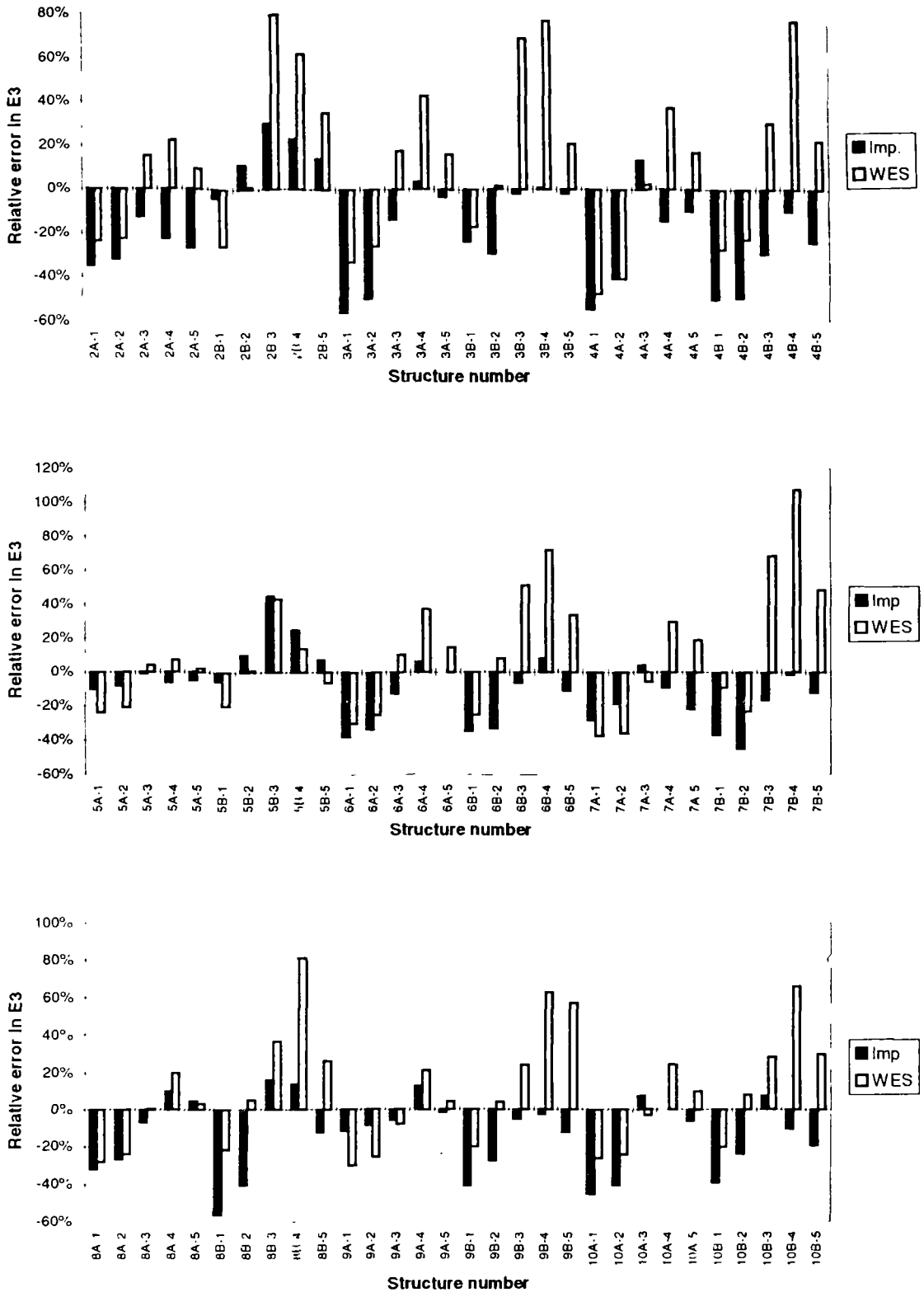


Figure 4. Relative error in predicting the modulus of unbound subbase using the improved and the WESDEF programs for the 90 pavement structures.

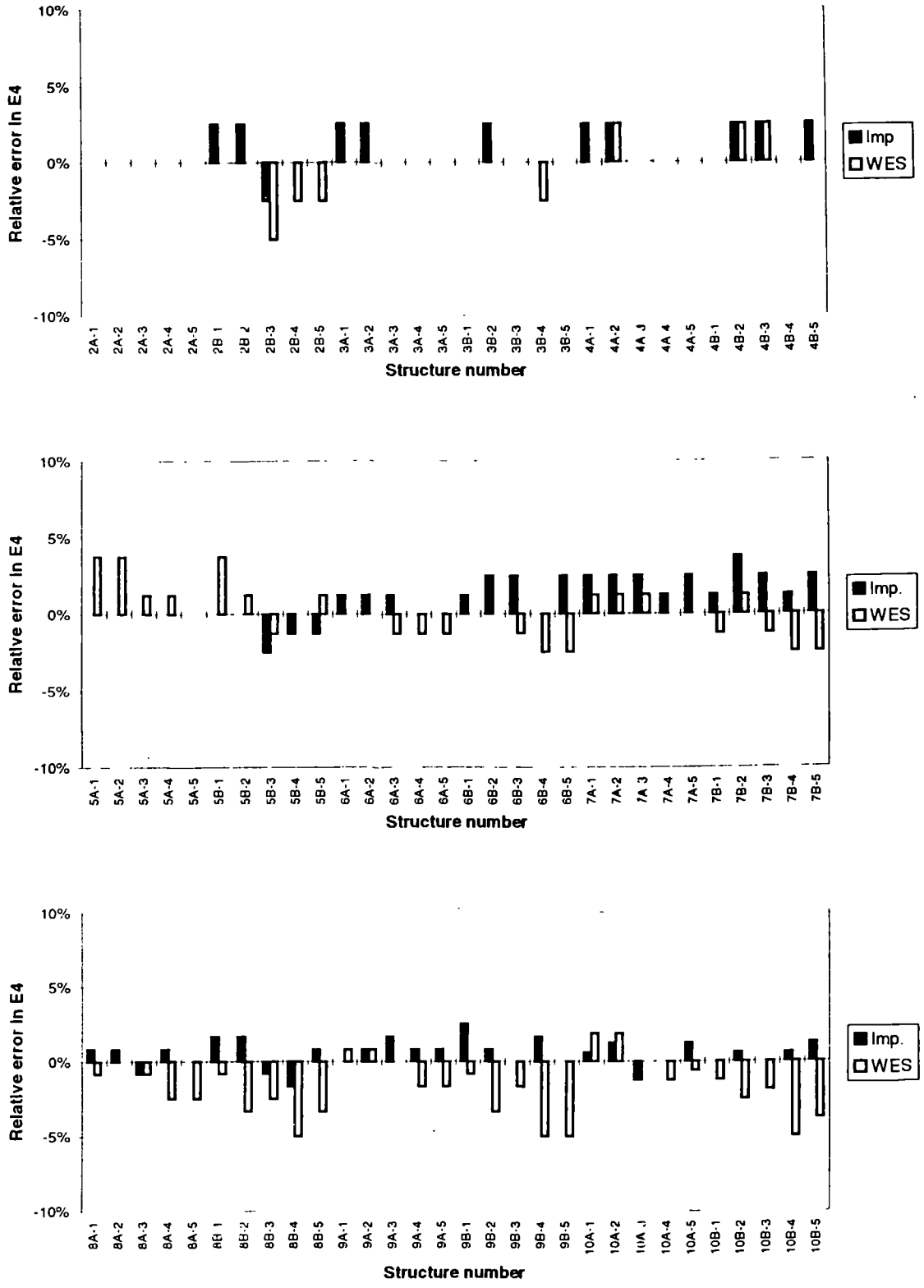


Figure 5, Relative error in predicting the modulus of subgrade using the improved and the WESDEF programs for the 90 pavement structures.